Synthesis and Evaluation of New Families of Polymer Electrolyte Membranes for Fuel Cell Applications

Patrick Gerard Gilbert

Submitted for the degree of Doctor of Philosophy
September 2011

Queen Mary, University of London

Acknowledgments

I would like to thank my supervisors, Prof Alice Sullivan and Dr Isaac Abrahams, for the help, guidance and advice given over the course of the PhD.

Without their support this PhD would not have been possible, they have taught me much about chemistry, research and life in general. I would also like to thank all the people that have been involved in the project; especially John Wilson (PhosphonicS Ltd) for guidance in multiple areas, Jovan Stankovic (QMUL) for patiently explaining the finer details of impedance spectroscopy and Nico Galaffu (PhosphonicS Ltd) for help with membrane synthesis and testing protocols.

Over the course of the PhD, many people made the long days (and quite a few long nights) spent in the lab both enjoyable and productive; especially those of the materials research group, Krystelle Mafina, Asma Qazi, Sai Madalla, Sebastien Guesene, Xi Liu. I would also like to acknowledge Barney who helped me retain my sanity during the difficult times over the course PhD.

There are many more people that I would like to say thank you to, the list is too long to write here, but it doesn't mean that you're any less appreciated!

Finally I would also like to thank PhosphonicS Ltd and Queen Mary for funding this project.

Pat Gilbert - September 2011

Abstract

Proton Exchange Membrane Fuel Cells (PEMFCs) are widely regarded as the next generation of portable power production devices, with uses ranging from powering automotive vehicles to laptops and smartphones. PEMFCs convert oxygen and hydrogen into water and usable electricity and have no moving parts, meaning that they can reach overall efficiencies of 60%. However current Polymer Electrolyte Membranes only work efficiently below 80 °C and at high humidity. At this low temperature, CO poisoning of the Pt electrocatalysts means that only high-grade fuel (low CO concentration $\leq$ 2 ppm) and high catalyst loading are required. This means that the overall cost of a PEMFC is prohibitively expensive. To dramatically the reduce cost and increase the efficiency of a PEMFC, new membranes are required which work at 120 °C, at which point CO poisoning is no longer a dominating issue.

In this thesis, the synthesis of novel organic/inorganic hybrid polyurethane Polymer Electrolyte Membranes (PEMs) with covalently bound phosphonic acid moieties (PA) made from cheap source materials have been reported, which, for the first time, demonstrate high conductivities at high temperatures, for example a PEM made from triethoxysilylpropyl isocyanate, polyethylene glycol, 4,4'-methylene diphenyl diisocyanate and PA displayed a conductivity of 3×10^{-2} S cm^{-1} at 120 °C and 100% RH. The membranes also display good mechanical, thermal and chemical stability making them ideal candidate PEMs for the use in PEMFCs. However further work needs to be done to reduce the thickness of the membranes from their current thickness of 200 μm to just 20-30 μm, which would dramatically increase their efficiency when used in a PEMFC, by reducing the Area Specific Resistance and increasing the output (usable) power.

Statement of Originality

I, Patrick Gerard Gilbert, hereby certify that all the experimental work stated in this thesis is my own work, with the exception of the synthesis of membrane 575C as well as the other initial formulation membranes as described in sections 4.0 and 4.1 which was synthesised by Dr Nico Galaffu of PhosphonicS Ltd.

Contents

List of Tables

List of Figures and schemes

List of Abbreviations

σ	Conductivity
λ	Water molecules per acid group in a hydrated PEM
AMS	Acrylamide ethylsulfide ethyltrimethoxysilane
ASR	Area Specific Resistance
DLS	Dynamic Light Scattering
DMDM	Dimethyl dimethoxysilane
DMP	Dimethyl phosphite
DPDM	Diphenyl dimethoxysilane
DPO	Dibenzoyl peroxide
EW	Mass of membrane which contains 1 mole of PA
GDE	Gas Diffusion Electrode
Glysil	3-Glycidyloxypropyl trimethoxysilane
IEC	Ion Exchange Capacity
HDI	Hexamethylene Diisocyanate
MDI	Methylene diphenyl diisocyanate (unless specified 4,4'-MDI)
MEA	Membrane Electrode Assembly
NMP	N-Methyl-2-pyrrolidone
PA	Phosphonic Acid Polysilsesquioxane
PA_E	Phosphonic Acid Ester Polysilsesquioxane
PBI	Polybenzimidazole
PEG	Polyethylene Glycol
PPG	Polypropylene Glycol
PTHF	Polytetrahydrofuran
PEEK	Polyether ether ketone
PEG	Polyethylene Glycol
PEM	Polymer Electrolyte Membrane
PEMFC	Proton Exchange Membrane Fuel Cell
PFA	Perfluoroalkoxy polymer (Copolymer of tetrafluroethylene and Perfluoropropylvinyl Ether)
PTMS	Phenyl trimethoxysilane
PU	Polyurethane
PWA	Phosphotungstic acid ($H_3PW_{12}O_{40}$)
SMA	3-(Triethoxysilyl)propyl methacrylate
SMEE	2,2'-(Ethylenedioxy) Diethanethiol trimethoxysilane
SPEEK	Sulfonated polyether ether ketone
TEG	Tetraethleneglycol dimethaacrylate
TEOS	Tetraethylorthosilicate
TSPI	3-Triethoxysilylpropyl isocyanate
VTMS	Vinyl trimethoxysilane

Chapter 1

Introduction to Polymer Electrolyte Membranes and Proton Exchange Membrane Fuel Cells

1.0 Introduction

The polymer electrolyte membrane (PEM), also called the proton exchange membrane, is the key component of proton exchange membrane fuel cells (PEMFCs). There are many different types and classes of membranes that have been explored, most notably those based on perfluorinated sulfonic acid and imidazole containing polymers. A schematic diagram for a single membrane fuel cell is shown below (Fig. 1.1). In reality, working fuel cells are made of stacks of many individual cells, with each cell producing *ca*. 0.7 V potential.[1]

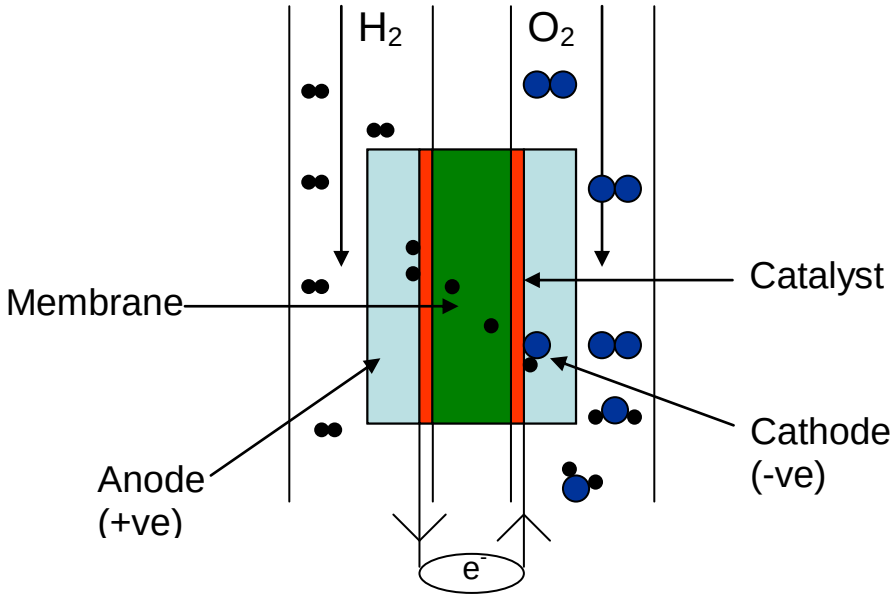

Fig. 1.1. Schematic diagram of a PEMFC

In a PEMFC a hydrogen gas stream is separated from an oxygen gas stream by the PEM, with a thin porous catalyst on the surface of the membrane. When hydrogen chemisorbs onto the catalyst layer it is oxidised into its constituent electrons and protons. The membrane is electronically insulating, but is proton conducting and therefore acts as an electrolyte. The protons are transported across the membrane as a result of a pressure gradient. The catalyst (which is usually Pt supported on porous carbon paper) also has the role of transporting the electrons to an electron capture

device which supplies the electrons to an external circuit before being channelled back to the catalyst on the cathode side of the cell. The electrons combine with the protons and with oxygen and undergo an electrochemical reaction to form water. Overall the equation can be written is summarised in Eq 1.1

$$2H_2 \rightarrow 4H^+ + 4e^- \text{ (Oxidation)}$$
$$4H^+ + 4e^- + O_2 \rightarrow 2H_2O \text{ (Reduction)} \quad (1.1)$$

The potential generated from a fuel cell is governed by the Nernst equation which is shown in Eq 1.2.1:

$$E = E^{\Theta} - \left(\frac{RT}{zF} \times \ln Q \right) \quad (1.2.1)$$

Where E^{Θ} is the standard cell potential, E is the electromotive force (EMF), R is the gas constant, T is temperature, z is the number of moles of charged species (protons), F is Faraday's constant (9.648456×10^4 C mol^{-1}) and Q is the reaction quotient and can be considered as the activities of products divided by the activities of reactants in the reaction occurring in a PEMFC, the substituted equation is given in Eq 1.2.2.

$$E_{cell} = E^{\theta}_{cell} + \frac{RT}{4F} \ln p_{O2} p_{H2} \quad (1.2.2)$$

PEMs have a variety of applications, but are chiefly used as electrolytes in fuel cells. Although currently expensive, fuel cells are seen as the next major advance in satisfying our energy needs, due to the relatively volatile nature of oil prices and the need for procurement of strategically accessible resources. Use of hydrogen produced either *in*-situ or commercially from agricultural crops, in fuel cells is seen as a way of breaking free of oil dependency. Originally touted as environmentally friendly, as there are no emissions other than water at the point of use, the use of hydrogen produced from bioethanol synthesized from agricultural crops is now realised to be just as detrimental to the environment as oil production and use.

The chemical reaction for hydrogen production and combustion from the steam reformation of ethanol is given in Eq. 1.3.

$$C_2H_5OH + 3H_2O \rightarrow 2CO_2 + 6H_2$$
$$6H_2 + 3O_2 \rightarrow 6H_2O \qquad (1.3)$$

From equation 1.3 it is evident that 1.91 kg of carbon dioxide is produced for every 1 kg of ethanol used. This is compensated by the fact then when the crops grow they absorb carbon dioxide from the air, so this part of the cycle is carbon neutral. The main concerns arise from fear of deforestation in developing countries for use as agricultural land to produce bioethanol and the planting of biofuel sources in preference to edible crops on economic grounds contributing to a global food crisis.

To cleanly produce hydrogen gas, the photovoltaic splitting of water into hydrogen and oxygen must be accomplished (Eq. 1.4) and this is seen as the 'holy grail' of cheap, renewable green energy.

$$2H_2O \xrightarrow{h\nu} 2H_2 + O_2 \qquad (1.4)$$

In this instance energy from sunlight is used to split water into hydrogen and oxygen, and when passed through a fuel cell they reform water. So the product is the starting material. Currently this is extremely limited and in addition the alternative electrolysis of water requires a tremendous amount of energy which makes this unviable.

1.1 Limiting Factors for PEMFC Commercialisation

Aside from hydrogen production there are three major technical requirements that need to be met before hydrogen fuel cells can truly become commercialised and scaled up for mass production. The first two requirements are not in the scope of this work, but to fully understand the technical challenges the problems should be mentioned.

1.1.1 Hydrogen Storage and Distribution

Hydrogen is a highly flammable gas and this leads to two problems. Firstly, the distribution and supply network is currently not set up to deliver gas fuels, but rather liquids, so this would require a huge initial investment (>£10 billion) to build the

required infrastructure. This currently limits the use of hydrogen fuel cells to centralised automotive fleets, such as buses where all the vehicles are based at a central depot. Secondly, there are problems associated with the portable storage of hydrogen gas in the vehicles themselves. To store enough hydrogen for a practical journey, the gas must be either compressed or stored in an effective hydrogen sponge. This then leads to safety concerns about compressed gases and risk of explosions in an accident.

1.1.2 Platinum Catalyst

For the dissociation of hydrogen gas into protons and electrons, platinum based catalysts are used. These are very expensive and consequently the platinum loading has been reduced dramatically over the past few years,[2,3] from 2.0 g cm^{-2} to 0.4 g cm^{-2}. However, the current working temperature for a PEM fuel cell is 80 °C. At this relatively low temperature carbon monoxide poisoning is a problem, as it adsorbs onto the surface, and due to the thermodynamic stability of the adsorbed species, it will not desorb from the surface. When the feed stream of hydrogen is not 'pure' (i.e. CO concentration. < 5 ppm) the electrodes become poisoned and the electrochemical reaction diminishes or stops with the fuel cell ceasing to function. This makes the purification of the hydrogen gas expensive as it has to undergo several cleaning steps.

1.1.3 Membrane

The role of the membrane is deceptively simple, to transport the protons produced at the anode to the cathode, whilst acting as a physical barrier to electrons. However, there are many factors that dramatically affect the operation and behaviour of the membrane and thus the fuel cell. Currently, the industry standard PEM is Nafion, which was developed and is marketed by DuPont. Nafion is the trade name for tetrafluoroethylene-perfluoro-3,6-dioxa-4-methyl-7-octenesulfonic acid, the structure of which is shown in Fig. 1.2.

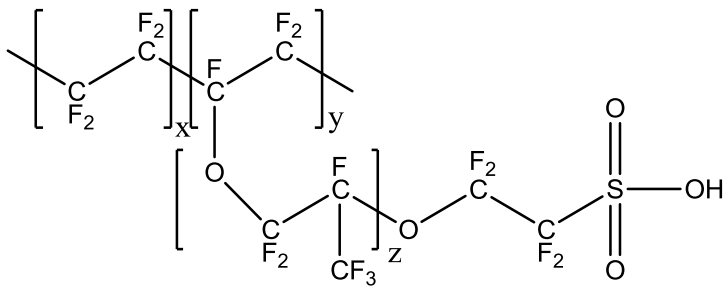

Fig. 1.2. Structure of Nafion

The polytetrafluoroethylene (PTFE) backbone makes Nafion extremely resistant to harsh chemical environments.[4] Originally Nafion was developed for use in chloro-alkali production cells, where the membrane transports sodium ions from brine solution to water, thus producing sodium hydroxide and chlorine gas.

Nafion has excellent mechanical and chemical durability, displays high conductivities at high temperatures ($\geq$ 0.1 S cm^{-1} at 80 °C) and reasonable conductivities at low temperature, which allow for a cold start up in fuel cells under ambient conditions. However, for use as a PEM in PEMFCs, Nafion is far from ideal.[4] Nafion's conductivity is highly dependent on the hydration state of the membrane; Nafion operates most efficiently at 100% relative humidity (RH) with efficiency dramatically decreasing with decreasing RH. Therefore, to achieve maximum conductivity the gas stream must be completely humidified by a humidification system. This adds to the bulk and complexity of the PEM fuel cell system and hence also adds considerable financial cost.

The second major disadvantage is the maximum working temperature of the membrane, which is 80 °C. At this temperature CO poisoning of the platinum catalysts is a major issue as mentioned above, ideally a membrane would work in the region of 150 °C, where CO poisoning would not be an issue (it would also be substantially improved at 120 °C), as the thermodynamics of CO adsorption would be overcome, thus allowing for less platinum to be used and the feed stream of hydrogen would not need to go through such an intensive purification process. At even higher temperatures, alcohol fuels could be used indirectly by being reformed *in*-situ, thus bypassing hydrogen storage and supply issues. At 80 °C the heat management of the fuel cell is a problem overcome by large radiator systems. At an operating temperature of 120 °C the heat elimination is easier to control so a radiator half the size could be used with traditional coolants such as ethylene glycol.

Thirdly, as Nafion is a fluorinated polymer, it is costly to produce and the fluorinated waste very expensive to dispose of in an environmentally friendly manner. There is also fluoride leaching when the polymer is in use which although minor, occurs constantly. This also leads to problems when trying to recover used platinum from Nafion based fuel cells as it is contaminated by fluoride ions.

So it is widely accepted that new materials must be developed, either by modifying existing membranes or from new formulations. Inorganic-organic hybrid polymers have been pointed out for their promising characteristics of high conductivities, high working temperatures and relatively lower humidity dependence.

1.2 Development of New PEMs

Many research groups are modifying Nafion to try and improve its characteristics; the vast majority of this work is through addition of inorganic components to Nafion solutions and then forming the membrane by sol-gel methods. This has led to higher working temperatures of up to 100 °C, but decreased proton conductivity and mechanical strength.

1.2.1 New PEM Targets

The United States Department of Energy (US DoE) has listed a set of criteria for new membranes for use as PEMs in fuel cells for automotive applications (80 kW stacks).[5,6] These are:

- 0.1 S cm^{-1} conductivity at operating temperature
- ≤ 0.07 S cm^{-1} conductivity at room temperature
- 5000 hr life span
- Survivability to -40 °C
- Cost $5 / kW
- $20 per m^2 for the membrane
- Less than 2mA cm^{-2} oxygen and hydrogen cross-over
- Thermal cyclability in condensed water

In 2007 the High Temperature Membrane Working Group (HTMWG) (a group set up by the US DoE) reviewed the then criteria and proposed new targets based on area specific resistance (ASR).

Area specific resistance is a measure preferred by engineers because the value does not take into account the thickness of the membrane. Conductivity does not always display a linear relationship with thickness, so ASR represents the true potential that can be achieved from a specific membrane. To achieve low ASR values, thin membranes need to be employed. For Nafion membranes the thickness has been decreased to between 25

to 50 μm. Nafion NRE 211 and 212 membranes are dispersion cast membranes instead of the previous generation Nafion 117 and 115 membranes which where extrusion cast. These membranes have also been further stabilized and exhibit lower fluoride ion leaching than the previous generation membranes. The tensile strengths of the NRE 211 membrane are between 30 to 50% lower than the extrusion cast membranes, but the elongation at break is considerably larger by *ca.* 50% (Nafion NRE-212 343% and N-117 225%, both at 50% RH and 23 °C).

The HTMWG also assessed the 2005, 2010 and 2015 targets against those actually achieved in 2006. The only target that has not been satisfactorily reached is that of the operating temperature. The same group also suggested a new approach to new membrane development in their R&D plan, which is listed below:

- New polymers with improved thermal stability
- Polymers with hydrophilic additives or improved hydrophilicity
- Polymers with added acids
- Water-dependent inorganic conductors
- Phosphoric acid based systems
- Emphasis on non-Nafion systems

New membranes should have the following attributes:

- Be low cost
- Exhibit high ionic conductivity
- Be electronically insulating
- Be gas impermeable
- Show conduction independent of water content
- Exhibit good high temperature performance (including improved CO tolerance)
- Maintain conduction in face of repeated exposure to condensed water
- Be able to conduct sufficiently at low temperature to allow bootstrapping of stack
- Be durable
- Show good interfacial properties
- Have mechanical strength
- Be recyclable

1.2.2 PEM Chemical Stability

To determine chemical stability in the working environment, membranes are tested *ex*-situ by peroxy radical attack. The United States Fuel Cell Council (USFCC) recommends that the test conditions should be immersing the membrane in 30% H_2O_2 and 20 ppm Fe^{2+} at 85 °C for 3 cycles, each lasting for 18 hours and using fresh reagents.[7]

This is called Fenton's reaction. The iron is catalytic, and is oxidised from FeII to FeIII by hydrogen peroxide producing a hydroxide anion and hydroxyl radical; the iron is then reduced by another molecule of hydrogen peroxide reforming Fe^{2+} and producing a proton and peroxide radical, the overall chemical equation is given in Eq 1.5. Iron sulphate is typically used as the source of iron.

$$\begin{aligned} Fe^{2+} + H_2O_2 &\rightarrow Fe^{3+} + OH\cdot + OH^- \\ Fe^{3+} + H_2O_2 &\rightarrow Fe^{2+} + OOH\cdot + H^+ \end{aligned} \qquad (1.5)$$

For milder conditions, 3% H_2O_2 and 2 ppm Fe^{2+} can be used, as this can give a good indication of chemical stability and can be employed in the screening process for membrane formulations.

1.2.3 Mechanical Strength

Despite the fact that mechanical strength is regarded as a critical feature of a membrane, there are no set requirements or protocols for testing mechanical strength. On the technical specification for Nafion, DuPont have given the tensile strength, non-standard modulus and the elongation to break in the machine and transverse directions. It is widely regarded that membranes have to be reasonably flexible and show good resistance to tears and other physical deformations during processing into membrane electrode assemblies (MEAs). Production of MEAs is typically performed by "hot pressing" which involves heat treatment, so the membranes also need to be chemically and mechanically stable at these elevated temperatures for short periods of time.

1.3 Proton Conductivity and Proton Transfer in PEMs

Proton conductivity in polymer electrolytes can occur via two different mechanisms, proton transfer or proton diffusion. The Grotthuss mechanism is widely accepted as describing proton transfer in water. Proton transfer is believed to be the dominant process in Nafion, as it displays poor conductivity at low hydration levels.[8]

1.3.1 The Grotthuss Mechanism

The Grotthuss mechanism was suggested over 200 years ago;[9] it simply stated that water effectively acted as a molecular wire for proton transfer, much like metal wires for electron transfer. This provides a simple reason why proton mobility is an order of magnitude greater than that of other ions both small such as Na^+ and even doubly positively charged cations such as Ca^{2+}. At the time it was proposed, the chemical composition of water was thought to be just OH, so the details in the original mechanism are clearly inaccurate. This has caused some groups to dispute the claim that the current mechanism should be called the Grotthuss mechanism.[10] Recently two camps argued that the proton transfer mechanism occurs via either a Zundel or an Eigen intermediate complex. These represent the two extremes of proton transfer, and thermodynamically there is little difference between the two complexes.

Zundel Complex

The Zundel complex has the chemical composition of $H_5O_2^+$, thereby consisting of two water molecules sharing a proton via hydrogen bonding (Fig. 1.3).

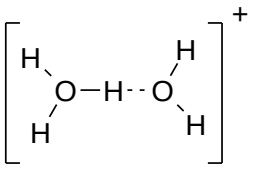

Fig. 1.3. Zundel Complex

The proton transfer is summarised in Fig. 1.4.

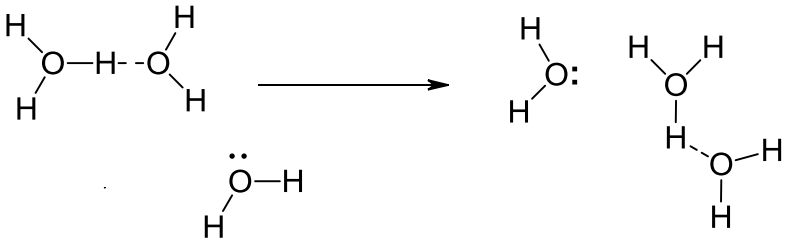

Fig. 1.4. Proton transfer via a Zundel complex (charges omitted for clarity)

This mechanism allows for near instantaneous transfer of protons. The energy required for this to occur is in the order of 0.025 – 0.1 eV, which is supplied via thermal vibrations at room temperature.

Eigen Complex

The Eigen complex has the chemical composition of $H_9O_4^+$, which makes it twice the size of the Zundel complex (Fig. 1.5).

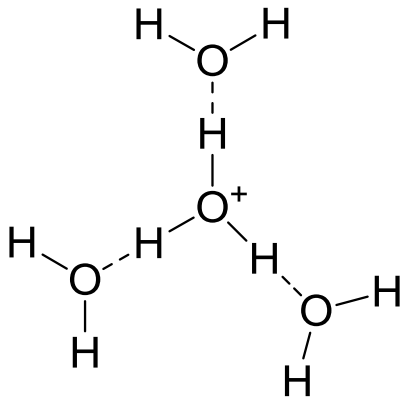

Fig. 1.5. Eigen Complex

In much the same way as the Zundel complex, the Eigen complex transfers protons across hydrogen bonds and again this transfer only requires a small amount of energy which is supplied by thermal vibrations.

It has been agreed by mathematical modelling that both Zundel and Eigen complexes exist for proton transfer in water. To many outside the field of quantum computational chemistry, the water molecules still act effectively as molecular wires, and hence the name the Grotthuss mechanism has stuck.

1.4 Current Electrolytes Being Developed For Use in PEMFCs: Nafion, PBI, (S)PEEK and Solid Acid

There are many types of PEMs which have been explored for use in PEMFCs, the three of most note are Nafion based membranes, phosphoric acid doped polybenzimidazole and sulfonated polyether ether ketone (SPEEK) PEMs. However, the search for potential new materials for use as PEMs has not just been limited to traditional polymers, certain solid acid ceramics have been shown to exhibit high proton conductivities. In the next section, a brief overview of these membranes is given.

1.4.1 Nafion

Nafion has been extensively studied in the literature; a quick search of Nafion using the Web of Science resulted in over 8400 hits[11] starting from 1975.[12] Seminal research

papers or reviews in this area have been cited over 500 times, indeed the most cited paper has been cited over 1100 times.[13] Nafion is a versatile material and has several other uses apart from in PEMFCs. These include being used as a ion exchange membrane in a chloroalkali cell, indeed this was the use for which Nafion was developed for;[4] use in nitric oxide microsensors,[14] while Harmer *et al.*[15] reported the use of Nafion as a catalyst for certain organic reactions.

1.4.1.1 Proton Conductivity in Nafion

For Nafion membranes, water enters into the hydrophilic cavities formed by the acid groups (Fig. 1.6). To do this it must first pass through the hydrophobic (fluorinated) hydrocarbon backbone. This is achieved by osmotic pressure. However, in some systems the water uptake actually exceeds that from the osmotic gradient. This is due to very strongly hydrophilic regions, but can cause the membrane to swell and even burst.[16]

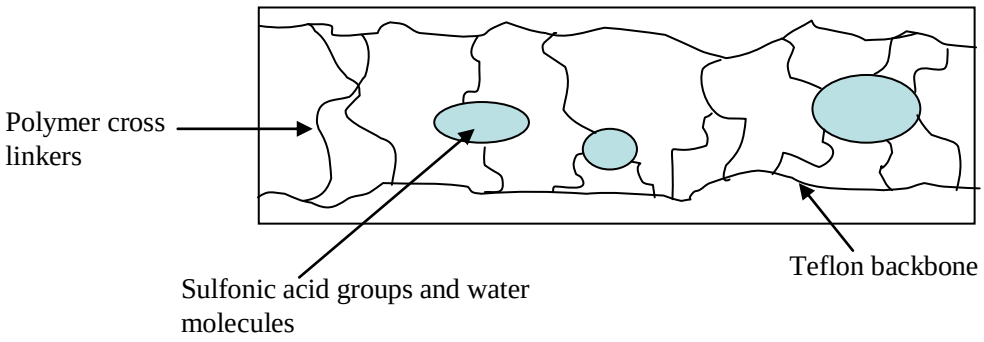

Fig. 1.6. Schematic cross section of a hydrated Nafion membrane

In anhydrous or low water volume systems, the proton transport mechanism is diffusion, occurring via the traditional ion hopping mechanism, or space jumping. This is driven by electrostatic forces or defects and the rate is usually an order of magnitude smaller than the molecular wire mechanism. However, as the electrolytes are only 100 – 200 microns thick this is still significant.

The mechanism for proton transfer can be approximated by determination of the proton diffusion coefficients. High proton diffusion values do not necessarily mean the mechanism is entirely due to proton transfer and therefore the true mechanism cannot be stated.

Zawodzinski *et al*. reported the conductivity of Nafion 117 using impedance spectroscopy in a two probe tangential cell.[17] The membrane was first conditioned by boiling in 3% H_2O_2 solution for one hour, and then the membrane was removed and boiled in dilute sulfuric acid (1 M) for one hour and then rinsed in boiling water for one hour. The membrane was then taken out and the surface water removed by wiping with filter paper. After measurement of the membrane thickness it was placed in the conductivity cell (as shown in Fig. 1.7). The impedance was measured at 5 kHz with the cell immersed in water (unspecified quality) at room temperature. Conductivities up to 0.1 S cm^{-1} were reported using this method. This is the literature value DuPont quote for Nafion conductivity on their product datasheets.[18]

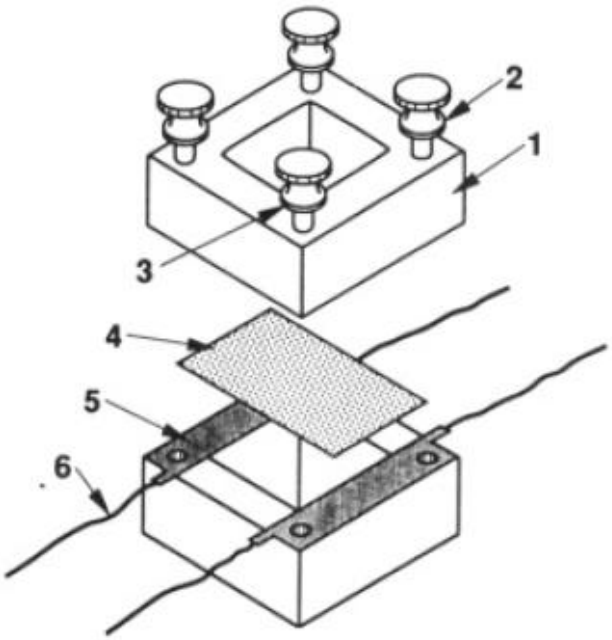

Fig. 1.7. Impedance cell set up taken from reference 17. Cell used for determination of membrane conductivity: (1) PTFE block; (2) thumbscrew; (3) open area to allow equilibration; (4) membrane sample; (5) blackened Pt foil; (6) Pt ribbon lead.

It is widely reported that the level of conductivity Nafion displayed is highly dependent on the membrane hydration state where hydration is measured by λ, the number of water molecules present in the membrane per acid group. Zawodzinski *et al*.[19] reported that although the conductivity for a fully hydrated Nafion membrane (λ = 24) at 25 °C was 0.1 S cm^{-1}, for a partially hydrated Nafion membrane (λ = 10) the conductivity was 0.04 S cm^{-1} and when λ = 5, the conductivity was only 0.02 S cm^{-1}. At higher temperatures, the reduction of conductivity is more pronounced for lower hydration states, as Nafion membranes lose more absorbed water

Hsu and Gierke[20] proposed that the high conductivity observed for Nafion was due to the morphology of the hydrated membrane. It was theorised from experimental SAXS and WAXD observations that in fully hydrated samples of Nafion, a cluster network forms with an inverted micelle structure, with narrow channels connecting the micelles spheres (Fig. 1.8). This would enable channels of water to form inside the membrane, thus enabling primary proton transport via the Grotthuss mechanism and secondary proton transport via the vehicular mechanism. Although in the years since the cluster network model was originally proposed, there has been much debate in the literature to the exact nature of the morphology of hydrated Nafion, the cluster network model and its derivatives have remained the most widely accepted model.[4] For example Haubold *et al*.[21] proposed a modified network model where in hydrated Nafion the solvent channels are a continuous phase throughout the membrane when used in a Direct Methanol Fuel Cell (DMFC) where methanol is used as the fuel instead of hydrogen gas (Fig. 1.9).

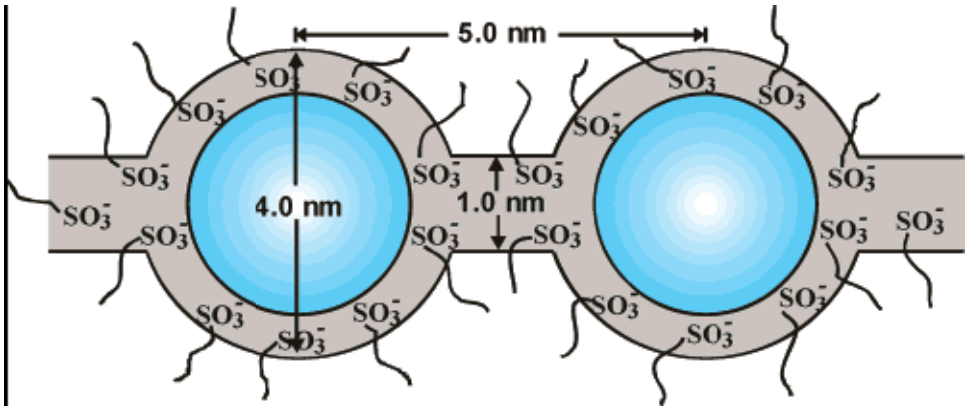

Fig. 1.8. Cluster network model of Nafion taken from reference 20

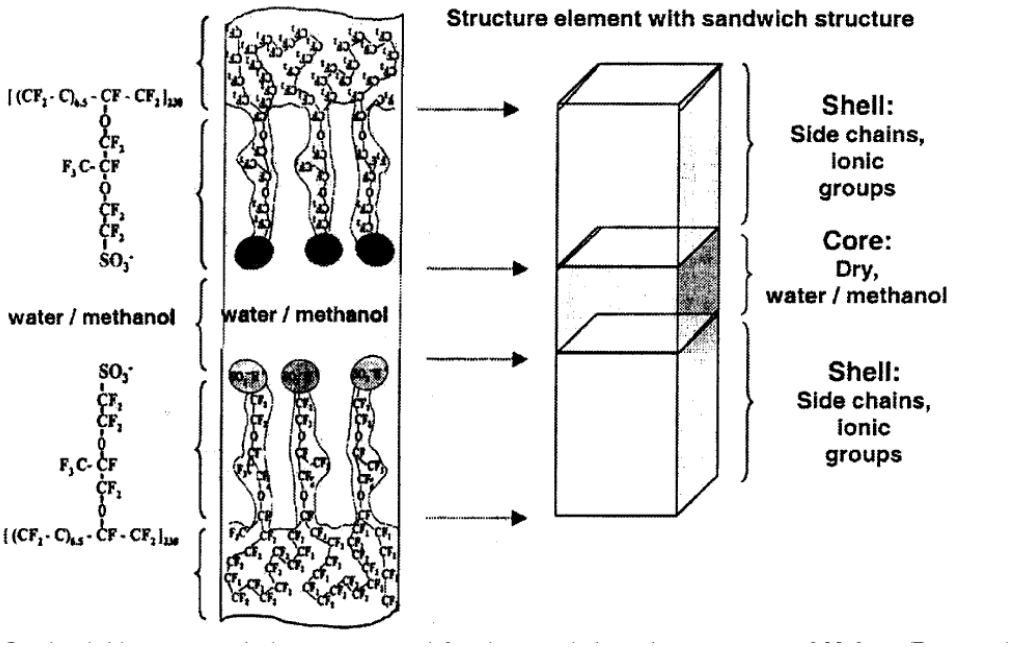

Fig. 1.9. Proposed sandwich network structure for hydrated Nafion when used in a DMFC, taken from ref 21

Recently, commercial Nafion membranes have changed from extrusion cast membranes to dispersion cast membranes. This has lead to a dramatic reduction in membrane thickness; Nafion 117 (an extrusion cast membrane) had a typical thickness of 183 μm[18] whereas Nafion NR 211 (a dispersion cast membrane) had a typical thickness of 25.4 μm.[22] Not only did this dramatically reduce the mass of membrane used in MEA fabrication (from 360 to 50 g m^{-2} respectively), it also reduced the overall MEA resistance and hence increased the PEMFC efficiency. The reduction in thickness did not result in a deterioration of mechanical properties. DuPont have also started to manufacture MEAs containing reinforced Nafion (Nafion XL),[23] which are more chemically stable, releasing 30 times less fluoride ions, have a tensile strength 1.5 times greater and exhibit 50% less water uptake/membrane swelling than the equivalent Nafion NR 211 membrane, although no specifications on the electrocatalyst had been released to date (e.g. Pt loadings). These new Nafion membranes, however, do not address the issue of low proton conductivity at low RH and/or at high temperatures.

To overcome the limitations of Nafion, many research groups have looked at modifying Nafion membranes with inorganic moieties to increase water uptake or to prevent membrane dehydration above 100 °C, including modification with SiO_2,[24,25] TiO_2[26] and PWA (phosphotungstic acid).[24,25,27] Generally these membranes exhibit higher proton

conductivities at elevated temperatures (above 80 °C) and lower relative humidities compared to untreated Nafion membranes, they display worse conductivity at low temperatures, poorer mechanical properties and more membrane swelling.

1.4.2 PBI

Polybenzimidazole is a high melting, high tensile strength and highly chemically stable polymer, which has a fully aromatic backbone as shown in Fig. 1.10.[28] Wainright *et al.* first proposed using phosphoric acid doped PBI membranes as a PEM for direct methanol fuel cell (DMFC) applications.[29] The PBI membranes were reported to have a conductivity of 2.5×10^{-3} S cm^{-1} at 130 °C in a dry atmosphere, for a membrane doped with 338 mol percent of H_3PO_4. Membranes were prepared by dissolving commercial PBI in dimethylacetamide, then cast onto glass plates, and heated until the solvent evaporated and the resulting films were then immersed in phosphoric acid.

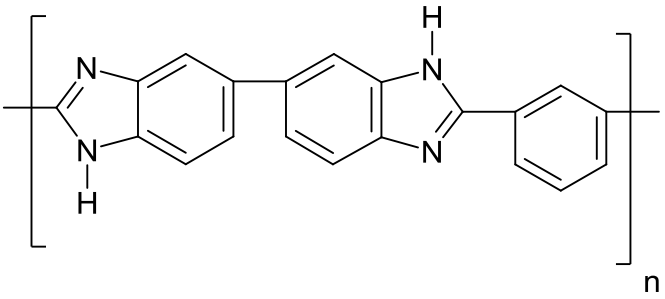

Fig. 1.10. Chemical structure of PBI

To further increase the conductivity of PBI membranes, Glipa *et al*. grafted sulfonic acid groups to the aromatic backbone.[30] This was done by reducing dissolved PBI in dimethylacetamide with LiH, and then adding sodium (4-bromomethyl) benzenesulfonate in varying mole percentages to produce partially sulfonated PBI membranes as shown in Fig. 1.11. Prior to conductivity measurements, the PBI membranes were soaked in phosphoric acid and then boiled in water. Conductivities of 1×10^{-2} S cm^{-1} at 50 °C and 100% RH were reported.

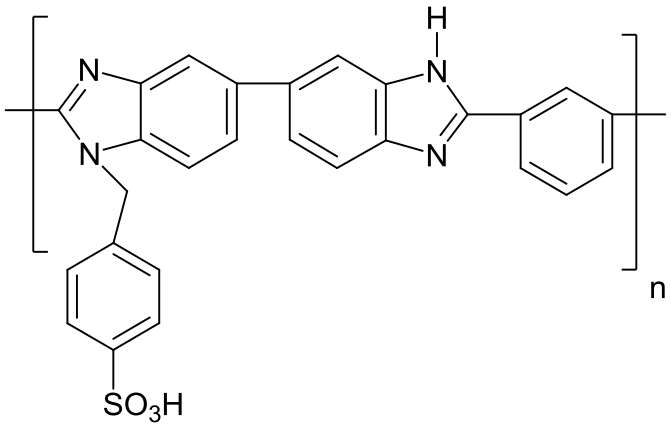

Fig. 1.11. Partially sulfonated PBI from reference 30

Bouchet and Seibert reported the use of sulfuric acid and hydrogen bromide as PBI membrane dopants as well as phosphoric acid.[31] Their A.C. impedance measurements were performed under vacuum, i.e. 0% RH. The presence of a significant volume of hydrogen bromide (100 mol%) showed little effect on the proton conductivity of PBI, this doped membrane only resulted in conductivities from 10^{-10} to 10^{-8} S cm^{-1} at 75 °C and 130 °C respectively. Whereas the phosphoric acid doped PBI membrane (305 mol%) gave a conductivity of 1×10^{-4} at 60 °C and the sulfuric acid doped PBI membrane (325 mol%) gave a conductivity of 4×10^{-4} at 45 °C, although at 30 °C the conductivity of the phosphoric acid doped PBI membrane was considerably lower than that of the sulfonic acid doped PBI membrane, 7×10^{-6} and 1×10^{-4} S cm^{-1} respectively.

PBI membranes with phosphoric acid dopant levels of up to 500 mol% have been reported in the literature with conductivities reaching 3.5×10^{-2} S cm^{-1} at 190 °C.[32] However, the long-term operation of doped PBI membranes remains a limiting factor as the acid dopants are not chemically attached to the PBI membrane backbone and can wash/leach out over long-term use thus reduce the overall efficiency of a PEMFC.[33] A secondary factor limiting the use of phosphoric acid, is that the phosphoric acid passivates the platinum electrocatalyst,[34] so typically higher Pt loadings are required to maintain fuel cell efficiency.[35]

1.4.3 PEEK membranes

Polyether ether ketone (**PEEK**) is a high melting point polymer (334 °C), which also has a high glass transition temperature (143 °C), the structure of which is shown in Fig. 1.12. PEEK is synthesised by nucleophilic polycondensation of either bis-phenols with

activated aromatic dihalides or from a single aromatic halide phenol monomer,[36] however most research groups use commercial grade PEEK from Polysciences and Victrex to synthesise membranes.

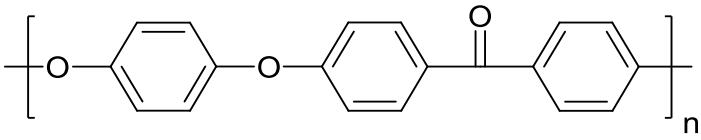

Fig. 1.12. PEEK polymer

PEEK membranes have very low intrinsic conductivity, so to increase the conductivity, PEEK membranes are partially sulfonated or synthesised containing sulfonic acid groups covalently bound to the polymer backbone. This forms sulfonated polyether ether ketone (**SPEEK**), the structure of which is shown in Fig. 1.13. PEEK membranes are sulfonated by dissolving PEEK polymer in concentrated sulfuric acid (95%).[37] In a typical synthesis, 20 g of PEEK is dissolved in 10 g of sulfuric acid, at room temperature and the solution then vigorously stirred for up to 120 hours. The polymer solution is then slowly precipitated in an excess of ice-cold water. The polymer precipitate is subsequently filtered and washed with deionised water until the pH of the washings is 7 and finally dried in a vacuum oven at 100 °C over night.

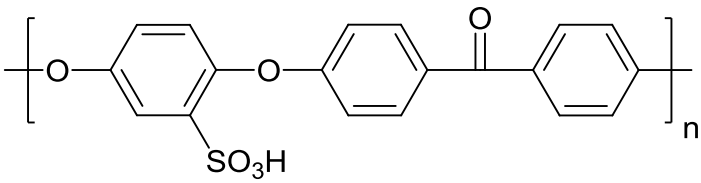

Fig. 1.13. SPEEK polymer

Zaidi *et al.* reported the incorporation of solid heteropolyacids into SPEEK membranes.[38] These were Phosphotungstic acid (**PWA**, Formula: $H_3PW_{12}O_{40}$), molybdo-phosphoric acid (**MPA**) and the disodium salt of PWA (**NaPWA**). To synthesise the composite membranes, SPEEK was dissolved in dimethylacetamide to produce a 5-10% weight solution. To this, the desired amount of heteropolyacid (60% w/w) was added and the reaction mixture was stirred for an additional 24 hours prior to membrane casting. It was found that below a sulfonation level of 80%, the introduction of a heteropolyacid increased the proton conductivity of the membranes at room temperature, but at 100 °C, the pristine SPEEK membrane had a higher proton conductivity than that of MPA and NaPWA, but a lower proton conductivity that the

PWA composite membrane (full results are shown in Table 1.1). Although the heteropolyacids increased the conductivities in most cases, they dramatically increased the water uptake of the membranes. The pristine SPEEK 80% sulfonated membrane absorbed 120% w/w water, whilst the PWA SPEEK 80% sulfonated composite membrane absorbed 600% w/w water. The lower proton conductivities for the NaPWA and MPA composite membranes at 100 °C was rationalized by the faster dehydration of these membranes compared to that of the pristine SPEEK and the PWA composite membranes. This meant that the membranes lost water during A. C. impedance measurements, which were performed under ambient air conditions, i.e. no external source of hydration and this resulted in the higher observed resistances.

Table 1.1 Water uptake and conductivities of composite SPEEK membranes (taken from Ref 38)

Membrane (% PEEK Sulfonated)	Thickness of wet membrane / μm	Water uptake / Weight %	Conductivity / S cm^{-1}	
			25 °C	100 °C
SPEEK 70	300	48	1.3×10^{-3}	6.7×10^{-3}
SPEEK 70 and PWA	170	64	3.5×10^{-3}	1.7×10^{-2}
SPEEK 70 and NaPWA	375	143	2.9×10^{-3}	1.5×10^{-2}
SPEEK 70 and MPA	200	94	3.1×10^{-3}	1.1×10^{-2}
SPEEK 74	300	62	2.1×10^{-3}	9.5×10^{-3}
SPEEK 74 and PWA	160	190	5.1×10^{-3}	2.0×10^{-2}
SPEEK 74 and NaPWA	300	160	4.5×10^{-3}	1.6×10^{-2}
SPEEK 74 and MPA	200	146	3.6×10^{-3}	1.2×10^{-2}
SPEEK 80	500	120	8.0×10^{-3}	7.6×10^{-2}
SPEEK 80 and PWA	300	600	2.0×10^{-2}	9.5×10^{-2}
SPEEK 80 and NaPWA	200	400	1.4×10^{-2}	5.8×10^{-2}
SPEEK 80 and MPA	160	320	1.2×10^{-2}	3.0×10^{-2}

Wang *et al*. reported the direct synthesis of sulfonic acid containing PEEK membranes which do not require post modification,[39] this has the advantage of avoiding the harsh conditions of PEEK sulfonation, allows a greater degree of control of sulfonation and avoids side reactions such as cross-linking of a sulfonic acid group and a phenyl proton creating an intermolecular sulfone group.[40]

Sodium 5,5'-carbonylbis(2-fluorobenzene sulfonate) was synthesised by sulfonating 4,4'-difluorobenzophenone by exposure to fuming sulfuric acid at 100 °C, which was then neutralised by adding sodium hydroxide and sodium chloride. To synthesise the SPEEK membrane, the desired amounts of sodium 5,5'-carbonylbis(2-fluorobenzene sulfonate) and 4,4'-difluorobenzophenone (up to 4:6 mol/mol ratio respectively) were dissolved in DMSO and bisphenol A was added with potassium carbonate as a catalyst. The membranes were synthesised in high yields (95 % and above). Although the electrochemical properties were not examined in this paper, other research groups have used this methodology to synthesise SPEEK membranes.

Gil *et al.* reported the synthesis of SPEEK membranes (the structure for which is shown in Fig. 1.14) from sodium 5,5'-carbonylbis(2-fluorobenzene sulfonate), 4,4'-difluorobenzophenone and 3,3',5,5'-tetramethyl-4,4'-biphenol instead of bisphenol A.[41] The ratio of sodium 5,5'-carbonylbis(2-fluorobenzene sulfonate) and 4,4'-difluorobenzophenone was also investigated, and the optimum ratio was found to be 60:40, as when the amount of sodium 5,5'-carbonylbis(2-fluorobenzene sulfonate) was increased further the SPEEK membrane became water soluble. However using this methodology, SPEEK membranes containing 1.1 moles of sulfonic acid per repeating unit were synthesised (60:40 ratio membrane), which is considerably higher than that of SPEEK membranes which were post-treated, which contained 0.8 moles of sulfonic acid per repeating unit. Conductivities of 0.07 and 0.11 S cm^{-1} were reported at 25 and 100 °C respectively. Conductivity measurements were performed using a similar experimental set up as described by Zawodzinski *et al.* (ref 17) and the conductivity cell was immersed in deionised water during measurements.

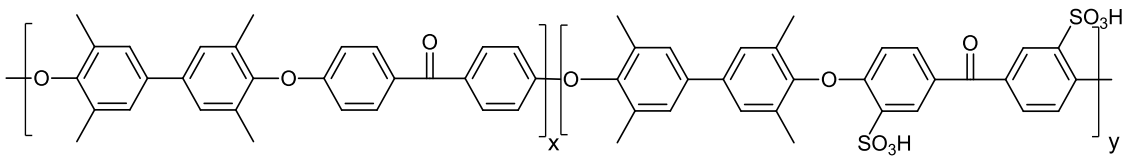

Fig. 1.14. SPEEK membrane synthesised in ref 41, x = 4 mol, y = 6 mol

The water uptake of the highly sulfonated PEEK membrane (1.1 mol per repeating unit) was only 54%, which is more favourable than those reported by Zaidi *et al*. (ref. 39, see Table 1.1), whereas SPEEK (0.8 mol per repeating unit) had a water uptake of 120%

and a lot less than those containing extra hetropolyacids. This was argued to be due to the extra hydrophobic phenyl ring and the methyl substituents.

Di Vona *et al*. reported the synthesis and characterisation of inorganic hybrid SPEEK membranes containing covalently attached silica groups[42] and titanium dioxide[43]. In both cases the PEEK was commercially supplied by Victrex and then sulfonated in sulfuric acid (described as above).

To synthesise the silica composite membrane, the SPEEK polymer was dissolved in dimethylacetamide and reacted with butyllithium to deprotonate the phenyl ring ortho to either the sulfonate or ketone functional groups. To this, $SiCl_4$ was added and the reaction mixture was refluxed overnight. The ethanol was added and refluxed for a further five hours before the polymer was precipitated at room temperature before being thoroughly washed with deionised water to remove the chloride ions, before heating at 120 °C for 10 hours and then at 80 °C for 4 hours under vacuum to cross link the siloxane groups via a condensation reaction. To activate the sulfonate groups into sulfonic acid, the membrane was immersed in 5 M sulfuric acid for one hour and then rinsed to remove excess sulfuric acid.

To synthesise the SPEEK/TiO_2 composite membrane, two synthetic routes were employed. In the first method the SPEEK polymer was dissolved in dimethylacetamide, titanium butoxide and pyridine were added and the reaction mixture was stirred for an hour. In the second route the SPEEK polymer was dissolved in dimethylacetamide, with titanium butoxide and 2,4-pentandione also dissolved in dimethylacetamide added and the reaction mixture stirred for an hour. The solutions were evaporated to dryness on PTFE sheets and the membranes were heated under vacuum.

The SiO_2/SPEEK composite membranes showed a higher water uptake compared to SPEEK membranes (ca. 240 %) and the conductivity at room temperature was 2.0×10^{-2} S cm^{-1}, which is higher than that of unmodified SPEEK membranes with a similar degree of sulfonation (*ca*. 2.0×10^{-2} S cm^{-1}). The TiO_2/SPEEK composite membranes have significantly less water uptake than those of unmodified SPEEK membranes, the membrane prepared by the first route had a water uptake of only 40%, whilst the membrane prepared by the second route had a water uptake of 125%. As proton

conductivity is highly dependent on water content, the membrane prepared by the first route had lower conductivity values, 3.0×10^{-3} S cm^{-1} at room temperature and 1.2×10^{-2} S cm^{-1} at 120 °C, whereas the membrane prepared by the second route had significantly higher proton conductivities at elevated temperatures, 5.8×10^{-2} S cm^{-1} at 120 °C, whilst having comparable conductivities at lower temperatures. Although the conductivities of the composite membrane are similar to the unmodified SPEEK membranes, the water uptake is just over half that of unmodified SPEEK membranes so the membranes would undergo less swelling in a PEMFC.

Similarly, inorganic hybrid SPEEK composite membranes have been synthesised which contained other inorganic moieties such as amorphous silica, zirconium phosphate sulfophenylphosphonate and zirconium phosphate and also exhibited enhanced properties.[44]

1.4.4 Solid Acid Electrolytes

The use of solid inorganic acids as electrolytes in high temperature PEMFCs was reported by Haile *et al*.[45] Caesium hydrogen sulfate ($CsHSO_4$) was shown to exhibit a 'superprotonic' phase in the temperature range of 140 to 230 °C. Although reasonable conductivities were obtained above this phase transition, typically about 10^{-2} S cm^{-1}, below the phase transition the conductivity dramatically reduces, at room temperature the conductivity was only approximately 10^{-7} to 10^{-6} S cm^{-1}. It was found that to obtain high conductivities at high temperatures the electrolytes had to be kept under humidified conditions of 3.1×10^{-3} atm. There are several major drawbacks to using $CsHSO_4$ as the electrolyte, firstly the electrolyte is soluble in water so water management in the PEMFC would be crucial and limit the operating life time of the fuel cell, secondly producing an ultra-thin electrolyte with no grain boundaries is currently not possible, the thinnest reported was approximately 1 mm, when ideally the thickness would be 30 μm. Thirdly the decomposition product is sulfur dioxide which would poison the Pt electrocatalysts.

More recently Caesium hydrogen phosphate (CsH_2PO_4) was shown to overcome some of the limitations of caesium hydrogen sulphate.[46] The solid acid electrolyte was thermally stable under both oxidative and reductive environments, with no decomposition products, which are poisonous to the electrocatalysts. The electrolyte

was made into films 260 μm, although this is still too thick for PEMFC applications, a schematic for a MEA based on a CsH_2PO_4 electrolyte is shown in Fig. 1.15, along with the dimensions of the components. Again the fuel stream must be kept humidified (ca. 0.3 atm) to prevent electrolyte dehydration. The disadvantage of caesium hydrogen phosphate was the superprotonic phase occurs at 238 °C, although it has a higher decomposition temperature than caesium hydrogen sulfate. Electrolytes of 25 μm thickness supported on porous stainless steel gas diffusion electrodes have been reported in the literature that have a power density of 415 mW cm^{-2} at 240 °C.[47]

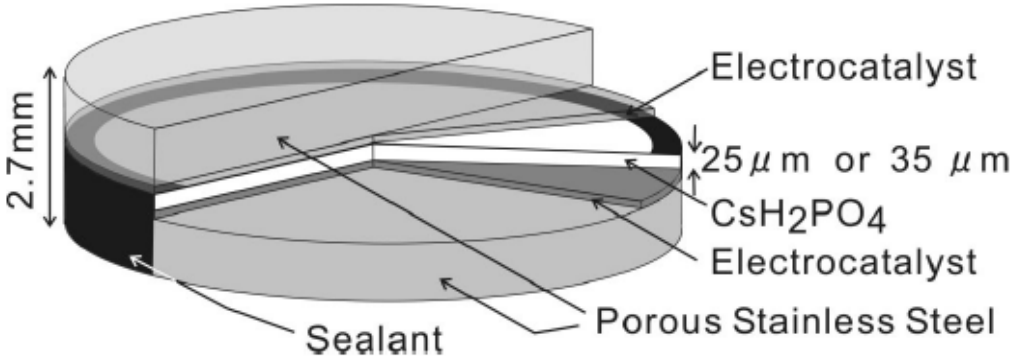

Fig 1.15. Schematic of Caesium hydrogen phosphate MEA from ref 47

However, using caesium hydrogen phosphate does not overcome all the problems of caesium hydrogen sulfate. CsH_2PO_4 is partially soluble in water, which like $CsHSO_4$ means water management is crucial in fuel cells using this electrolyte. Secondly CsH_2PO_4 has an even higher temperature for the superprotonic phase (238 °C), which means cold start up of the PEMFC would be impossible without a considerable secondary power source to be used for the power application and simultaneously heating up the PEMFC to the required operating temperature. These problems severely impact the suitably of solid acid electrolytes for fuel cell applications.

1.5 Polyurethane Formation, Properties and Hybrid Polyurethane PEMs

In the present work, PEMs were based on hybrid inorganic/organic polyurethane (PU) polymers with covalently bound phosphonic acid groups. The use of hybrid PUs as the basis of a PEM for a PEMFC has been discussed in the literature for over 10 years, however in all instances to date the protogenic group has not been covalently bound into the polymer matrix and the highest proton conductivity reported above 100 °C was 5

mS cm^{-1} at 110 °C and 100% RH. In this section the formation of a urethane bond and polyurethane polymer is described, as well as the properties of PUs along with the synthesis and the proton conductivities of hybrid PU PEMs in the literature also being briefly discussed.

1.5.1 Polyurethanes (PUs)

PUs are formed in a stepwise reaction typically using monomers containing diols and diisocyanates, although higher polyols and polyisocyanates can be used to form a more cross linked and rigid polymer. The reaction only requires heat to proceed, although in commercial synthesis, catalysts are often employed to increase the rate of reaction and to lower the temperature required for the reaction to occur. The most common catalyst used in PU formation is DABCO (1,4-diazabicyclo[2.2.2]octane). The formation of urethane and polyurethane bonds are shown in Fig. 1.16, whilst the proposed mechanism of the non-catalysed and catalysed urethane bond formation are given in Figs. 1.17 and 1.18, respectively.

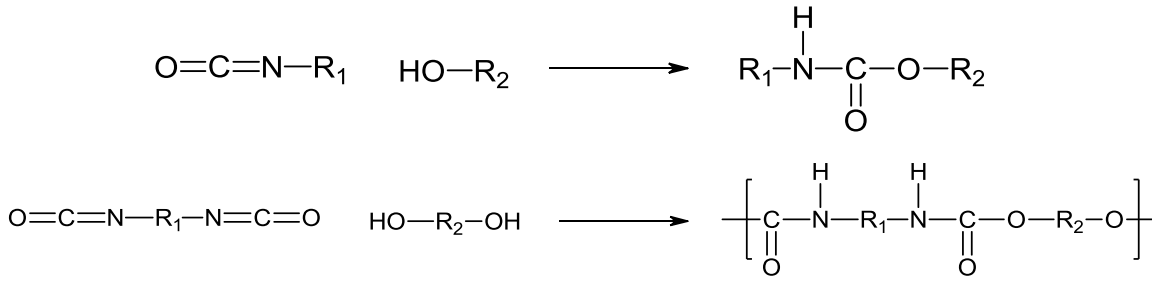

Fig. 1.16. Synthesis of a urethane and polyurethane

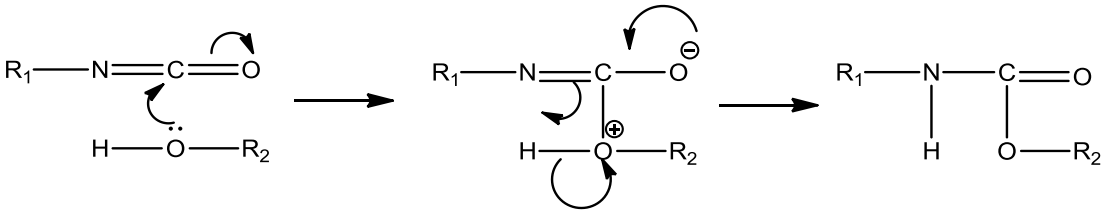

Fig. 1.17. Proposed mechanism for urethane bond formation

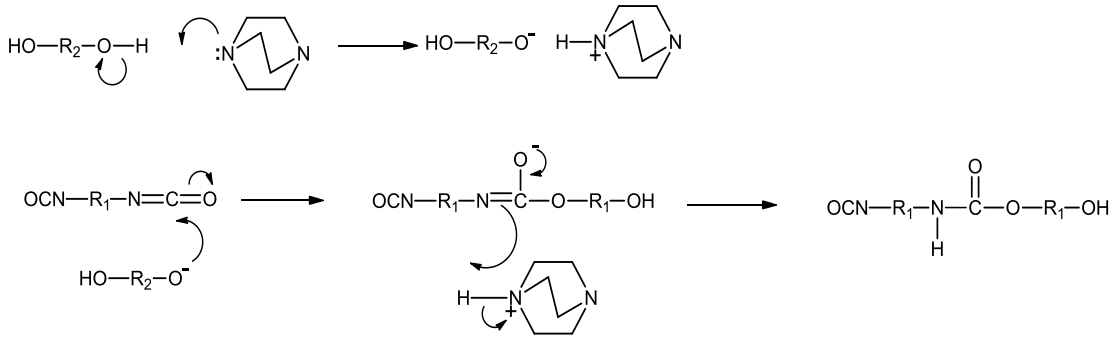

Fig. 1.18. Urethane bond formed using DABCO catalyst

Generally the diols used are polyethers such as polyethylene glycol, polypropylene glycol and polytetrahydrofuran and the diisocynates used are 4,4'-methylenediphenyl diisocyanate (MDI), 2,4'-methylenediphenyl diisocyanate (2,4'-MDI), 2,4-toulene diisocyanate (TDI) and 1,6-diisocyanatohexane. A list of common diol and diisocyanates precursors along with chemical structures is given in Table 1.2.

Table 1.2: PU precursors

Precursor	Structure
Polyethylene glycol (**PEG**)	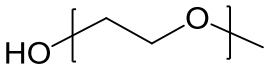
Polypropylene glycol (**PPG**)	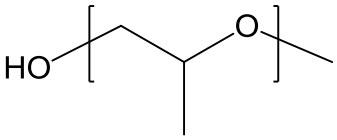
Polytetrahydrofuran (**PTHF**)	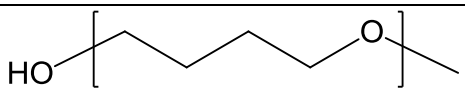
4,4'-methylenediphenyl diisocyanate (**MDI**)	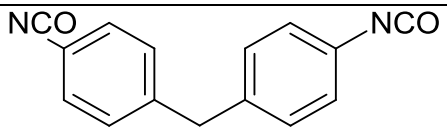
2,4'-methylenediphenyl diisocyanate (**2,4'-MDI**)	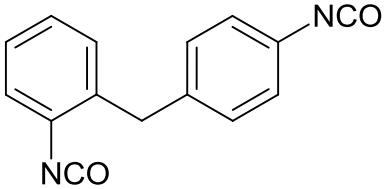

2,4-toluene diisocyanate (**TDI**)	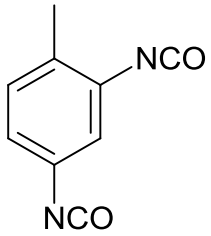
1,6-diisocyanatohexane (**HDI**)	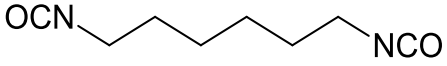

PEG is synthesised by the polymerisation of ethylene oxide. This can be achieved by free radical and ionic initiation and propagation steps, but typically commercial PEG uses the ionic synthetic route as the free radical route can lead to a high degree of branching and less control of the end PEG molecular weight (MW).

PPG is synthesized by polymerisation of propylene oxide in the presence of an initiator and a base. Commercial PPG synthesis uses ethylene glycol as the initiator and potassium hydroxide as the base. If a higher polyol is used as the initiator (e.g. glycerol) the resulting polymer is branched. Using a simple base (KOH) results in random orientation of the pendant methyl chain, thus the polypropylene glycol is atactic.

PTHF is synthesised by acid catalytic ring opening and step-wise addition of tetrahydrofuran. The acid catalysts used are typically trifluoromethanesulfonic acid, fluorosulfonic acid or chlorosulfuric acid.

MDI and 2,4'-MDI are synthesised from the phosgenation of methylene dianiline. The ratio of each isomer is determined by the purity of the starting amine, and these can then be purified to pure MDI and 2,4'-MDI. Recently, investigations into new synthetic routes to produce MDI without the use of phosgene have been carried out, with methyl carbamate and dimethyl carbamate shown to be promising candidates, although heavy metal (Pb) catalysts are required.

TDI is synthesised in a similar fashion to MDI. Toluene is nitrated with nitric and sulfuric acid to produce 2,4-dinitrotoluene, which in turn is hydrogenated into 2,4-diaminetoluene. 2,4-Diaminetoluene is then reacted with phosgene to produce pure 2,4-toluene diisocyanate. HDI is synthesised from the phosgenation of hexamethylene diamine.

On exposure to sunlight, aromatic containing PUs discolours, although this generally does not affect the properties. To avoid discolouration in applications, where this would not be acceptable (e.g. for material coatings), aliphatic diisocyanates are used instead.

For synthesis of flexible and elastomeric polyurethanes, the PU is typically comprised of soft and hard segments. The soft segments are high MW diols (100 kDa – 10 MDa), which are used in tandem with hard segments, such as aromatic diisocyanates or multiple aromatic diisocyanates, with low MW diols used as spacers. The flexibility and elasticity is due to the soft segments uncoiling and the tear resistance is due to the hard segments, as represented in Fig. 1.19.

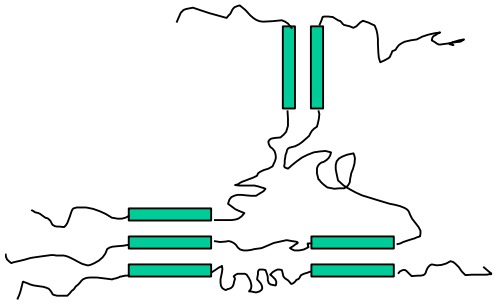

Fig. 1.19 Schematic representation of a PU polymer, filled boxes represent hard segments and lines soft segments

PU polymers exhibit two main types of intermolecular forces, these are hydrogen bonding and π-π stacking. There is extensive hydrogen bonding between the polyether components and the urethane segments in the membrane between chains. When saturated with water the hydrogen bonding between the polymer segments decreases.

There is also extensive π-π stacking between the hard aromatic rings. This stacking still occurs at high water saturation, as the aromatic rings are hydrophobic, this prevents water molecules from moving between the two aromatic rings. However this π-π stacking is not thermally stable.

An additional form of intermolecular bonding can be introduced by free-radical reactions, as represented in Fig. 1.20. This is achieved by immersing or boiling the polymer in an organic peroxide. The suggested preferred position for coupling is on the methylene position between the two phenyl rings in MDI. This type of cross-linking has the advantage of being both chemically and thermally stable.

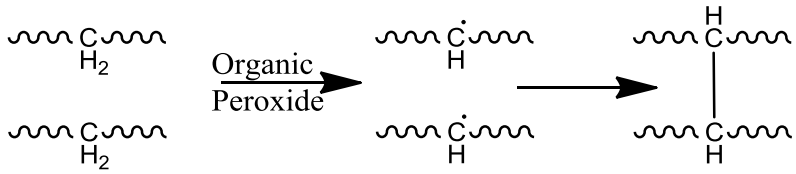

Fig. 1.20. Peroxide radical initiated cross-linking

Inorganic hybrid PUs were originally synthesised by reacting 3-aminopropyltriethoxysilane with residual isocyanates in the PU polymer[48] to investigate whether incorporation of inorganic cross linking affected the gas permeability of the polymer. The reaction proceeds in a similar manner to that of an alcohol. Once this coupling is complete, the silane is hydrolysed to form a siloxane, which in turn is condensed to form additional Si-O-Si linkages. It was found that the incorporation of inorganic components had no apparent affect on the gas permeability of the polymer.

1.5.2 Hybrid PU PEMs

Honma *et al.* reported the synthesis of a new class of hybrid PEMs using a PEG polyurethane/silica polymer matrix with a surfactant, monododecylphosphate (MDP) as the proton source.[49,50] The incorporation of other inorganic network formers was explored by the addition of monophenyltriethoxysilane (MPTS) to the prepolymer polymer matrix.

To synthesise the membranes, the end-capped PEG prepolymer was first formed by mixing the PEG (MW 200, 300, 400, 600, 1000 or 2000) and 3-(triethoxysilyl)propyl isocyanate (TSPI) in a 1:2 (mol/mol) ratio, under continuous stirring for 5 days at 70 °C in a nitrogen environment. Separately MTPS (0.2 g) was dissolved in THF (0.2 g). This was then dispersed in isopropanol (2 g) and the desired amount of MDP was added whilst stirring to this solution. The desired amount of PEG end-capped prepolymer was then added, whilst stirring (the combined mass of the prepolymer and MTPS was kept at 2 g). To this a small volume of dilute HCl was added as a catalyst to hydrolyse the alkoxysilanes, and after 30 seconds of stirring the polymer solution was cast onto polystyrene petri dishes and annealed at 60 °C for 12 hours to evaporate solvent and condense the hydroxysilyl groups. After this time, the free standing membrane was removed from the petri dish and further annealed at 100 °C in nitrogen to promote

further condensation to obtain a more cross linked membrane and improved mechanical stability. The amount of MDP was increased as a weight ratio with respect to the membrane, from 20 to 40% mass (MDP % = mass MDP/(mass prepolymer + mass MPTS). The optimal PEG MW was reported to be 600.

Proton conductivity was determined by A.C. impedance spectroscopy using a Solartron 1260 FRA, with a frequency range of 2 MHz to 1 Hz, in a normal cell configuration. The conductivity of a 40% (w/w) MDP membrane was measured as a function of RH at 110 °C; it was found that conductivity dramatically reduced under 75% RH. At 100% RH the proton conductivity was around 1×10^{-3} S cm^{-1} and below 75% RH the conductivity was *ca*. 1×10^{-6} S cm^{-1}. For the 30% MDP membrane, the conductivity at 110 °C and 100% RH was *ca*. 6×10^{-4} S cm^{-1} and the conductivity of the 20% MDP membrane at 110 °C and 100% RH was 1.5×10^{-4} S cm^{-1}. Due to the relatively low conductivities observed at high temperatures, coupled with the fact that the surfactant acid, MDP, would leach out of the PEM during use in a PEMFC, this would reduce the already low proton conductivity of the PEM and hence lower the efficiency of the PEMFC over the lifetime of use. Hence, these membranes are unsuitable for use in actual PEMFCs.

The use of phosphotungstic acid (PWA) instead of MDP was also reported.[50] Membranes containing 10% to 40% (w/w) PWA were synthesised. For PWA containing membranes no catalytic HCl was needed during membrane synthesis and the PWA was effectively immobilised in the polymer matrix due to the size of the molecule, limiting the problem of acid group leaching. Moreover the proton conductivities for the 10% (w/w) and 40% (w/w) PWA membranes at 110 °C and 100% RH were 2×10^{-3} S cm^{-1} and 9×10^{-4} S cm^{-1} respectively, however at 80 °C the conductivities were 5×10^{-3} S cm^{-1} and 4×10^{-3} S cm^{-1} respectively. Although the PWA and MDP membranes have similar conductivities (2×10^{-3} S cm^{-1} and 1×10^{-3} S cm^{-1}) respectively, this was surprising as both phosphonic acids contain one phosphonic acid group but a large difference in MW, a 40% w/w MDP membrane would contain significantly more phosphonic acid groups than a 40% w/w PWA membrane. This suggests that whilst the phosphonic acid groups are important to proton conductivity, other factors are equally important, such as the mode of proton transport which is determined by water uptake and diffusion, which is influenced by the choice of protogenic group.

Lin and Thangamutha reported the use of a PEG polyurethane/silica polymer matrix with a sulfonic acid surfactant, 4-dodecylbenzene sulfonic acid (DBSA).[51] The membranes were synthesised as above (Honma *et al*[49]). These membranes showed similar conductivities to those containing MDP, and no discernable difference in membrane properties was reported.

Ma *et al*. reported the use of a membrane containing PEG polyurethane/silica polymer matrix with partially phosphorylated polyvinyl alcohol as the proton donor moiety.[52] The membranes were synthesised as described by Honma.[49] Using partially phosphorylated polyvinyl alcohol, conductivities of up to 1.7×10^{-3} S cm^{-1} at 160 °C were reported, although these authors state that the membrane conductivities were performed in a humidified air flow, they did not state specifically what the humidity conditions were. The relatively high conductivities reported at 160 °C were attributed to the PEG acting as the proton solvent at low water contents.

1.6 Conclusions

Currently there are no PEMs which meet all the desired targets for use in PEMFCs so new PEMs still need to be developed. Inorganic additives (including silica based additives) have been shown to increase the water retention in Nafion membranes above the optimal 80 °C for unmodified Nafion membranes and it has been suggested that phosphonic acid would also retain water above 100 °C, therefore new PEMs which contain both inorganic components and phosphonic acid have the potential to exhibit the crucial requirement of high conductivity at and above 120 °C.

Chapter 2
Experimental Procedures and Techniques

2.0 Introduction

This chapter details the reaction conditions and reagents used in the synthesis of the components and the PEMs studied in the present work, from the phosphonate ester and its hydrolysis to PEM Types A to F. The casting and curing conditions and set up are also described. An introduction to the main characterisation technique, that of A. C. impedance spectroscopy is given, as well as conductivity cell and environment controlled heating chamber design and set up, along with a brief description to the other experimental techniques used in the present work.

2.1 Phosphonic Acid Ester Syntheses

The reaction scheme of the phosphonic acid ester synthesis is shown in Fig 2.1.

2.1.1 Synthesis of Dimethylphosphonatoethyltriethoxysilane (5) and 2,4-*Bis*(triethoxysilyl)-1-dimethyl Phosphonatobutane (7) Mixture Using Drop Wise Addition of VTES (Blend 1)

A three neck round bottom flask with an overhead stirrer, gas outlet, dropping funnel and a condenser was connected to a schlenk line, the flask was evacuated and filled with nitrogen gas. Dimethylphosphite (DMP) (45 mL, 0.490 mL) and di-tert butoxide (DTB) were added to the flask and heated to 130 °C and stirred. Once at this temperature vinyl triethoxy silane (VTES) (62 mL, 0.404 mol) was added slowly dropwise over the course of 3 hours, with further DTB (1 mL) added after 2 hours. The reaction mixture was heated for a further 15 hours at 130 °C until the reaction was complete, as determined by ^{1}H NMR (when the vinyl peaks disappeared), the unreacted DMP was removed by distillation under reduced pressure. This gave a mono to bis ratio of 98:2.

2.1.2 Synthesis of Dimethylphosphonatoethyltriethoxysilane (5) and 2,4-*Bis*(triethoxysilyl)-1-dimethyl Phosphonatobutane (7) Mixture Using a One Pot Method (Blend 6)

A three neck round bottom flask with an overhead stirrer, gas outlet and a condenser were connected to a schlenk line, the flask was evacuated and filled with nitrogen gas. VTES (90 mL, 0.588 mol), DMP (43 mL, 0.471 mol) and DTB (3 mL) were added to

the flask. The reaction mixture was then heated to 130 °C and constantly stirred for 18 hours. After the reaction was complete, as determined by ^{1}H NMR (when the vinyl peaks disappeared), the unreacted DMP was removed by distillation under reduced pressure. This gave a mono dimethylphosphonatoethyltriethoxysilane to bis 2,4-*bis*(triethoxysilyl)-1-dimethyl phosphonatobutane ratio of 60:40 (by ^{31}P NMR δ 35, 33).

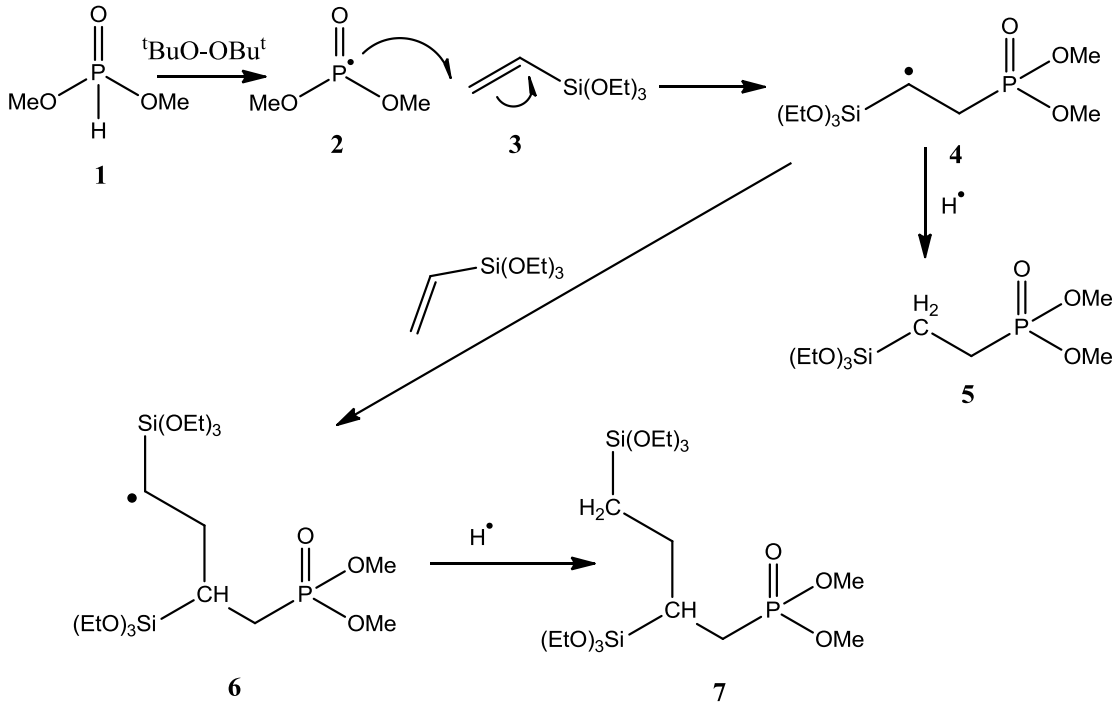

Scheme. 2.1. Synthesis of the phosphonate ester PA precursors, dimethylphosphonatoethyltriethoxysilane (**5**, mono) and 2,4-*bis*(triethoxysilyl)-1-dimethyl phosphonatobutane (**7**, bis).

2.1.3 Blends With Varying Mono Phosphonate Ester to Bis Phosphonate Ester Ratios

Blends of the one pot (Blend 6) and drop wise (Blend 1) phosphonate ester mixtures were made to achieve varying mono to bis ratios between the two extremes of 60:40 to 98:2. To calculate the mass required from each of the Blend 1 and Blend 6 mixtures for a particular blend, the ratio of mono to bis was converted into the mole fractions required from the two components, and then the mass from each mixture (as given in Table 2.1) was combined to create the desired mono to bis ratio.

Table 2.1. Masses (g) of blend 1 and blend 6 ester mixtures required to make desired blends of intermediate mole ratios of mono:bis

Blend	Mole % Mono Required in Blend	Blend 6 (g)	Blend 1 (g)
1	98	0	1
2	96	1	4
3	94	1	3
4	90	1	0.9
5	80	1	0.25
6	60	1	0

2.2 Phosphonate Ester Hydrolysis

Four methods were employed in this project to hydrolyse the phosphonate ester to the phosphonic acid.

2.2.1 Method 1

Dimethylphosphonatoethyltriethoxysilane and 2,4-*bis*(triethoxysilyl)-1-dimethyl phosphonatobutane (Blend 1, 100 mL), prepared as in the blend 1 process above, was placed in a two-neck round bottomed flask with HCl (6 M, 100 mL) and refluxed at 110 °C for 24 hours. After this period, the volume was reduced under reduced pressure, and methanol (100 mL) was added; this mixture was concentrated again and then redispersed in MeOH (100 mL). This process was repeated, and the phosphonate ester was dispersed in MeOH (100 mL). A 2 mL aliquot of this solution was then dried overnight to obtain the mass of phosphonic acid dispersed in 1 mL of methanol (ρ 0.33 g mL^{-1}).

2.2.2 Method 2

Dimethylphosphonatoethyltriethoxysilane and 2,4-*bis*(triethoxysilyl)-1-dimethyl phosphonatobutane (Blend 1, 100 mL), prepared as in the blend 1 process above, was placed in a two-neck round bottomed flask with HCl (6 M, 100 mL) and refluxed at 110 °C for 24 hours. After this period, the volume was reduced under reduced pressure, and methanol (100 mL) was added; this mixture was concentrated again and then redispersed in MeOH (100 mL). This process was repeated, but deionised water (100 mL) was used in place of methanol for the redispersion step. A 2 mL aliquot of this solution was then dried overnight to obtain the mass of phosphonic acid dispersed in 1 mL of water (ρ 0.30 g mL^{-1}).

2.2.3 Method 3

Dimethylphosphonatoethyltriethoxysilane and 2,4-*bis*(triethoxysilyl)-1-dimethyl phosphonatobutane (Blend 1) (100 mL) was placed in a two-neck round bottomed flask with HCl (6M, 100 mL). The reaction mixture was refluxed for 2 h and then the methanol produced was distilled out with a Dean-Stark trap. When the temperature of the mixture reached 104-108 ºC, the Dean-Stark was disconnected and the volume of methanol extracted was replaced with HCl (6 M). The reaction mixture was then refluxed for an additional 6 h at 115 °C. After this period, the volume was reduced under reduced pressure, and methanol (100 mL) was added; this mixture was concentrated again and then redispersed in MeOH (100 mL). This process was repeated, but deionised water (100 mL) was used in place of methanol for the redispersion step. A 2 mL aliquot of this solution was then dried overnight to obtain the mass of phosphonic acid dispersed in 1 mL of water (ρ 0.30 g mL^{-1}).

2.2.4 Method 4

Ethyl dimethylphosphonate trimethoxy silane and 2,4-*bis*(triethoxysilyl)-1-dimethyl phosphonatobutane (Blend 1) (100 mL) was placed in a two-neck round bottomed flask with HCl (6M, 200 mL) and refluxed at 120 °C for 24 hours. After this period, the volume was reduced under reduced pressure, and methanol (100 mL) was added; this mixture was concentrated again and then redispersed in MeOH (100 mL). This process was repeated, but deionised water (100 mL) was used in place of methanol for the redispersion step. A 2 mL aliquot of this solution was then dried overnight to obtain the mass of phosphonic acid dispersed in 1 mL of water (ρ 0.30 g mL^{-1}).

To hydrolyse blends 2 to 6, the same procedures were used as blend 1, just replacing blend 1 with the desired blend

2.2.5 Determination of the Extent of Hydrolysis

In all cases the degree of hydrolysis was determined by comparison of the ^{31}P NMR spectra. Measurements were performed on a JEOL 270 FT-NMR spectrometer; ^{31}P NMR spectra were collected at a frequency of 109.13 MHz. To determine the extent of acid hydrolysis in the PA during hydrolysis of the ester mixture as function of time and temperature, an aliquot (*ca.* 1 mL) of PA solution was removed from the reaction

mixture using a syringe. This sample was placed in a glass vial and heated in an oven at 100 ºC overnight. Once cooled, a portion of the glass was crushed in a mortar (cryo-grinding with liquid nitrogen when required) using a pestle. The crushed and ground glass was transferred to a sample vial and 2 mL of NaOH solution (14 M) was added. The glass was then digested by heating the solution moderately (*ca*. 50 ºC) for about 30 minutes. The solution was then transferred into a NMR tube for analysis.

2.3.1 PEM Type A Synthesis

2.3.1.1 PEG 200

3-(Triethoxysilyl)propyl isocyanate (TSPI) (Sigma-Aldrich, 95%, 2 g, 8 mmol) was placed in a dried flask filled with nitrogen. To this PEG (Alfa Aesar, MW 200, 0.8 g, 4 mmol) was added. The reaction mixture was heated at 70 °C and stirred gently for five days to produce the desired silyl end capped prepolymer. To make the 0% PA membrane, the polymer matrix was hydrolysed by adding HCl (1 M, 1 mL). To make the membranes containing PA, the PA blend was added in the amount stated in Table 2.2.

2.3.1.2 PEG 400-1000

TSPI (Sigma-Aldrich, 95%, 1 g, 4 mmol) was placed in a dried flask filled under nitrogen. To this PEG (Alfa Aesar, MW 400, 600 or 1000, 2 mmol) was added. The reaction mixture was heated at 70 °C and stirred gently for five days to produce the desired silyl end capped prepolymer. To make the 0% PA membranes, the polymer matrix was hydrolysed by adding HCl (1 M, 1 mL). To make the membranes containing PA, the PA was added in the type and amount stated in Table 2.2.

2.3.2 PEM Type B Synthesis

NMP (99%, 20 mL) was placed in a dried flask filled with nitrogen. To this, TSPI (95%, 1.5 g, 6 mmol) and PEG (MW 100, 200, 400 600 or 1000, 6 mmol) were added. The solution was heated to 70 °C and stirred slowly. After 3 hours, MDI (99%, 0.75 g, 3 mmol) was added and the reaction mixture was stirred for an additional 3 hours to produce the desired silyl end capped prepolymer. To make the 0 % PA membranes, the polymer matrix was hydrolysed by adding HCl (1 M, 1 mL). As indicated in Table 2.2, membranes that were prehydrolysed (PH) had HCl (1 M, 1 mL) added just prior to the

addition of PA. The volume, blend and hydrolysis method of the PA added is also given in Table 2.2.

2.3.3 PEM Type C Synthesis

NMP (99%, 20 mL) was placed in a dried flask filled with nitrogen. To this, TSPI (95%, 1.5 g, 6 mmol) and PEG (MW 200, 400 or 600, 6 mmol) were added. The solution was heated to 70 °C and stirred slowly. After 3 hours hexamethylene diisocyanate (HDI, 95%, 0.50 g, 3 mmol) was added, and the reaction mixture was stirred for an additional 3 hours to produce the desired silyl end capped prepolymer. To make the 0% PA membranes, the polymer matrix was hydrolysed by adding HCl (1 M, 1 mL). The membranes containing PA were all first prehydrolysed by the addition of HCl (1 M, 1 mL) prior to the addition of PA. The volume of PA added is given in Table 2.2.

2.3.4 PEM Type D Synthesis

PEG (denoted as PEG 1 in Table 2.2) (MW 200, 400 or 600, 3 mmol) and MDI (1.5 g, 6 mmol) were placed in NMP (20 mL) and heated to 70 °C and stirred gently for 3 hours. Simultaneously, TSPI (1.5 g, 6 mmol) and PEG (denoted as PEG 2 in table 2.2) (MW 200, 400 or 600, 6 mmol) were heated to 70 °C and stirred gently for 3 hours. After this time the reaction mixtures were combined and stirred for an additional 3 hours at 70 °C to produce the desired silyl end capped prepolymer. To make the 0% PA membranes, the polymer matrix was hydrolysed by adding HCl (1 M, 1 mL). Where indicated in Table 2.2, membranes that were prehydrolysed (PH) had HCl (1 M, 1 mL) added just prior to the addition of PA. The volume, blend and hydrolysis method of the PA added is also given in Table 2.2. For the membranes that were made with Glysil and TEOS as additional network formers, the Glysil and TEOS were added, whilst continuously being stirred, one minute prior to the addition of PA.

2.3.5 PEM Type E Synthesis

TSPI (2 g, 8 mmol) was placed in a dried flask filled with nitrogen. To this, polypropylene glycol (PPG, Alfa Aesar, MW 400 or 1000, 4 mmol) was added. The reaction mixture was heated at 70 °C and stirred gently for five days to produce the desired silyl end capped prepolymer. To make the 0% PA membranes, the polymer matrix was hydrolysed by adding HCl (1 M, 1 mL). The membranes containing PA

were all first prehydrolysed by the addition of HCl (1 M, 1 mL) prior to the addition of PA. The volume of PA added is given in Table 2.2.

2.3.5 PEM Type F Synthesis

TSPI (2 g, 8 mmol) was placed in a dried flask filled with nitrogen. To this polytetrahydrofuran (PTHF, Sigma-Aldrich, MW 250, 650 or 1000, 4 mmol) was added. The reaction mixture was heated at 70 °C and stirred gently for five days to produce the desired silyl end capped prepolymer. To make the 0% PA membranes, the polymer matrix was hydrolysed by adding HCl (1 M, 1 mL). The membranes containing PA were all first prehydrolysed by the addition of HCl (1 M, 1 mL) prior to the addition of PA. The volume of PA added is given in Table 2.2.

Table 2.2 List of PEMs and PA volumes added

Membrane Number	PEG MW	PA Blend	Hydrolysis Method	PA Volume Added / mL	Additional Notes	PA Loading % w/w
Type A						
001	200	-	-	-	-	0
002	200	1	2	1.0	-	10
003	200	1	2	1.8	-	16
004	200	1	2	2.3	-	20
005	200	1	2	2.9	-	24
006	200	1	2	4.0	-	30
007	200	1	2	6.2	-	40
008	200	1	2	9.3	-	50
009	200	1	2	14	-	60
010	400	-	-	-	-	0
011	400	1	2	0.3	-	5
012	400	1	2	0.7	-	10
013	400	1	2	1.1	-	15
014	400	1	2	1.5	-	20
015	400	1	2	2.6	-	30
016	400	1	2	4.0	-	40
017	400	1	2	6.0	-	50
018	400	1	2	9.0	-	60
019	600	-	-	-	-	0
020	600	1	2	0.4	-	5
021	600	1	2	0.8	-	10
022	600	1	2	1.3	-	15
023	600	1	2	1.8	-	20
024	600	1	3	1.6	-	20

Table 2.2 Continued

025	600	1	2	3.1	-	30
026	600	1	3	2.8	-	30
027	600	1	2	4.9	-	40
028	600	1	3	4.5	-	40
029	600	1	2	7.3	-	50
030	600	1	3	6.6	-	50
031	600	1	2	11	-	60
032	600	1	3	10	-	60
033	600	1	2	17	-	70
034	1000	1	-	-	-	0
035	1000	1	2	1.1	-	10
036	1000	1	2	2.5	-	20
037	1000	1	2	4.3	-	30
038	1000	1	2	6.7	-	40
039	1000	1	2	10	-	50

Type B

Membrane Number	**PEG MW**	**PA Blend**	**Hydrolysis Method**	**PA Volume Added / mL**	**Additional Notes**	**PA Loading % w/w**
040	100	-	-	-	-	0
041	100	1	3	1.1	-	10
042	100	1	3	2.4	-	20
043	100	1	3	4.1	-	30
044	100	1	3	4.7	-	33
045	100	1	3	5.2	-	35
046	200	-	-	-	-	-
047	200	1	3	0.6	-	5
048	200	1	3	0.6	PH	5
049	200	1	3	1.3	-	10
050	200	1	3	1.3	PH	10
051	200	1	3	2.0	-	15
052	200	1	3	2.0	PH	15
053	200	1	3	2.9	-	20
054	200	1	3	2.9	PH	20
055	200	2	2	2.9	-	20
056	200	2	3	2.9	-	20
057	200	2	4	2.9	-	20
058	200	3	3	2.9	-	20
059	200	1	3	3.8	-	25
060	200	1	3	3.8	PH	25
061	200	1	3	4.9	-	30
062	200	1	3	4.9	PH	30
063	200	1	3	5.7	-	33
064	200	1	3	5.7	PH	33
065	200	1	4	5.7	-	33
066	200	1	4	5.7	PH	33
067	200	1	2	5.7	-	33

Table 2.2 Continued

068	200	1	2	5.7	PH	33
069	200	2	4	5.7	-	33
070	200	2	4	5.7	PH	33
071	200	1	3	6.2	-	35
072	200	1	3	6.2	PH	35
073	200	1	3	7.7	-	40
074	200	1	3	7.7	PH	40
075	200	1	3	9.4	-	45
076	200	1	3	9.4	PH	45
077	200	1	3	11.5	-	50
078	200	1	3	11.5	PH	50
079	400	-	-	-	-	0
080	400	1	3	1.7	-	10
081	400	1	3	2.8	-	15
082	400	1	3	3.9	-	20
083	400	1	3	6.6	-	30
084	400	1	3	7.6	-	33
085	400	1	3	8.3	-	35
086	600	-	-	-	-	0
087	600	1	3	2.2	-	5
088	600	1	3	3.6	-	10
089	600	1	3	4.2	-	15
090	600	1	3	4.9	-	20
091	600	1	3	8.4	-	30
092	600	1	3	9.6	-	33
093	600	1	3	10.5	-	35
094	1000	-	-	-	-	0
095	1000	1	3	3.1	-	10
096	1000	1	3	4.9	-	15
097	1000	1	3	6.9	-	20
098	1000	1	3	11.8	-	30
099	1000	1	3	13.5	-	33
100	1000	1	3	14.8	-	35

Type C

Membrane Number	**PEG MW**	**PA Blend**	**Hydrolysis Method**	**PA Volume Added / mL**	**Additional Notes**	**PA Loading % w/w**
101	200	-	-	-	-	0
102	200	1	3	1.2	PH	10
103	200	1	3	2.7	PH	20
104	200	1	3	4.6	PH	30
105	200	1	3	5.3	PH	33
106	400	-	-	-	-	0
107	400	1	3	1.6	PH	10
108	400	1	3	3.7	PH	20
109	400	1	3	6.3	PH	30
110	400	1	3	7.2	PH	33

Table 2.2 Continued

111	600	-	-	-	-	0
112	600	1	3	2.1	PH	10
113	600	1	3	4.7	PH	20
114	600	1	3	8.0	PH	30
115	600	1	3	9.2	PH	33

Type D

Membrane Number	**PEG 1 MW**	**PEG 2 MW**	**PA Blend**	**Hydrolysis Method**	**PA Volume Added / mL**	**Additional Notes**	**PA Loading % w/w**
116	200	200	-	-	-	-	0
117	200	200	1	3	1.8	-	10
118	200	200	1	3	2.8	-	15
119	200	200	1	3	4.0	-	20
120	200	200	1	3	5.3	-	25
121	200	400	-	-	-	-	0
122	200	400	1	3	2.0	-	10
123	200	400	1	3	3.2	-	15
124	200	400	1	3	4.6	-	20
125	200	400	1	3	6.1	-	25
126	200	600	-	-	-	-	0
127	200	600	1	3	2.2	-	10
128	200	600	1	3	3.5	-	15
129	200	600	1	3	5.0	-	20
130	200	600	1	3	6.7	-	25
131	400	200	-	-	-	-	0
132	400	200	1	3	2.2	-	10
133	400	200	1	3	3.5	-	15
134	400	200	1	3	5.0	-	20
135	400	200	1	3	6.7	-	25
136	400	400	-	-	-	-	0
137	400	400	1	3	2.4	-	10
138	400	400	1	3	3.9	-	15
139	400	400	1	3	5.5	-	20
140	400	400	1	3	7.3	-	25
141	400	600	-	-	-	-	0
142	400	600	1	3	2.7	-	10
143	400	600	1	3	4.4	-	15
144	400	600	1	3	6.0	-	20
145	400	600	1	3	8.0	-	25
146	600	200	-	-	-	-	0
147	600	200	1	3	2.7	-	10
148	600	200	1	3	4.2	-	15
149	600	200	1	3	4.5	TEOS (0.5 g)	15
150	600	200	1	3	4.5	Glysil (0.5 g)	15
151	600	200	1	3	6.0	-	20
152	600	200	1	3	8.0	-	25
153	600	400	-	-	-	-	0

Table 2.2 Continued

154	600	400	1	3	2.9	-	10
155	600	400	1	3	4.6	-	15
156	600	400	1	3	6.5	-	20
157	600	400	1	3	8.7	-	25
158	600	600	-	-	-	-	0
159	600	600	1	3	3.1	-	10
160	600	600	1	3	4.9	-	15
161	600	600	1	3	7.0	-	20
162	600	600	1	3	9.3	-	25

Type E

Membrane Number	**PPG MW**	**PA Blend**	**Hydrolysis Method**	**PA Volume Added / mL**	**Additional Notes**	**PA Loading % w/w**
163	400	-	-	-	-	0
164	400	1	3	1.3	PH	10
165	400	1	3	3.0	PH	20
166	400	1	3	5.1	PH	30
167	400	1	3	5.9	PH	33
168	1000	-	-	-	-	0
169	1000	1	3	2.2	PH	10
170	1000	1	3	5.0	PH	20
171	1000	1	3	8.6	PH	30
172	1000	1	3	9.9	PH	33

Type F

Membrane Number	**PTHF MW**	**PA Blend**	**Hydrolysis Method**	**PA Volume Added / mL**	**Additional Notes**	**PA Loading % w/w**
173	250	-	-	-	-	0
174	250	1	3	1.1	PH	10
175	250	1	3	2.5	PH	20
176	250	1	3	4.3	PH	30
177	250	1	3	4.9	PH	33
178	650	-	-	-	-	0
179	650	1	3	1.7	PH	10
180	650	1	3	3.8	PH	20
181	650	1	3	6.6	PH	30
182	650	1	3	7.6	PH	33
183	1000	-	-	-	-	0
184	1000	1	3	2.2	PH	10
185	1000	1	3	5.0	PH	20
186	1000	1	3	8.6	PH	30
187	1000	1	3	9.9	PH	33

PH signifies the polymer was prehydrolysed by addition of HCl prior to addition of PA

2.4 Casting and Curing of Polymer Suspension

Four methods were explored for the casting and curing of the polymer suspensions produced in the present work.

2.4.1 Casting on a Perfluoroalkoxy Substrate

The membrane solution was cast onto a thin Perfluoroalkoxy (**PFA**) film, which was attached to a glass sheet for stability, and a PTFE frame clipped on top of the film/glass slide (as shown in Fig. 2.2). The polymer solution was aged for 1 hr at room temperature before being placed in an oven at 100 ºC for at least 16 hrs. The membrane was allowed to cool to room temperature before being removed from the PFA film. This method was unsuccessful for all PEG/PPG and PTHF membrane formulations, as the surface was too hydrophobic for the solution to spread. The resulting membranes curled and were glassy and had inhomogeneous thicknesses so membranes produced were not good enough for testing and evaluation.

Fig. 2.2. Typical PFA substrate casting set up. Glass slide with a PFA film on the surface and a PTFE liner, held in place by clips

2.4.2 Casting on a Polystyrene Substrate

Between 5 mL and 10 mL of neat polymer (not containing NMP as a solvent, *i.e.* polymer matrixes type A, E and F) was cast into sterile polystyrene Petri dishes (5 cm diameter). After curing for one hour at room temperature, the membranes were then heated over night in an oven at 70 °C. The membranes were then allowed to cool to room temperature before they were removed from the polystyrene Petri dish. The

membranes were then placed on a PTFE sheet and placed in the oven at 100 °C for at least six hours. Depending on the volume and density of the polymer solution used, membranes were formed with a wide range of thicknesses, *ca.* 50 – 500 μm. The major limitation to this method of casting was that NMP (and similar solvents) could not be used as it dissolved the polystyrene Petri dishes. NMP dissolves nearly all thermoplastics and is widely used in the polymer industry for this property.

2.4.3 Casting onto a Modified Glass Substrate

This method was similar to that employed to when casting onto a PFA (substrate, but instead of PFA, a modified glass surface was used. The polymer covalently bonded to an unmodified glass surface (condensation reaction) when curing in the oven. The glass surface was modified by replacing the surface hydroxyl groups with hydrophobic octadecyl surface groups.

The modification of the surface was achieved by using the following procedure. The glass sheet was cleaned with warm soapy water, and rinsed well with deionised water; the sheet was then immersed in nitric acid (1M) for 72 hours, removed and rinsed well with deionised water and oven dried for 2 hours. The glass sheet was then immersed in a solution of ocatadecyltrichlorosilane in toluene (2% v/v) for one hour, and then turned over and immersed for another hour. The glass sheet was then removed and washed with copious methanol, followed by warm soapy water, rinsed well with deionised water, and then placed in an oven at 120 ºC for 16 hours. The glass sheet was then allowed to cool and could be used as a casting surface.

When the polymer solution was cast onto the modified glass surface, it spread very well and covered the glass surface. The polymer solution was aged 1 hr before placing in an oven at 100 ºC for at least 16 hrs. The membrane was then allowed to cool down before being carefully removed/peeled from the glass surface (using a microspatula or Stanley knife blade). The advantage of using this technique is that NMP can be used as a solvent, which is essential for membranes containing MDI. The disadvantage of this technique is that the modified glass surface can become scratched or damaged, and this results in surface hydroxyl groups becoming available for cross-linking to the membrane when curing in the oven, which makes it impossible to remove the membrane in one piece.

2.4.4 Casting on a PTFE Substrate

The approach used for casting on PTFE was similar to that of when casting on a PFA and modified glass surface, but instead using a sheet of PTFE (Fig 2.3). This had the advantage of being able to easily remove the membrane from the surface, even if the surface was scratched (*i.e.* damaged). The polymer solution was aged for one hour at room temperature and then placed in an oven at 100 ºC for at least 16 hours. The membranes were allowed to cool before being removed from the surface.

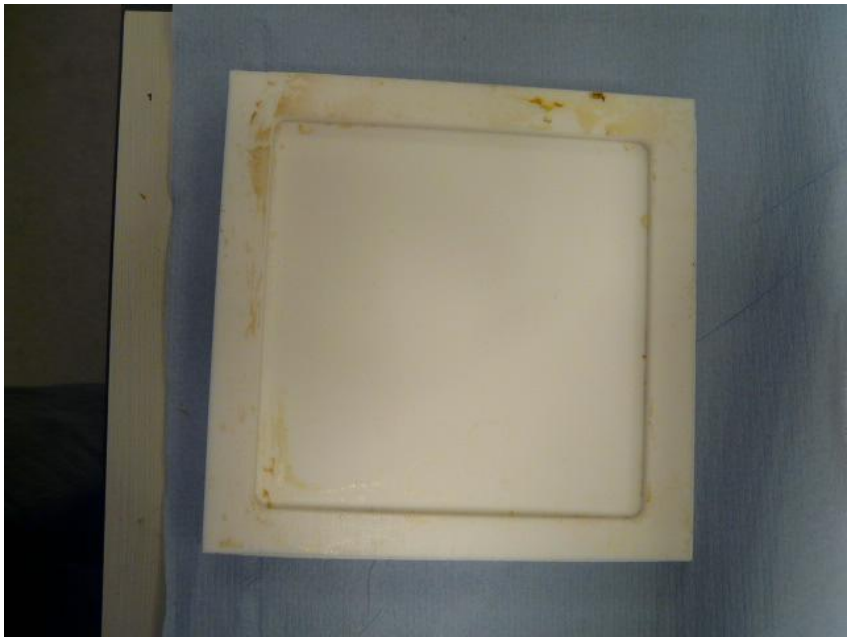

Fig. 2.3. PTFE sheet and lining used for membrane casting, external dimensions 150 mm × 150 mm, internal dimensions 120 mm × 120 mm

2.5 Membrane Conditioning in Preparation for Impedance Measurements

Prior to conductivity measurements, the membranes were conditioned by various methods; these included steaming, immersion and boiling in deionised water.

2.5.1 Steaming

A portion of membrane, *ca*. 2 cm × 2 cm was placed in a standard vegetable steamer containing deionised water and steamed for one hour. After this time the membrane was removed from the steamer and the surface water was removed with filter paper.

2.5.2 Boiling

A portion of membrane, *ca.* 2 cm × 2 cm was placed in a beaker of boiling deionised water and boiled for one hour. After this time the membrane was removed and the surface water was removed with filter paper.

2.5.3 Immersion

A portion of membrane, *ca.* 2 cm × 2 cm was placed in a beaker of deionised water at room temperature. Membranes were left to soak for either 30 minutes, 1 hour, 2 hours, 4 hours or 24 hours. After this time the membrane was removed and the surface water was removed with filter paper.

2.6 Impedance Spectroscopy

2.6.1 Introduction[53]

A. C. impedance spectroscopy (ACIS) is a form of electrochemical measurement. ACIS, by requirement has to use alternating current (AC) and not direct current (DC). In ACIS, the difference in the phase of the applied voltage and current is measured during passage through an electrolyte at different frequencies, hence the need of AC and not DC. From this information, the total resistance of an electrolyte can be determined.

As the frequency of the current is changed, so does the phase difference (θ) (Fig 2.4), and thus the impedance. Thereby, by incrementally changing the frequency over which the phase difference is measured, an impedance spectrum is obtained. In this project, the frequencies at which measurements were made ranged from 1 MHz to 1 Hz.

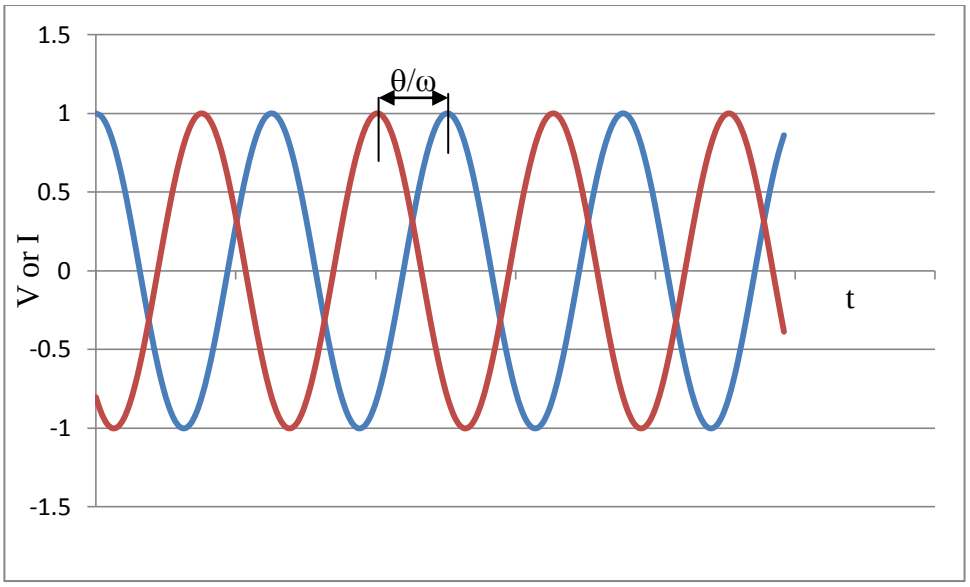

Fig. 2.4. Phase difference θ, between current and voltage at one frequency; blue and red lines represent voltage and current respectively and ω is 2πf

The impedance itself is a complex number, comprising of a real and imaginary component, and these are plotted against each other in an impedance plot. The real component of impedance is labelled *Z*' (which is displayed on the *x*-axis) and the imaginary component of the impedance is labelled Z" (which is displayed on the *y*-axis), equation 2.1 defines the real and imaginary components of the impedance.

$$Z' = |Z| \cos\theta$$
$$Z'' = |Z| \sin\theta \qquad (2.1)$$

Where θ is the phase difference between voltage and current.

When there is no phase difference, θ is 0, then cos (0) = 1 and sin (0) = 0, therefore the impedance is entirely real, and so is due to the resistance, and thus this point of the spectrum can be used to determine the total resistance of the sample.

2.6.2 Ideal Impedance Spectra

The real component, which is shown on the *x*-axis of an impedance spectrum, is related to the resistivity of the system being measured and the *y*-axis of an impedance spectrum is related to the capacitance of the system.

An ideal simple electrolyte system can be modelled by a simple equivalent circuit consisting of a resistor (R) and capacitor (C) connected in parallel as shown in Fig. 2.5. An equivalent circuit is representative of the physical process taking place within the membranes when a current and voltage are applied, and is at best an approximation when the response is linear in behaviour in regard to current and voltage and independent of signal amplitude.

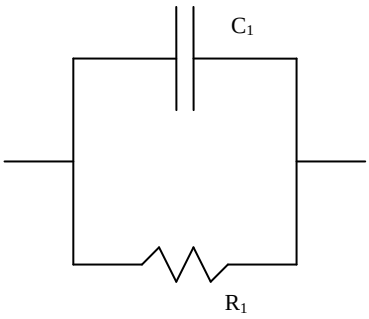

Fig. 2.5 Simple equivalent Circuit with C_1 (capacitance of membrane) and R_1 (resistance of membrane) in parallel as model for the physical process occurring within the PEM

The ideal impedance spectrum of a conductive sample should be represented by a semi-circle as shown in Fig. 2.6, with frequency decreasing from left to right. The resistance is taken as the intercept at low frequency on the *x*-axis, with the high frequency intercept subtracted from this, ideally the intercept at high frequencies should be 0. Due to the fact the electrodes used in this project (stainless steel and platinum) cannot conduct the protons from the electrolyte membrane, there is a blocking spike at low frequencies, and an idealised blocking spike is shown in Fig. 2.7.

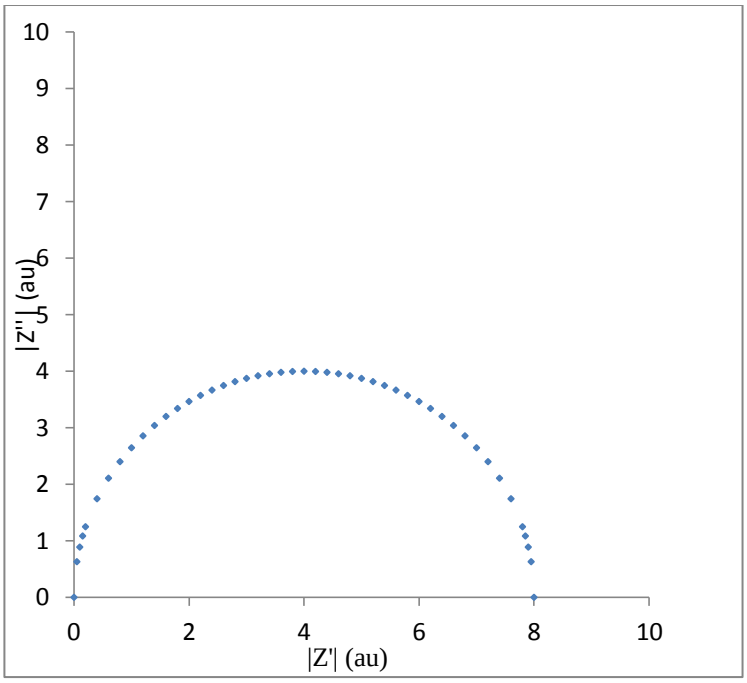

Fig. 2.6. Impedance plot of a simple system as depicted by the equivalent circuit in Fig 2.5

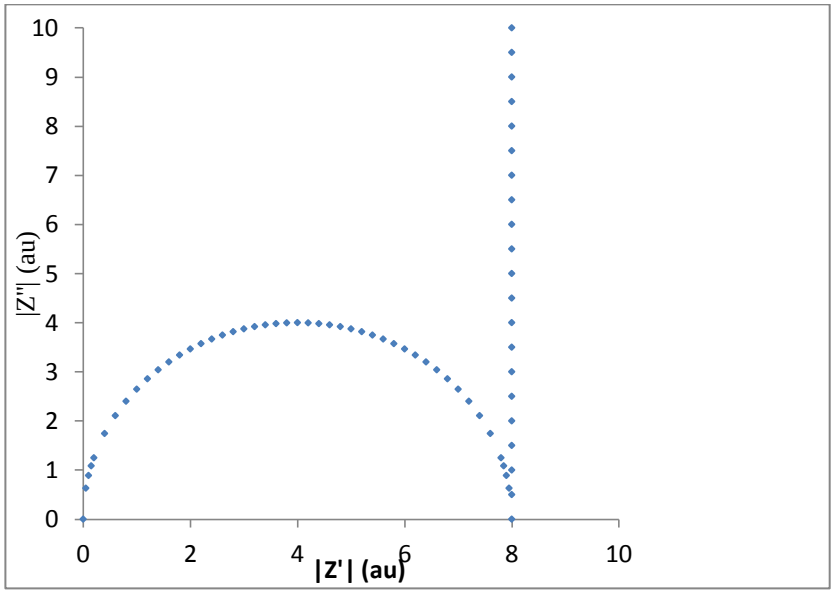

Fig. 2.7. Impedance plot of a simple system with a blocking spike caused by blocking electrodes

Again with an ideal impedance spectrum, the intercept on the Z' axis at low frequencies is taken as the impedance of the electrolyte, as the high frequency intercept should pass through the origin.

In reality, due to the nature of the blocking electrodes at the interface between the electrode and membrane, a double layer dominates the spectra at lower frequencies, and

at slightly higher frequencies non-ideal double capacitance layer responses dominate as shown in Fig. 2.8.

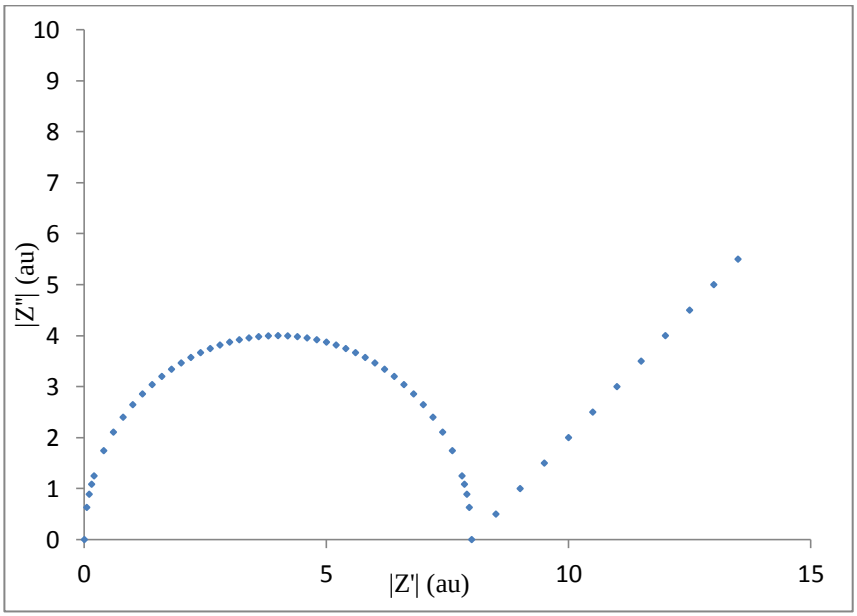

Fig. 2.8 Impedance plot of a simple system with a blocking spike caused by blocking electrodes, the angle of the blocking spike is caused by a double capacitance layer forming at the membrane electrode interface.

2.6.3 Real Impedance Spectra

As is often the case in reality, the actual recorded impedance spectra can substantially differ from that of the idealised spectra and this can be caused by numerous factors, the main causes are given below.

(i) Semi-circle does not go through the origin of the real plane

This can be caused by either $R_{\infty} \neq 0$ or that there is an additional semi-circle at higher frequencies, which cannot be measured/observed due to the frequencies being higher than those available experimentally (above 1 MHz in this work).

(ii) Overlapping semi-circles.

This can be caused by having two process of ionic transport through an electrolyte and could be modelled by more complex equivalent circuits than the one shown in Fig. 2.5.

(iii) Depressed Semi-circles.

The semi-circles observed in this project are depressed in shape rather than full semi-circles. This is due to the nature of proton transport through disordered media. When a structure (such as a ceramic) has a regular repeat unit (cell), the mode of ion transport

throughout the electrolyte is uniform, as such a semi-circle is observed in the impedance spectrum from the electrolyte response. However in disordered medium (such as an amorphous polymer) there are multiple discrete channels through which ion transport can occur, each requiring different (albeit slightly different) energies, thus the overall response, and impedance spectrum, is a combination of all the different pathways, and this makes the semi-circle depressed. When these spectra are modelled, the capacitor element (C) in the equivalent circuit is replaced with a constant phase element (CPE).

(iv) Merged semi-circle and blocking spike.

In impedance spectra the semicircle and blocking spike can merge, an extreme example of which is shown in Fig 2.9. This is due to the response from the electrodes dominating at higher frequencies as well as the lower frequencies. In this situation, the only way to reasonably determine the resistance from the electrolyte is to fit the impedance spectrum to an appropriate equivalent circuit, in this instance, where the electrolyte is a disordered system, the appropriate equivalent circuit would be the "ZARC" which models a depressed semicircle directly as a system which has a distribution of time elements, with an extra CPE element in series to represent the blocking electrode, as represented in Fig 2.10. Typically, if the electrodes were completely smooth/polished, then the extra element would be a capacitor, however due to the slight roughness of the actual electrodes, a CPE would provide the better fit for the spectrum.

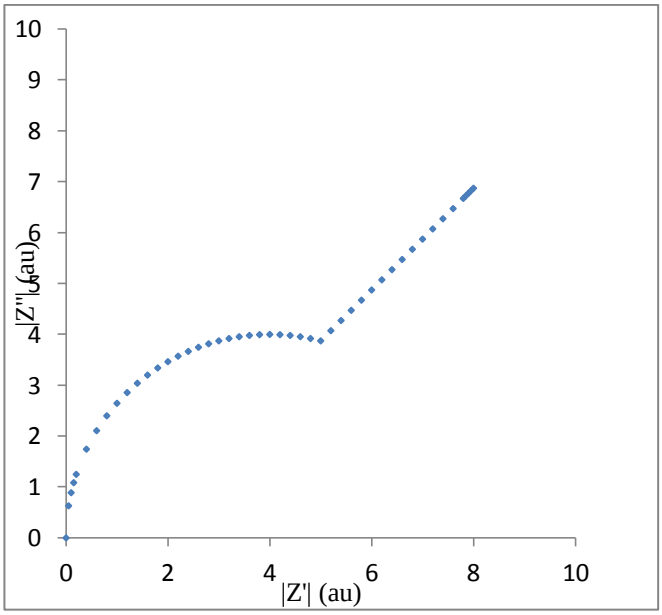

Fig. 2.9. Impedance spectrum where the response from the blocking electrodes dominate the response from the electrolyte at high frequencies

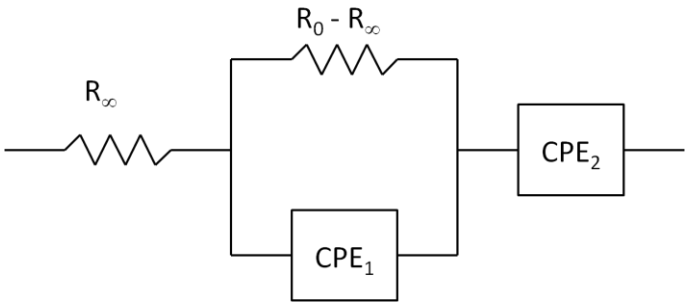

Fig. 2.10. Modified ZARC equivalent circuit for modelling spectra which exhibit behaviour shown in Fig 2.9

(v) Only the end of the semi-circle or only the blocking spike visible.

Often, only the end of the semi-circle or only a blocking spike may be visible on the impedance spectra, an example of which is shown in figure 2.11. In these cases, the bulk of the semi-circle is not visible as the response from this region occurs at a higher frequency than measured (*i.e.* greater than 1 MHz). The most accurate methods for determining the resistances in these cases would be to perform a linear regression on the blocking spike to the real *x*-axis, or if the bulk of the semi circle was visible then the origin of the semi-circle may be extrapolated.

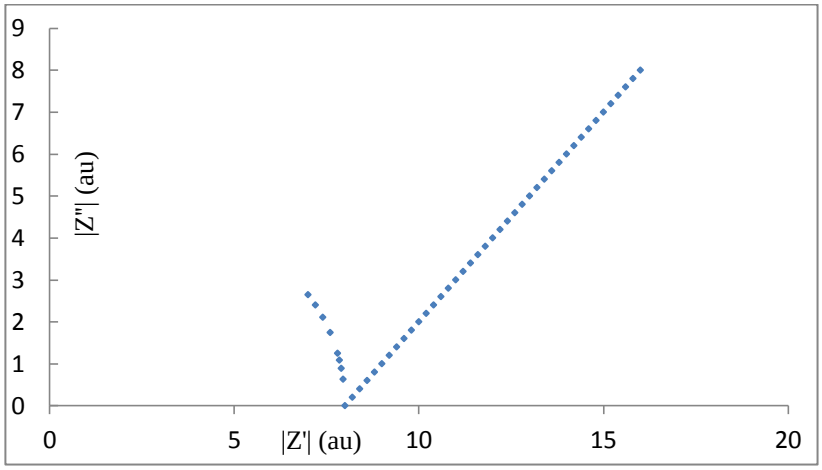

Fig. 2.11. Impedance spectrum of a highly conductive electrolyte, the response causing the rest of the semi-circle occurs at frequencies higher than 1 MHz

In some instances, especially in highly conductive samples, all that is visible in the spectra are the blocking spikes resulting from the electrode-electrode/electrolyte interface being the dominating over the electrolyte impedance at all the frequencies measured, again the most accurate method for determining the resistances in these cases would be to perform a linear regression on the blocking spike to the real x-axis.

In some instances, there is a lack of response from the electrolyte and determining the resistance from linear regression of the blocking spike accurately can be difficult, e.g. as in Fig. 2.12.

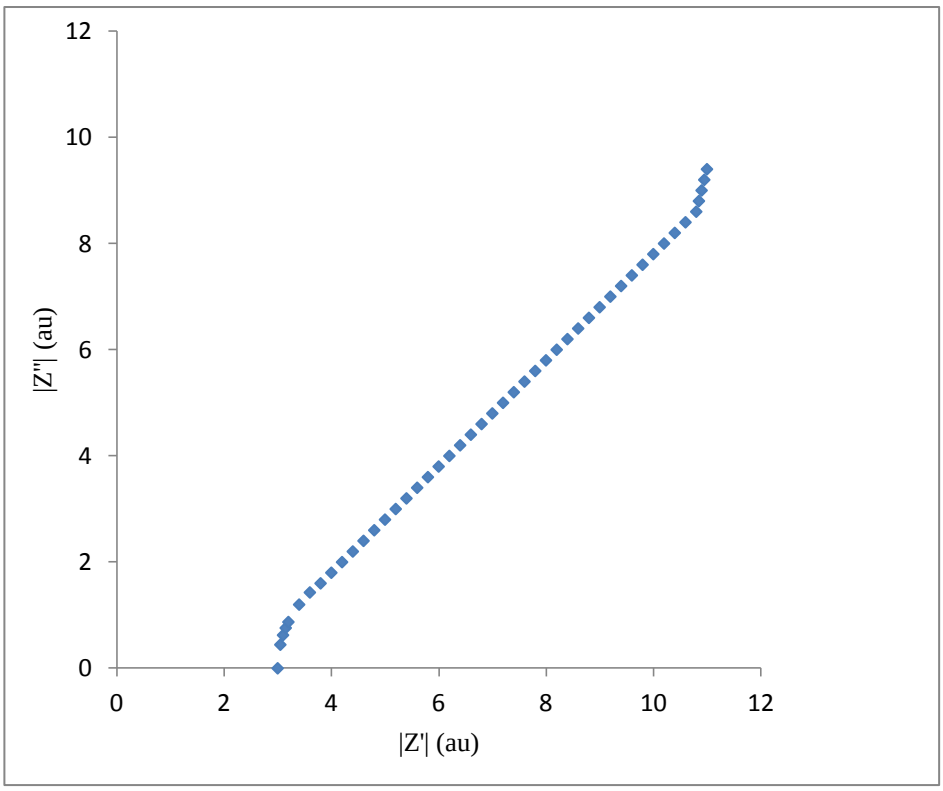

Fig. 2.12. Impedance spectrum showing just a blocking spike

In such cases the resistance is taken at the *x*-axis intercept, rather than a linear regression of the blocking spike which would result in an underestimated resistance. There are several factors that result in the blocking spike not intercepting the *x*-axis at a 45° angle, the two most important of which, is that there could be a small contribution to the impedance from the electrolyte (but which cannot be reasonably determined by fitting the data to a sensible equivalent circuit) and also a contribution from the electrolyte-electrode interface, again this could be due to roughness of the surface of the electrode, which can be modelled using a fractal geometry and appropriate equivalent circuit. The contribution of the membrane-electrode interface to the total impedance would be typically significantly less than that of the impedance resulting from the electrolyte itself, thus should not significantly change the determined resistance of the electrolyte.

However there are times when the interpretation of the impedance spectra can be ambiguous. In these cases, the analysis of the impedance spectrum of the membrane is taken in context with those spectra of the same sample at similar temperatures and also on different cycles, if this is still ambiguous, equivalent circuit modelling is used to make a conservative estimate of resistance and hence a conservative determination of conductivity.

There are two directions in which the impedance of the membranes can be measured, these are through the membrane and across the membrane in the transverse direction; these are called normal and tangential modes, respectively. Both are equally valid if the membrane is homogenous in nature.[54] Determination of resistances and conductivities ideally should be performed in the normal mode due to the fact this is the direction in which the protons will travel in a PEMFC, in the tangential mode it is possible for the current and voltage to travel across the surface of the PEM instead of through the PEM bulk in impedance measurements if the surface would have a lower resistance, thus giving higher conductivities than would be observed in the normal mode. All measurements in this project are 2-probe in both the normal and tangential modes, and were originally performed on a Solartron 1255, and then on an Autolab PGSTAT302N.

2.6.4 Calculation of Conductivity

The value of conductivity from resistance is determined using equation 2.2,

$$\sigma = \frac{l}{A \times R} \qquad (2.2)$$

where σ = conductivity (S cm^{-1}), l distance between electrodes (cm), A cross-sectional area (cm^2) and R resistance in Ω.

In the normal cell, the distance between the electrodes is equal to the thickness of the membrane and the cross-sectional area is the surface area of the membrane (if the membrane is smaller than the electrodes). In the tangential cell, the distance between the electrodes is set to 1 cm, and the cross sectional area of the membrane is the thickness (measured with a micrometer) multiplied by the width of the membrane, and in all cases, the resistance is the determined resistance from ACIS.

Area Specific Resistance (ASR) can be determined using equation 2.3,

$$ASR = R \times A \qquad (2.3)$$

where R is resistance (Ω) and A is the cross sectional area (cm^2).

Normal cell measurements were acquired in the frequency range from 1 MHz to 1 Hz, measuring 50 frequency points in a decreasing logarithmic scale and using 10 mV amplitude. Tangential cell measurements were acquired using a frequency range from 1 MHz to 1 Hz, measuring 50 frequency points in a decreasing logarithmic scale and using 150 mV amplitude.

2.6.5 Normal Cell Set-Up

In this cell set-up, the membrane was sandwiched between two solid stainless steel blocking electrodes (Figs. 2.13 and 2.14). The area of the membrane measured was relatively small, approximately 0.25 cm^2.

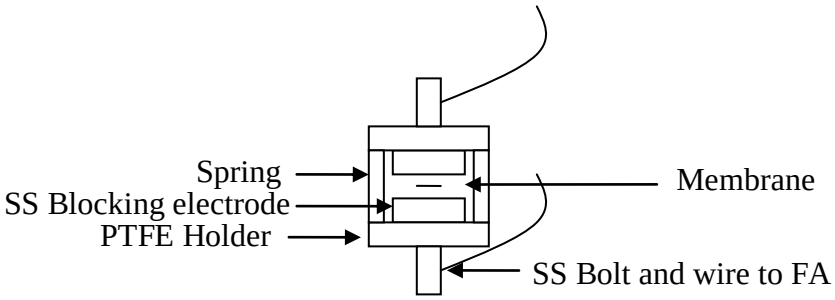

Fig. 2.13. Schematic diagram showing normal mode cell

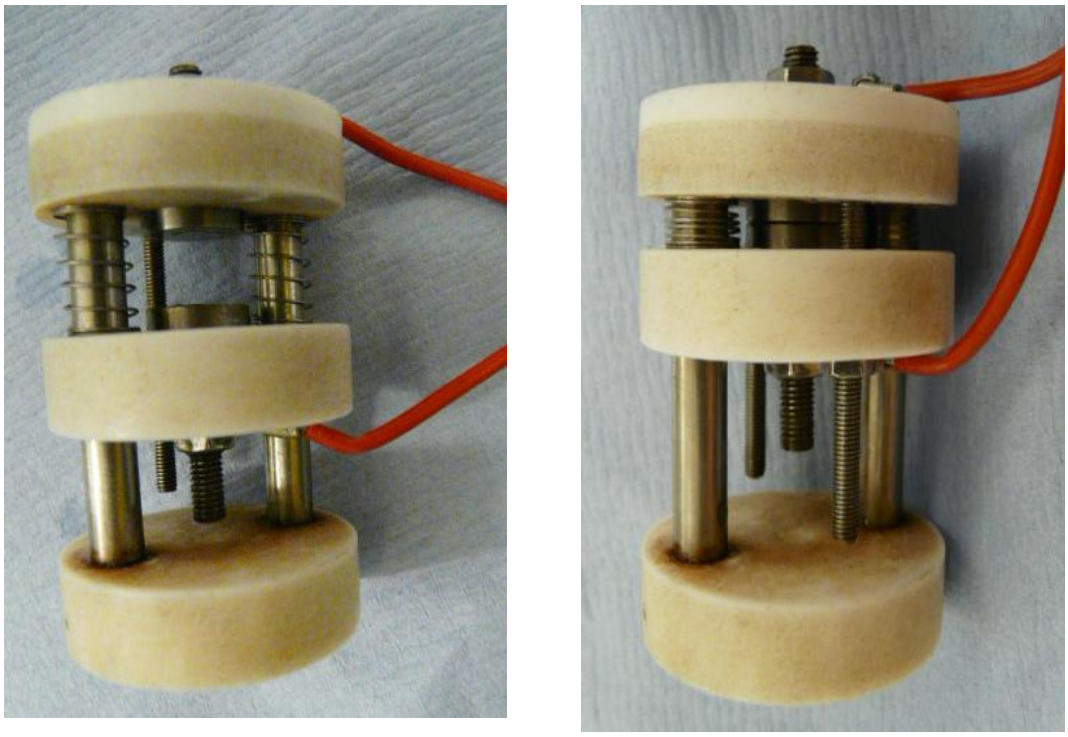

Fig. 2.14. The normal cell open (right) and closed (left)

2.6.6 Tangential Cell Set-Up

In this project the design of the tangential cell evolved through several versions. To achieve good contact between the two interfaces, the membrane and electrode needed to be pressed firmly against each other. In the tangential cell developed for this project this was achieved using screws, which ran through the cell and electrode.[17] The membrane was sandwiched between two PTFE blocks (Fig. 2.16). The screws were then tightened significantly to achieve adequate contact. When heated to 120 °C the PTFE segments of the tightened tangential cell deformed irreversibly thus effectively destroying the contact between the membrane and electrodes. For high temperature measurements, different cell materials need to be explored to overcome this design flaw, one option is to use ceramic materials, however these are generally more expensive than PTFE and more difficult to machine or fabricate.

In the exposed tangential cells (versions 1 to 3), there was a hole in the centre of the cell, which was 1 cm × 1 cm. This was to allow the membrane to equilibrate faster with the environment in the humidity chamber. Initially blackened platinum electrodes were used. This cell design and materials used were based on a design published by Zawodzinski *et al*.[17] This cell design and set-up were used to measure the impedance of Nafion 117 membranes immersed in water (or suspended above a saturated salt

solution) at room temperature. In the tangential cell version 1, the Pt electrodes were blackened to increase the surface area of the electrode and provide better contact between the membrane and electrodes.[17] However the Pt foil originally used was only 125 μm thick and needed to be cleaned and re-blackened after every use. This procedure quickly resulted in damaging the Pt foil used as the electrodes. Thicker Pt electrodes were then used in the tangential cell (0.125 mm). These were coated in the same way as the thinner electrodes and were more robust to the cleaning and blackening. Measurements were then performed (with Nafion 117) using blackened Pt and non-blackened Pt electrodes yielding similar results, thus indicating that the blackening, and hence increased surface area of the electrodes was not needed in this experimental set-up. However, the Pt wire used to connect the electrodes to the BNC connectors in the chamber lid often became loose or would break from the electrode thus would have to be re-welded which would damage the electrodes.

At this point it was decided to try a more robust alternative to the Pt electrodes and wires previously employed. Mikhailenko *et al.*[55] reported the design of a two-probe tangential cell with stainless steel being used as both the electrode and wire material (Fig. 2.15). Their cell reportedly produced repeatable results comparable to published four-electrode tangential cell measurements of Nafion 117 membranes, with the added advantage of fewer stray points.

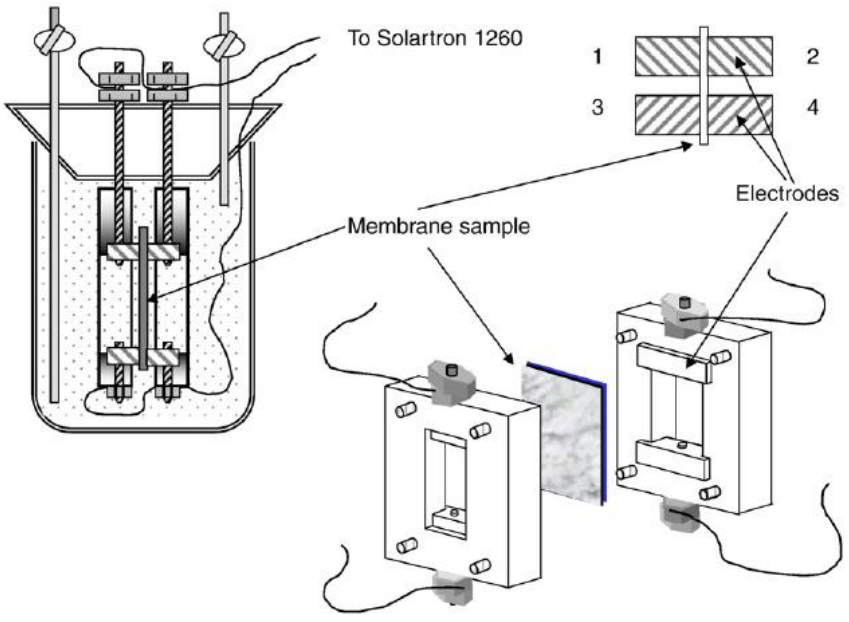

Fig. 2.15. Two-electrode tangential cell by Mikhailenko *et al.* ref 55

As stainless steel had been shown to be a good electrode material in the normal cell, and there was precedence in the literature that stainless steel could successfully be used in a two-electrode tangential cell and given the huge reduction in cost of the electrode material, thicker stainless steel electrodes (0.25 mm) were used, which would be more durable. The wires connecting the electrodes to the BNC connectors were also replaced with annealed stainless steel (2 mm diameter).

2.6.6.1 Version 1 Cell

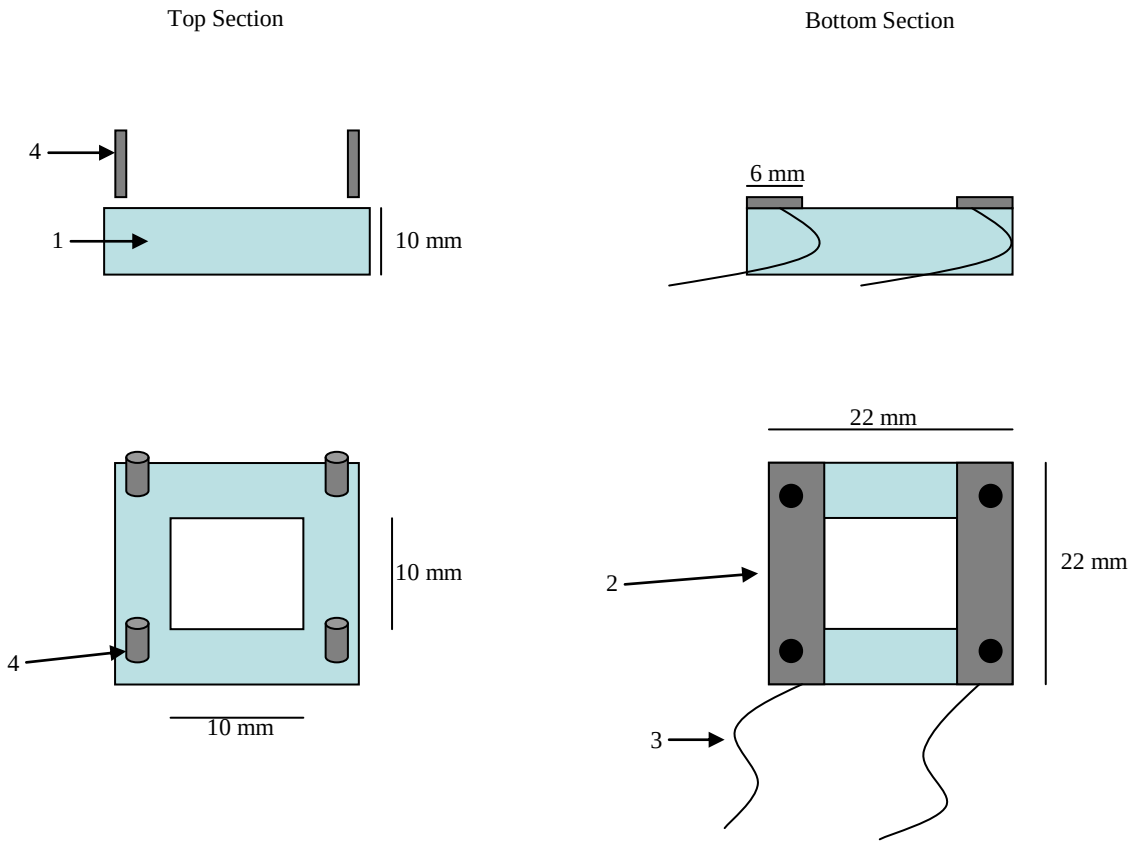

Fig. 2.16. Schematic diagram of a tangential mode cell. 1 Virgin PTFE block, 2 Blackened Pt foil (125 μm), 3 Pt wire, 4 Stainless steel screws. Design based on Ref 17

The platinum foil was blackened by electrodepositing Pt colloids onto the surface.[56] The platinum foil was first cleaned in 50 % aqua regia (4 parts water, 3 parts 12 M HCl and 1 part 16 M HNO_3), and then washed in water. The Pt foil was used as a cathode in 0.01M H_2SO_4, rewashed and then platinised by passing a 30 mA cm^{-2} current through the foil with a platinum counter anode in 72 mM chloroplatinic acid solution. The solution was stirred constantly to obtain an even coating of platinum. When the current was too high, then the platinum coating formed larger crystallites (lower surface area) which formed a bright reflective layer instead of a black one.

2.6.6.2 Version 2 Cell

This cell was as version 1, but the platinum electrodes were not blackened.

2.6.6.3 Version 3 Cell

This cell was as version 1, but the platinum electrodes and wire were replaced with stainless steel (grade A4). The electrodes were annealed stainless steel, 0.25 mm thick and the wire was annealed stainless steel, 2 mm diameter.

2.6.6.4 Version 4 Cell

This cell was as version 3, but the PTFE cells were remade with no hole in the centre of the cell, *i.e*. the bulk of the membrane surface was not exposed to the atmosphere.

2.6.7 Conditions used for normal and tangential cell measurements

Measurements were performed by heating the cell and membrane in a pressure tight stainless steel chamber that had fresh deionised water in the bottom. This was to maintain 100% RH during measurements. The environment control chamber is shown in Fig. 2.17, with the dimensions of the chamber given in Fig. 2.18, along with the dimensions of the chamber lid in Fig. 2.19.

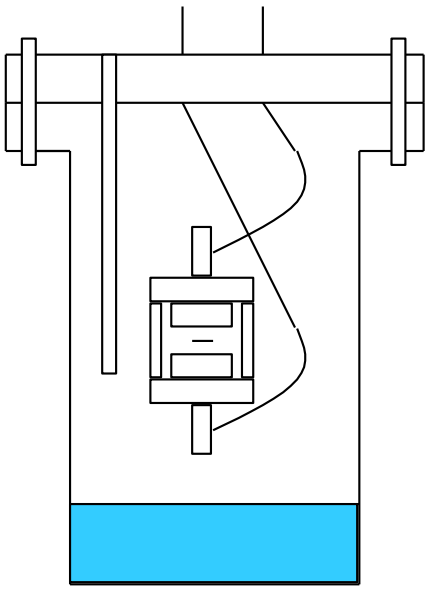

Fig. 2.17. Schematic representation of the chamber housing the measurement cell under operating conditions

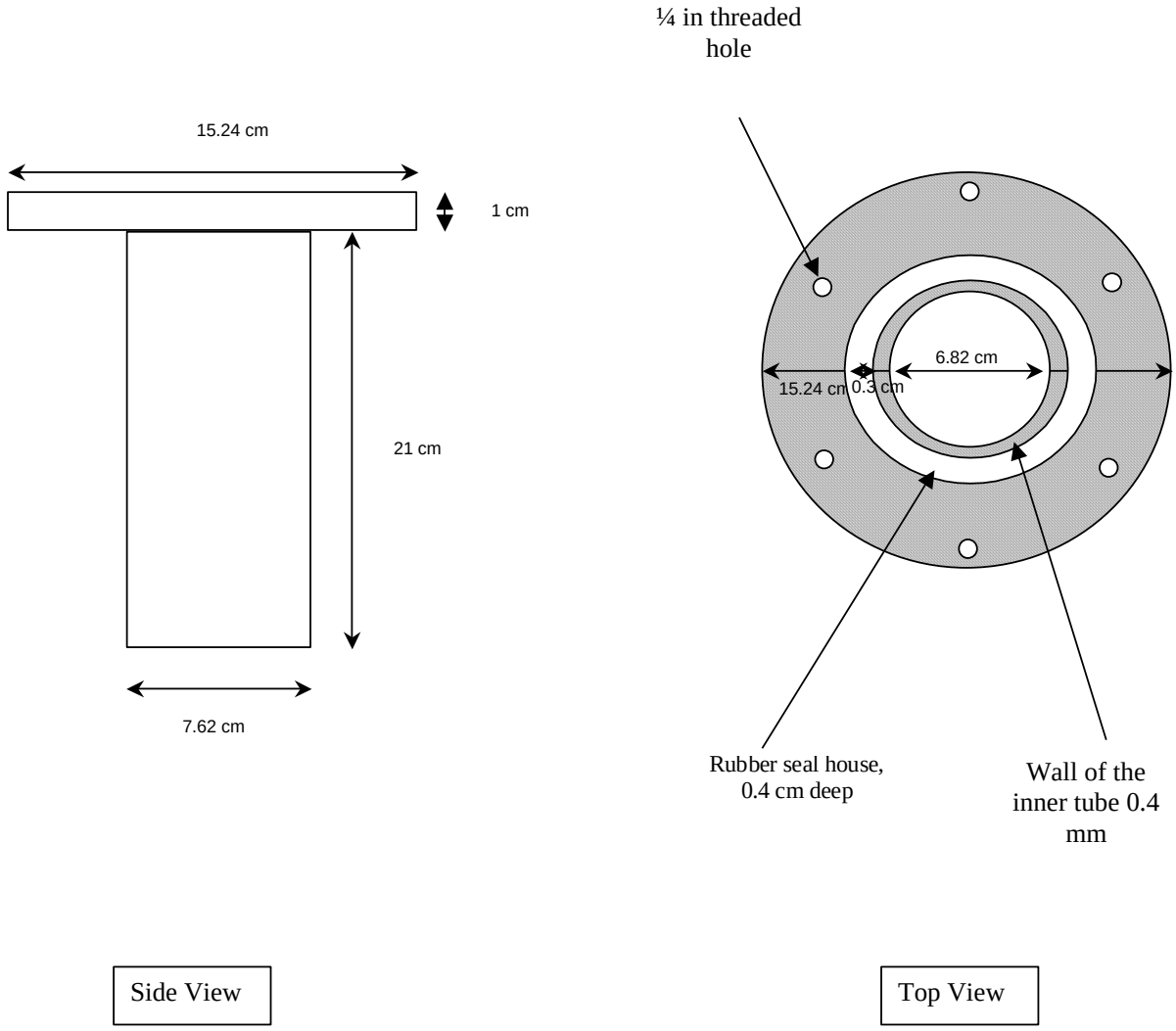

Fig. 2.18. Dimensions of an environmental control chamber

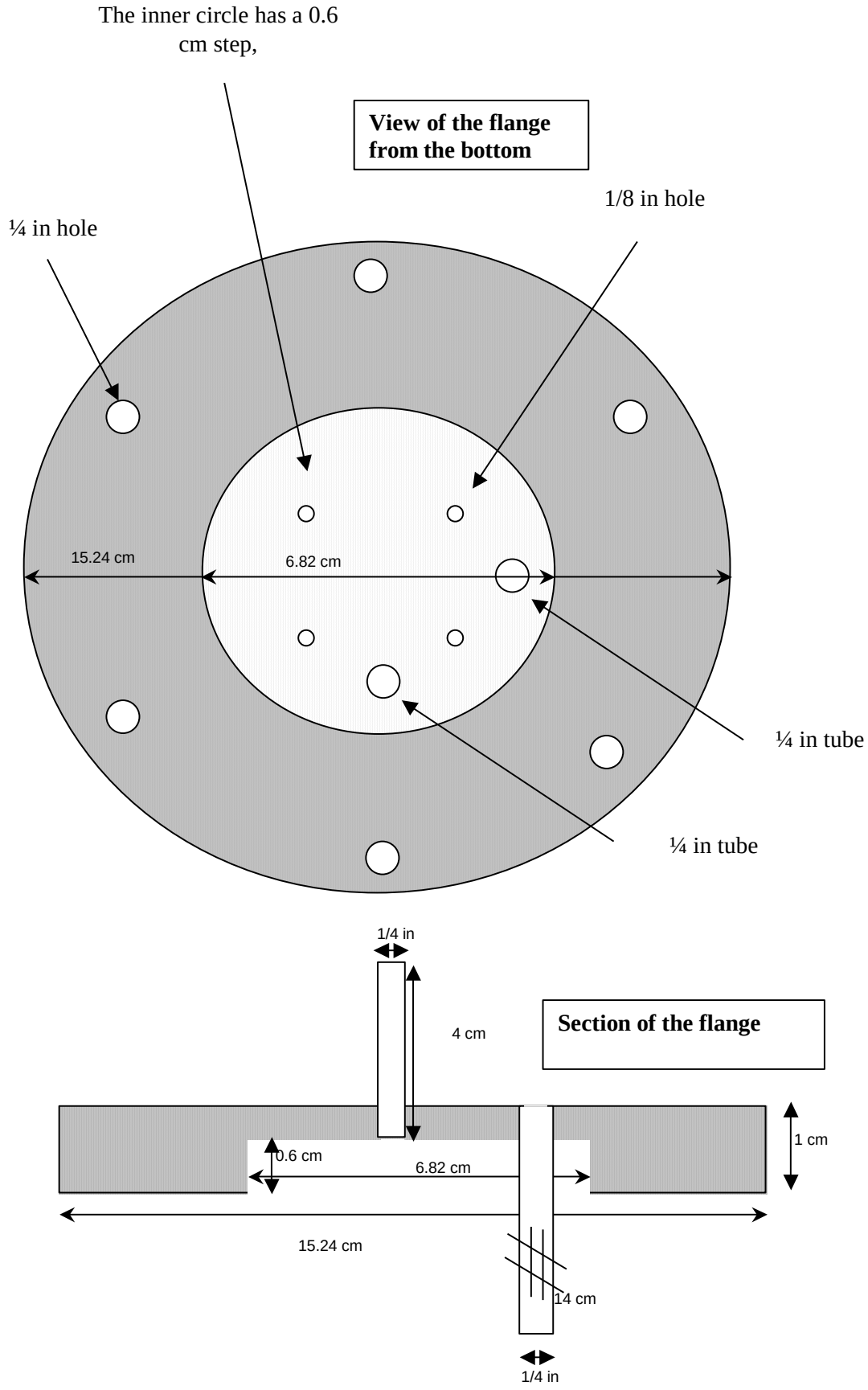

Fig. 2.19: Dimensions of the chamber lid

The chamber was heated using heating tape with a percentage controller (Omega HTWC102-002/004). The temperature was controlled by a temperature controller (Omega CN132) with a k-type thermocouple.

Measurements were recorded at room temperature (*ca.* 21 ºC), 30, 40, 50, 60, 70, 80, 90, 100, 110 and 120 ºC. After reaching the required temperature and prior to each measurement the chamber was vented briefly so the chamber was at atmospheric pressure. The membrane was allowed to equilibrate for at least 20 minutes with the environment which was at 100% RH (after 20 minutes in the normal cell, repeat measurements in the normal cell produced comparable spectra). The impedance was measured on average over three cycles on the heating ramp only.

2.6.8 Impedance Spectroscopy Measurements of Neat PA

Proton conductivities of neat PA were measured for both blends 1 and 6. Blend 6 which was a powder, was firstly compressed into a pellet of approximate dimensions 10 mm diameter, 2 mm thickness. The surfaces of the pellet were polished and then painted with silver conductive paint to provide to a good electrode/electrolyte interface. Blend 1 was used in the form of a glassy film which was prepared by placing a 2 mL aliquot of dispersed blend 1 hydrolysed by method 3 in an oven overnight at 100 °C on a PTFE slide, after which time the slide was removed from the oven and the film of PA obtained. When the film was placed in boiling water it rapidly dissolved.

2.6.9 Intermediate RH ACIS Measurements

Two methods to control RH were employed during the course of this project, the first of which was the use of saturated salt solutions. Different saturated salt solutions have different vapour pressures over a given temperature range, thus can be used as a control for relative humidity. A non-comprehensive list of salt solutions and RH over a temperature range from 0 to 100 °C is given in Fig 2.20. However, there were several draw backs to this method. Firstly, to maintain a saturated solution at 100 °C during measurement, the solute/salt needed to be added at this temperature to form a saturated solution, this required a very large quantity of salt to be added (thus making this method uneconomical), and when the solution cooled, salt precipitated out. Secondly, using saturated salt solutions as a control for RH, the maximum temperature for which RH could be maintained was 100 °C, well below the 120 °C target of the project. Thirdly,

the salt solutions were corrosive to the stainless steel chamber, the conductivity cell and the humidity sensor, seriously limiting the life span of each.

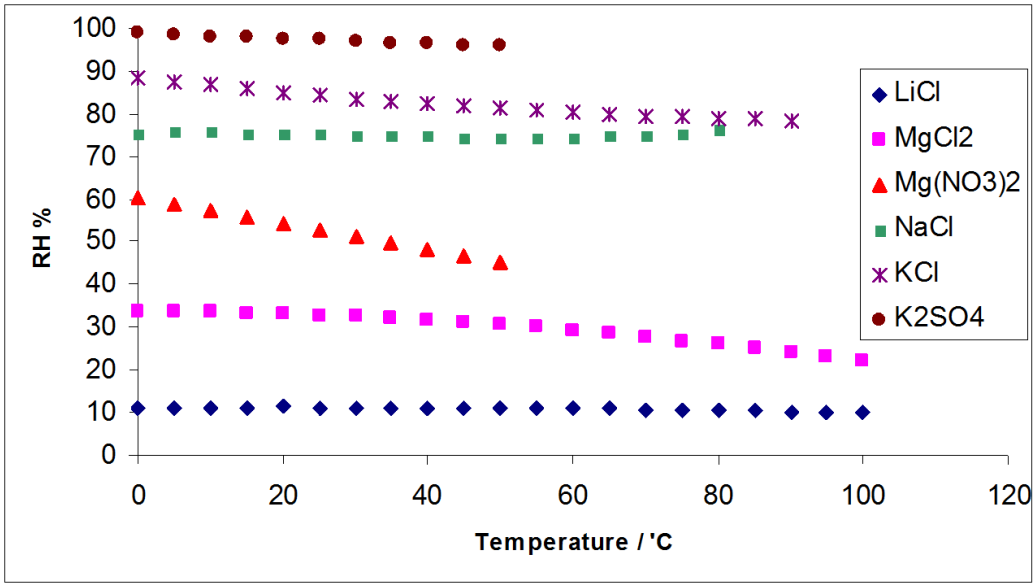

Fig. 2.20: Graph showing the RH of certain saturated salt solutions over 0-100 °C temperature range

The second method for the control of RH was the use of two interconnected chambers as shown in Fig. 2.21. The first chamber contained the conductivity cell, and the second chamber contained deionised water, with both chambers being heated independently. To maintain 100 % RH, both chambers would be kept at the same temperature. To lower the RH, the chamber which contained the deionised water would be kept at a lower temperature, dependent on the temperature of the chamber containing the conductivity cell and desired RH. The calculation was based on the specific vapour pressure of water, and is given in equation 2.4.

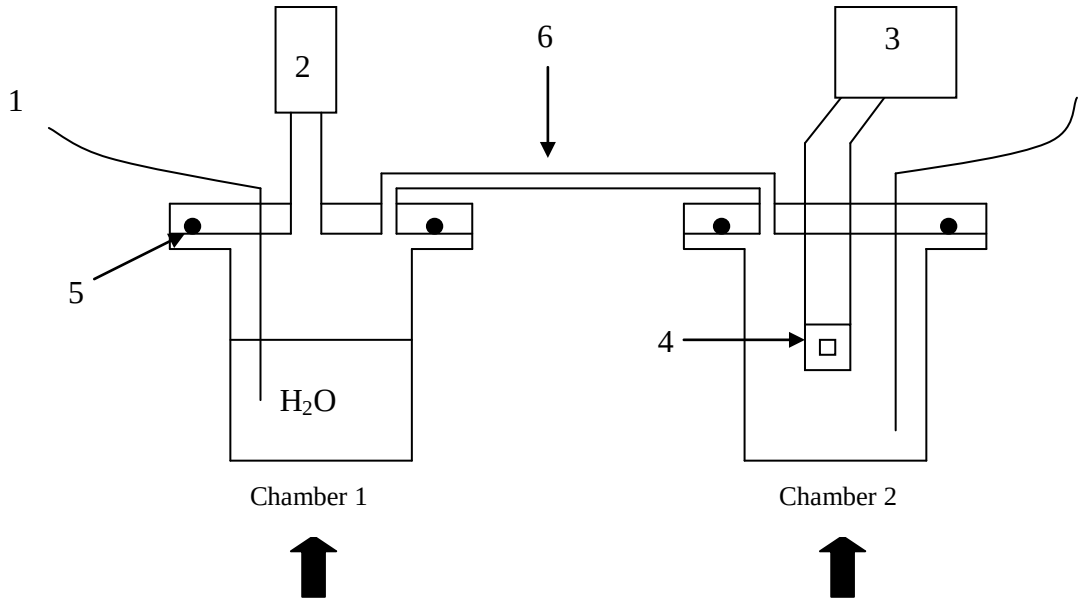

Fig. 2.21. Control of RH using 2 chambers. Key: 1 Thermocouples, 2 pressure transducer, 3 frequency analyser, 4 membrane cell, 5 rubber flanges, 6 stainless steel tube. RH in chamber 2 calculated using equation 2.4.

$$RH = \left(\frac{p_{C2}}{P_{C1}} \right) \times 100 \tag{2.4}$$

To check the validity of this experimental set-up to obtain specific RH/water vapour pressure, a calibrated pressure transducer was attached to the system. To obtain the pressure from solely the water vapour, the system was firstly purged of air; this was achieved by boiling the water and then opening the system, thereby causing the steam to purge the air from the system. The cell was then closed, so any pressure reading from the transducer was solely due to the water vapour in the system. To achieve accurate readings from the pressure transducer, the system needed to be pressure tight at elevated temperatures for 3 days to allow measurements from each heating cycle to be recorded. However, the pressure inside the system slowly increased at room temperature after purging the air and cooling but before heating, which meant that the system was not adequately vacuum sealed, thus meaning that the RH in chamber two could not be determined.

2.7 FT-IR Spectroscopy

FTIR measurements were performed using a Bruker Tensor 27 FT IR spectrometer with a Pike MIRacle single reflection attenuated total reflection infrared accessory and a

diamond/ZnSe crystal plate. Measurements were collected from 4000 to 525 cm^{-1} over 128 scans at 4 cm^{-1} resolution.

2.8 NMR spectroscopy of membranes

NMR measurements were performed on a JEOL 270 FT-NMR spectrometer. ^{31}P NMR spectra were collected at a frequency of 109.13 MHz. To determine the extent of acid hydrolysis in the PA during hydrolysis of the ester mixture as function of time and temperature, an aliquot (*ca.* 1 mL) of PA solution was removed from the reaction mixture using a syringe. This sample was placed in a glass vial and heated in an oven at 100 ºC overnight. Once cooled a portion of the glass was crushed in a mortar (cryo-grinding with liquid nitrogen when required) using a pestle. The crushed and ground glass was transferred to a sample vial and 2 mL of NaOH solution (14M) was added. The glass was then digested by heating the solution moderately (*ca*. 50 ºC) for about 30 minutes. The solution was then transferred into a NMR tube for analysis.

2.9 Water uptake

The water uptake was determined by placing a portion of pre-weighed dry membrane (stored in phosphorus pentoxide for 24 hours) in deionsed water (50 mL). After 30 minutes the membrane was removed, the surface water removed with filter paper and the sample reweighed. The membrane was then re-immersed in the water and the procedure repeated after 1 hour, 2 hours, 3 hours, 4 hours, 6 hours and 24 hours.

2.10 Ion exchange capacity (IEC)

In this technique, a portion of membrane *ca.* 200-350 mg was suspended in 50 cm^3 0.5 M sodium formate (HC(O)ONa) solution for several days, shaking occasionally. After this time, the protons from the membrane exchanged with sodium ions from the formate solution, to give a membrane containing a mixture of sodium phosphonate and phosphonic acid, and a solution containing a mixture of formic acid (HCO_2H) and sodium formate. A 10 cm^3 aliquot of the sodium formate/formic acid solution was titrated against dilute sodium hydroxide (typically 20 mM) using phenolphthalein as an indicator, and an average of at least three titres used in calculations. To determine the IEC, equation 2.5 was used. The prefactor 5 was used because each titre measured the concentration of formic acid from one fifth of the total volume of the sodium formate/

formic acid solution used in the experiment. IEC has units of mol g^{-1} equivalents (of dry membrane), but are generally presented as mmol g^{-1} equiv.

$$IEC = \frac{5 \times [NaOH] \times Volume\ NaOH}{dry\ membrane\ mass} \tag{2.5}$$

For comparison, the IEC capacity of Nafion 117 was determined using sodium formate solution and compared to the literature value of sodium chloride solution. The Nafion membrane was firstly conditioned to activate the sulfonic acid groups and to remove contaminants. This was achieved with the same conditioning regime used in impedance conditioning, boiling in hydrogen peroxide, then sulfuric acid and finally in deionised water. Once fully conditioned, the membrane was stored over phosphorus pentoxide for 72 hours to completely dehydrate it, and the dry membrane mass recorded. After this, the Nafion membrane was stored in sodium formate solution (0.5 M, 50 mL) for 48 hours with occasional stirring. A 10 mL aliquot was then removed and placed in a small beaker with a magnetic stirrer bar and pH electrode. To this solution dilute sodium hydroxide solution (0.01 M) was added dropwise whilst constantly stirring. After each addition of sodium hydroxide the pH was then recorded and a pH neutralisation curve obtained. The end point was recorded and used to determine the IEC. This procedure was repeated twice to obtain an average end point. The IEC was calculated according to equation 2.6.

$$IEC = \frac{5 \times 0.01\ M \times 0.0061\ dm^3}{0.3311\ g} = 0.92\ mmol\ g^{-1}\ equiv \tag{2.6}$$

Using this methodology, the IEC of Nafion was determined to be 0.92 mmol g^{-1} equiv, with an equivalent weight (EW) of 1087 g mol^{-1}. This agrees with the literature values quoted by DuPont of an IEC of 0.91 mmol g^{-1} equivalence and an EW of 1100 g mol^{-1}.[22] Therefore, using sodium formate instead of sodium chloride is a valid method for determining the IEC of PEMs.

To obtain accurate end point analysis for phosphonic acid PEMs, and to determine whether any PA leaching from the membrane occurred, both phosphorous acid and formic acid were separately titrated against sodium hydroxide.

2.11 Equivalent Weight (EW) Determination

The EW was determined by taking the reciprocal of the IEC in mol g^{-1} and is quoted as g mol^{-1}.

2.12 λ Value Determination

λ values are the number of water molecules present in the membrane per each PA group in the membrane. To hydrate the membrane, it is either immersed in deionised water for at last 48 hours or boiled in deionised water for one hour. The λ value was determined using equation 2.7.

$$\lambda = EW \times \frac{Water\ Uptake\ (\%)}{RMM\ of\ Water} \tag{2.7}$$

2.13 TGA

TGA measurements were performed on a TA Q500 series instrument using either nitrogen or air as the purge gas, both with a gas flow rate of 50 cm^3 min^{-1}. Isothermal measurements were performed by heating the sample to 120 ºC at a 10 ºC min^{-1} ramp, and then holding at 120 ºC for 24 hours. For heating experiments the membrane was heated to 500 ºC at a rate of 10 ºC min^{-1}.

2.14 Differential Scanning Calorimetry (DSC)

DSC measurements were performed on a Mettler Toledo DSC with a robotic auto sampler. All measurements were carried out with nitrogen as the balance and purge gas (gas flow rate of 150 and 50 cm^3 min^{-1} respectively). DSC traces were recorded from 3 heating and cooling cycles from 10 ºC to 150 ºC to 10 ºC at a rate of 10 ºC min^{-1}.

2.15 Fenton's Reagent

Fenton's reagent was prepared by dissolving $FeSO_4$ (1.0 g) in deionised water (1000 mL), a 10 mL aliquot of this solution was then further diluted in deionised water (500 mL) to give a Fe^{2+} concentration of 20 ppm. Half of this solution (250 mL) was added to 6% hydrogen peroxide solution (250 mL) to give Fe^{2+} 10 ppm in 3% hydrogen peroxide.

A portion of membrane, with a known mass, was placed in boiling Fenton's reagent for up to 1 hr.

Chapter 3

Synthesis and Characterisation of Phosphonic Acid Polysilsesquioxane

3.0 Introduction

The component responsible for the majority of proton conductivity in the polymer electrolyte membranes (PEMs) being investigated in the present work is phosphonic acid polysilsesquioxane (PA). In this chapter, the synthesis and characterisation of PA are discussed.

PA when considered on a molecular basis is a diprotic phosphonic acid attached to a siloxane group via a short carbon chain (Fig. 3.1). However, this is a somewhat simplistic representation of a complex molecule (as PA actually exists as a complex oligomer) in which the structure is highly dependent on the synthetic route used to produce the PA (discussed later 3.5 and 3.6). The acidity of PA is close to that of the parent phosphorous acid (H-P(O)$(OH)_2$), with pKa values of 1.3 and 6.7 for the two acidic protons.[57]

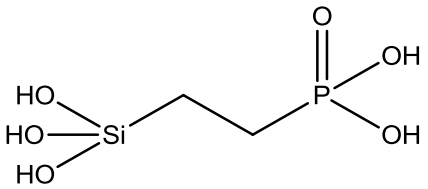

Fig. 3.1 Structure of monomeric PA

PA has several uses; it can be used as a metal scavenger,[58] as an effective catalyst (when combined with transition metals such as Pd and Pt)[59] and more recently as a proton source in PEMFCs.[60]

Phosphonic acids of general formula R-P(O)$(OH)_2$ have been promoted as a potential way of overcoming problems associated with sulfonic acid containing PEMs such as Nafion, which are currently used in commercial PEMs and phosphoric acids which are used in polybenzylimidazole PEMs (PBI PEMs).[61] Although phosphonic acids are less acidic than sulfonic acids, PEMs based on these acids have been shown to retain absorbed water above 100 °C,[61] compared to sulfonic acid PEMs, which have an optimal operating temperature of 80 °C, above which their performance rapidly

deteriorates. This makes phosphonic acids ideal candidates for development for use in high temperature PEMFCs with operating temperatures of 120 °C and above. Phosphonic acid membranes also have advantages over phosphoric acid doped PBI PEMs, [62] in which the phosphoric acid gradually washes out of the membrane and also into the Pt containing electrodes acting as a poison which reduces PEM efficiency over time.[63] In contrast, in phosphonic acid membranes, the acid is typically covalently bound into the polymer matrix and is not easily removed, although there are some cases where phosphonic acid surfactants are used where the acid is not covalently bound to the matrix[50]. One negative aspect of use of phosphonic acid is that condensation of the acid groups may occur in anhydrous conditions.

3.1 PA Ester Synthesis

PA may be synthesised by the hydrolysis of the parent phosphonate ester (**PA_E**). The phosphonate ester is actually a mixture of two esters, dimethylphosphonatoethyltriethoxysilane (**5**) and 2,4-*bis*(triethoxysilyl)-1-dimethyl phosphonatobutane (**7**), the reaction mechanism for the formation of **5** and **7** using the reaction conditions described in 2.1 is shown in Fig. 3.2.

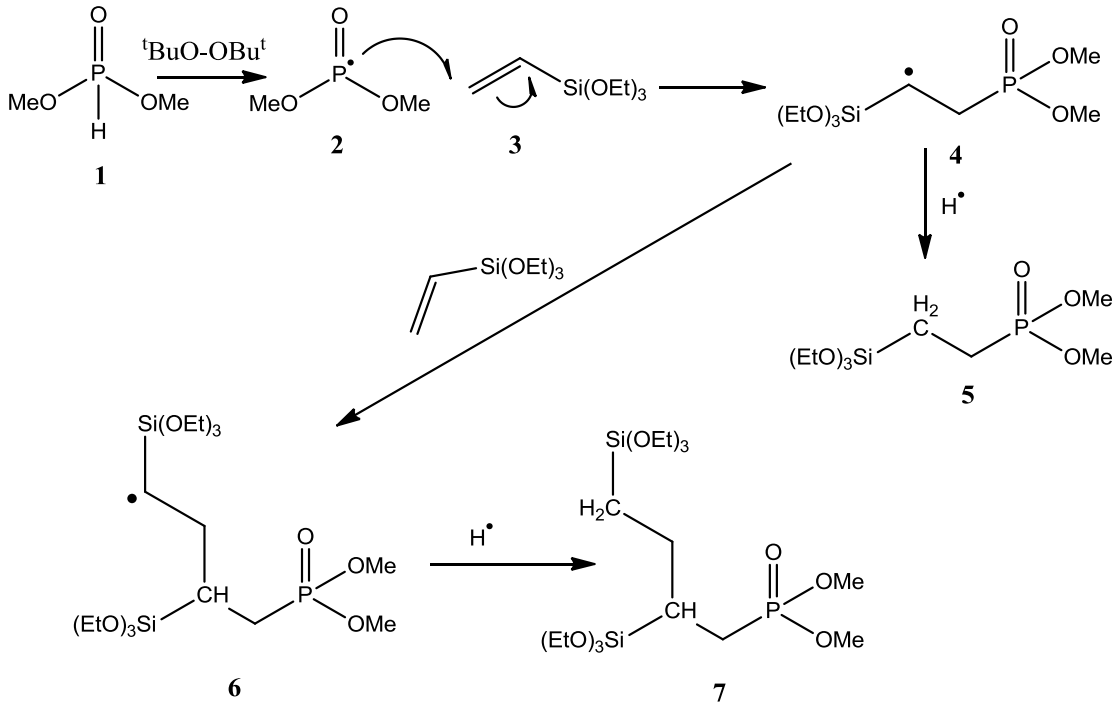

Scheme. 3.2. Synthesis of the phosphonate ester PA precursors, dimethylphosphonatoethyltriethoxysilane and 2,4-*bis*(triethoxysilyl)-1-dimethyl phosphonatobutane.

The ratio of **5** to **7** is determined by the reaction conditions employed during the synthesis, and two different ratios 98:2 and 60:40 were used in the present work (blends 1 and 6, respectively).

In the blend 1 synthesis, vinyltriethoxysilane (VTES) was added slowly to the dimethylphosphite/di-tertbutoxide mixture. This kept the concentration of dimethylphosphite (DMP) radicals greater than the concentration of VTES in the reaction mixture, thus one molecule of VTES would react with one radical DMP species, and then gain a radical hydrogen, before there was a chance to react with another molecule of VTES. This effectively meant that very little **7** was formed, *ca*. 2%. This blend is also referred to as the "dropwise" blend, as the VTES was added in dropwise. As in this blend, the DMP and VTES reacted in an almost 1:1 stoichiometric ratio, there was little residual DMP left at the end of the reaction. This meant the PA_E did not require distillation to remove residual DMP. Fig. 3.3 shows a ^{31}P solution state NMR spectrum obtained for a typical blend 1 PA_E sample.

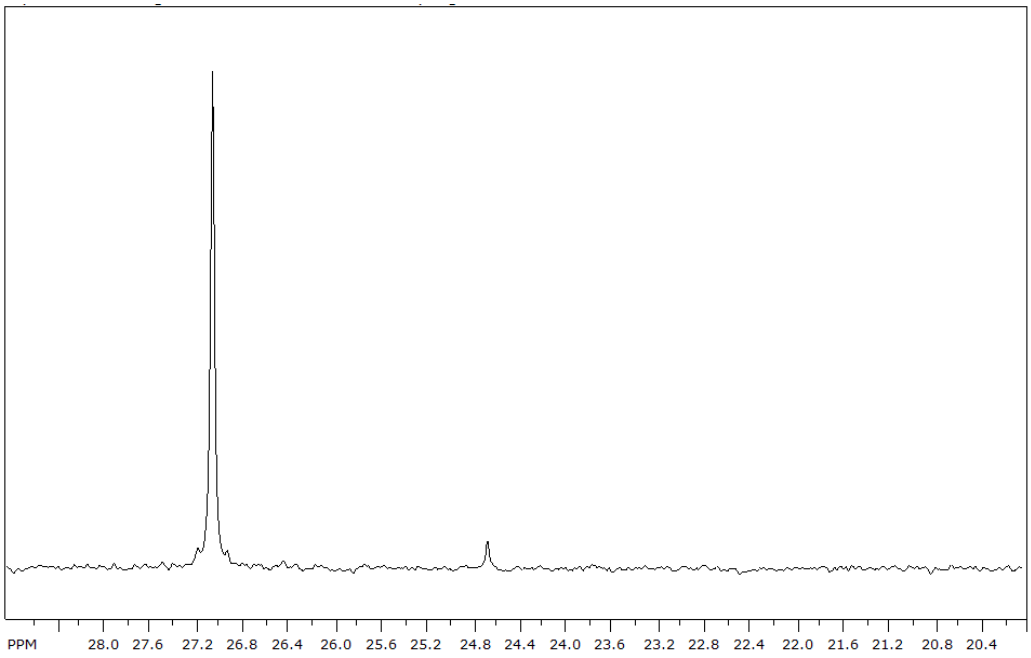

Fig. 3.3. ^{31}P NMR spectrum of blend 1 PA_E showing resonances for **5** (δ 26.9) and **7** (δ 24.6)

In the blend 6 synthesis, the VTES, DMP and di-tertbutoxide were all added at the same time and then the reaction mixture was heated. Under these conditions, intermediate **4**

has a good chance of reacting with another molecule of VTES (instead of a hydrogen radical) to form intermediate **6,** which would then react with a hydrogen radical to form phosphonate ester **7**. The blend 6 product therefore contains more **7** (40%) than the blend 1 product. This leaves a significant amount of unreacted DMP in the reaction mixture, which needs to be removed by vacuum distillation, otherwise when the blend is hydrolysed, the DMP is hydrolysed into phosphorous acid which would affect the conductivity of the derived membrane.

The solution state ^{31}P NMR spectrum of the blend 6 product showed no evidence of tri-substitued silyl phosphonate esters being formed. This can be explained by considering that the bulky ethoxy substituents on the silyl ester sterically hinder access to the radical site in intermediate **6**, thus preventing the molecule from reacting with another VTES molecule.

To synthesise blends containing intermediate ratios of **5** and **7**, the desired amounts of blends 1 and 6 were mixed together as described in section 2.1.3. These were labelled Blends 2 to 5.

3.2 Hydrolysis of PA_E

To be used in a PEMFC, the phosphonate ester groups need to be converted to hydroxyl groups to form the desired phosphonic acid. There are three methods which can be used for the ester hydrolysis, *viz*: base hydrolysis, acid hydrolysis and nucleophilic attack. The method of hydrolysis has a direct impact on the silsesquioxane bonding of the PA.

The base hydrolysis for molecule **5** is summarised in Fig. 3.4 and the mechanism shown in Fig 3.5. PA_E as stated previously is a mixture of molecules **5** and **7** and molecule **7** undergoes base hydrolysis in a similar way.

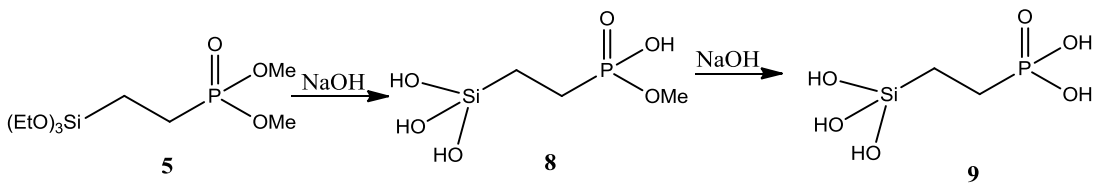

Fig. 3.4. Base hydrolysis of **5**

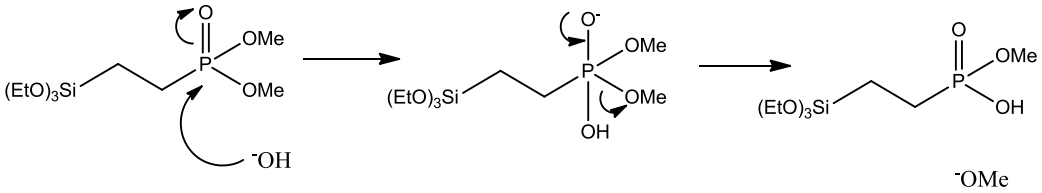

Fig. 3.5. Mechanism of base hydrolysis of the phosphonate ester of molecule **5**

A strong base would be needed to hydrolyse the ester groups, typically sodium hydroxide (NaOH) would be used, and the reaction mixture heated for an extended period of time. The advantage of base hydrolysis is that molecular (*i.e.* non-condensed PA) would be synthesised. The major disadvantage of base hydrolysis of PA_E is that the sodium salt of the acid is formed at the high pH used in this reaction (Fig. 3.6). Under reflux conditions the NaOH attacks the Si-O-Si linkages resulting in two Si-O-Na groups.

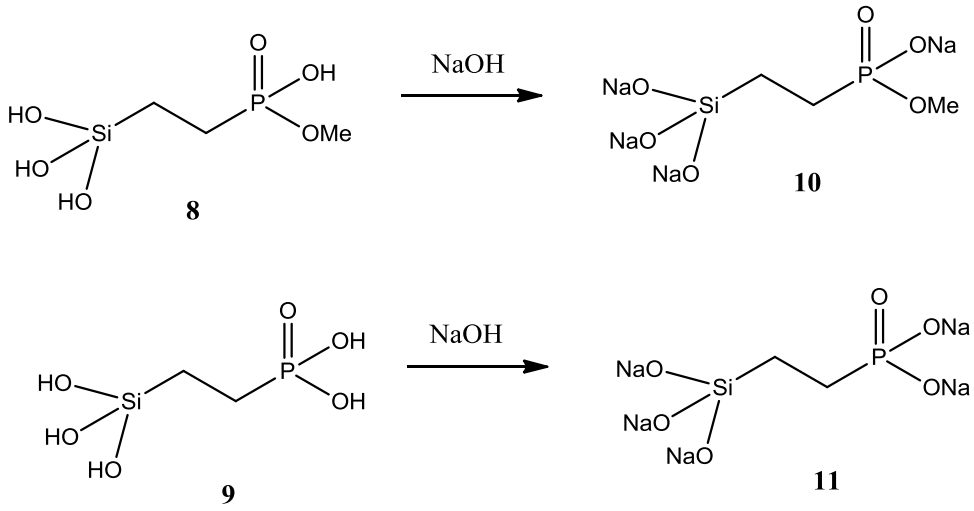

Fig. 3.6. Sodium salts of **8** and **9**

To convert **10** and **11** into **8** and **9**, (as well as the molecule **7** derivatives), the compounds would need to be hydrolysed with a strong acid to lower the pH and could be achieved by refluxing the reaction mixture in concentrated HCl. This would convert the phosphonate sodium salt into the phosphonic acid, but also would convert the Si-O-Na group into Si-OH, whereupon condensation could occur, forming a partially polymerised silyl chain. This method would also produce substantial amounts of sodium chloride, which would need to be washed out of the reaction mixture.

Acid hydrolysis of PA_E would result in a cross-condensed oligomer, of which examples of molecules **5** and **7** are given in Fig. 3.7. Intermediates **12** and **14** show partially hydrolysed phosphonate ester groups, with only one methoxy group converted into a hydroxyl group. The first methoxy group is easily hydrolysed by both acid and base hydrolysis and again in both cases, the second methoxy group requires a longer reaction time or stronger conditions (higher temperature and/or higher acid concentration) to fully hydrolyse the PA_E.

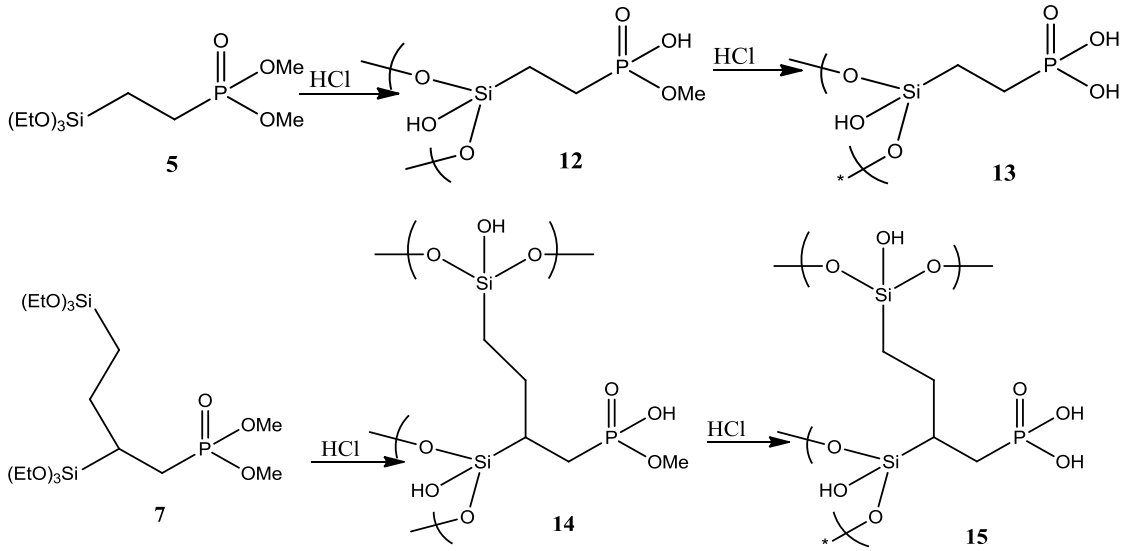

Fig. 3.7. Acid hydrolysis of **5** and **7**

Acid hydrolysis is used in the present work, as the final product does not need to undergo further chemical reaction. The product is simply washed to remove residual HCl, before redispersing in solvent. In contrast, after base hydrolysis, the sodium salt of PA would need to be refluxed in strong acid to fully convert it to the acid, thus adding an extra step into the synthesis.

Molecule **13** (Fig. 3.7) is a representation of a condensed and hydrolysed version of molecule **5**. Since PA is a mixture of hydrolysed **5** and **7**, the condensed PA contains oligomers of hydrolysed **5** and **7**. The level of condensation in the PA is unknown, but it is likely to be less than 100%. The degree of condensation in siloxanes is usually determined by ^{29}Si NMR.[64,65,66,67] Unfortunately, due to the relatively low abundance of ^{29}Si and the dilute nature of the dispersed PA in a solution state NMR experiment, the sample signals could not be distinguished above the background noise in ^{29}Si spectra for PA collected in the present study.

If 100% hydrolysis is assumed, then the formula for PA may be represented as $[(ECH_2R)_x((ECHR(CH_2)_2E)_y]_z$ where $E=(HO)_nO_{3-n}Si$, $R=CH_2PO(OH)_2$, *x* and *y* represent the molar ratio of **5** and **7** in the blend used, respectively and *z* is the degree of polymerisation.

The extent of phosphonic acid hydrolysis can be determined by ^{31}P solution state NMR and the size of the resulting dispersed PA particles can be determined by dynamic light scattering (DLS).

3.3 Suitability of Blends 1 to 6 for use in PEM Formation

Blends of phosphonate esters, 1 through to 6, as summarised in Table 3.1 were formed as stable viscous liquids. When blends 5 and 6 were hydrolysed, the resultant PAs formed were solid powders, which could not be redispersed in methanol, ethanol or water and thus were unsuitable for use in PEM synthesis

Table 3.1. Physical state of PA blends after hydrolysis

Blend	5:7 Ratio	State of hydrolysed blend	Suitable for PEM synthesis
1	98:2	Viscous liquid	✓
2	96:4	Viscous liquid	✓
3	94:6	Viscous liquid	✓
4	90:10	Viscous liquid-semi solid	✓
5	80:20	Solid residue	×
6	60:40	Solid residue	×

Hydrolysis products of blends 1 to 3 were viscous liquids which could be redispersed in methanol or water, resulting in visually homogenous suspensions. Hydrolysis of blend 4 gave a viscous liquid, which contained some solid material. However, when methanol was added and the mixture shaken vigorously, the PA dispersed into solution.

The fact that the hydrolysis products of blends **5** and **6** (PA) were solids, which could not be redispersed in solvent, was due to the formation of larger particles as a result of the higher content of **7**. These hydrolysis products could be digested in concentrated sodium hydroxide at elevated temperatures. It is believed that the NaOH hydrolyses the

condensed Si-O-Si linkages, thus breaking up the oligomer into the constituent molecules. The hydrolysis product of blend 4, was a semi-solid viscous liquid. This suggests that the larger particles formed were agglomerates of smaller particles, which broke apart when the suspension in methanol or water was shaken vigorously.

As the hydrolysis products of blends 1 to 4 all formed stable dispersions they could be used in PEM synthesis. Several methods were employed to hydrolyse the PA_E blends into PA and are described in chapter 2.2.

3.4 PA_E Hydrolysis Results

Initially PA_E hydrolysis was carried out by refluxing 6 M HCl for 24 hours at 110 °C (method one). To determine the extent of phosphonate ester hydrolysis, dispersed PA was placed in an oven and heated at 100 °C overnight to produce a condensed glass. This condensed glass was then digested in concentrated sodium hydroxide solution, before being diluted with D_2O and ^{31}P NMR spectrum recorded (Fig. 3.8).

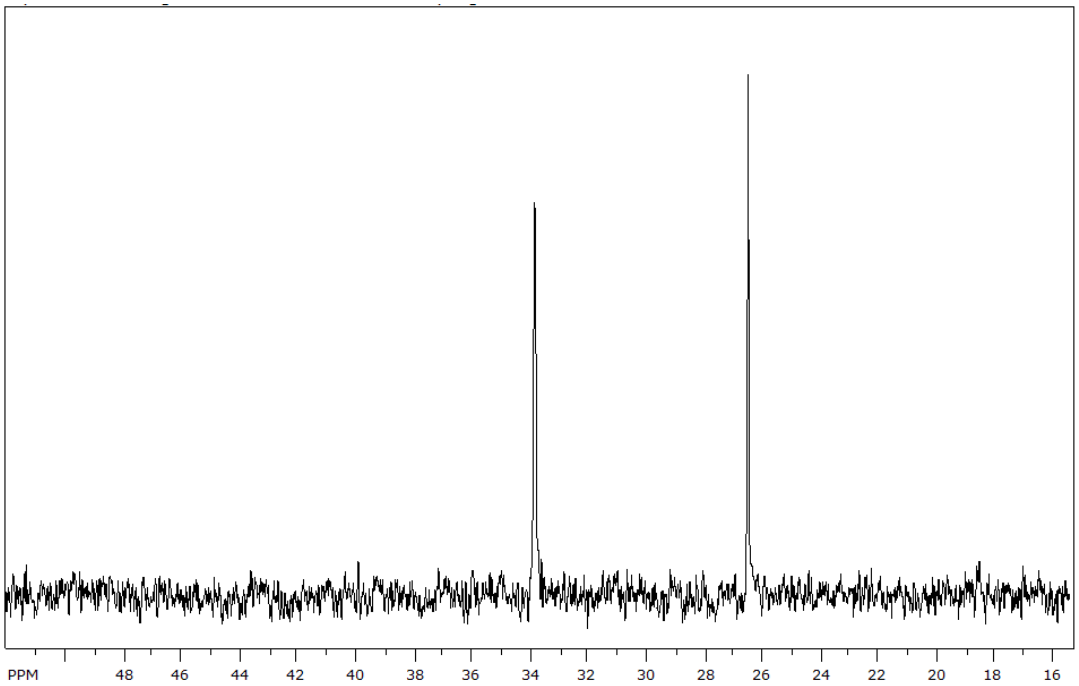

Fig. 3.8. ^{31}P NMR spectrum of PA blend 1, hydrolysed by method one.

The spectrum shows resonances at δ 33.8 and δ 26.5. The four possible phosphorus environments are shown in Fig 3.6 on molecules **12**, **13**, **14** and **15**. The presence of significant amounts of molecules **14** and **15** in blend 1 after hydrolysis is unlikely and therefore, the two observed resonances are likely to be associated with the sodium salts

of molecules **12** and **13,** which correspond to molecules **10** and **11** (Fig. 3.5), respectively. The disodium salt **11** would be expected to have a more deshielded phosphorus environment than the monosodium salt **10**. It is therefore possible to assign the resonance at δ 26.5 to the disodium salt **11** and the resonance at δ 33.8 to the monosodium salt **10**. Further support for this assignment comes from the fact that the resonance at δ 33.8 decreases in intensity after prolonged refluxing in HCl. By comparing the integrals of the two peaks, the molar ratio of **10** to **11** can be determined, and hence the extent of hydrolysis into the di-acid species.

Different hydrolysis conditions were explored for blend 1. Originally method one was tried, however when the PA dispersion was added to the prepolymer mixture (membrane formulation types A and B, the other formulations were not tested with PA hydrolysed by method one), a visually inhomogeneous mixture was formed. When the polymer solution was cast and cured, the resultant membranes were visually inhomogeneous and brittle.

Method two hydrolysis used the same reaction conditions and work up as used as method one, however the PA was dispersed in water instead of methanol. When this PA dispersion was added to the prepolymer solution, a visually homogeneous solution was formed, and when this solution was cast and cured, the resultant membranes appeared visually homogenous in nature. Following digestion in NaOH the ^{31}P NMR spectrum revealed that the extent of hydrolysis was only 73%, with 27% remaining as the monoester monoacid in the PA dispersion.

This significant amount of mono-ester, mono-acid **12** could lead to a significantly lower proton conductivity than the di-acid **13** when incorporated into a PEM. Although the second acid group is significantly weaker than the first acid group, this would still mean 13.5% less acid groups available in the PA.

To maximise the proton conductivity of derived PEMs, a method of hydrolysis was investigated to produce fully hydrolysed PA **13** and **15**. In method three, Dean-Stark distillation was used for the first two hours of hydrolysis, after which time the Dean-Stark apparatus was removed. An amount of concentrated HCl was added, which was equivalent to the volume of methanol removed and the reaction mixture refluxed for an

additional 22 hours. This was to remove methanol formed from the hydrolysis of the phosphonate ester groups and ethanol produced from the hydrolysis of the silyl ester groups. According to Le Chatelier's principle, a system moves to oppose any changes placed on it, thus by removing the methanol produced by hydrolysis, the system moves to produce more methanol by hydrolysing more of the phosphonate ester, thus creating a more hydrolysed PA. Using this method of hydrolysis, 100 % hydrolysed PA was produced.

Method four was employed to determine whether an increase in temperature and HCl volume could also increase the hydrolysis conversion of the phosphonate ester. In this method, the reflux temperature was increased to 115 °C and the volume of 6 M HCl added was doubled to twice that of the volume of PA_E to be hydrolysed. This method also produced PA which was 100 % hydrolysed into the di-acid form.

To determine the relative efficiencies of methods 2 to 4, a small aliquot of each reaction was taken at 1, 2, 4, 6 and 24 hours. Each aliquot was placed in an oven at 100 °C overnight, and the resultant glass was digested in $NaOD/D_2O$ and the ^{31}P NMR spectrum was then recorded for each specimen using a phosphoric acid standard. As an example, the spectra for method four are shown in Fig 3.9. As can clearly be seen in the spectra, the peak at δ 34 gradually decreases in intensity to where in the NMR spectrum and after 24 hours it is no longer visible leaving only the peak at δ 26.5 associated with the disodium salt **11**. The extent of hydrolysis as a function of time for methods two, three and four is summarised graphically in Fig. 3.10.

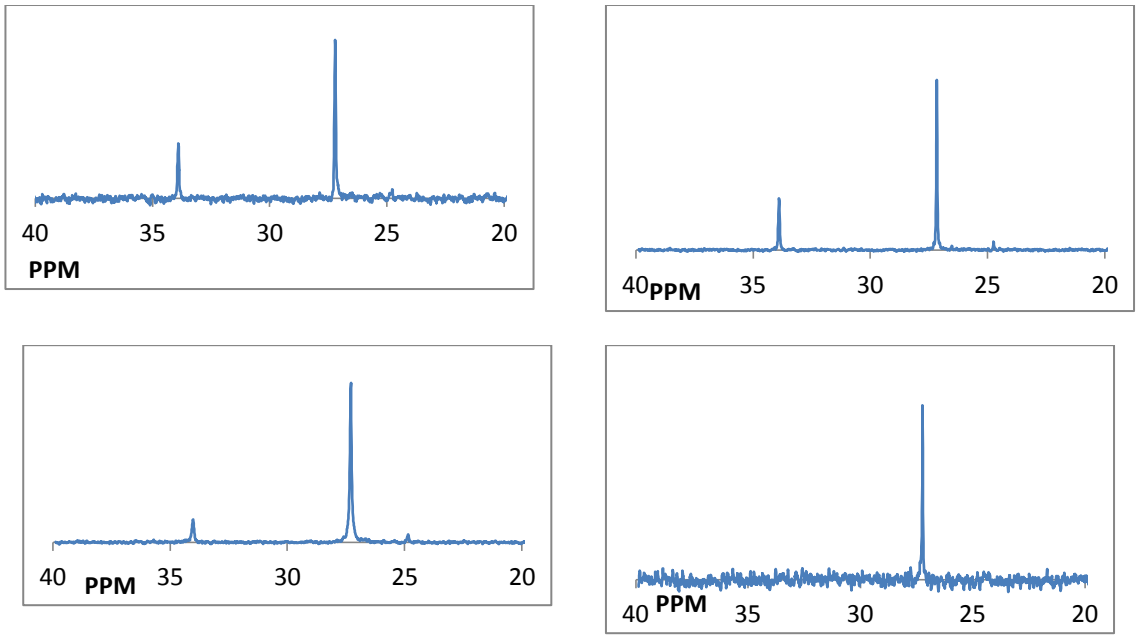

Fig. 3.9. ^{31}P NMR spectra of PA hydrolysis by method 4. Top left after 2 hours, top right after 4 hours, bottom left after 6 hours and bottom right after 24 hours

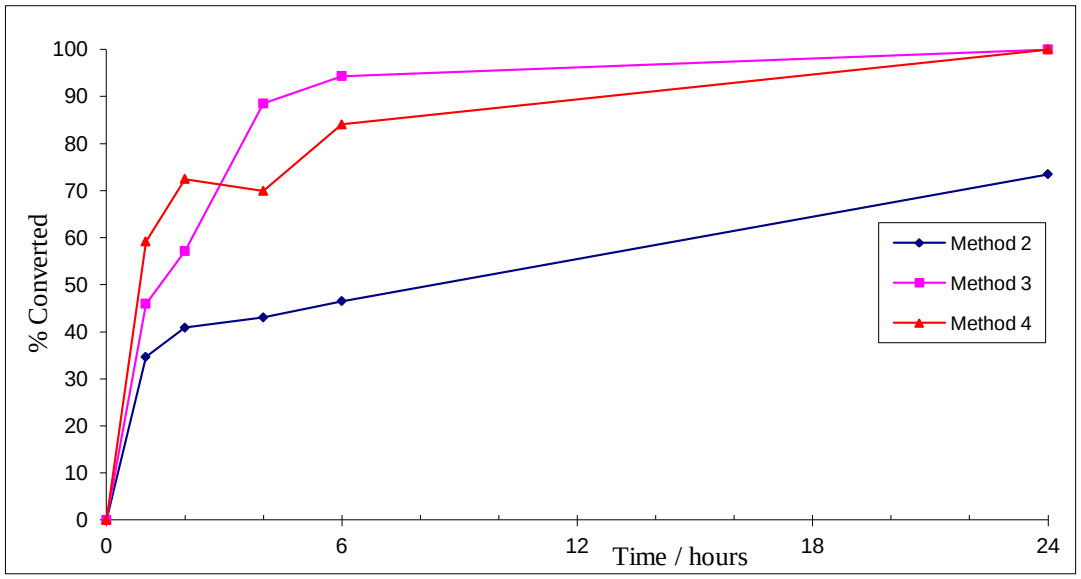

Fig. 3.10. Hydrolysis of PA_E blend 1 as a function of time and conditions (methods two to four).

As can be seen in Fig 3.10, for method two hydrolysis there is a rapid conversion into the di-acid during the course of the first hour under reflux. The rate rapidly decreases after this time, to a maximum conversion of 73% after 24 hours. If the rate of conversion remains constant as it does between 2 and 24 hours, then 100% conversion

of the PA_E into the di-acid would occur after refluxing under these conditions for 48 hours.

Method three is a more efficient hydrolysis than method four. This is due to the fact that smaller amounts of reagents were used as well as a lower temperature. The conversion of PA_E into the di-acid PA was 97% complete by 6 hours, compared to 83% for method four and 46% for method two. Thus PA blends hydrolysed by method three were predominantly used in this project.

3.5 PA Particle Size Distribution

The particle size of the PA used is crucial for PEM synthesis and PEM properties. Ideally particle sizes should be small so that an even distribution of PA particles is obtained throughout the polymer matrix when used in PEM synthesis thus avoiding phase separation. Smaller particle sizes should also prevent phase separation between inorganic and organic components, which could effectively inhibit proton conductivity through the membrane. If the particles are too large, then they might not form a stable dispersion and would therefore be unsuitable for use in PEM synthesis (blends 5 and 6). Smaller PA particles should also improve the mechanical properties of the PEMs by enabling better cross-linking between particles with organic plasticisers.

In the present study particle size distributions were determined by dynamic light scattering (DLS). This technique measures the particle size of the PA in a dispersed medium (in this case water). For particle sizes to be accurately determined, the concentration of PA particles is reduced 100 times of that used in PEM synthesis. The major disadvantage of this technique is that the particle size measured is that of the PA particle and its surrounding solvent shell. This means that this technique overestimates the size of the particles. As a reference, the particle size of the PA_E of blend 1 was also recorded at similar concentrations to that of the hydrolysed PA. The results for particle size analysis by DLS for blend 1 hydrolysed by methods two to four are shown in Fig. 3.11. Results are also shown for aged PA hydrolysed by methods three and four. PA hydrolysed by method two did not show a noticeable difference in particle size after 1 year.

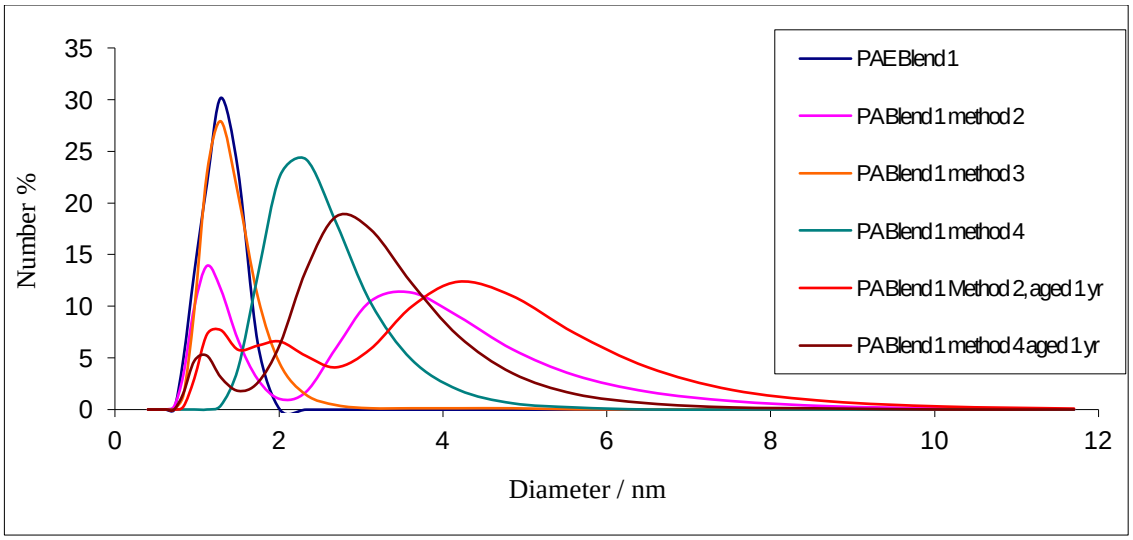

Fig. 3.11. DLS analysis of PA particle size, hydrolysed by different methods and aged

The average particle size of the PA_E was 1.3 nm (13 Å), or approximately 8 carbon-carbon single bonds. This very small particle size is consistent with the PA_E containing discrete molecules of **5** and **7** and not oligomers as in the hydrolysed PA. However, when the PA_E is hydrolysed by method three, the particle size of the resultant PA is nearly identical to that of the PA_E. This suggests only limited oligomerisation for PA_E hydrolysed by method three.

Method two hydrolysis resulted in an average particle size of 3.5 nm. This is over twice the size of the particles observed when method three hydrolysis is used. After aging for one year, a sample of the PA was re-measured and the particle size of the PA had increased significantly to 4.2 nm, with a broader particle size distribution observed. This indicates that during this time the PA particles agglomerated and condensed forming larger particles.

The PA_E hydrolysed by method four shows an intermediate particle size to those hydrolysed by methods two and three, with an average particle size of 2.3 nm, which increased to 2.9 nm when the dispersion was aged for one year. The decreased concentration of PA_E when refluxing (due to the doubling the volume of HCl added) helped prevent particles from forming larger oligomers. Again the increase in particle size over time can be rationalised by PA particles agglomerating and then condensing further to form the larger particles, which in turn also explains the larger distribution of particle size.

The average volume of the particles can be estimated from the average particle size by assuming the particles to be spherical (Eq 3.1)

$$v = \frac{4}{3}\pi\left(\frac{d}{2}\right)^3 \tag{3.1}$$

where d is the particle size diameter, and v is volume. From the volume, the number of condensed PA units making up the oligomer can be roughly determined assuming that volume of one PA monomer is that of 1.15 nm^3 as derived from the average particle size of 1.3 nm for non-hydrolysed PA_E.

Table 3.2: Estimated particle size volume as determined by DLS

Patricle Size diameter /nm	Particle size volume /nm^3	Number of PA units in oligomer
1.3	1.15	1
1.6	2.30	2
2.1	4.6	4
2.5	8	7
2.8	12	10
3.5	25	20
4.0	35	30
4.5	50	40
5.0	65	55
5.5	90	75
6.0	110	100

Therefore the PA hydrolysed by method three is typically composed of 1 hydrolysed unit of PA_E, whereas using method two, the PA oligomer is comprised of approximately 12 units of PA and when aged for a year this increases to an average of over 30 units, with a substantial number reaching 100 units in size (*ca*. 6 nm). The PA oligomer produced when hydrolysed by method four is typically comprised of approximately of 5 units of PA increasing to around 12 units after one year. The fact that the PA produced by hydrolysis method three does not increase in particle size upon aging for a year, indicates that using this method the PA dispersion formed is very stable.

3.6: Summary of PA_E Hydrolysis Results

Table 3.3 summarises the results of the hydrolysis experiments on PA blends 1 to 6. From these results, hydrolysis of PA blend 1 using method three was selected as the most efficient protocol to use for subsequent experiments.

Table 3.3. Preliminary results of PA hydrolysis of the different blends and hydrolysis methods for use in PEM synthesis

PA Blend	Hydrolysis method 1	Hydrolysis method 2	Hydrolysis method 3	Hydrolysis method 4
1	Formed inhomogeneous membranes	Incomplete hydrolysis, stable dispersion	**Complete hydrolysis, stable dispersion**	Complete hydrolysis, stable dispersion
2	Not tested	Incomplete hydrolysis, stable dispersion	Complete hydrolysis, stable dispersion	Complete hydrolysis, stable dispersion
3	Not tested	Not tested	stable dispersion	Not tested
4	Not tested	Not tested	stable dispersion	Not tested
5	Not tested	Not tested	Solid, not suitable for PEM synthesis	Not tested
6	Not tested	Not tested	Solid, not suitable for PEM synthesis	Not tested

3.7 Conductivity Measurements on Neat PA

Neat PA would be expected to exhibit higher proton conductivities than when the PA is distributed in a polymer matrix as part of a PEM. This would be due to the neat PA polymer having a much higher ion exchange capacity (IEC) and a much smaller equivalent weight (EW) than when it is diluted within another polymer matrix. In addition, the neat PA polymer would be expected to have greater proton conductivities under anhydrous conditions due to the fact that the concentration of the phosphonic acid groups would be large enough to act as the medium/proton solvent through which the Grotthuss mechanism of proton conductivity could occur. Considering the high concentration of phosphonic acid groups in close proximity to each other, when the neat PA polymer is exposed to high temperatures under anhydrous conditions the phosphonic acid groups can condense, reducing the number of available phosphonic acid groups from the polymer (Fig 3.12), thus reducing the IEC. Initially this condensation may actually improve proton conductivity for a short while as the condensation product is water, thus the system becomes self-humidifying for a short period of time, the length of which depends on the how high a temperature is used.

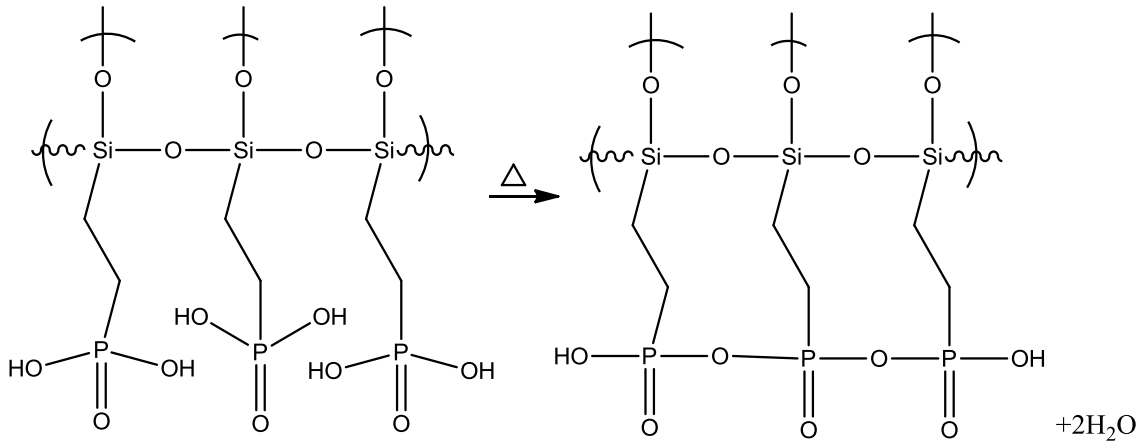

Fig. 3.12. Schematic representation of condensation reaction in neat PA polymer

As the blend 6 PA was a compressed powder, the measured resistances were larger than those of the blend 1 film. This is due to polycrystalline nature of the blend 6 PA sample, which resulted in a large concentration of grain boundaries with an associated resistance. As for the blend 1 sample which was a glassy film, no grain boundaries were present and thus the measured total resistance was lower.

The proton conductivity of blend 1 PA hydrolysed by method 3 was tested in the normal cell with no pre-conditioning, at 100% RH. When the sample of blend 1 PA was placed in the normal conductivity cell, heated to 120 °C and kept at that temperature for 1 hour the resistance decreased significantly. The results for blend 1 PA are summarised in table 3.4

Table 3.4. Variation of total resistance and total conductivity for blend 1 PA glassy film heated at 120 °C for 1 hour

Temperature / °C	Time / min	Resistance / Ω	Conductivity / S cm^{-1}
21	0	7900	5.0×10^{-6}
120	0	17	2.4×10^{-3}
120	30	7.5	5.3×10^{-3}
120	45	5.6	7.1×10^{-3}

The measured resistance at 120 °C after 1 hour was only 0.25 Ω, when the internal resistance of the cell was subtracted from this, it left a calculated resistance of just 0.05 Ω, which equates to a conductivity of 800 mS cm^{-1}. After this measurement, the chamber was allowed to cool and the cell removed allowing the sample to be inspected.

The sample had significantly degraded to the extent where a short circuit between the two electrodes occurred. This is in keeping with the observation that the film dissolved in boiling water. These two results showed the unsuitably for using neat PA blend 1 in humidified conditions for PEMFC applications.

The proton conductivity of the PA blend 1 film was also determined under ambient RH at room temperature and 0% RH at 120 °C, the results are shown in Table 3.5.

Table 3.5. Variation of total resistance and total conductivity for blend 1 PA glassy film heated at 120 °C for 1 hour at 0% RH over 2 heating cycles

Temperature / °C	Heating Cycle	Time / min	Resistance / Ω	Conductivity / S cm^{-1}
21	1	0	284000	3.2×10^{-7}
120	1	15	200	4.4×10^{-4}
120	1	30	160	5.6×10^{-4}
21	2	-	8500	1.1×10^{-5}
120	2	60	140	6.6×10^{-4}
120	2	120	140	6.6×10^{-4}
120	2	180	130	7.0×10^{-4}
21	3	-	7100	1.3×10^{-5}

As can be seen in Table 3.5, the proton conductivity of the dry membrane at 0% RH was significantly lower than that of the membrane at 100% RH. However, the proton conductivity at 120 °C was stable over the 3 hours of the second heating cycle measured during the second heating cycle. At the end of the end of the experiment there was no visible deterioration of the film. The long term stability of the proton conductivity of the PA film at 120 °C was not determined. It is possible that the proton conductivity would decrease over an extended period, due to acid condensation and the resultant water produced evaporating from the film.

3.8 Conclusions

PA can successfully be synthesised by the hydrolysis of esters dimethylphosphonatoethyltriethoxysilane and 2,4-*bis*(triethoxysilyl)-1-dimethyl phosphonatobutane. The ratio of these esters to each other is dependent on the reaction conditions used in their preparation. 98% pure dimethylphosphonatoethyltriethoxysilane can be prepared by slow dropwise addition of VTES during synthesis (blend 1). A variety of methods for hydrolysis of the ester were investigated, 100% acid hydrolysis

was efficiently achieved using a Dean-Stark apparatus and concentrated HCl (method three). This yielded PA particles of approximately 1.3 nm, a dispersion of which in water was stable up to one year. Proton conductivities of around 10^{-3} S cm^{-1} were observed for neat PA polymer at 120 °C in 100% RH. However, the neat PA polymer degraded under these conditions, so its use in as a PEM is limited. Nevertheless, PA prepared using blend 1 and method three could serve as a component in hybrid membranes for application in PEMFCs.

Chapter 4

Hybrid Polymer Electrolyte Membranes Incorporating PA as the Proton Source

4.0 Introduction

As described at the end of chapter 3, neat PA polymer is unsuitable for use in PEMFCs due to its lack of water stability. Therefore the aim of the project was to find a suitable polymer matrix to make a highly conductive, water stable and mechanically strong PEM using PA as the acid moiety. In the literature, there have been several different polymer formulations reported for phosphonic acid containing PEMs. Following preliminary studies carried out at Queen Mary, University of London and PhosphonicS Ltd on a variety of polymer formulations, a set of initial formulations was selected for further investigation in the present study. These formulations were based on mixtures of DPDM, glysil, SMEE, AMS, SMA, DVB, TEOS, DPO and PA (see Table 4.1 for structures and full names). Variation in the formulation and the effects of changes in the preparation conditions on the resulting membranes were investigated. Membrane stability and mechanical properties (elongation at break and flexibility) as well as the electrical conductivity were used to assess the suitability of the polymer electrolyte membranes (PEMs) for potential use in a proton exchange membrane fuel cell (PEMFC).

Table 4.1: Precursors used in original PEM synthesis

Name	Chemical Structure	Abbreviation
Dimethyl dimethoxy silane	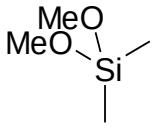	DMDM
Diphenyl dimethoxy silane	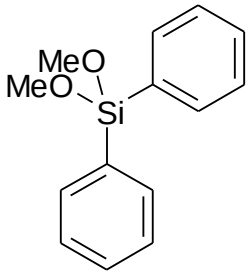	DPDM

Table 4.1 Continued

Phenyl trimethoxy silane	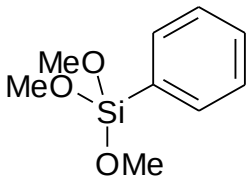	PTMS
Tetraethyl orthosilicate	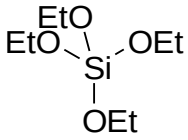	TEOS
3-(Trimethoxysilyl)propyl methacrylate	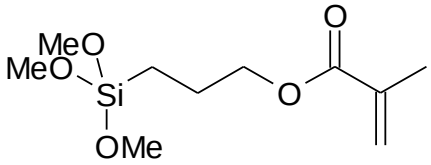	SMA
Acrylamide N-ethylsulfide ethyl trimethoxy silane	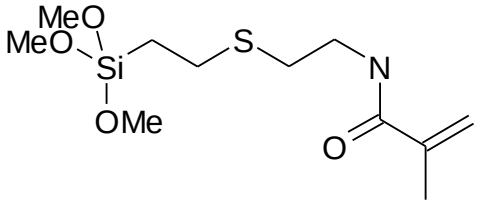	AMS
Tetraethylene glycol dimethaacrylate	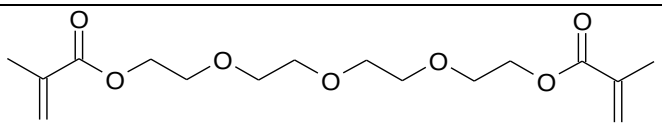	TEG
Divinyl benzene	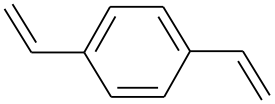	DVB
(3-Glycidyloxypropyl) trimethoxysilane	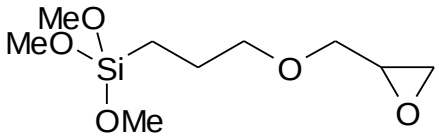	Glysil
2,2′-(Ethylenedioxy) Diethanethiol trimethoxysilane	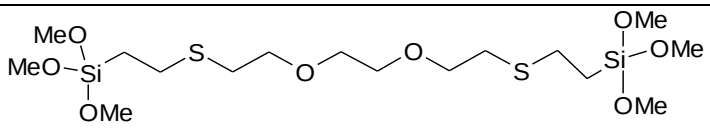	SMEE

4.1 Initial Polymer Formulation of PEMs

The concept of this method of PEM formulation was to create cross linked polymers via vinyl free radical polymerisation in addition to siloxane condensation between precursors. Some precursors such as TEG and DVB had only vinyl groups, some only had silyl ether groups for cross linking via siloxane condensation such as TEOS,

PERSIL and SMEE whilst others had a mixture of both silyl ether groups and vinyl groups such as AMS and SMA.

In a typical membrane synthesis, varying amounts of several (3-7) of the precursors shown in Table 4.1 were placed in a small reactor, along with PA (dispersed in methanol) with a free radical initiator (dibenzoyl peroxide, DPO) and refluxed overnight, whereupon the solution was then cast onto PFA sheets before being cured in an vacuum oven. There were a large number of membranes (several hundred) synthesised (by Dr Nico Galaffu at PhosphonicS Ltd) using a SOP which were evaluated (at QMUL as part of the present work) on the following criteria: water stability, mechanical properties and proton conductivity. The initial screening process involved immersing the membrane in boiling water. If the membrane survived the proton conductivity was measured at room temperature, 80 and 120 °C at 100% RH and preliminary mechanical properties were evaluated by bending the membrane around a cup. Due to the large quantity of PEMs synthesised, the majority of membranes were only tested once over three heating cycles, with the more promising membranes retested and remade to evaluate reproducibility.

All of the membranes synthesised from these precursors were brittle and had poor mechanical strength and tear resistance, as determined by dynamic mechanical analysis (DMA) and a simple test of bending the membrane around a cup of 60 mm diameter. The observed glassiness of the membranes was rationalised to have resulted from the relatively short polymer chains formed between the inorganic containing network formers and the PA. In addition, the nature of the free radical polymerisation used in the synthesis of the membranes meant that membrane reproducibility was not easily achieved. Another major problem with this approach was significant PA leaching from the membrane (1-10%) was observed for multiple membranes, thus showing that the PA was not being completely bound into the polymer matrix via adequate cross linking.

One of the better performing PEMs synthesised in these initial polymer formulations was that of membrane **575C**. This membrane was made from DPDM (2 mL), Glysil (1.5 mL), SMEE (1.5 mL), AMS (0.5 mL), SMA (1.5 mL), DVB (0.5 mL) TEOS (0.3 mL), DPO (0.5 mL), PA (6 mL), HCl (1 M, 2 mL) and methanol (15 mL). The DPO was dissolved in the methanol and heated to 50 °C, to which the SMA, DVB and AMS

were added and refluxed for one hour, DPDM, Glysil, SMEE and TEOS were then added and the mixture refluxed for an additional 30 minutes. Finally the PA and HCl were added and the reaction mixture was then refluxed for an additional 16 hours. The polymer solution was then cast and aged at room temperature for 16 hours before being heated for an additional 16 hours at 80 °C in a vacuum oven.

The proton conductivities of this membrane after various conditioning (none, steaming and immersion in deionised water) are shown in Table 4.2.

Table 4.2a Variation of total Resistance and total conductivity for 575C membrane heated at 120 °C over four heating cycles, no pre-conditioning, 100% RH

Temperature / ºC	Cycle	Resistance / Ω	Conductivity / S cm^{-1}
20	1	52800	4.2×10^{-6}
80	1	260	8.4×10^{-4}
120	1	25	9.5×10^{-3}
20	2	630	3.5×10^{-4}
80	2	55	3.9×10^{-3}
120	2	45	5.1×10^{-3}
20	3	1470	1.5×10^{-4}
80	3	180	1.2×10^{-3}
120	3	17	1.3×10^{-2}
20	4	55	3.9×10^{-3}
80	4	33	6.6×10^{-3}
120	4	25	8.8×10^{-3}

Table 4.2b: Variation of total resistance and total conductivity for 575C membrane heated at 120 °C over four heating cycles, conditioned by immersion in deionised water 5 days, 100% RH

Temperature / ºC	Cycle	Resistance / Ω	Conductivity / S cm^{-1}
20	1	31000	7.7×10^{-6}
80	1	550	4.4×10^{-4}
120	1	50	4.8×10^{-3}
20	2	570	4.2×10^{-4}
80	2	75	3.2×10^{-3}
120	2	50	4.8×10^{-3}
20	3	700	3.4×10^{-4}
80	3	50	5.0×10^{-3}
120	3	35	6.9×10^{-3}
20	4	55	4.5×10^{-3}
80	4	35	6.9×10^{-3}
120	4	30	8.0×10^{-3}

Table 4.2c: Variation of total resistance and total conductivity for 575C membrane heated at 120 °C over two heating cycles, steam conditioned, 100% RH

Temperature / ºC	Cycle	Resistance / Ω	Conductivity / S cm^{-1}
20	1	5500	5.3×10^{-5}
80	1	480	6.0×10^{-4}
120	1	7	4.3×10^{-2}
20	2	5650	5.1×10^{-5}
80	2	15	2.1×10^{-2}
120	2	160	1.8×10^{-3}
20	3	8000	3.6×10^{-5}

As can be seen from Tables 4.2a-c, the proton conductivity of the 575C membrane for the non-conditioned and immersed condition membranes was similar over the different cycles, with almost identical conductivities on the fourth heating cycles. Whereas the immersed conditioned membrane showed improvement in proton conductivity in subsequent heating cycles, the non-conditioned membrane showed the highest conductivity on the 3rd heating cycle and subsequently the 4th heating cycle showed lower proton conductivities (albeit the same as the immersed conditioned membrane). This implied that first heating cycles for the non-conditioned membrane acted as a conditioning step, which resulted in the higher observed conductivities.

The steamed conditioned membrane unsurprisingly showed the highest proton conductivities on the first heating cycle, this was due to the higher initial water absorption observed on steaming compared to immersing in water. However, the observed proton conductivity drops significantly on the second heating cycle to below the immersed and non-conditioned membrane values at 120 °C. This indicated that steaming had a detrimental effect on the membrane, which suggested that long term direct exposure to high temperature water vapour would result in membrane degradation, thus reducing the efficiency of the PEMFC.

The proton conductivities observed at low temperatures over the first heating cycles were very low, ranging from 10^{-6} to 10^{-4} S cm^{-1}, which is significantly lower than the requirements needed for a cold start of a PEMFC (0.01 S cm^{-1}).[6] The reason for the low observed proton conductivities for the 575C membrane was rationalised as resulting from low PA loading of the membranes which was 12%, when the acid content of the

membrane was increased to try and increase the proton conductivities the membranes became unstable in boiling water and dissolved.

The ion exchange capacity (IEC), equivalent weight (EW) and water molecules per acid group (λ) values of the 575 membrane was determined from several membranes synthesised at different times, this enabled the reproducibility of the membrane to be evaluated, and the results are shown in Table 4.3.

Table 4.3. Properties of 575C membrane

Membrane	IEC / mmol g^{-1} equiv	Water uptake / %	EW	λ
575C Original	1.39	12.9	719	5
Repeat 1	1.58	12.8	632	5
Repeat 2	1.23	14.1	813	7
Repeat 3	1.04	8.6	961	5
Mean	1.31	12.1	781	5
Standard Deviation	0.23	2.4	141	1.2
% S.D.	18%	20%	18%	24%

As shown in Table 4.3, the results of the IEC and water uptake of the different 575C membranes vary considerably, the IEC range from 1.04 to 1.58 mmol g^{-1} equiv over the four membranes tested, with a standard deviation for IEC and water uptake of 18 and 20% respectively. This shows that this method of membrane synthesis and preparation does not produce PEMs with very reproducible properties.

One of the major problems with the 575C membrane was the brittleness and glassy nature of the membrane. When the membrane was in the dry state, cutting it resulted in numerous fractures appearing along the edge of the membrane, which ranged in size from micro-fractures (visible via optical microscopy) and visible fractures of up to 5 mm. It was observed that when the membranes were softened by conditioning (immersing in water and steaming) the visible fractures were substantially reduced; however when looked at through an optical microscope, the micro-fractures were still visible.

Thus because of the poor mechanical properties, low room temperature proton conductivities and reproducibility issues of membrane synthesis, it was decided that a

new approach was needed to synthesise PEMs containing PA as the functional proton donor group. To achieve more reproducible results, free-radical polymerisation should be avoided; to improve the mechanical properties of the membrane a flexible spacer should be used and to improve low temperature (and high temperature and/or low humidity) proton conductivities the polymer matrix should be able to act as a proton solvent, enabling transport of the proton through the membrane.

4.2 Polyethylene Glycol Polymer Formulation

Polyethylene Glycol (PEG) which is also known as polyethylene oxide (PEO) has been widely used in lithium batteries as a low cost ion conductor for the transport of lithium ions under anhydrous conditions.[68,69] High molecular weight (MW) PEG forms a coil, (which also forms the basis of the elasticity Spandex/lycra) which due to the ether bonds can efficiently transport lithium ions through the core of the coil when a voltage is applied.[70] Thus PEG was seen as an ideal candidate for the basis of a polymer matrix of a PEM, however whether the PEM would be capable of proton conductivity needed to be determined, under anhydrous and humidified conditions.

The next stage in evaluating PEG for use as the prepolymer for PEM synthesis was to find a way in which to covalently bond the PEG to the PA, either directly or indirectly. The PEG has terminal hydroxyl groups and the only way to covalently bond them directly to PA is for condensation to occur between them and the silanol hydroxyl groups. However, there was no evidence in the literature that supported that this reaction would occur in sufficient quantity to form a fully condensed polymer. In fact, alcohols, including polyols, act as a mediator in silanol cross-condensation to form siloxane bonds.[71]

A literature search of inorganic-organic hybrid polymers containing PEG and SiO_2 revealed several approaches for synthesising hybrid materials. Reports on the use of low concentrations of inorganic material to enhance the stability of highly elastic polyurethane material, was not applicable to this project.[72,73] However, there were two approaches that have been employed to create hybrid PEG-SiO_2 polymers for use as PEMs for PEMFC applications. The first method involved doping a hybrid membrane with a low MW PEG (400 Da) which was not covalently bound into the polymer matrix.[74] The second method was to firstly react the PEG with an isocyantate or amine

terminated silyl ether, and then hydrolyse the silyl ether to form a cross linked siloxane polymer network.[50,75] However, for these membranes, acid containing surfactants were used as the proton sources.

To determine whether or not the latter approach could be applied when PA was used as the proton source instead of a surfactant dopant, and to determine whether the PA would be covalently bonded into the polymer matrix, the procedure employed by Honma *et al.*[49,50] was initially used, replacing the surfactant with PA to make a membrane that contained 20% w/w PA. The PEG used was 600 Da as this was the optimal chain length reported in the literature by Honma *et al*. However when blend 1 PA hydrolysed by method 1 (dispersed in methanol) was added to this prepolymer, an inhomogeneous solution was formed. When the PA was hydrolysed by method 2 (dispersed in water), the solution formed was visually homogeneous and this was used to cast a membrane successfully (membrane 023, see chapter 2 for synthesis conditions).

This initial membrane showed that the approach Honma *et al.* used could successfully be applied to synthesise membranes containing covalently bound PA. To determine the effects of PEM formulation, both the PEG MW and amount of PA added to the membranes were varied and this formed the **Type A** PEMs. These PEMs had high water uptake and swelling properties, which lead to modifications to the polymer matrix to form the **Type B** PEMs, which included an aromatic component (MDI) which made the PEM more hydrophobic, thus reducing both swelling and water uptake; however the mechanical properties (flexibility) of the membranes were generally poorer compared to those of the Type A PEMs. This, in turn lead to the development of **Type C** PEMs, which replaced the aromatic group by an aliphatic group, thus retaining the hydrophobicity of the Type B PEMs whilst having similar mechanical properties to those of Type A PEMs. However the mechanical properties were not discernibly different from those of Type B PEMs. **Type D** PEMs were developed to improve the mechanical properties and decrease the water uptake and swelling over Type B PEMs, and consisted of a "hard segment" of two bis aromatic groups separated by a short PEG spacer, these PEMs had excellent mechanical properties, exceeding those exhibited by Type A PEMs and lower water uptake and swelling than Type B and C PEMs. However, due to the increased size of the organic chain/spacer, the EW and IEC of the

Type D PEMs were reduced, and hence the observed conductivity was lower than Types A, B and C.

At this point it was decided to modify Type A PEMs to change the PEG chain with other polyethers to give **Type E** PEMs which contained polypropylene glycol (PPG) and **Type F** PEMs which contained polytetrahydrofuran (PTHF) to counter problems arising from Type A, B, C and D PEMs. An overview of PEM formulation history is shown in a flow chart in Fig 4.1. The flow chart gives a brief description of the (desirable and undesirable) properties of each PEM type. For the mechanism of polyurethane bond formation see chapter 1.5.1.

The overall aim was to synthesise a PEM that meets the criteria listed in chapter 1.2.1

- 0.1 S cm^{-1} conductivity at operating temperature
- $\leq$ 0.07 S cm^{-1} conductivity at room temperature
- Be low cost
- Exhibit high ionic conductivity
- Be electronically insulating
- Be gas impermeable
- Show conduction independent of water content
- Exhibit good high temperature performance (including improved CO tolerance)
- Maintain conduction in face of repeated exposure to condensed water
- Be able to conduct sufficiently at low temperature to allow bootstrapping of stack
- Be durable
- Show good interfacial properties
- Have mechanical strength

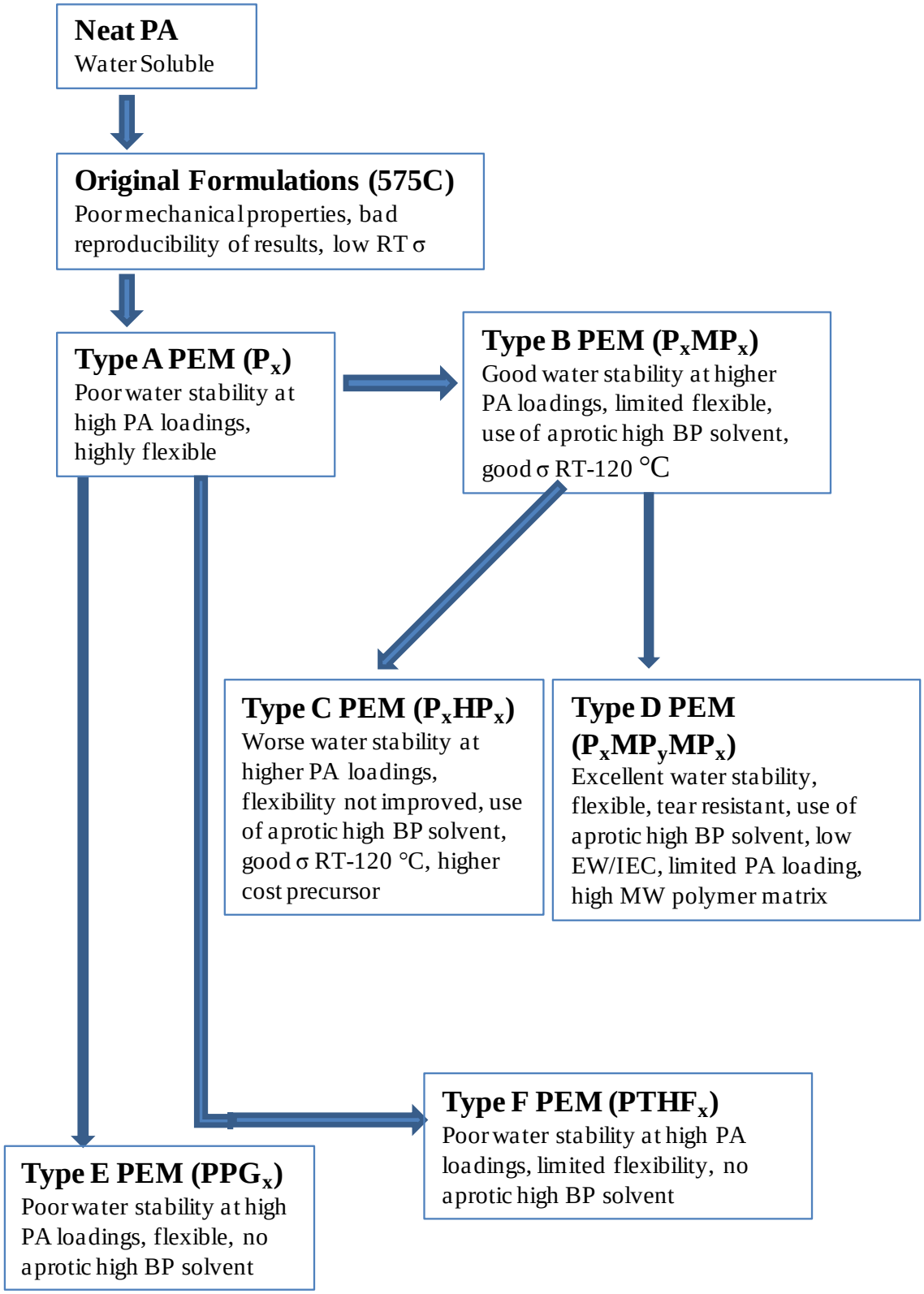

Fig. 4.1. Flow chart of PEM type synthesis evolution, P = PEG, M = MDI, H = HDI, *x* and *y* denote polyether MW ÷ 100 (eg PEG MW 200 is represented by P_2)

4.3.1 Type A PEM Synthesis

Typically, to synthesise Type A polymer matrices, 8 mmol of TPSI and 4 mmol PEG were reacted together without the use of a solvent at 70 °C and with continuous stirring for 5 days as described by Honma *et al.*[49,50,] to form the desired silyl end-capped prepolymer (as shown in Fig 4.2). Honma *et al.* reported that membranes using PEG 600 showed optimal mechanical properties and proton conductivity, so this formulation was tried first.

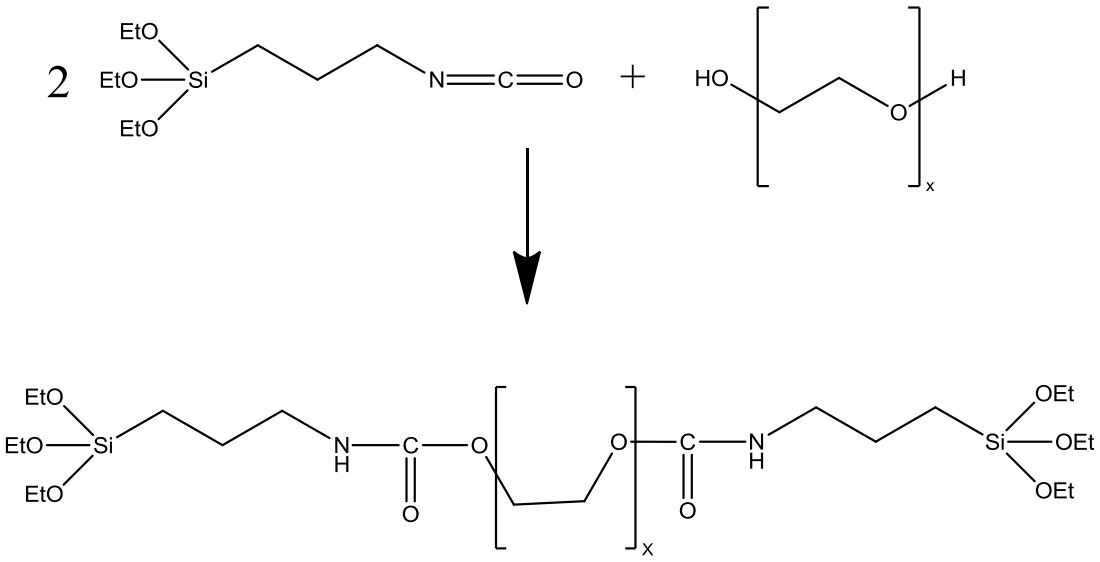

Fig. 4.2. Reaction of Type A pre-polymer formation

The higher molecular weight PEGs (600 and 1000 Da) were solids, which melted upon reaching 70 °C, however PEG 600 was sometimes difficult to manipulate as it has a melting point just above ambient room temperature (*ca.* 24 °C) so it was stored in the fridge to keep solidified and removed as required.

Once the prepolymer was formed (as shown in Fig. 4.2), PA was added to hydrolyse and condense the polymer matrix to form a sol. Blend 1 PA, hydrolysed by method 1 was originally tried. However upon addition of the PA a homogenous suspension was not formed, but rather discrete large agglomerates were visible. When this sol-gel was cast onto a polystyrene Petri dish and cured in an oven overnight at 60 °C, the resulting membrane was visibly inhomogeneous and had poor mechanical properties.

This membrane formulation was then repeated but instead used addition of Blend 1 PA hydrolysed by method 2 (membrane 024). When this PA was added (dispersed in water

instead of methanol), the sol formed was homogenous in nature, and when cast onto a polystyrene Petri dish and cured in an oven overnight at 60 °C, the resulting membrane was visibly homogenous. This indicated that for future membrane formulations and synthesis, blend 1 PA should be dispersed in water and not methanol. The difference in homogeneity between PA dispersed in methanol and water was likely to be caused by the hydrolytic polycondensation being much faster for all the components when the PA was dispersed in water and this factor prevented the phase separation as observed when the PA is dispersed in methanol.

Membranes containing PEG with MWs 200, 400, 600 and 1000 were then systematically synthesised with different PA (blend 1, method 2) loadings (membranes 001 to 039 respectively).

4.3.2 Type A Results

It was found that membranes that contained higher MW PEG had better mechanical properties and higher proton conductivities. Indeed membrane 038 (PEG 1000, 40% PA w/w, blend 1 method 2) exhibited excellent proton conductivities over a wide temperature range, from room temperature to 120 °C, the results of which are shown in Table 4.4 and Fig. 4.3 (Nyquist plots of the impedance spectra from the steamed membrane). The conductivities obtained were also stable for up to 52 hours at elevated temperatures, and the conductivities obtained were comparable with those obtained from different membrane conditioning regimes, such as steaming for one hour or immersion in warm deionised water for one hour, as shown in Table 4.5.

Table 4.4: Variation of total resistance and total conductivity for membrane 038 (PEG 1000, 40% PA w/w, blend 1 method 2), heated at 120 °C over two heating cycles, conditioned by steaming for 1 hour and measured at 100% RH, 290 μm thick.

Temperature / °C	Cycle	Resistance / Ω	Conductivity / S cm^{-1}
30	1	37	3.1×10^{-2}
80	1	3	3.5×10^{-2}
27	2	5.9	2.0×10^{-2}
40	2	2.6	4.5×10^{-2}
60	2	2.4	4.8×10^{-2}
80	2	2.6	4.5×10^{-2}
100	2	5	2.3×10^{-2}
120	2	2.5	4.6×10^{-2}

120 °C after 17 hours, cycle 2, R = 1.8 Ω, $\sigma = 6.4 \times 10^{-2}$ S cm^{-1}

Table 4.5. Variation of total resistance and total conductivity for membrane 038 (PEG 1000, 40% PA w/w, blend 1 method 2), heated at 80 °C for 52 hours, conditioned by immersion in warm deionised water for 1 hour and measured at 100% RH, 350 μm thick.

Temperature / °C	Time / hour	Resistance / Ω	Conductivity / S cm^{-1}
30	-	6.1	2.3×10^{-2}
80	1	2.5	5.6×10^{-2}
80	52	3.4	4.1×10^{-2}

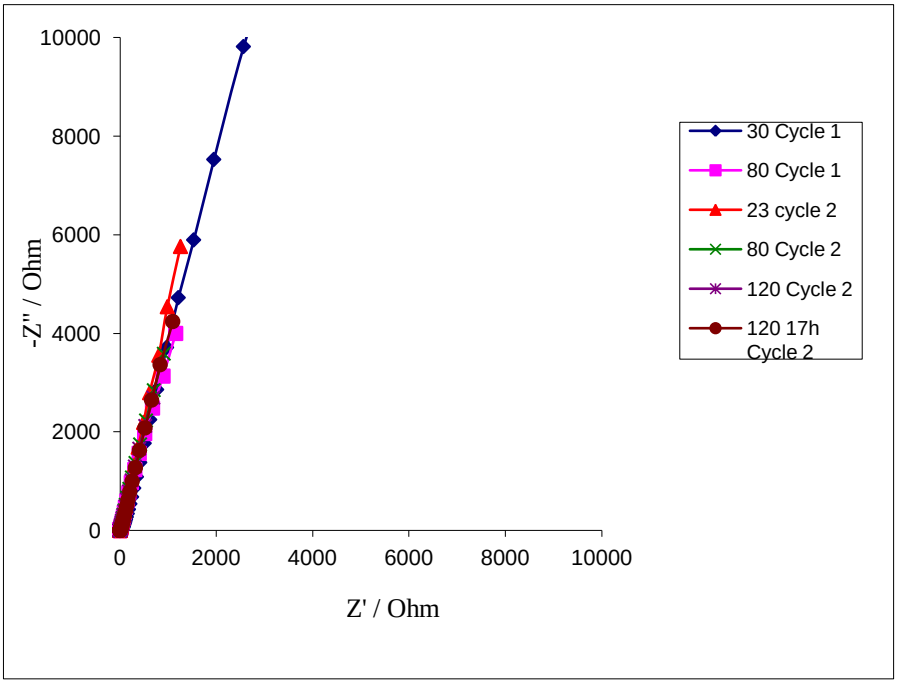

Fig 4.3a: Impedance spectra for membrane 038, heated at 120 °C over two heating cycles, conditioned by steaming for 1 hour and measured at 100% RH

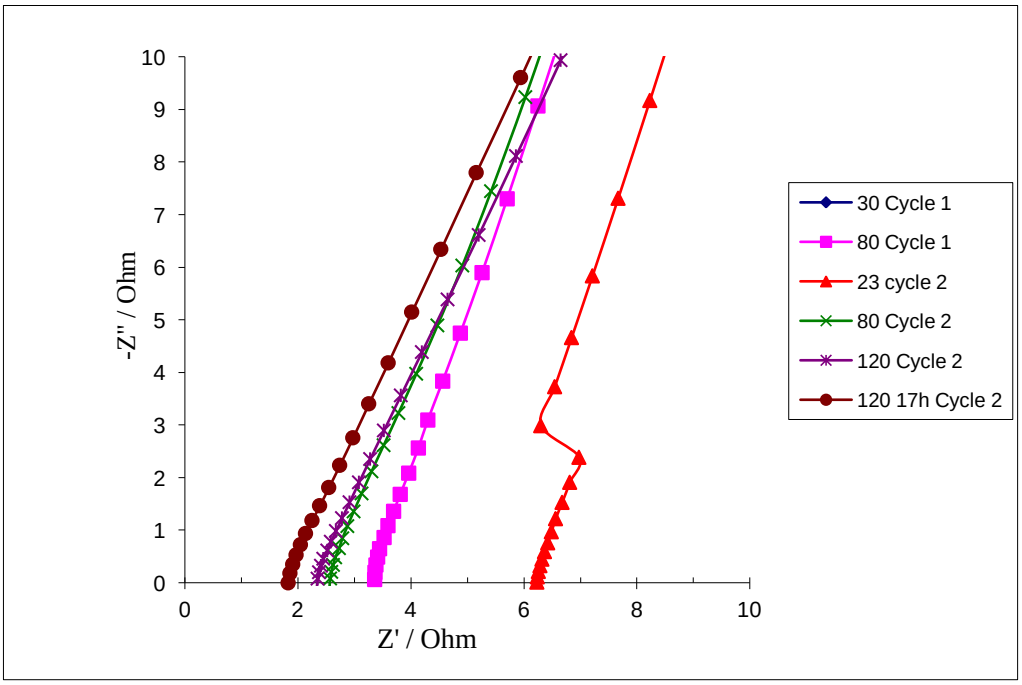

Fig 4.3b: Very high frequency impedance spectra for membrane 038 heated at 120 °C over two heating cycles, conditioned by steaming for 1 hour and measured at 100% RH

4.3.3 Comparison of PA Hydrolysis methods 2 and 3 for Type A PEMs

Two batches of Type A PEMs with PEG 600 were produced, one containing Blend 1 PA hydrolysed by method 2, and the other by method 3, to determine whether or not

there was any difference in proton conductivity between the membranes which had PA which was partially hydrolysed and membranes that had fully hydrolysed PA. The two PA loadings investigated were 30% and 60% PA w/w. The 60% PA loaded membranes were both immersed in warm deionised water prior to measurements for one hour. Due to their poor water stability, the membranes prepared using both types of PA substantially deteriorated during the course of this preconditioning step.

The membranes containing 30% PA were labelled membrane 031 (PA hydrolysed by method 2) and membrane 032 (PA hydrolysed by method 3). Both membranes were immersed in warm deionised water for a preconditioning step and did not visibly deteriorate. The results are shown in Table 4.6 and show that the PEM containing Blend 1 PA hydrolysed by method 2 (membrane 031) had a room temperature proton conductivity that was an order of magnitude lower than the membrane which contained Blend 1 PA hydrolysed by method 3. Membrane 031 had a proton conductivity of 4 mS cm^{-1} at 80 °C, however this value reduced substantially over the course of 5 hours to 1.2 mS cm^{-1}, after this time, the sample was removed from cell and had not visually deteriorated. This decrease is in contrast to membrane 038 which was also made using PA Blend 1 hydrolysed by method 2 and had a relatively stable conductivity over 52 hours at 80 °C (Table 4.5) , this implies that there was a difference to the extent of PA hydrolysis between batches of PA hydrolysed by method 2. The proton conductivity of membrane 032 was stable at around 2.4 to 2.7 mS cm^{-1} over the same time range and conditions.

Table 4.6: Total Proton Conductivities of membranes 031 and 032 at 21 and 80 °C, measured at 100% RH in the normal cell

Temperature / °C	Membrane 031 Conductivity / mS cm^{-1}	Membrane 032 Conductivity (sample 1) / mS cm^{-1}	Membrane 032 Conductivity (sample 2) / mS cm^{-1}
21	0.092	1.2	0.91
80	4*	2.7	2.4

*After 5 hours at 80 °C, the Conductivity of membrane 031 decreased to 1.2 mS cm^{-1}

These results indicated that Blend 1 PA hydrolysed by method 3 was more suitable for use as a precursor in PEM formulation than Blend 1 PA hydrolysed by method 2. To determine whether the membranes synthesised using PA hydrolysed by method 3 were reproducible, a second membrane of formulation 032 was made and this membrane

(sample 2) displayed similar proton conductivities to that of the original membrane 032 when measured under identical conditions, as shown in Table 4.7.

Table 4.7. Total proton conductivities of two samples of membrane 032 heated to 120 °C at 100% RH, measured in the normal cell

Temperature / °C	Sample 1 Conductivity / mS cm^{-1}	Sample 2 Conductivity / mS cm^{-1}
21	1.2	0.91
30	1.2	0.97
40	0.98	1.2
50	1.1	1.9
60	1.5	1.9
70	2.1	2.2
80	2.7	2.4
90	2.7	2.5
100	2.1	2.3
110	1.9	2.1
120	1.9	2.1

The results of the two samples of membrane 032 indicated that the Type A PEMs could be synthesised so that reproducible results could be obtained, unlike those membranes made using the initial PEM formulations that employed free radical reactions, such as those described in sections 4.0 and 4.1 (*i.e.* membrane 575C).

4.3.4 Discussion of A.C. Impedance Spectroscopy, derived resistances, conductivities and activation energies

Before the A.C. Impedance Spectroscopy (ACIS) results can be analysed in depth, the limitations of the technique must first be considered. ACIS is a qualitative tool for the evaluation of proton conductivities in PEMs, due to the many factors influencing the results of a frequency sweep, as well the different methods of interpreting impedance spectra. The quality and accuracy of the results can be improved by performing repeated measurements of the same sample of the membrane over repeated heating cycles and different samples of the same membrane over repeated heating cycles.

Despite ACIS being a qualitative technique, ACIS can be used as a routine way of determining the approximate conductivities of the sample under investigation at different conditions quickly and non-destructively. Therefore all given values of conductivities in the present work are only approximate for the specific conditions stated and not absolute. With this being considered, values of conductivity for a membrane can be considered the same if they vary within the same order of magnitude.

The graphs showing total conductivities of membranes over a temperature range are displayed with axis of Log_{10} σ vs 1000 / K (where σ is S cm^{-1}), although logarithms do not have units, the original units of S cm^{-1} are shown on the y-axis for clarity. In much the same way the data points of each membrane and heating cycle are connected with a line, which are not lines of best fit, this is to aid the reader to distinguish between heating cycles and different membranes. The axis Log σ was chosen due to the prevalence of reporting the results in this format in the primary literature, with Ln σ, Ln σT and Log σT also used in a lesser extent.

Lines of best fit can be plotted through one data series to determine activation energies of proton transport in graphs where the y-axis is Ln σ from the Arrhenius equation ($A=A_0e^{-Ea/RT}$) however due to the qualitative nature of the results this only gives an insight into the nature of conductivity within the PEM and not an unequivocal mechanism. To improve the quality of the line of best fit, conductivities at each temperature should be pooled and processed with error-bars included on the graph. However it must also be considered whether a PEM is the same or a different material at each temperature, even at the same RH, and whether or not repeated heating cycles also alters the PEM. In ceramic conductors, the chemical structure of the ceramic is a fixed unit cell, which is dependent on the conditions (pressure, temperature etc), upon changing of the temperature the structure will remain the same unless a phase transition is reached and passed, thus the activation energy of each phase can be determined by repeated measurements over many heating cycles. In glass conductors, there is no long range order to the chemical structure; however the chemical structure is still fixed as long as the glass is kept below the glass transition or melting temperature. However in polymers, the chemical structure is not fixed and has a certain degree of freedom for motion which varies from polymer to polymer, as well as with additives and conditions employed such as temperature and pressure. This means that it is possible that a PEM

has a different structure and morphology at each temperature, thus the PEM is not the same material at each temperature, and if it is a different material then the activation energies cannot be determined by fitting a line of best fit through the data points. The system gets even more complex when the water content of the membranes is taken into consideration. Water uptake by PEMs causes swelling (a change in physical dimensions) as well as a change in membrane morphology, as the water content of the membrane changes (from different temperatures, water vapour pressures and equilibration times) so would the structure of the membrane. Thus even if an impedance spectrum was re-recorded after a relatively short period of time (say 5 minutes) the membrane could have a different structure, thus a different conductivity than the previous measurement. So not only would determining the activation energy of proton transport accurately by this method be impossible, this leads to more errors in determining the conductivities of the material itself compared to glass and ceramic type conductors. Lastly another important factor must be considered when studying polymer materials in this experimental set up is that of polymer creep, which is the slow movement or deformation of the polymer when under stress. In the normal cell set-up the membrane was sandwiched between two solid stainless steel electrodes with pressure applied by screws going through the PTFE part of the conductivity cell. When heated the membrane could deform depending on what the final temperature was and how long it was maintained. In the present work, some membranes had suffered from significant creep, with the thickness of the sample decreasing and the area increasing. Again, this would not only effect the determination of activation energies, but also the conductivities.

A major problem with ACIS is that the technique cannot specify which ions are responsible for the observed conductivity or always distinguish different ions if they have similar mobilities through an electrolyte. In the present work the ion most likely to be responsible for the observed conductivities is that of protons, however the possibility that it could be a hydronium ion (via molecular diffusion instead of proton hopping) as well as non-bound PA and phosphorous acid diffusing across the membrane. To test the hypothesis that the observed conductivities is due to protons, a test similar to that of a leak test can be carried out to determine hydrogen mobility through the membrane (preferably when part of an MEA). In a leak test, an MEA is used as a separator between two chambers, in one chamber there is a low pressure of inert gas (nitrogen or

argon) and on the other side the chamber the chamber is filled with either air or oxygen. If oxygen is detected on the side which has the inert gas, then there is gas cross-over which is undesirable. By replacing oxygen with hydrogen gas, the mobility of hydrogen can be determined through the PEM/MEA. If hydrogen is detected then this means that the PEM is capable of proton transfer.

4.3.5 Type A PEMs conclusions and development to Type B membranes

Although membranes of polymer matrix type A were successfully synthesised and displayed excellent proton conductivities (40-64 mS cm^{-1}) up to 120 °C, they displayed poor water stability. The membranes containing high MW PEG and high PA loadings became very swollen when hydrated. When a sufficiently high perpendicular force was applied to the hydrated PEG 1000 membranes (as when measuring the thickness of the swollen membrane with a micrometer), they then disintegrated. In addition, the high MW PEG and PA loaded membranes, after impedance measurements were deformed (membrane creep); the thickness had decreased and the area of the membrane increased on the electrodes. For example, membrane 038 which was 290 μm thick and had an area of 0.25 cm^2 prior to impedance measurements, after being heated as described in Table 4.4, these dimensions had changed to approximately 135 μm thickness and an area of 0.34 cm^2, thus decreasing the cell constant (k) from 0.116 cm^{-1} to 0.0397 cm^{-1}. Due to the highly sticky nature of these membranes, they could not be successfully removed in their entirety from the electrodes so these dimension changes could not be recorded accurately. For a measured total resistance of 1.8 Ω (as measured at 120 °C after 17 hours on the second heating cycle) this would decrease the total conductivity from 64 mS cm^{-1} to 22 mS cm^{-1}. However, it is reasonable to assume that the change in dimensions occurred gradually over time when the PEM was heated at 100% RH, and thus the dimensions of the PEM (and hence the cell constant) would be different to those mentioned previously, making the accurate determination of total conductivity for the PEM impossible.

To improve the membrane water stability, composite PEMs that contained two different molecular weight PEG precursors were synthesised with various PA loadings. These included PEG 200/400, 200/600, 200/1000, 400/600, 400/1000 and 600/1000 pairs. However, this change in membrane formulation did not improve the water stability

properties of the Type A polymer matrix membranes, and so the results of these PEMs are not discussed in the present work.

There are two types of molecular forces between the polymer chains in Type A PEMs. One of these was the covalent siloxane bonds which formed from condensation between the silyl ether end-capped pre-polymer and the silanol groups on the PA; the siloxane bonds were formed during membrane curing. The second type of bonding was hydrogen bonding between the urethane bonds from two or more polymer chains when the PEM is in a dry state.[76] However in a PEMFC and for conductivity measurements, the PEMs were hydrated by exposure to water vapour (from membrane preconditioning and when heated at 100% RH). These water molecules diffuse through the membrane and disrupt the hydrogen bonding between the polymer chains, thus preventing the hydrogen bonds forming directly between polymer chains,[77] a representation of this is shown in Fig. 4.4. This swelling therefore also reduces the mechanical properties of the membranes. In PEMs that contain higher MW PEG (most notably PEG 1000), the membranes absorbed so much water that they became completely saturated and lost all mechanical stability, membrane 038 for instance absorbed 32% mass water and increased in thickness by 23%.

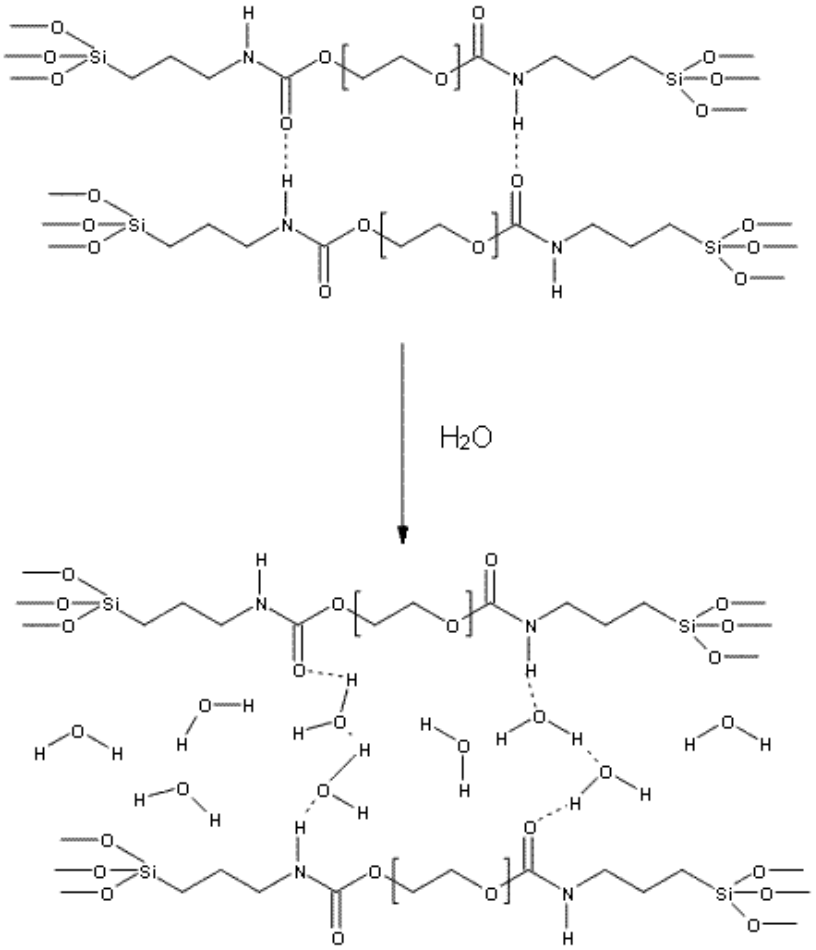

Fig 4.4: Representation of molecular forces in an anhydrous and hydrated Type A PEM

To improve the water stability of the PEMs, it was rationalised that the incorporation of hydrophobic components into the polymer matrix would decrease both water uptake and swelling of the membrane. PUs typically consist of two components, a soft segment and a hard segment. The hard segments are generally (hydrophobic) aromatic diisocyanates, the most common of which is MDI. MDI has also been used in the synthesis of organic/inorganic hybrid PUs,[78] although there have been no reports of MDI containing hybrid PUs for PEMFC applications in the literature to date.

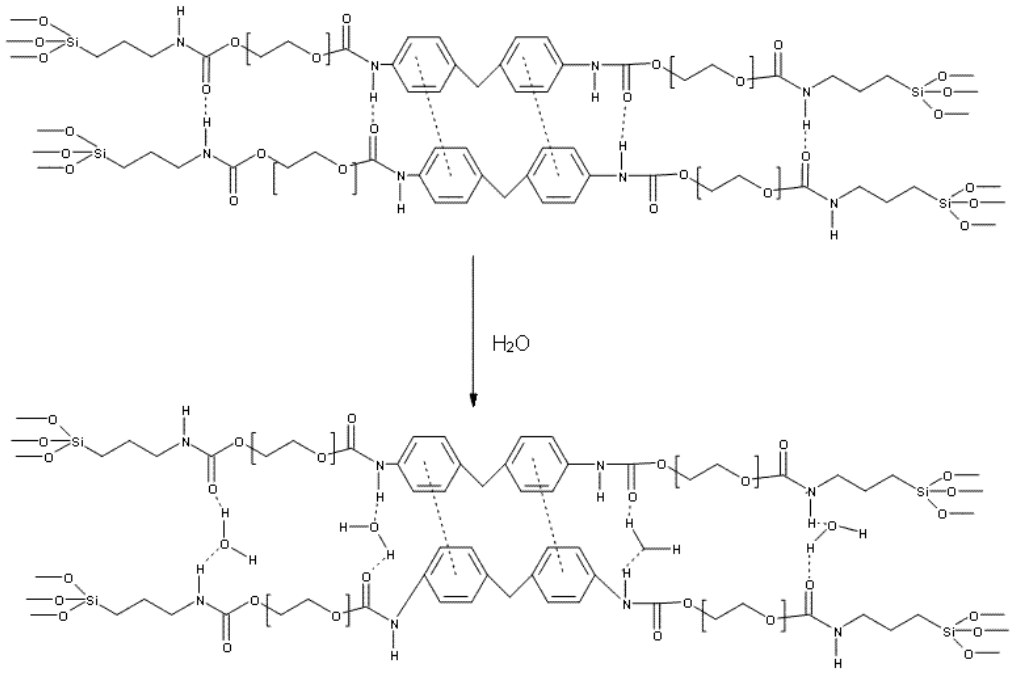

Fig. 4.5. Representation of molecular forces in an anhydrous and hydrated type B PEM.

The MDI introduces a third type of intramolecular bonding between polymer chains, that of π-π stacking of the aromatic ring systems (as illustrated in Fig. 4.5). As the aromatic rings are hydrophobic this bonding is not disrupted by absorbed water, so this limits the water uptake and hence the swelling of the hydrophilic parts of the polymer matrix. However, due to the nature of the forces in π-π stacking, this form of intermolecular bonding is not thermally stable and at higher temperatures becomes weaker.[79] There is also additional hydrogen bonding introduced from the urethane bonds on the hard (aromatic) segments and it was found that the thermal behaviour of this hydrogen bonding was independent of the morphology and depended primarily on the glass transition temperature of the hard segment.[80,81]

Elastomeric PUs typically consist of high MW diols (e.g. PEGs of MW 100 kDA and above) with low MW aromatic diisocyanates (e.g. MDI).[82] The high MW diols are typically coiled, and when a transverse force is applied they uncoil, thus enabling the PU to effectively stretch to many times its original length.[83] In this project relatively short chain PUs were synthesised and hence this mechanical property was not observed.

4.4.1 Type B Synthesis

The synthesis of MDI containing hybrid PU PEMs is described in detail in chapter 2.3.2.

Initially no solvent was used in the Type B synthesis as MDI has a low melting point (37 °C), which was well below the 70 °C reaction temperature employed. However, upon hydrolysis of the prepolymer a very hard resin was formed which could not be further manipulated. The literature indicated that an aprotic polar solvent was required, with the most commonly employed being NMP,[84] DMF[85] or DMSO.[86] Membrane synthesis was attempted with THF,[87] although due to the low boiling point the prepolymer synthesis was carried out at 60 °C. The use of THF as the solvent was unsuccessful as an inhomogeneous precipitate was formed upon hydrolysis, even after 5 days of stirring at 60 °C, which could be attributed to the lower temperature used for the reaction, or phase separation occurring when the PA dispersed in water was added. For similar reasons, the use of acetone as the solvent was not attempted, due to its lower boiling point than THF. NMP was chosen as the solvent due to its lower cost, lower volatility and lower toxicity compared to DMF and DMSO.

According to the literature, for organic/inorganic PUs syntheses involving MDI and using a polar aprotic solvent, each step of the reaction only took three hours without the addition of a catalyst,[88,89,90] *i.e.* the desired prepolymer was formed after six hours and not five days as needed for Type A PEM synthesis. This had the advantage of allowing synthesis of the desired prepolymer, hydrolysis of the prepolymer; addition of the PA followed by casting and curing the resultant sol-gel to produce a PEM within 24 hours.

As NMP was used as the solvent, polystyrene Petri dishes could not be used to cast the sol-gel. NMP is widely used in the plastics industry due its desirable properties (low volatility, toxicity and cost, and the ability to dissolve most polymers). New casting surfaces were needed for the Type B PEM synthesis. Various substrates were tried unsuccessfully, the results of which are shown in Table 4.8.

Table 4.8: List of different casting substrates used in Type B PEM curing

Substrate	Outcome
Polystyrene Petri dish	Sol-gel dissolved Petri dish
PFA	Sol-gel would not spread across PFA surface, resulted in very poor PEMs
Glass	PEM stuck to glass surface after curing, could not remove
Silicon wafer	PEM stuck to silicon wafer after curing, could not remove
PTFE	Sol-gel would not always spread evenly across PTFE, PEMs not always formed to adequate standard
OTS modified glass	Sol-gel spread well over the OTS glass surface, good PEMs routinely formed. However due to the modified glass surface prone to being damaged, recoating regularly was required

The PEMs formed when cast onto glass could not be removed in one piece, in many places they had to be scraped off with a blade, destroying the PEM. This was due to the fact that the glass forms surface hydroxyl groups, when curing; these hydroxyl groups undergo condensation with hydroxyl groups from the polymer, thus there was covalent Si-O-Si bond formation between the glass surface and PEM, a representation of this condensation is shown in Fig. 4.6.

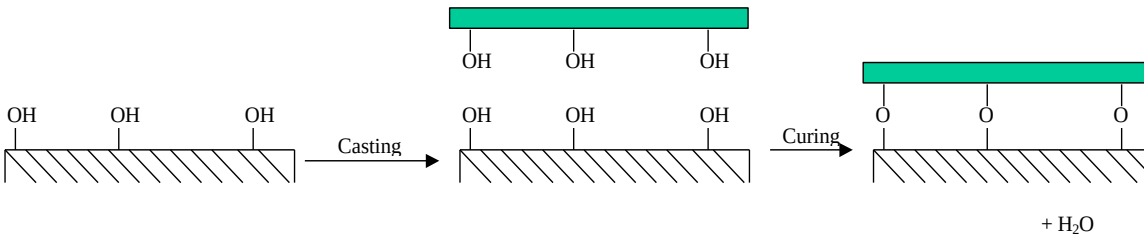

Fig 4.6: Si-O-Si condensation occurring between PEM and glass surface during casting and curing

As the PEM covalently bonded to the glass surface via surface hydroxyl groups, it was rationalised that if these surface hydroxyl groups were removed then the PEM formed could be removed from the glass surface, thus making glass an ideal casting substrate. This was achieved by modifying the glass surface with octadecyltrichlorosilane (OTS),[91] as illustrated in Fig 4.7 and described in chapter 2.4.3.

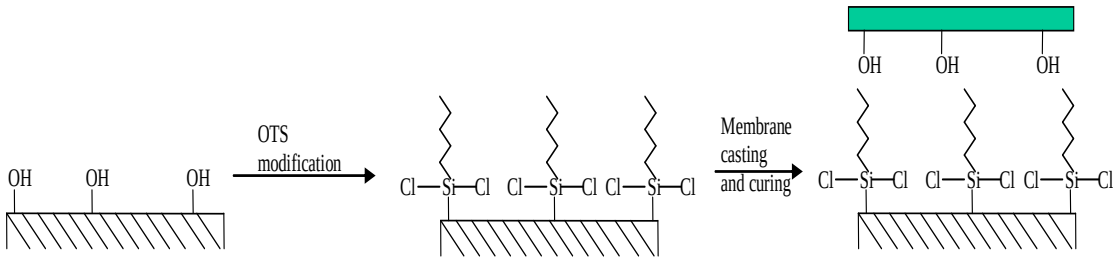

Fig 4.7: Representation of modification of glass surface with OTS, followed by PEM casting and curing

The coating of the glass effectively made the alkyl hydrophobic tail groups the casting surface. The sol-gel spread very well over the modified glass surface, and peeled off easily in one piece once the membrane was cooled after curing. However, when removing the membrane from the glass slide, the modified glass surface was often damaged which led to subsequent membranes sticking to the surface in places, and thus not being able to be removed in one complete piece. To prevent this from occurring, the glass sheets were retreated with OTS after several uses.

Initially, membranes containing PEG 100 to 1000 were synthesised in a systematic fashion with varying amounts of PA loadings as described in the experimental section 2.3.2 and Table 2.2. The general reaction conditions and precursors for the prepolymer synthesis are shown in Fig 4.8.

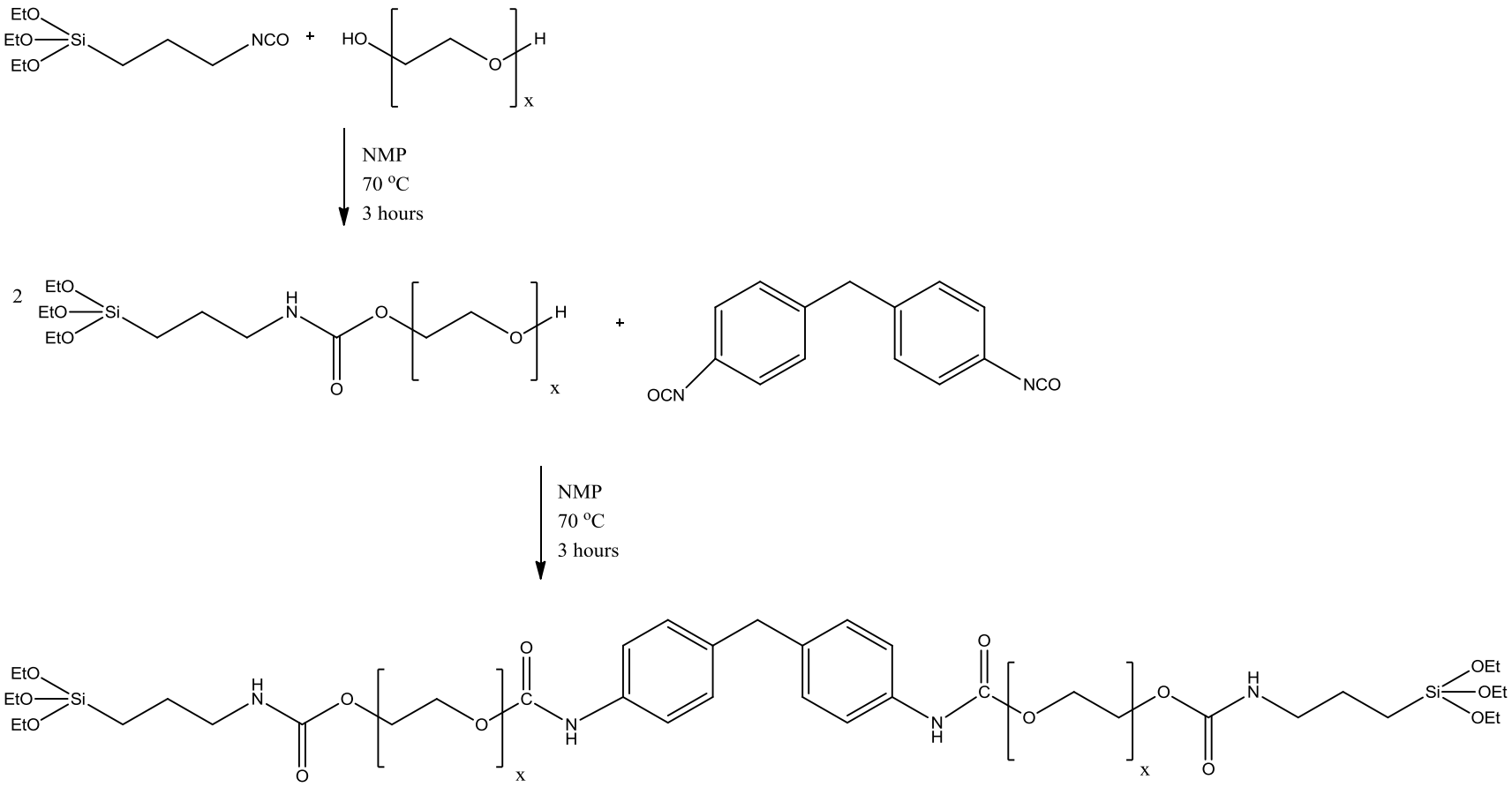

Fig 4.8: Structures of Type B precursors and prepolymer with reaction conditions, x varies depending on PEG MW, PEMs contain PEG MW 200 are denoted as P_2MP_2, PEG 400 as P_4MP_4, and PEG MW 600 as P_6MP_6

4.4.2 Type B Blend 1 Results

PEMs synthesised using PEG 200 showed good mechanical properties, these membranes were flexible enough to bend around a cup without breaking, and had comparatively low swelling (*ca.* 10-15%) compared to the equivalent Type A membranes which did not contain MDI (*ca.* 15-25% depending on PA content). As the PEG MW was increased the mechanical properties (most notably the flexibility) improved further, however the swelling and water uptake of the membranes increased significantly. For the PEMs synthesised from PEG 1000 for example, where $x \approx 6$, the membranes were flexible when dry, however when they were conditioned to perform impedance spectroscopy measurements, the membranes became very swollen, for instance membrane 098 (30% PA) absorbed 40% mass water and increased in thickness by 31% when hydrated, these membranes were easily torn when hydrated and upon application of a perpendicular force, the membranes disintegrated into a powder (*i.e.* they behaved like a gel). This was due to the fact that there were two PEG 1000 molecules incorporated into the prepolymer, effectively making a total of 12 repeating units of ethylene glycol per polymer chain, which made the PEM very hydrophilic, absorbing a significant amount of water. This made ACIS studies impossible to perform on these membranes. Table 4.9 states the water uptake and swelling of dry membranes when hydrated for selected Type B PEMs with increasing PEG MW and PA content. PEG 100 polymers were brittle and glassy, they could not be bent around a cup without breaking and when the membranes were cut, they visibly fractured, indicating that the PEG chain was too short/low MW to be used as a precursor for PEM synthesis. This initial testing indicated that the Type B PEMs of interest were those containing PEG 200, 400 and 600.

Table 4.9: Water uptake and swelling for selected Type B PEMs after being dried and then immersed in deionised water for 48 hours

	15% PA Loading		30% PA Loading	
PEG MW	Mass Uptake (% w/w)	Swelling (%)	Mass Uptake (% w/w)	Swelling (%)
200	11	11	12	13
400	14	15	16	17
600	19	18	23	21
1000	32	27	40	31

To compare the proton conductivity of the Type B PEMs, PEMs containing 15% PA w/w (Blend 1 hydrolysed by method 3) and PEG 200 (membrane 051), PEG 400 (membrane 081) and PEG 600 (membrane 089) were synthesised in a similar fashion and conditioned in the same way, by steaming for one hour prior to measurement. During measurements the membranes were kept at 100% RH by placing deionised water in the bottom of the humidity chamber. As each membrane had the same equivalent weight (EW) this enabled a direct comparison between the PEMs. The results are shown in Table 4.10.

Table 4.10: Calculated conductivities of Type B PEMs containing 15% PA over two heating cycles at 100% RH with steam conditioning, all conductivity values are in mS cm^{-1}

	Cycle 1 Conductivities / mS cm^{-1}			Cycle 2 Conductivities / mS cm^{-1}		
Temperature / °C	PEG 200	PEG 400	PEG 600	PEG 200	PEG 400	PEG 600
20	0.2	0.3	0.9	0.5	-	3.0
30	0.3	0.7	1.5	1.0	-	4.3
40	0.4	1.3	2.0	1.9	5.3	5.2
50	0.5	1.6	1.9	1.5	5.9	5.2
60	0.8	2.2	1.4	1.8	6.2	3.0
70	1.6	3.2	1.4	2.4	6.2	2.1
80	3.4	19.5	1.4	4.2	5.5	1.9
90	4.5	18.2	1.3	4.0	5.3	1.8
100	4.0	16.5	1.3	3.8	5.5	2.0
110	4.0	5.0	1.7	4.2	5.2	2.4
120	4.2	5.3	2.6	4.5	5.9	3.7

Membrane 051 showed a steady increase in conductivity with increasing temperature up to 50 °C, above this temperature the conductivity dramatically increased reaching a maximum of 4.5 mS cm^{-1} at 90 °C, whereupon further heating to 120 °C the conductivity plateaued. This meant that for membrane 051 the energy required for proton transport through the membrane at high temperatures was relatively small (0.035 eV) compared to that of Nafion at 80 °C (0.12 eV) which implied that proton transport was occurring predominantly via the Grothuss mechanism.[92]

Membrane 081 showed a similar trend to that of membrane 051, although membrane 081 exhibited higher conductivities in the first heating cycle. In the second heating

cycle, membrane 081 showed a change in the observed trend in proton conductivity. The proton conductivity was independent of temperature and was nearly constant around 5.5 mS cm^{-1} with an E_a of 0.0035 eV (Fig 4.11). This was unexpected, and was at first thought to be an anomalous result; however a similar trend was observed for membrane 089 (Fig. 4.12), although in that case the trend was not as extreme.

Membrane 089 exhibited the highest proton conductivity at room temperature after steam conditioning of the three membranes tested (membranes 051, 081 and 089). This was due to the fact that the P_6MP_6 membranes were more hydrophilic than those of P_4MP_4 and P_2MP_2. The proton conductivity of membrane 089 ranged from 1-5 mS cm^{-1} at all temperatures at which the impedance was measured, with the second cycle reaching slightly higher conductivities than the first cycle, as can clearly be seen in Table 4.10. Reasons for the observed higher conductivities could include that there was better contact between the membrane and electrode in the 2^{nd} heating cycle, membrane creep meaning that the cell constant had changed and the membrane reaching a higher hydration state or equilibrium after the first measurement cycle. When the conductivity cell was removed from the chamber and opened, it was found that the membrane had suffered from membrane creep; however the membrane could not be removed from the electrode of the cell to ascertain the new dimensions.

Membrane 051 was remade using the same sample preparation, and the proton conductivity was determined by A.C. impedance spectroscopy using the same sample conditioning and measurement settings, however the membrane piece measured was significantly thicker (*ca.* 50% thicker) than that of sample 1 (580 μm compared to 370 μm). This resulted in the membrane showing greater water uptake and swelling than sample 1 (18% water uptake and 20% swelling). The thicker membrane had a different conductivity profile than that of the thinner membrane sample, as can be seen in Fig. 4.9. The differences in proton conductivity between the two samples showed that the proton conductivity was not independent of membrane thickness in the temperature range of 20 to 100 °C, and resulted from the difference in water uptake and retention. Above 100 °C the conductivities of the two samples were the same due to the extra absorbed water in the thicker membrane being lost through dehydration.

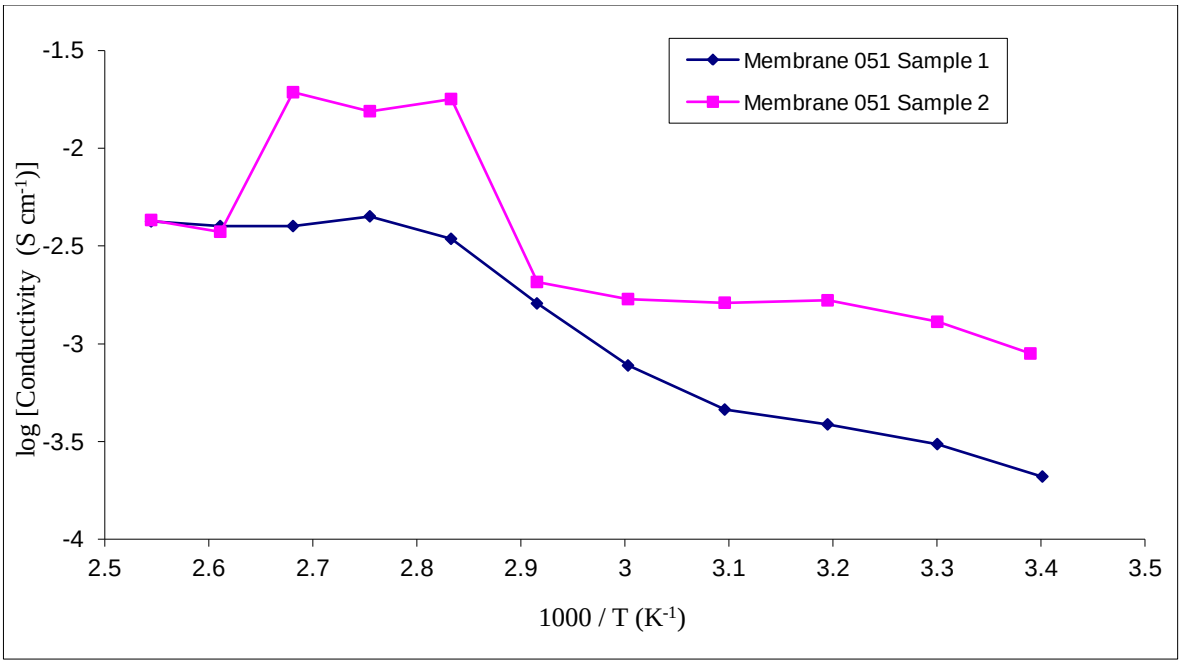

Fig. 4.9. Measured conductivities of two samples of membrane 051, sample 1 was 370 μm and sample 2 580 μm, heated to 120 °C at 100% RH

From these initial impedance measurements two potential candidates, P_2MP_2 and P_4MP_4 membranes were identified for further studies for the Type B PEMs; P_6MP_6 PEMs suffered from membrane creep during impedance measurements and displayed significantly higher swelling and water uptake. The P_2MP_2 membranes were chosen over P_4MP_4 membranes to be further refined at this stage due to the lower water uptake these membranes displayed. This enabled PEMs with higher PA loadings to be synthesised, with lower water uptake and swelling properties, as well as higher proton conductivities. PEMs containing high PA loadings were successfully synthesised, but at loadings above 35%, the membranes displayed limited water stability.

Membrane 059 (P_2MP_2, 25% w/w PA) was synthesised in a similar fashion to membrane 051. The conductivity of this membrane was determined by a segment of membrane that was conditioned by steaming for one hour, and then measurements performed at 100% RH and on a second segment of the same membrane which was not conditioned at all with measurements performed in the dry state (*i.e.* 0% RH), the results are shown in Fig. 4.10.

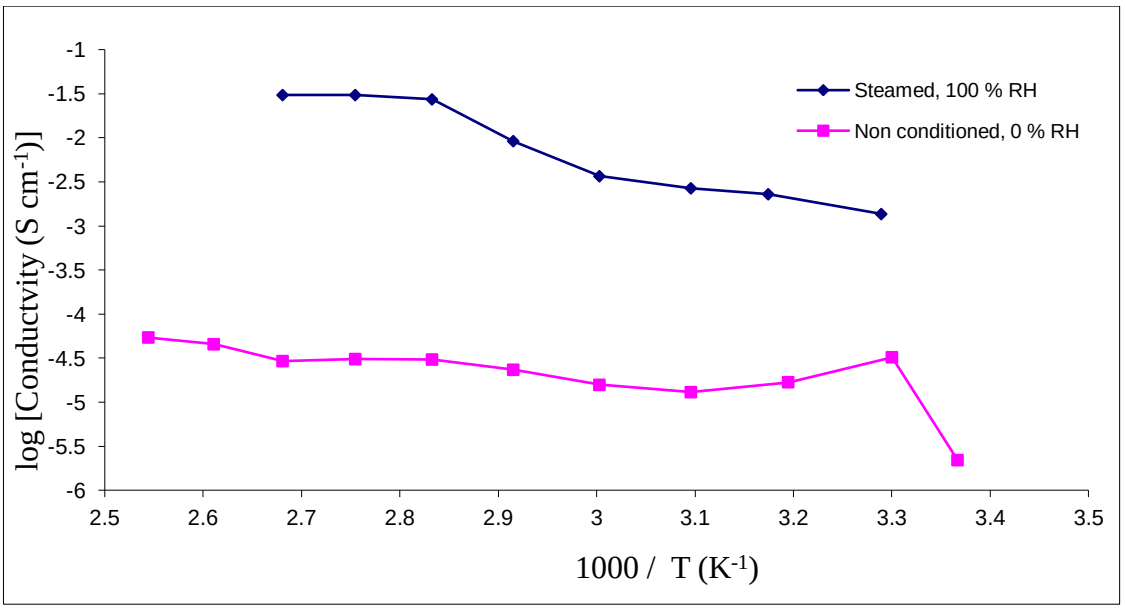

Fig. 4.10: Measured proton conductivities of membrane 059, heated to 120 °C over one heating cycle conditioned by steaming (100% RH) and non conditioned (NC, 0% RH), P_2MP_2 25% PA

Unsurprisingly the conductivity for the hydrated membrane was far greater than that of the non-hydrated membrane. This was due to the water molecules acting as a charge carrier, allowing quick hopping of the proton charge via the Grothuss mechanism (Chapter 1.3.1), with an E_a of 0.064 eV in the 80 to 100 °C temperature range. In the non-hydrated membrane the PEG acts as the proton solvent, allowing slow diffusion of the protonic species through the membrane. This results in much higher resistances, and does not vary much over the temperature range, this results in a relatively high E_a of 0.22 eV over the temperature range of 40 °C to 120 °C.

As expected, the proton conductivity observed for membrane 059 was significantly higher than that of membrane 051, as membrane 059 contained an extra 10% PA w/w, with the same trend displayed in both instances as is shown in Fig. 4.11. On the second heating cycle however, the proton conductivity of membrane 059 dropped dramatically at higher temperatures for example at 90 °C, from 34 to 8 mS cm^{-1} on the 1st and 2nd heating cycle respectively, though this was still higher than the proton conductivity of membrane 051 at 90 °C which was 4 mS cm^{-1}. Upon immersion in boiling water for one hour, there was no visible deterioration of the membrane, indicating the membrane was water stable. This suggested that the steaming conditioning may have affected the proton conductivities of some membranes in an unexplained way.

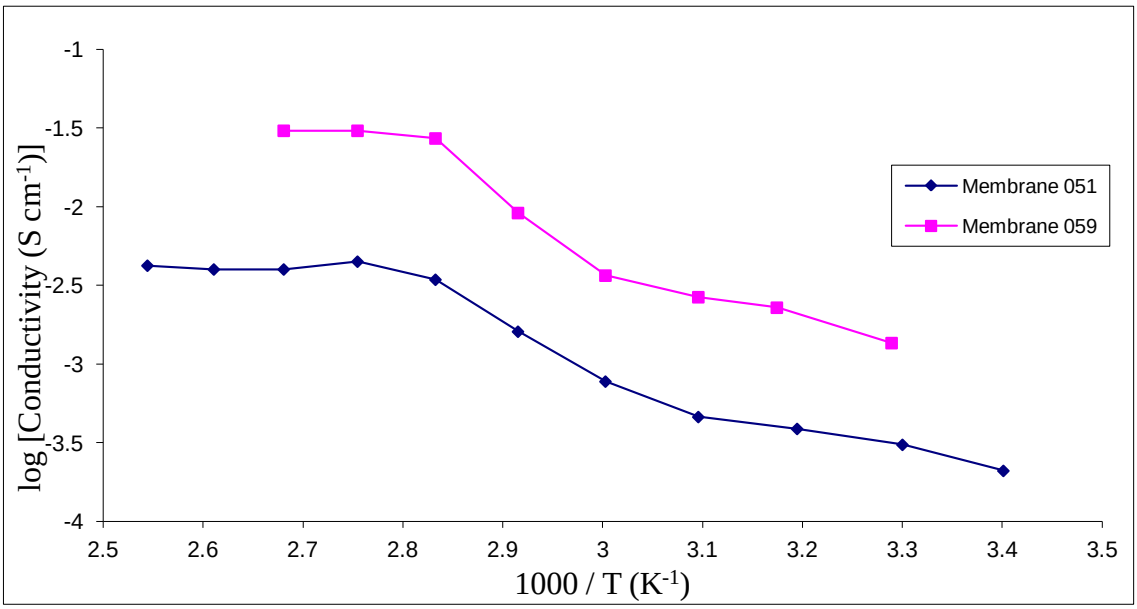

Fig. 4.11: Measured proton conductivities for membranes 051 (15% PA 350 μm thick) and 059 (25% PA 320 μm thick) on the first heating cycles at 100% RH, with both membranes steamed pre-conditioned.

4.4.3: Type B PEMs with additional network formers (Glysil and TEOS)

Type B P_2MP_2 membranes with a PA loading of 25% PA containing Glysil and TEOS in the formulation were also prepared. These membranes displayed the same IEC and EW as membrane 059. The membrane with Glysil in the formulation, when steamed showed similar conductivity to that of membrane 059. However, when the Glysil membrane was boiled for one hour in deionised water, instead of being steamed for one hour, the proton conductivity values observed were significantly lower at low temperatures (below 60 °C) than that of the steamed membrane, as shown in Fig. 4.12. Above this temperature the proton conductivities were similar, albeit lower than both the steamed Glysil membrane and membrane 059, indicating that steaming of the membrane had a more beneficial effect than placing the membrane in boiling water.

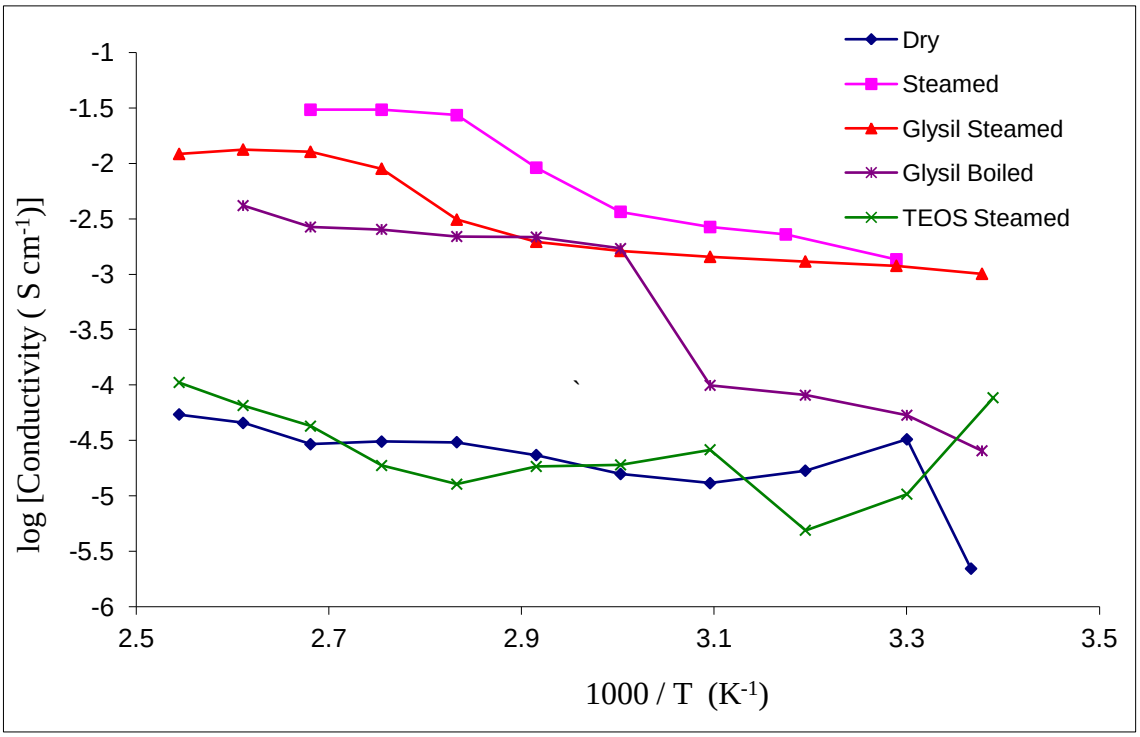

Fig. 4.12. Total proton conductivities of PEMs based on membrane 059 under various conditions, heated to 120 °C

The decrease in conductivity at lower temperatures for the boiled Glysil membrane can be rationalised by considering the nature of the water absorption. During steaming the membrane absorbs more water than when boiled (9% and 6% mass increase respectively). This mass change may seem insignificant, but it was a 50% increase in water absorption and could explain the difference in conductivity values observed at low temperatures. The proton conductivities for both the boiled and steamed conditioned samples are given in Table 4.11.

Table 4.11. Variation of Total Conductivity for Glysil containing membrane 059, heated at 120 °C over two heating cycles with steam conditioning, and over one heating cycle for boiled conditioning, all measurements at 100% RH

Temperature / °C	Steamed conditioned (1^{st} heating) σ / mS cm^{-1}	Steamed conditioned (2^{nd} heating) σ / mS cm^{-1}	Boiled conditioned (1^{st} heating)σ / mS cm^{-1}
21	1.0	1.2	0.039
30	1.2	1.3	0.077
40	1.3	1.6	0.068
50	1.4	2.1	0.13
60	1.6	4.3	1.8
70	2.0	6.0	1.9
80	3.1	9.4	1.9
90	9.0	9.7	2.7
100	13	9.2	2.5
110	13	8.3	4.0
120	12	8.4	-

Alternatively, the difference in observed conductivities between boiled and steamed membranes could be that the boiling pre-treatment resulted in acid leaching from the membrane. This acid would not be covalently bound into the membrane, and could be from residual undistilled DMP, which had been hydrolysed into phosphorous acid. When the membranes were steamed, this was not washed out and hence these membranes exhibit higher conductivities over both heating cycles measured.

To test this hypothesis, two experiments were performed. The first was to boil a large piece of membrane (3 cm × 3 cm) in deionised water for one hour. The acidity of the water was then determined by titrimetric analysis with dilute sodium hydroxide solution and measured using a calibrated pH meter. The proportion of acid in the water was determined to be equivalent to only 2% of the PA content of the membrane piece.

Two segments of this boiled membrane were removed, one segment was used for impedance spectroscopy measurements and the second placed over P_2O_5 for two days to dry. The 2^{nd} segment of membrane was then steamed in the same way as the previously steamed Gylsil membrane and the proton conductivities determined by impedance

spectroscopy. The measured conductivities for both pieces were similar to those of the boiled membrane and steamed membrane respectively (on the first heating cycle), thus showing that the small acid loss upon boiling does not impact on the observed proton conductivities of the membrane, and the difference in proton conductivities between the steamed and boiled Glysil membranes was due to the nature of the membrane conditioning.

The membrane synthesised with TEOS in the formulation was conditioned by steaming over water for one hour before being placed in the normal cell. The proton conductivities observed for this membrane at 100% RH were considerably less than those of both the Glysil and non-Glysil membrane 059 (as shown in Fig. 4.15). The actual conductivities recorded were similar to the non-conditioned membrane 059 which was measured at 0% RH. In the anhydrous membrane, there is no water to act as a "molecular wire" so the proton transport is limited to diffusion rather than charge hopping (Grothuss mechanism). The TEOS membrane absorbed a significant amount of water (6% w/w). This would suggest that the added TEOS disrupts the mode of proton transport through the membrane, *i.e*. the TEOS forms small particles of silica which block the water diffusion channels which in turn prevents the charge hopping and results in a comparable conductivity to that of the anhydrous membrane 059.

4.4.4 Type B PEM Conclusions

After an initial assessment of PEM formulations based on mechanical properties and water stability it was clear that P_1MP_1 and $P_{10}MP_{10}$ Type B PEMs were unsuitable for use in PEMFC applications. On further investigation, based on the P_2MP_2 PEM formulation, the incorporation of additional inorganic network formers derived from Glysil and TEOS, lowered the observed conductivities of the PEMs, although TEOS had a much more severe impact. It was also observed that conditioning the membranes by steaming prior to conductivity measurements produced unexplained results, so a less harsh conditioning of immersion in deionised water was employed. It was found that at high temperatures the E_a of proton transport was typically less than 0.1 eV which indicated that proton transport occurred primarily through proton transfer rather than via diffusion, thus relying on absorbed water in the PEM. However, the change in PEM formulation from Type A to Type B resulted in membranes which had poorer flexibility

and brittleness, but lower water uptake and swelling, thus it was decided to further modify the polymer formulation to make the polymer more flexible.

4.5 Type C PEMs

In the type C polymer matrix, the MDI component was replaced with an aliphatic diisocyanate, hexamethylene diisocyanate (HDI) which is shown in Fig. 4.13.

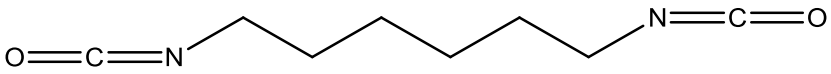

Fig. 4.13. Structure of HDI

HDI is the most common aliphatic diisocyanate used in the synthesis of polyurethanes.[79] At room temperature it is a liquid and is considerably more toxic than MDI (the material safety data sheet (MSDS) states that HDI inhalation/ingestion is fatal), as HDI is a toxic liquid, further handling precautions needed be taken compared to MDI. HDI is synthesised by the phosgenation of hexamethylene diamine, which is then purified. As well as being more toxic, HDI is significantly more expensive than MDI in laboratory scale quantities; MDI costs £8.90 per 100 g whilst HDI costs £17.70 per 50 g.[93]

HDI was used instead of MDI to improve the mechanical properties of the membranes. The optimal PEG MW for Type B membranes was quite low, 200 Da. MDI has limited flexibility due to the rigidity of the two-phenyl rings in the molecule, with only one centre of rotation in the middle of the molecule, that being the bridging carbon. HDI on the other hand is similar to PEG in that the hydrocarbon chain is more flexible as there is no limited rotation in the molecule.

4.5.1 Type C PEMs Proton Conductivities

The change from MDI to HDI in the polymer matrix had several negative impacts on the PEM properties, although the proton conductivities were similar to those membranes containing MDI as can be seen in Fig 4.14.

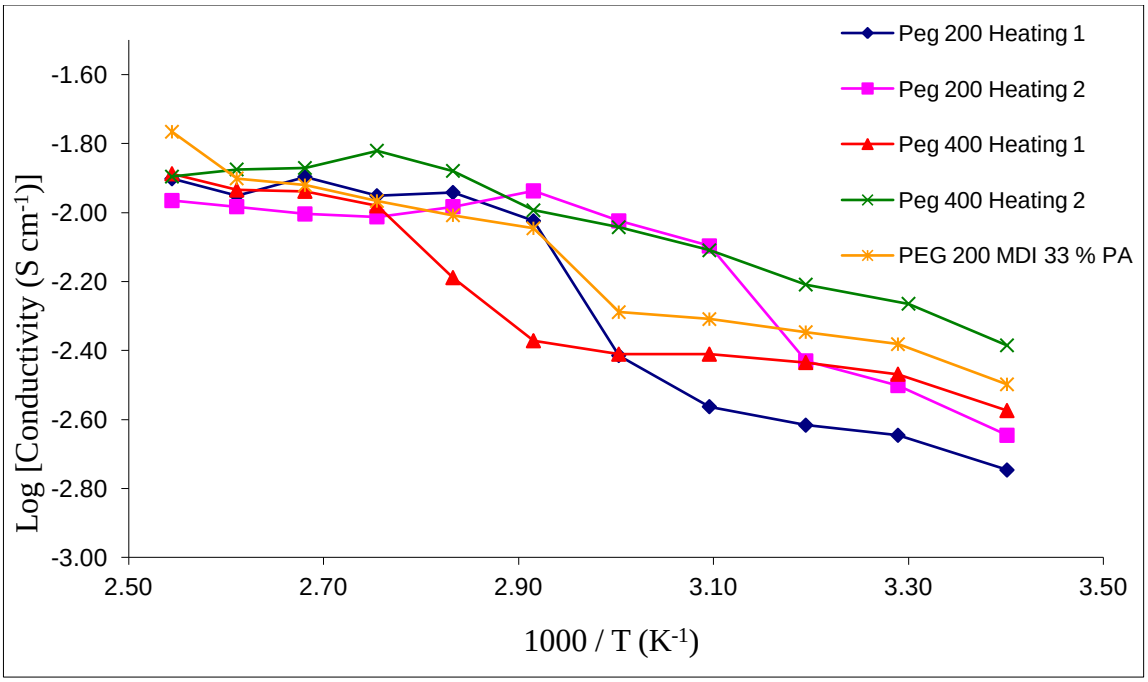

Fig 4.14. Total proton conductivities of Type C PEMs (P_2HP_2 and P_4HP_4) containing 30% PA heated to 120 °C over two heating cycles at 100% RH. Type B membrane 064 is shown for comparison.

Both the P_2HP_2 and P_4HP_4 Type C PEMs with 30% PA loadings (membranes 104 and 109 respectively) had proton conductivities between 1.5-2.5 mS cm^{-1} at room temperature on the first heating cycle and 2-4 mS cm^{-1} on the second heating cycle. Both membranes had the same proton conductivity (13.0 ± 1 mS cm^{-1}) at 120 °C on both heating cycles. The MDI containing membrane 064 had a room temperature proton conductivity of 3.2 mS cm^{-1} and at 120 °C a proton conductivity of 17 mS cm^{-1}, which was only slightly higher at both temperatures than both the Type C membranes as can be seen in Fig 4.21.

4.5.2 Type C PEMs: Mechanical Properties

The Type C PEMs displayed similar flexibility to their Type B PEM counterparts. There was no visual improvement in flexibility when dry; however there was a marked deterioration in tear resistance for the dry membrane. Also the membrane flexibility was markedly poorer when the membrane was hydrated. The membrane was easy to tear/damage when hydrated after conditioning for ACIS studies.

This degradation in mechanical properties although initially unexpected can be rationalised by the removal of the aromatic rings, as these were no longer present in the

membrane there was no π-π stacking between the diisocyanate groups. The water uptake of the Type C PEMs was also higher than their Type B counterparts. Membrane 104 (P_2HP_2, 30% PA) absorbed 15% mass water over 48 hours and membrane 109 ((P_4HP_4, 30% PA) absorbed 17% mass water over 48 hours, both of which are considerably higher than the 12% mass increase observed for membrane 064 (P_2MP_2, 33% PA).

The overall decrease in performance and increase of cost makes the HDI containing membranes (polymer matrix type C) a non-ideal candidate for development compared to those containing MDI (polymer matrix type B).

4.6 Type D PEMs

As replacing the aromatic MDI group with an aliphatic HDI group resulted in a reduction of mechanical properties of the PEMs when dry and hydrated, it was decided that another approach was needed to improve the mechanical properties of the PEMs. The Type B polymer matrix was modified to contain an extra MDI and PEG group as described in Fig. 4.15. To synthesise this type of PEM, the hard segment, (MDI-PEG-MDI) was made separately to that of the silane end capped PEG as described in section 2.3.4. This allowed for two PEG monomers with different chain lengths (*x* and *y*) to be included in the polymer matrix and hence to have a greater degree of control of membrane characteristics than the membranes made by the Type B and Type C PEM syntheses.

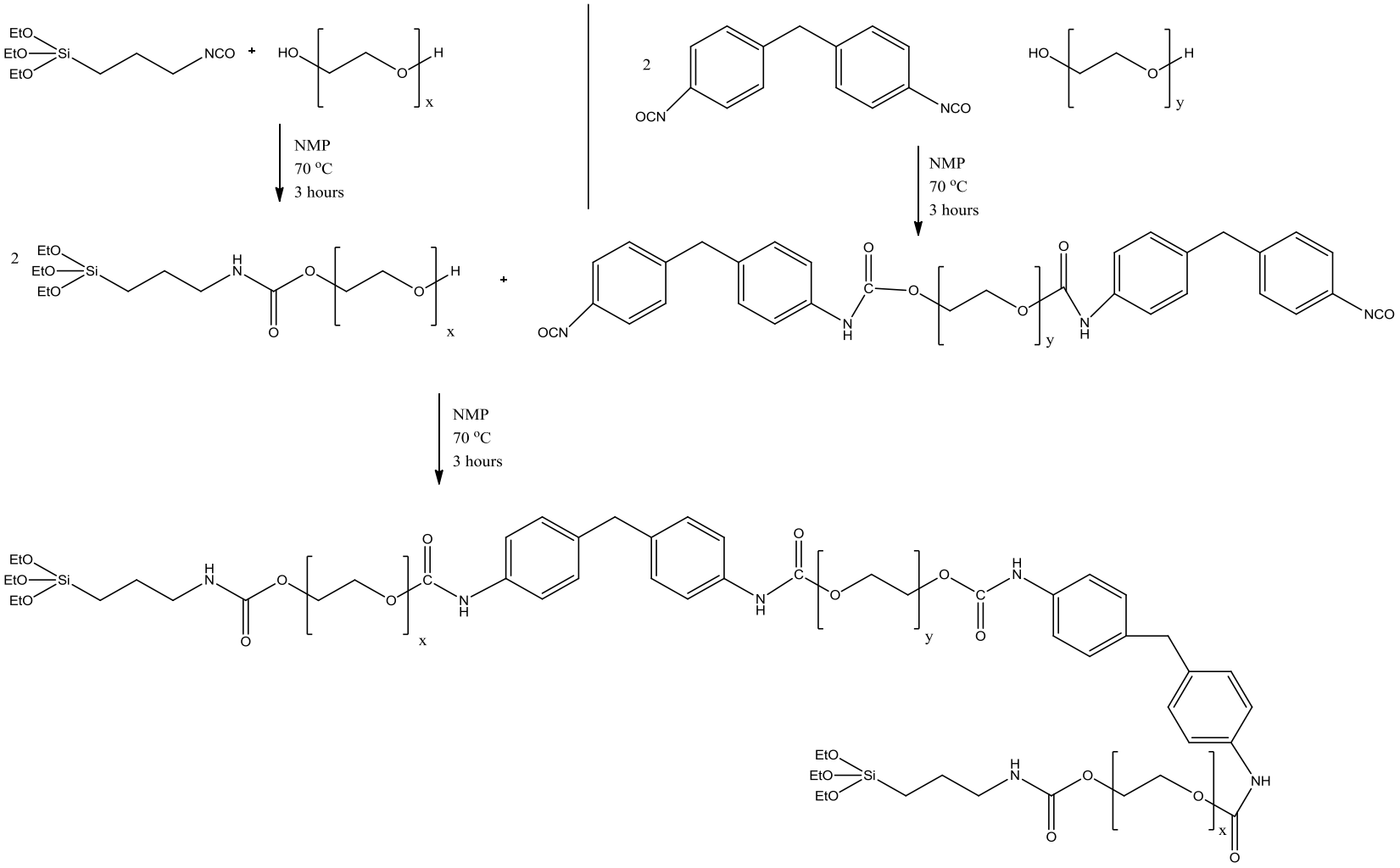

Fig. 4.15. Type D PEM prepolymer synthesis

Type D PEMs were prepared in a methodical fashion, first by keeping the molecular weight (MW) of PEG_x the same (200 Da), whilst increasing the MW of PEG_y from 200 to 1000 Da. The MW of PEG_x was then increased (400 Da) and that of PEG_y was varied. This was then repeated to produce PEG_x 600 Da PEMs. PA loadings for each prepolymer formulation were varied from 0% to 25% in 5% increments to make membranes 116 to 162.

Membranes were primarily characterised by determination of conductivities up to 120 °C at 100% RH in the normal cell, boiling water stability and also mechanical properties (including flexibility and tear resistance) were also recorded. Membranes containing high MW PEG_y (600 Da) were found to be non-boiling water stable at any PA loadings. The membranes where PEG_y was 400 Da showed considerably better boiling water stability. This was improved further when the MW of PEG_y was further decreased to 200 Da.

This initial investigation revealed three polymer matrices for further investigation. Those of $P_2MP_2MP_2$, $P_4MP_2MP_4$ and $P_6MP_2MP_6$. Membranes where the MWs of PEG_x and PEG_y were both 200 Da were fairly rigid and brittle, irrespective of PA loading. When these membranes were cut when dry they visibly fractured; when these membranes were hydrated prior to cutting, fracturing was less severe, but still visually noticeable. This rigidity/glassiness was due to the membranes only having relatively short PEG groups coupled with two fairly rigid MDI groups. The PEG_x 400 and 600 Da membranes were mechanically superior to the PEG_x 200 Da membranes, with the extra length in the PEG chains allowing enhanced flexibility and tear resistance, when both hydrated and dry. These membranes did not fracture when cut and were considerably more rubbery in nature, especially the PEG_x 600 Da membranes. However the PEG_x 600 Da containing membranes were only stable in boiling water up to 15% PA loadings.

4.6.1 Type D PEMs: Proton Conductivity

As clearly shown in Fig. 4.16, increasing the PEG_x chain length dramatically reduced the proton conductivities of the membranes (15% PA loadings) at all temperatures. Membrane 118 (PEG_x 200 Da) showed comparable conductivity to that of membrane 051 (Type B, P_2MP_2 15% PA) at high temperatures and slightly higher conductivities at low temperatures (below 60 °C) when conditioned by the same process (steaming for

one hour). The slight increase in proton conductivities at lower temperatures can be attributed to the incorporation of an extra hydrophilic B PEG chain in the Type D polymer matrix. However the mechanical properties of membrane 118 were far inferior to that of the membrane 051, where membrane 051 could be bent around a cup with an outer diameter of 95 mm without breaking, membrane 118 could not.

The dramatic drop in proton conductivity observed for membrane 133 (PEG_x 400 Da) and even larger drop for membrane 148 (PEG_x 600 Da) is attributed to the longer PEG chains disrupting the path of proton conduction. Indeed, membrane 148 has lower proton conductivity than that of Type B membrane 048 (P2MP2) which only had a PA loading of 5%.

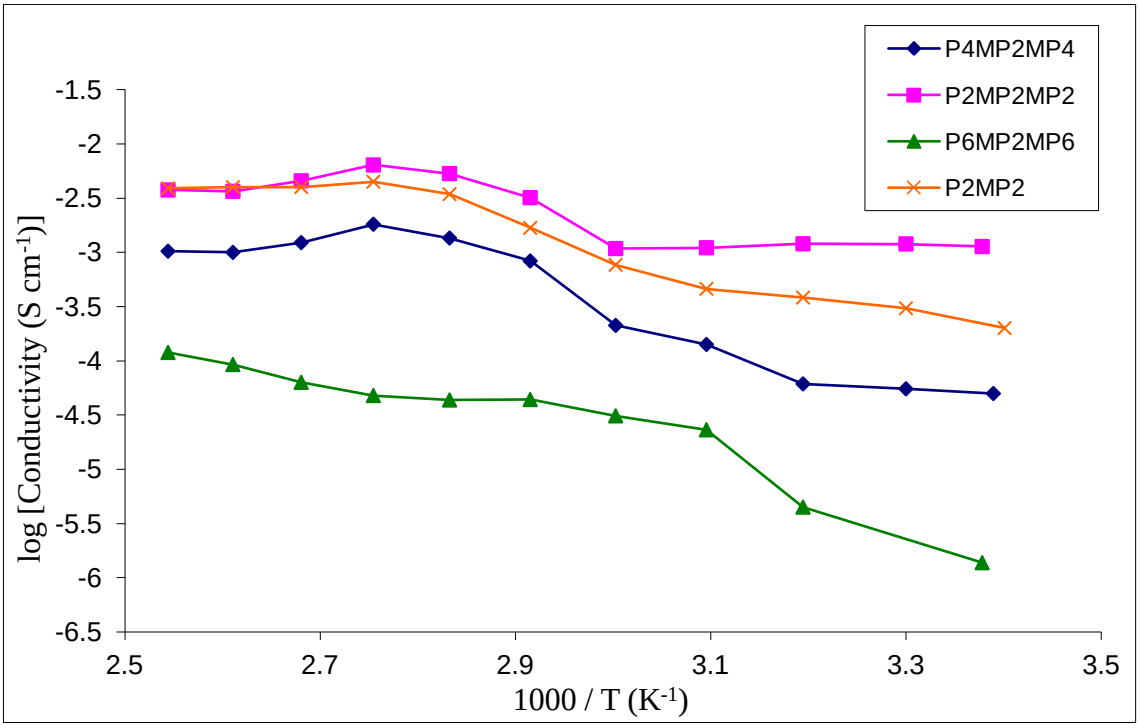

Fig. 4.16. Total proton conductivities for Type D PEMs, PEG_x 200 Da (membrane 118) 400 Da (membrane 133) and 600 Da (membrane 148) with 15% PA loadings, heated to 120 °C at 100% RH over one heating cycle. Type B Membrane 051 is shown for comparison.

If the primary mode for proton transport in the PEM is via the Grothuss mechanism, then the decrease in proton conductivity could be explained by decreased water uptake. However this is not the case as membrane 148 absorbed more water (19%) than membrane 133 (16%), which in turn absorbed more water than membrane 118 (10%)

when all membranes were stored in deionised water for 48 hours at room temperature after drying over phosphorus pentoxide for 24 hours. This indicates that either the absorbed water does not contribute to the proton conductivity and hence the mechanism is not primarily via the Grothuss mechanism or that the absorbed water actually disrupts the proton transport occurring via the Grothuss mechanism, through the polymer matrix swelling and forming isolated hydrated regions in the membrane, thus making charge transfer less favourable over the vehicular/diffusion mechanism.

Alternatively an argument can be made relating to the decreased inorganic component ($SiO_{3/2}$) of the prepolymers containing higher MW PEG_x's. The organic part of the membrane has a different affinity for water than the inorganic part of the membrane, thus when the proportion of the organic component of the prepolymer is increased in comparison to the inorganic component (which is achieved when PEG_x is increased in MW), this in turn can cause a phase separation between the inorganic and organic components of the membranes when hydrated, which resulted in the lower proton conductivities

To determine whether the latter was the case, two membranes based on membrane 148 were synthesised, but doped with an additional inorganic containing precursor, one derived from TEOS (membrane 149) and the other from Glysil (membrane 150). The TEOS membrane showed very low conductivity, similar to that of the TEOS containing membrane 059, for which the same reasoning to the decrease of proton conductivity can be made. The proton conductivity of membranes 148 and 150 are shown in Fig. 4.17.

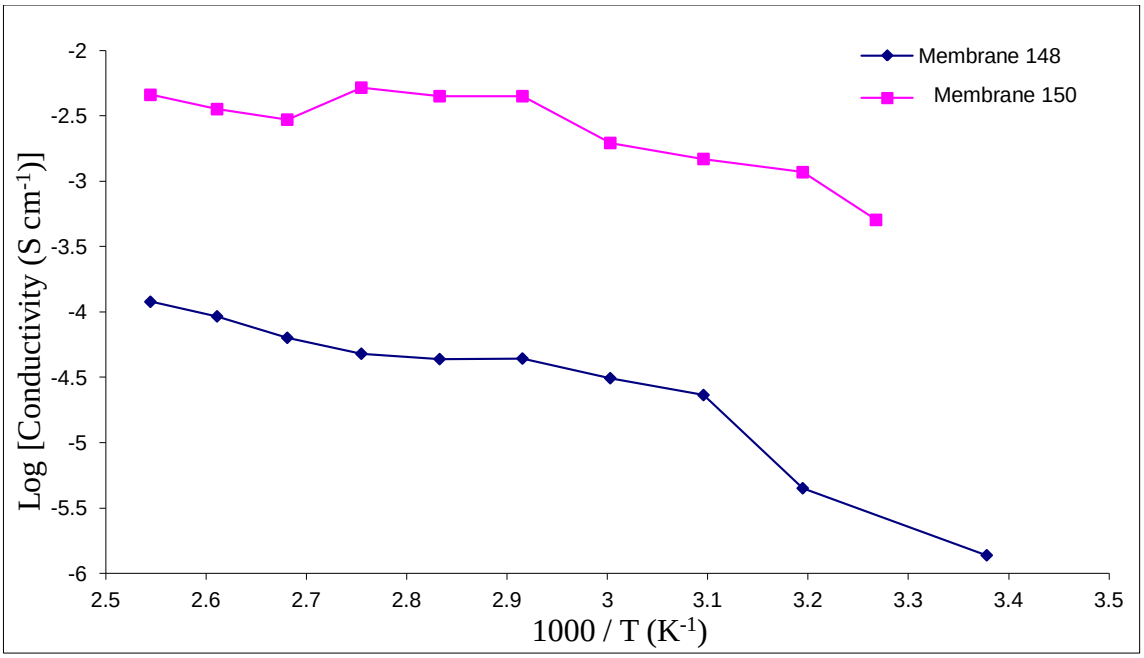

Fig. 4.17. Total conductivities of membranes 148 and 150 (modified by Glysil addition) heated to 120 °C at 100% RH over one heating cycle

As can be seen in Fig. 4.17, the addition of Glysil dramatically improved the proton conductivity of the membrane, showing similar conductivities to membranes 118 and 051. The mechanical properties of this membrane were also far superior to that of membrane 148. The membrane was very tough and rubbery, and when cut no fracturing was visible. The improvement in proton conductivity can be attributed to the increased inorganic content of the membrane.

Despite the excellent mechanical properties of this class of membrane (especially membranes 148 and 150) these membranes were not suitable for PEMFC applications due to their relatively low proton conductivities which ranged from 10^{-4} S cm^{-1} at room temperature to 10^{-3} S cm^{-1} at 80 and 120 °C, compared to the $10^{-2}/10^{-1}$ S cm^{-1} targets of the High Temperature Membrane Working Group, of the United States Department of Energy (HTMWG, US DoE). These low conductivities resulted from the low PA loadings in the polymer matrix, yielding low IEC and EW values for these PEMs, and cannot be overcome with further modification of the Type D polymer matrix.

4.7 Type E PEMs

Type E membranes were prepared in the same fashion as Type A PEMs, however replacing the PEG with polypropylene glycol (PPG) of either 400 or 1000 Da. The structure of PPG is shown in Fig. 4.18.

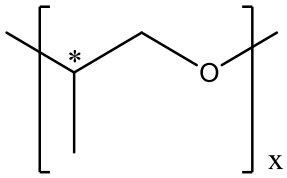

Fig 4.18. Structure of PPG repeating unit. The asterisk highlights the chiral centre

PPG is similar in nature to PEG, however there is an additional pendant methyl group in each repeating unit of the polymer. This creates a chiral centre in each repeating unit (highlighted in Fig. 4.26 by an asterisk). The PPG used in this project was atactic (random S and R). Isotactic PPG can be used, although this would greatly increase the cost of the membrane for no perceivable benefit. The extra methyl group should alter the mechanical properties of the membrane, whilst reducing the water uptake, in theory making better PEMs than Type A membranes, thus avoiding high boiling point aprotic solvents used in Type B membrane synthesis and reducing the processing conditions and costs of the PEMs.

4.7.1 Type E PEMs: Proton Conductivity

As can be seen in Fig. 4.19 the proton conductivities of the PPG 400 and 1000 membranes were similar to each other at low temperatures (below 60 °C), however the observed values were over an order of magnitude less (20-30 times) than that observed for membrane 064 which had a similar PA loading when the membranes were conditioned in the same fashion. Ideally PEMFCs would need to operate from a cold start-up, thus putting PPG membranes at a disadvantage over Type A and B membranes.

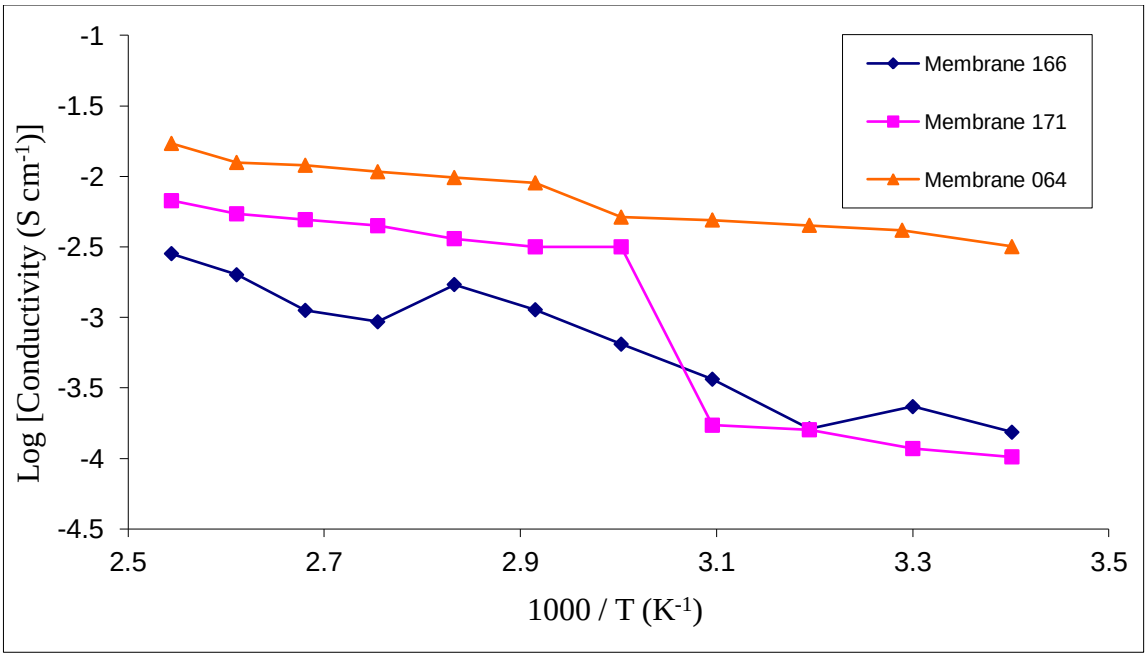

Fig 4.19: Total Proton conductivities of membranes 166 and 171 (Type E PPG 400 and 1000 respectively, 30% PA) heated to 120 °C over one heating cycle at 100% RH, membrane 064 (Type B P_2MP_2 33% PA) shown for comparison

4.8 Type F PEMs

Polytetrahydrofuran (**PTHF**) or (polytetramethylene glycol) was incorporated into the polymer matrix in the same fashion as PPG in type E membranes. Whereas PPG has a pendant methyl group, PTHF is similar to PEG in that it is a linear chain polymer, the structure of PTHF is shown in Fig. 4.20. As type A membranes were very hydrophilic, absorbing too much water upon hydration, decreasing the hydrophilicity of the membrane is crucial for improving PEM properties. PTHF reduces the oxygen content of the polymer backbone by having a longer alkyl chain, four carbon atoms long compared to PEG which only has two.

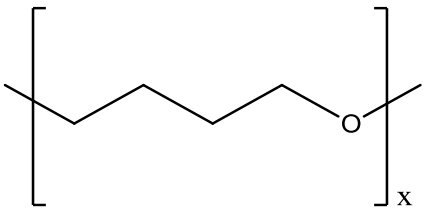

4.20. Structure of PTHF

Polytetrahydrofuran, or poly(tetramethylene ether) glycol, is made by the ring opening polymerisation of tetrahydrofuran. Invista, formerly a DuPont company markets PTHF as Tetrathane and used in the manufacture of spandex (Lycra) and other high performance elastomers.[94] However, the MW of the PTHF used for these applications is usually in the k - MDa range and in this project the MW ranged from 250 to 1000 Da so as to enable the IEC of the produced PEMs to be kept at reasonably high values.

The PTHF of 250 Da was liquid, whilst those of 650 and 1000 Da were white waxy resins, which had low melting points just above room temperature (but below 30 °C). When the polymer solutions of PEMs using PTHF 250 Da were cast into polystyrene Petri dishes, they adhered to the surface and could not be removed without tearing or breaking the formed PEM. To allow the removal of the PEM from the casting substrate, the casting procedure for Type B membranes was used (OTS modified glass). However, these membranes were easily torn and quite brittle. PEMs made using PTHF 650 and 1000 Da were visibly inhomogeneous and were also not stable in boiling water, and no impedance measurements were carried out. The poor membranes could be a result of an added stabiliser, butylated hydroxytoluene (BHT), which was not present in other precursors, adversely affecting the desired prepolymers from forming, reacting in competition with the PTHF for the isocyanate groups on the TSPI, thus the resulting PEMs were not fully cross-linked and this could explain their poor properties.

4.9 Summary of Selected Types A-F PEMs

PEM	Plasticser	PA %	Boiling Water Stable	Swelling %	Water Uptake %	IEC mmol g^{-1}	Cup test	Fractured when cut	Conditioning	σ RT / mS cm^{-1}	σ 80 °C / mS cm^{-1}	σ 120 °C / mS cm^{-1}	Comments
575C	-	10	✓	12	10	1.31	✓	✓	none	0.0042	0.84	9.5	
									immersed	0.0077	0.44	4.8	
									steamed	0.053	0.6	4.3	
Type A													
	PEG 400	30	-	17	16	2.71	✓	×	Steamed	1.9	1.1	1.5	Membrane Creep
	PEG 400	50	×	-	-		✓	×	Steamed	9.9	65	29	Membrane Creep
	PEG 600	30	-	25	28	2.64	✓	×	Steamed	1.2	2.7	1.9	Membrane Creep
	PEG 1000	40	-	30	41		✓	×	Steamed	20	45	46	Severe membrane creep
Type B													
	P_1MP_1	30	✓			2.60	×	✓	-	-	-	-	
	P_2MP_2	15	✓	11	11	1.35	✓	×	Steamed	0.2	3.4	4.2	
	P_2MP_2	25	✓			2.35	✓	×	Steamed	1.3	27	25	
									0% RH	0.0022	0.031	0.054	
									Steamed	1.0	3.1	12	Contained Glysil
									Steamed	0.077	0.013	0.11	Contained TEOS
	P_4MP_4	15	✓	15	14	1.40	✓	×	Steamed	3.4	20	1.4	
	P_6MP_6	15	✓	18	19	1.41	✓	×	Steamed	4.2	5.3	2.6	Membrane creep
	$P_{10}MP_{10}$	15	×	27	32	1.39	✓	×	-	-	-	-	
Type C													
	P_2HP_2	30	-	13	15	2.59	✓	×	Immersed	1.8	11	13	
	P_4HP_4	30	-	15	17	2.55	✓	×	Immersed	2.7	6.5	13	
Type D													
	$P_2MP_2MP_2$	15	✓	8	10	1.36	✓	✓	Steamed	1.1	5.3	3.8	
	$P_4MP_2MP_4$	15	✓	12	16	1.42	✓	×	Steamed	0.05	1.4	1.0	
	$P_6MP_2MP_6$	15	✓	14	19	1.39	✓	×	Steamed	0.0014	0.044	0.012	

PEM	Plasticser	PA %	Boiling Water Stable	Swelling %	Water Uptake %	IEC mmol g^{-1}	Cup test	Fractured when cut	Conditioning	σ RT / mS cm^{-1}	σ 80 °C / mS cm^{-1}	σ 120 °C / mS cm^{-1}	Comments
	$P_6MP_2MP_6$	15	✓			1.43	✓	×	Steamed	0.051	4.5	4.5	Contained Glysil
Type E													
	PPG 400	30	✓			2.63	✓	×	Immersed	0.15	1.7	2.8	
	PPG 1000	30	✓			2.62	✓	×	Immersed	0.10	3.6	6.8	
Type F													
	PTHF 250	-											Inhomogeneous
	PTHF 650	-											Inhomogeneous
	PTHF 1000	-											Inhomogeneous

4.10 Further Development of PEMs and incorporation into a PEMFC as a MEA

To choose a PEM for further development and optimisation, the role of a PEM in a PEMFC needs to be considered as well as how it is physically included. A PEM in a PEMFC is a critical component of the membrane electrode assembly (**MEA**). A MEA contains the PEM sandwiched between two gas diffusion electrodes (**GDEs**). The gas diffusion electrodes are typically made from porous carbon paper with an electrocatylst deposited on the surface. The electrocatalysts are typically nano-sized colloids of Pt, but those containing other Pt group metals are becoming more important. To make the MEA, the PEM and GDEs undergo a process called "hot pressing". In this process the PEM and GDEs are pressed together under some force at elevated temperatures. The pressure applied, temperature used, as well as length of time being pressed varies dramatically and depends on the membrane and the GDEs being used to make the MEA (but generally above 130 °C and 1000 psi pressure for over a minute), and even slightly different conditions can dramatically affect the performance of the MEA.[95] The process of hot pressing can easily damage the membrane, creating hot spots on the surface of the PEM and causing thermal degradation which can be observed as pinhole formation in the surface and propagates under working conditions, this dramatically reduces the working life span of the MEA (and hence PEMFC) as well as the power output of the MEA. To form proton conducting channels from the PEM and catalyst sites on the GDEs, ionomer solution of the PEM is used as a paste between the GDE and PEM. During hot pressing the ionomer solution, which is usually a solution or suspension of similar if not the same composition to the PEM, sets and thus acts as these essential conduction pathways. The use of the ionomer solutions allows for better contact between the components in the MEA than just hot pressing alone, and for performance and long life spans of the MEA, good contact must be present and maintained.

When a PEM swells due to absorbing water, this causes pressure in the MEA and results in the MEA expanding. If the PEM is then allowed to dry out, this causes the PEM to contract. Depending on the adhesion between the GDEs and PEM, the extent of swelling and contraction of the PEM and how many cycles of hydration and dehydration the MEA undergoes could cause delamination between the PEM and GDEs thus increasing the resistance of the system and hence power output. For MEAs which

use Nafion as the MEA, delamination is a significant problem due to the large swelling when hydrated, the difficulty in keeping the membrane hydrated at elevated temperatures for prolonged periods of time and the chemical composition of the membrane (PTFE backbone) which effectively makes the surface of the membrane non-stick.[96] Similarly, membrane creep needs to be minimised to prevent MEA delamination as well pin-hole formation.

Thus when selecting a PEM for further evaluation for use in a PEMFC, the long term stability of the MEA is a key consideration, and this can be maximised by the selection of PEMs with low water uptake which results in low swelling, do not exhibit membrane creep, and have good adhesion properties. This would reduce the effect of multiple hydration and dehydration cycles, and keeping the MEA at elevated temperatures for prolong periods of time would have on the MEA. Membrane creep must also be minimised due to the hot pressing technique employed to manufacture MEAs. This effectively rules out the original formulation (575C etc), Type A which exhibited excellent conductivities and flexibility but very high swelling. Whereas Type D and E PEMs had conductivities too low to be considered for optimisation and homogenous Type F PEMs were not successfully synthesised. This leaves the option of Type B and C PEMs for possible optimisation, Type B PEMs exhibited slightly higher conductivities at comparable PA loadings, as can be seen in section 4.9, smaller swelling, lower water uptake and used less expensive and toxic precursors, thus are a better candidate for optimisation studies and more in-depth analysis.

Chapter 5

PEM selection, modification, characterisation and comparison to other phosphonic acid/hybrid polyurethane PEMs

5.0 Introduction

Of all the PEMs synthesised in the current work, those of Type B showed the most promise for use in PEMFC applications, in particular the membranes that had the prepolymer formulation of P_2MP_2. This type of membrane was stable in boiling water. They were flexible enough to bend around a cup without breaking, when cut did not fracture, displayed low water uptake and swelling with PA loadings up to 35% w/w, and did not visibly deteriorate after being immersed in Fenton's Reagent (3% H_2O_2, 5 ppm Fe^{2+}) at 80 °C for one hour. These membranes however, displayed conductivities an order of magnitude lower than those desired (100 mS cm^{-1}). To improve the observed total conductivities and area specific resistances of this type of membrane, variations in casting and curing were explored as well as modification of PA composition. These membranes were also characterised to enable more detailed understanding of the effect increased PA loading has on the water stability, uptake and swelling has on this composition. The thermal stability and membrane morphology was also studied.

5.1 Type B Blend 1 Optimisation

Membranes were prepared by prehydrolysing the prepolymer with dilute hydrochloric acid prior to the addition of PA. The proton conductivities of these membranes were determined by ACIS in the same way as the non-prehydrolysed membranes.

In related work by Honma *et al.* the authors prehydrolysed the prepolymers formed using dilute HCl (0.1 M, 1 mL) before the addition of the DBSA.[49] In this project the prepolymer was prehydrolysed using HCl, the addition of the PA occurred 30 seconds after the

prehydrolysis. If the PA was added after this amount of time elapsed, an inhomogeneous polymer solution was formed, which in turn lead to inhomogeneous membranes being formed.

5.2 Type B Blend 1 Optimisation: Normal Cell Proton Conductivity Results

The proton conductivities of the prehydrolysed membranes are shown in Fig. 5.1. The pre-hydrolysed membranes were conditioned by immersing in deionised water for one hour at room temperature, this was a very mild preconditioning step compared to boiling, steaming and the Nafion conditioning regime. The results for Nafion 117 are shown for comparison (the Nafion 117 membrane was boiled in 3% H_2O_2 for one hour followed by boiling in 1 M sulfuric acid for one hour and then boiling in deionised water for one hour).

The conductivity of Nafion is in agreement with published literature values for comparable experimental set-ups (two-probe normal cell, same conditioning), ranging from 20 mS cm^{-1} at room temperature to 55 mS cm^{-1} at 80 °C,[97] albeit slightly less than the literature values of Nafion 117 membranes measured in 4-probe tangential cell.[98] At and above 100 °C the conductivity of the Nafion membrane dropped dramatically, at 110 °C the conductivity dropped to 0.8 mS cm^{-1}, whereas membrane 064 which had a PA loading of 33% had a conductivity of 11 mS cm^{-1} at 120 °C. It is these high temperature conductivities which is where this new type of membrane can offer improved performance over established PEMs such as PBIs and Nafion.

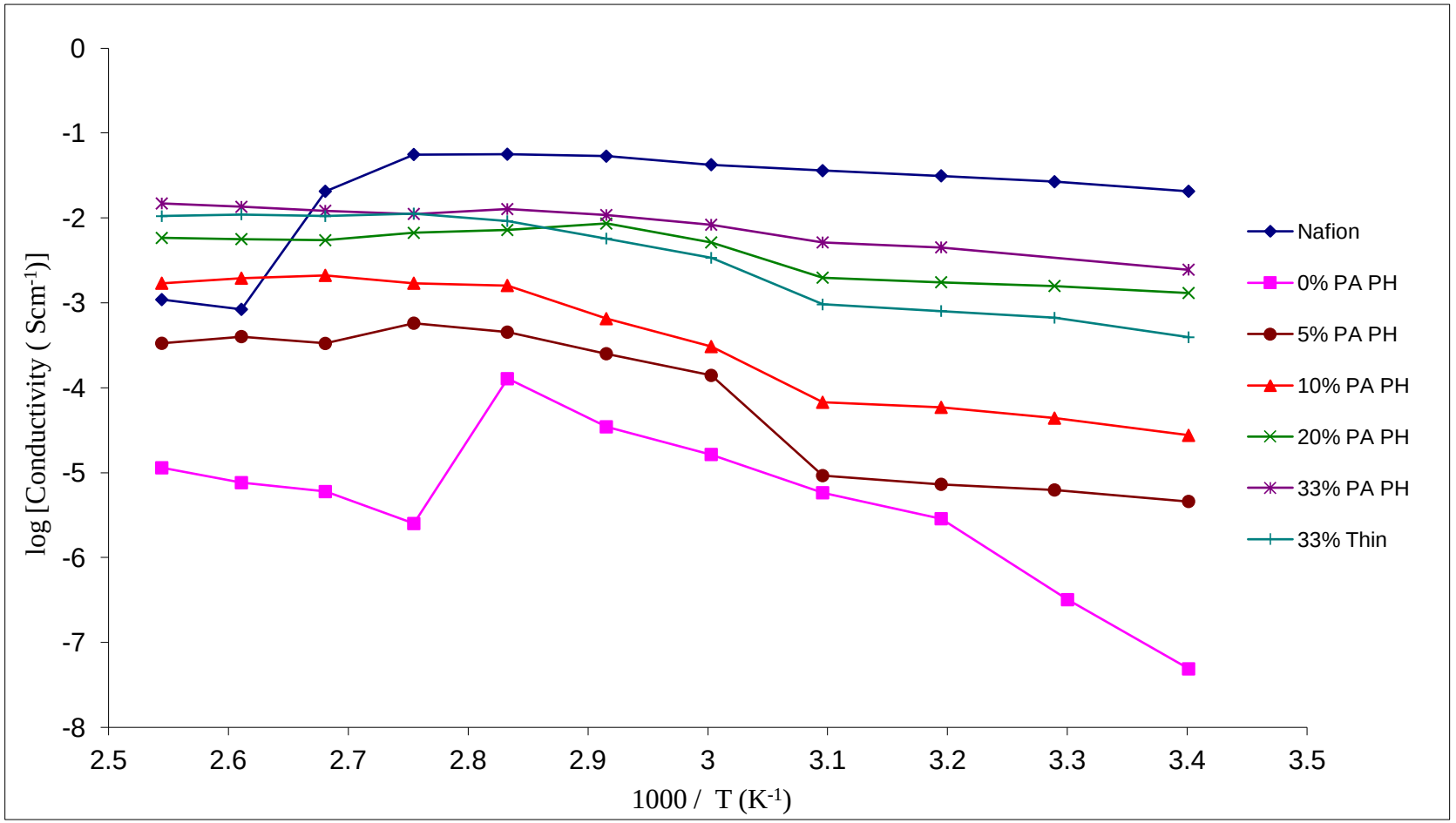

Fig. 5.1: Proton conductivities for Type B P_2MP_2 membranes (Pre-hydrolysed) at 100% RH and immersion conditioning heated to 120 °C, the proton conductivity for Nafion 117 measured under the same conditions is shown for comparison

The conductivities observed for the prehydrolysed Type B membranes that contained PA showed similar trends to each other. In the first heating cycle there was a step up in proton conductivity for the membranes between 50 and 60 °C or 60 and 70 °C. The observed increase in proton conductivities between these temperatures was less pronounced with increasing PA content. In the Type B PEM containing no PA, there was a large decrease in proton conductivity from 80 to 90 °C, indicating that the membrane started to dehydrate. This suggests that the phosphonic acid group helps to retain the absorbed water above 100 °C, as theorised by Kreur *et al*.[61] The E_a of proton conductivity at different temperature ranges for the PEMs tested is given in Table 5.1 (see chapter 4.3.4 for discussion on Ea values and reliabilities). The E_a value determined for Nafion 117 membrane was in good agreement with published literature values.[92] The E_a of membrane 064 was found to be under half of that for Nafion at lower temperatures and two-thirds of the value at higher temperatures, meaning that the energy required for proton transport to occur in membrane 064 is substantially less than that required for Nafion.

Table 5.1: Table showing activation energy of proton transport at different temperature ranges through Type B PEMs (Nafion E_a, determined under identical conditions shown for comparison)

PEM	Temperature Range	E_a / eV
Nafion	20 – 90 °C	0.14
048 (5% PA)	20 – 50 °C	0.55
	70 – 120 °C	0.022
050 (10% PA)	20 – 60 °C	0.42
	70 – 120 °C	0.17
054 (20% PA)	20 – 60 °C	0.14
	70 – 120 °C	0.20
064 (33% PA)	20 – 60 °C	0.065
	70 – 120 °C	0.098

The proton conductivities of the 1st, 2nd and 3rd heating cycles were reproducible at both high and low temperatures (RT and 120 °C) for all prehydrolysed membranes. A table of total conductivities shown in Table 5.2 of three membranes for comparison, those of membranes 050, 054 and 064 (10%, 20% and 33% PA loadings respectively).

Table. 5.2. Proton conductivities for membrane 050 (P_2MP_2 10% PA PH) measured over two heating cycles and heated to 120 °C at 100 % RH, immersed conditioning. All conductivities are in mS cm^{-1}.

	Membrane 050 Conductivities		Membrane 054 Conductivities			Membrane 064 Conductivities		
Temperature / °C	Heating 1	Heating 2	Heating 1	Heating 2	Heating 3	Heating 1	Heating 2	Heating 3
21	0.026	0.027	1.0	1.3	1.7	3.2	2.8	2.5
30	0.042	0.044	1.3	1.6	2.0	4.2	4.9	3.6
40	0.056	0.059	1.6	1.7	2.4	4.5	8.3	4.5
50	0.088	0.067	1.7	2.0	3.5	4.9	9.8	5.1
60	0.20	0.31	1.7	5.1	4.3	5.1	13	8.3
70	0.66	0.65	2.1	8.6	6.7	9.0	15	11
80	0.91	1.6	3.1	7.2	7.2	9.8	13	13
90	0.86	1.7	9.5	6.7	5.6	11	12	11
100	0.87	2.1	12	5.5	4.3	12	13	12
110	1.1	2.0	8.6	5.6	4.7	13	14	14
120	1.7	1.7	7.2	5.8	5.0	17	15	15

Membrane 064 also showed similar proton conductivities over three heating cycles when preconditioned by immersing in deionised water as shown in Table 5.2. The proton conductivity of a sample of membrane 064 which had been steam conditioned was also measured up to 120 °C, the results of which are also given in Table 5.3.

Table 5.3: Total proton conductivities of membrane 064, measured to 120 °C over 3 heating cycles at 100% RH, immersed conditioned. Also shown membrane 064 steam conditioned measured over one heating cycle

Temperature / °C	σ Cycle 1 / mS cm^{-1}	σ Cycle 2 / mS cm^{-1}	σ Cycle 3 / mS cm^{-1}	σ Steamed conditioned / mS cm^{-1}
21	3.2	2.8	2.5	48
80	9.8	13	13	36
120	17	15	15	34

As can clearly be seen from Table 5.3, the proton conductivity of the sample of membrane 064 which had been conditioned by steaming was significantly higher than the sample which had been immersed in deionised water. This was a similar effect to that observed in Type B PEMs with additional network formers from Glysil and TEOS (section 4.4.3), where upon steaming, the Glysil containing membrane 059 displayed higher proton conductivities than the membrane that was conditioned by boiling in deionised water. A sample of membrane 064 which had been conditioned by immersion in deionised water was heated to 120 °C in the normal cell at 100% RH, and maintained at this temperature for 102 hours. Initially the proton conductivity was 17 mS cm^{-1}, after 102 hours the proton conductivity was re-measured and was found to be 14 mS cm^{-1} which indicates stability of conductivity at temperatures above 100 °C at 100% RH.

5.3 Type B Blend 1 optimisation: Tangential Cell Proton Conductivity Results

Due to the relatively high conductivities of membrane 064 (P_2MP_2 33% PA PH), the proton conductivity was also measured in the tangential cell. Two pieces of membrane were tested with different conditioning, one of boiling in deionised water for 30 minutes and one of immersing the membrane in deionised water for 3 hours prior to measurement. The results are summarised in Table 5.4. Resistance and conductivity values are quoted to only two significant figures due to the qualitative nature of ACIS.

Table 5.4: Calculated total resistances and conductivities for membrane 064 in the tangential conductivity cell with both boiled (5.3a) and immersed (5.3b-d) conditionings.

5.4a: Calculated total resistance and conductivity for membrane 064 heated to 100 °C at 100% RH in the tangential cell, conditioned by boiling in deionised water

Temperature / °C	Resistance / Ω	Conductivity / mS cm^{-1}
21	7700	5.0
80	2600	15
100	3200	12

5.4b: Calculated Total Resistance and Conductivity for membrane 064 heated to 80 °C at 100% RH in the Tangential Cell over the 1st heating cycle, conditioned by immersing in deionised water

Temperature / °C	Resistance / Ω	Conductivity / mS cm^{-1}
21	23000	1.6
80	2500	14
80 (19 h)	2400	15

5.4c: Calculated total resistance and conductivity for membrane 064 heated to 80 °C at 100% RH in the tangential cell over the 2nd heating cycle, conditioned by immersing in deionised water

Temperature / °C	Resistance / Ω	Conductivity / mS cm^{-1}
25	3800	9.3
21 (1 week)	2100	17
80	2700	13

5.4d: Calculated total resistance and conductivity for membrane 064 heated to 80 °C at 100% RH in the tangential cell over the 3rd heating cycle, conditioned by immersing in deionised water

Temperature / °C	Resistance / Ω	Conductivity / mS cm^{-1}
21	5500	6.4
21 (1 week)	4100	8.7
80	3500	10

The results for the boiled membrane 064 in the tangential cell showed high conductivity at room temperature which was twice that of the same membrane immersed in water and measured in the normal cell, but still significantly less than that of the steamed conditioned sample in the normal cell however the high temperature conductivities for both the tangential and normal cell measurements were comparable. In the normal cell, the impedance is measured through the membrane in the direction of which the protons would travel in a working PEMFC, however in the tangential cell set up this is not the case, the impedance is measured laterally through the membrane in a transverse direction to which the protons would be transported in a working PEMFC. The applied current will travel along the path of least resistance, and in the tangential cell configuration this may not necessarily be through the bulk of the PEM but rather the surface of the PEM, which would deflate the determined resistance values. As in this case the conductivities of both the normal and tangential cells were similar, the actual direction of current travel did not affect the conductivity results. The fact that the boiled and immersed conductivities were comparable indicated that boiling the membrane did not result in acid leaching for this membrane formulation, this was confirmed by titrametric analysis of the deionised water the PEM was boiled and immersed in.

When the membrane was heated to 100 °C in the tangential cell, the membrane warped irreversibly. The impedance plot obtained once the membrane had cooled could not be used to extract the resistance of the membrane. This membrane warping was also observed for Nafion membranes in the tangential cell. This was caused by the cell design of the two-electrode tangential cell. In a four-electrode configuration the outer

pair of electrodes are current collectors and the inner pair of electrodes are used to measure the phase difference of the applied potential (*i.e*. impedance).[97] This means that in the four-electrode method the contact between the electrolyte (the membrane) and the outer electrodes is not a big issue. In the two-electrode method the one set of electrodes has both functions, thus membrane-electrode contact crucial. If the contact is not adequate then very noisy impedance spectra are obtained which cannot be used to extract the electrolyte resistance.

To limit membrane deformation, the cell was redesigned to remove the window in the centre of the cell. The redesign of the cell then allowed adequate contact between the electrodes and PEMs for proton conductivities to be measured over several cycles at room temperature to 80 °C. Impedance spectra were not obtained between these temperatures, as due to the new cell design, long equilibration times were required. However the results at these two temperatures for membrane 064 show comparable conductivities to the membrane when measured in the normal cell with the same conditioning. The determined proton conductivities when measured in the tangential cell are shown in Fig. 5.2.

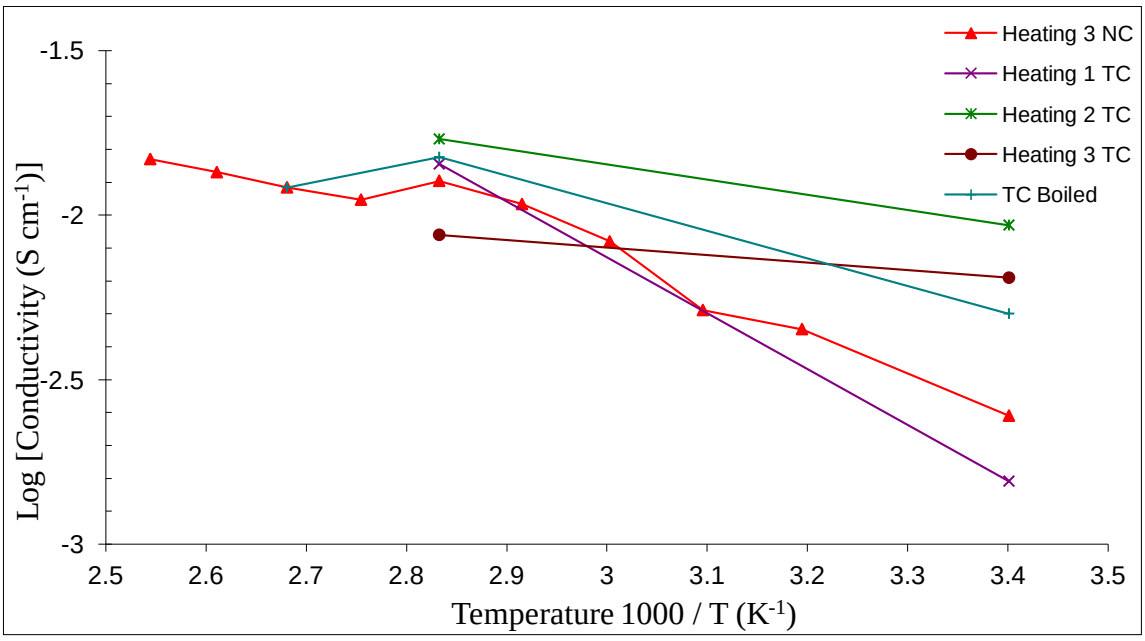

Fig 5.2: Proton Conductivities of membrane 064 measured in the normal cell (NC) and tangential cell (TC). Heating 1-3 TC the membrane was pre-conditioned by immersion in deionised water and heated to 80 °C over 3 heating cycles at 100% RH. TC boiled was conditioned by boiling in deionised water and heating to 80 °C over one heating cycle. Heating 3 of membrane 064 measured in the normal cell is shown for comparison

After each heating cycle in the tangential cell, the membrane was allowed to cool back down to room temperature and the impedance was remeasured. The membrane was then left in the humidity chamber over water (100% RH) for a week before the impedance was remeasured before heating again to 80 °C. This delay for a week prior to measurements was to allow further equilibration between the membrane and the environment. After this time the membranes showed a slightly higher conductivity than just after the PEM had cooled down, a typical spectrum obtained at room temperature is shown in Fig. 5.3. On the first heating cycle of the immersed conditioned membrane, the membrane was kept at 80 °C for 19 hours to determine if there was a significant change in conductivity. The difference in conductivity was negligible (14 and 15 mS cm^{-1} for initial and final measurements, respectively) as can be seen from the Nyquist plot of the impedance spectra shown in Fig. 5.4, thus indicating that conductivity of the membrane was stable at elevated temperatures for prolonged time in the tangential cell.

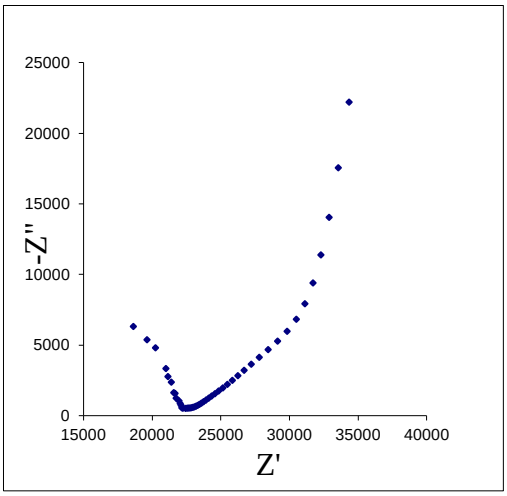

Fig. 5.3. Nyquist plot of impedance spectrum of membrane 064 at RT in the tangential conductivity cell, immersed conditioning, 1st heating cycle

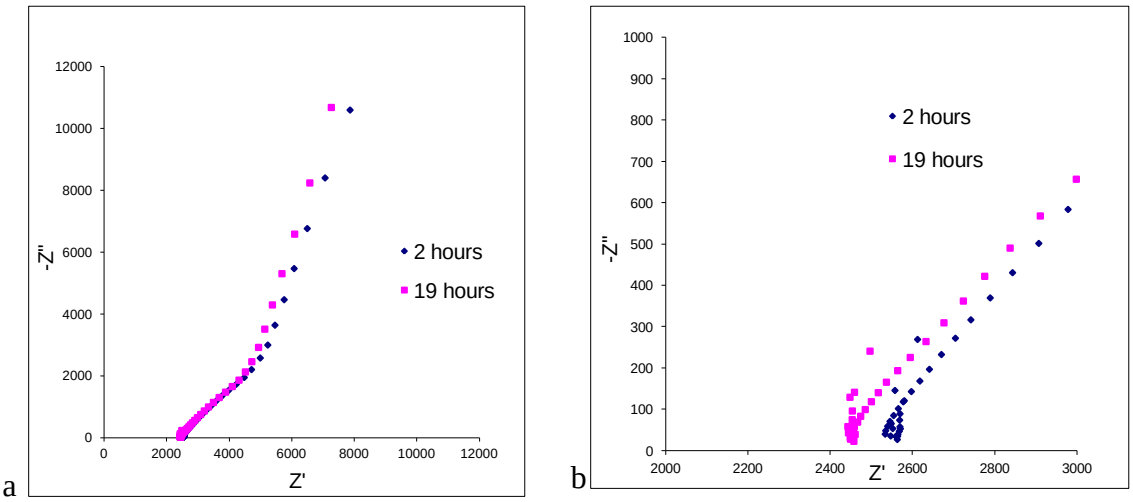

Fig. 5.4. Nyquist plots of impedance spectra of Membrane 064 in the tangential conductivity cell at 80 °C after 2 and 19 hours respectively, 1st heating cycle. a) entire spectra, b) high frequency region.

At room temperature in the impedance spectra, the end of the semi-circle (the response from the bulk electrolyte) was clearly visible (Fig. 5.3). At higher temperatures (80 °C), the end of the semi-circle was not clearly visible, although there were a few points indicating the very end of the semi-circle (Fig. 5.4). After being kept at 80 °C for two hours, there was a loop at the high frequency range of the impedance spectra, indicating that the impedance and thus the resistance was not constant during measurement and was consistent with the membrane not being fully equilibrated, resulting from the long measurement times. After 19 hours the loop was less pronounced which indicated that the membrane was closer to equilibration (Fig. 5.4b). Although the determined resistance after heating for 19 hours was less than that after 2 hours, there was only *ca.* 4% difference. The disappearance of the bulk semi-circle response was due to the frequency shift of the bulk electrolyte response not being detected due to the upper limits of the frequency range being measured (1 MHz) and interference from the membrane/electrode interface which became the dominant response in the measured frequency range.[97]

For highly conductive materials in the tangential cell (and even the normal cell) the bulk electrolyte signal (the semi-circle) is observed at high frequencies, typically above 1 MHz. For most of the semi-circle to be recorded, frequencies of up to 100 MHz need to

be measured,[55] which unfortunately was beyond the capability of the frequency response analyser used in this work (Autolab PGSTAT302N).

There were two gradients to the blocking spike recorded at both RT and 80 °C, as can be seen in Figs. 5.3 and 5.4 (around 40 and 75° respectively). The lower gradient part of the blocking spike was caused by the membrane-electrode interface not being ideal, thus creating interfacial impedance, which causes the blocking spike to be ≈ 40-degree angle.[99] The interfacial impedance was probably caused by the electrode being damaged (scratched) thus creating the interfacial impedance.[100] However the observed interfacial impedance does not directly affect the determination of electrolyte resistance from the impedance spectra. At even lower frequencies, this interfacial response was not visible and the blocking spike reverts to typical behaviour.

By the third heating cycle the proton conductivity of the membrane in the tangential cell was significantly lower at 80 °C than that in both the first and second heating cycles. After this heating cycle the tangential cell was removed from the humidity chamber, and was then dismantled. The membrane had not visibly deformed over the three heating cycles, which was also the case when the membrane was heated in the normal cell over several heating cycles.

5.4 Blend 2-4 PA Type B PEMs

Membranes with the different ratio of **13**:**15** (mono:bis) phosphonic acid (the structures of which are shown in Fig. 5.5) were also prepared to determine the difference in physical properties that the introduction of more bis PA would have. Blends of PA were prepared by mixing the desired quantities of phosphonate esters dimethylphosphonatoethyltriethoxysilane and 2,4-*bis*(triethoxysilyl)-1-dimethyl phosphonatobutane, which were then hydrolysed to produce the desired PA. The P_2MP_2 polymer matrix was chosen due to the desirable properties displayed by those membranes made from Blend 1 PA.

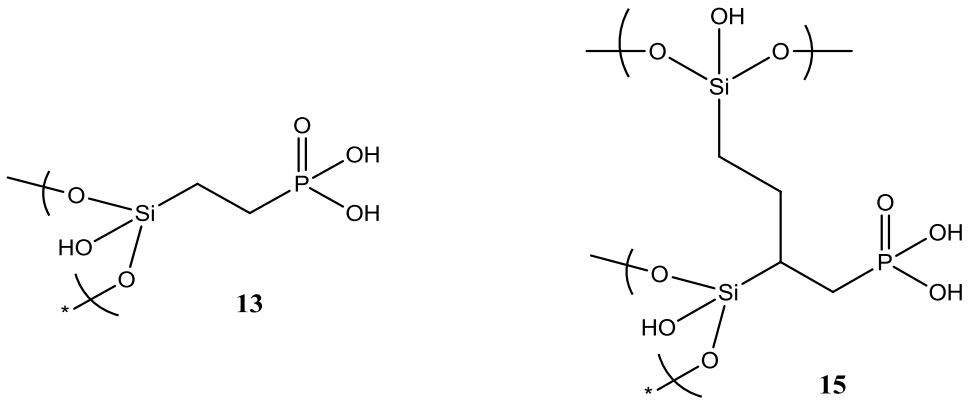

Fig 5.5: Structure of molecules (PA) **13** (mono) and **15** (bis)

Initially Blend 4 (90% **13**: 10% **15**) was used as the PA precursor and was hydrolysed by method 3. This was then added to the prepolymer matrix to produce a membrane with 20% PA loading. However, the membrane produced was visibly inhomogeneous with very poor mechanical properties being very brittle, indicating that this Blend was not suitable for PEM synthesis. It was reasoned that the poor physical characteristics of this membrane was due to **15** being present in too high an amount, making the PA particle size too large to form a homogenous dispersion. Due to this initial result, the synthesis of a membrane incorporating Blend 5, which had a **15** content of 30%, was not attempted.

The amount of bis PA was then reduced to make Blend 3, which had a 6% **15** component. The membrane produced was of a similar quality to that of the membrane produced using Blend 4. No further work was carried out on this membrane.

The amount of **15** in the PA was then further decreased to only 4%, which is 2% greater than that of Blend 1 to synthesise membranes with Blend 2 PA. The membranes produced in this fashion had similar mechanical and physical properties to those membranes made with Blend 1. The proton conductivities of membrane 056 (P_2MP_2, 20% PA Blend 2) which was measured over three heating cycles are shown in Fig. 4.17. A second membrane was tested which had a higher PA loading, membrane 069 (P_2MP_2 35% PA), the proton conductivities of this membrane are also shown in Fig. 5.6.

5.4.1 Blend 2-4 PA Type B PEMs Proton Conductivities

The impedance spectra obtained from the membrane containing blend 4 PA were of very bad quality and could not be used to determine the membrane resistances, and thus their proton conductivities could not be determined.

The ACIS results for the membranes made with blend 2 were surprising as both the 20% and 35% PA loaded membranes display similar conductivities to each other at higher temperatures (at and above 80 °C) as can be seen in Fig. 5.6. In the membranes that contained blend 1 PA, the conductivity of the 35% PA membrane was nearly double that of the 20% membrane (12.7 mS cm^{-1} and 7.2 mS cm^{-1} respectively) at 120 °C and the difference in conductivity was an order of magnitude greater (30.7 mS cm^{-1} and 3.1 mS cm^{-1} respectively) at 80 °C (the results of which are shown in Fig. 5.7). The blend 2 membranes also displayed lower conductivities than their blend 1 counterparts, which had the same PA w/w loading as can be seen in Fig. 5.8. The blend 1 membranes exhibited higher conductivities on their first heating cycle at both low and high temperatures. This initial testing indicated that the membranes containing blend 1 PA were more suitable than those containing blend 2 PA.

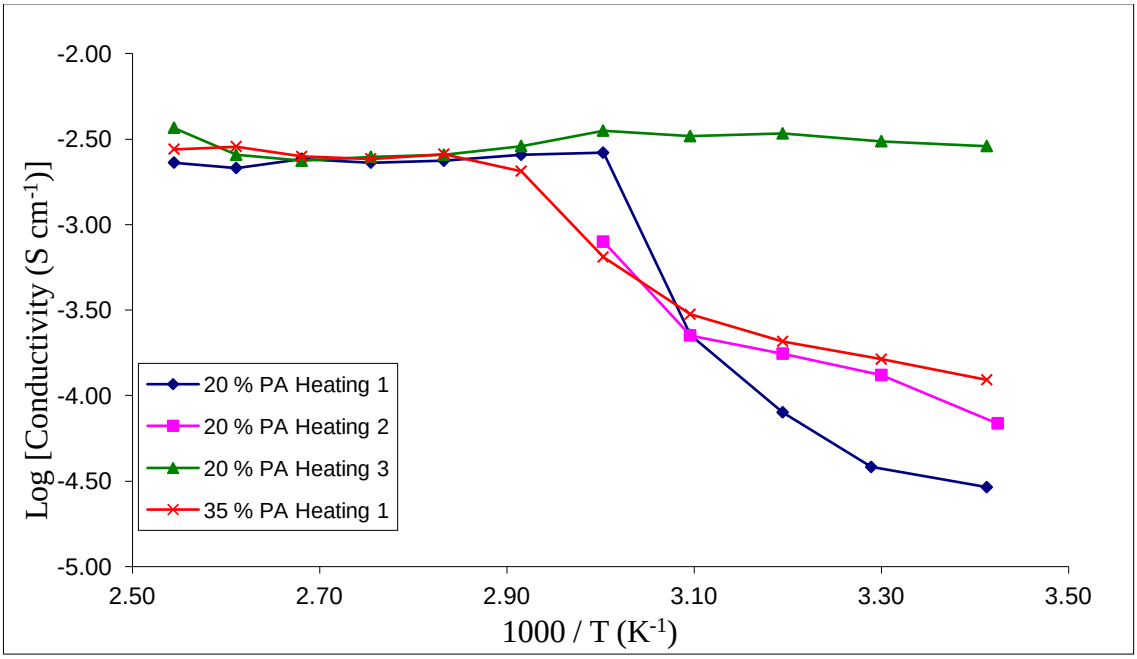

Fig. 5.6. Total proton conductivities of membrane 056 (20% PA) heated to 120 °C over 3 heating cycles, and membrane 069 (35% PA) heated to 120 °C over 1 heating cycle, both at 100% RH

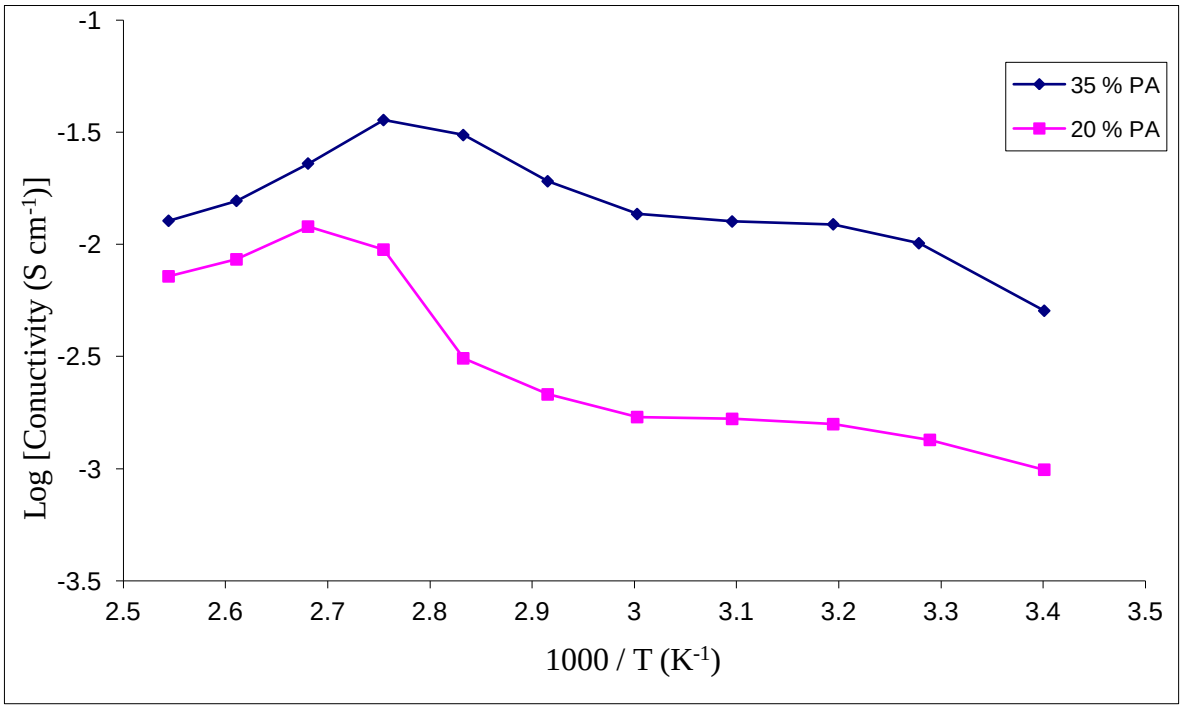

Fig. 5.7. Total proton conductivities of Blend 1 PA membranes 054 (20% PA) and 072 (35%) heated to 120 °C over one heating cycle at 100% RH, preconditioned by immersion in deionised water

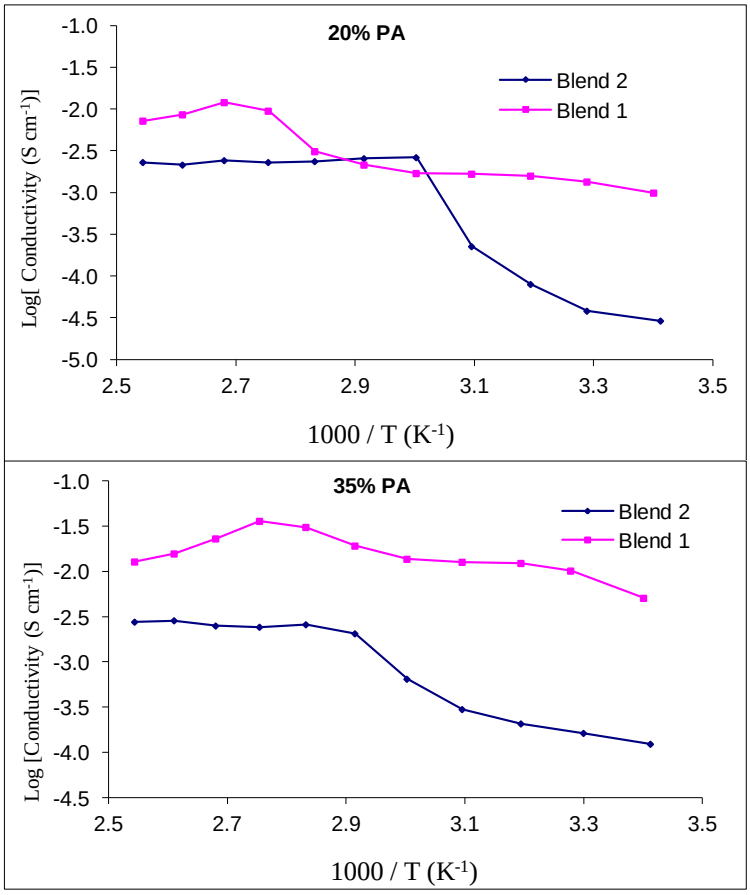

Fig. 5.8. Comparison of total proton conductivity comparison for Blend 1 and 2 membranes with PA loadings of 20 and 35% loading, heated to 120 °C at 100% RH on the first heating cycle, all membranes were preconditioned by immersion in deionised water

As discussed in chapter 1, although the proton conductivity of a PEM is a critical property, it is not the only property that needs to be taken into consideration in the development of new PEMs. The thermal and oxidative stability of the PEMs are vital for long term use in PEMFCs. To determine the thermal properties of the PEMs, TGA and DSC can be employed. Other properties which are important and need to be determined are IEC/EW, water uptake, chemical structure of the PEM and PEM surface morphology. These are discussed for the Type B P_2MP_2 formulation in the next few sections.

5.5.1 Type B Blend 1 Optimisation: Thermal Testing Results: TGA

The thermal stability of the membranes was recorded by thermal gravimetric analysis (TGA), which was performed on hydrated membranes in air to determine the oxidative stability of the membranes at elevated temperatures. A TGA trace of hydrated membrane 064 is shown in Fig. 5.9.

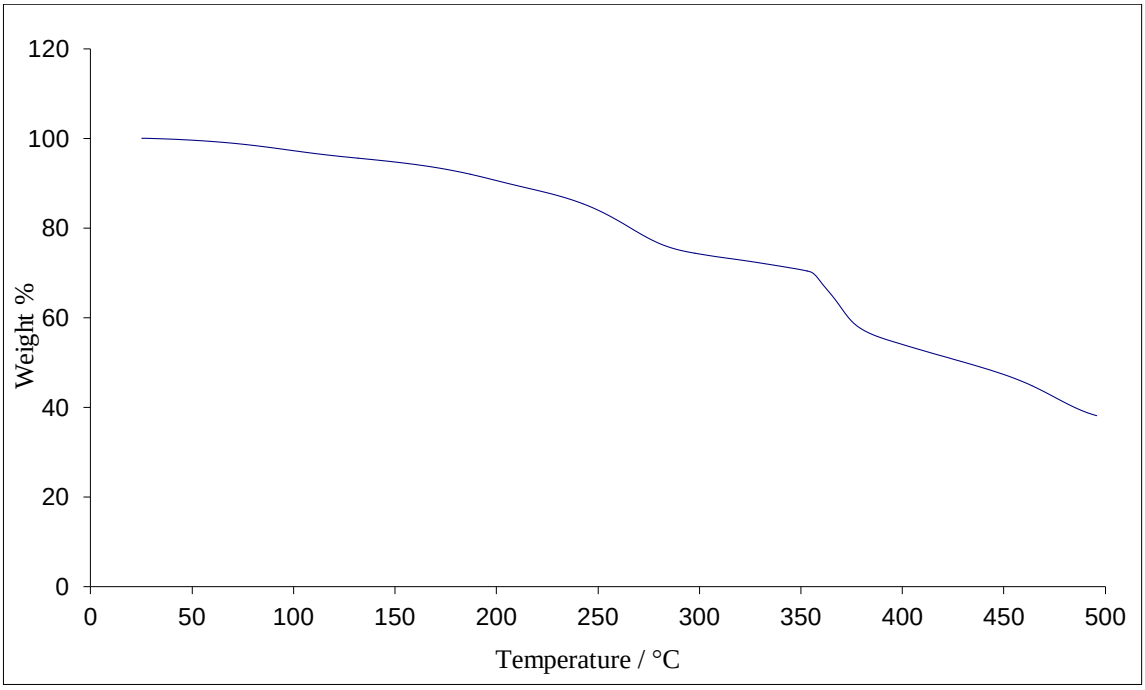

Fig. 5.9. TGA trace of hydrated membrane 064 in air, heating ramp 10 K min^{-1}

The membrane was first stored over phosphorus pentoxide for 24 hours and the dry mass recorded and then conditioned by immersing in deionised water for 24 hours prior to measurement and the mass re-recorded just prior to measurement. The membrane gradually lost 14% mass up to 240 °C, which was from the membrane losing absorbed water, the mass loss was in agreement with the water uptake from the conditioning step. Further mass loss was recorded on further heating with the mass loss up to 300 °C resulting from the decomposition of urethane bonds, releasing both water and carbon dioxide, and the mass loss over 300 °C from the oxidation of the organic polymer segments. After the sample was heated to 500 °C, the membrane was cooled and visually inspected. The membrane had turned black and was stiff and very brittle (it was easily snapped). This 40% mass left after the experiment was the inorganic component of the membrane with some residual carbon retained in the residue. This is in reasonable agreement with the amount of inorganic (SiO_2) in the membrane from a 33% PA loading as well as the SiO_2 terminal groups on the PU polymer matrix. This simple experiment indicated that this membrane was stable in an oxidative environment, such as would be present in the PEMFC in the operating temperature range (RT-120 °C).

To determine the long-term oxidative/thermal stability of the membrane, as in a working PEMFC environment where the temperature would routinely be kept at elevated levels for extended periods, an isothermal TGA experiment was performed. In this experiment a hydrated membrane was quickly heated to 120 °C and then kept at this temperature for 24 hours. The TGA trace for this experiment is shown in Fig. 5.10.

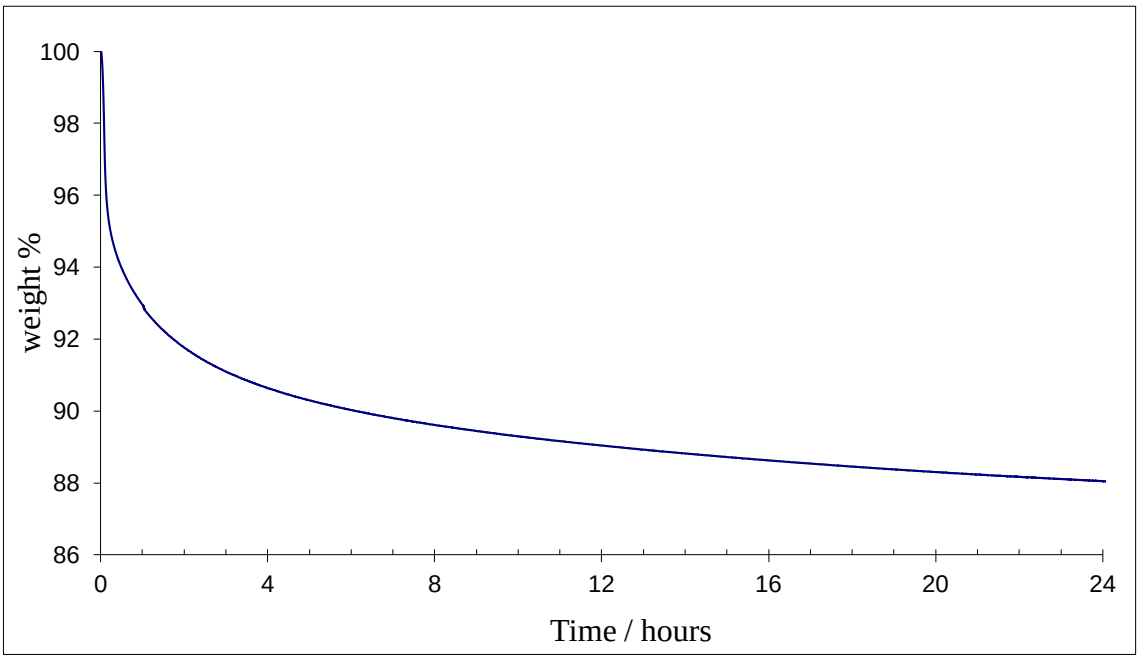

Fig. 5.10. Isothermal TGA trace of hydrated membrane 064, 120 °C for 24 hours

As can clearly been seen in the TGA trace (Fig. 5.9), the membrane rapidly lost 7% mass during the first hour. The rate of mass loss after this time dramatically decreased, over the next 7 hours, only a further 3% mass was lost and in total over the 24 hours measured at 120 °C the membrane only lost a total of 12% mass. This gradual loss of mass was associated with the dehydration of the hydrated membrane. This gradual water loss indicated that the absorbed water was tightly bound in the polymer matrix via chemical and/or physical interactions, notably that of hydrogen bonding. This strong interaction between the membrane and the absorbed water was also supported by DSC frozen water experiments (section 5.4.2). Ideally the isothermal TGA experiment should be performed under humidified conditions to replicate the conditions in a PEMFC and impedance testing, this would be beneficial as the water absorbtion/desorbtion kinetics could be determined for different temperatures and also different temperature ramps. However, this was not possible in this project, as no access to the specialised equipment to perform these experiments could be obtained. Despite this, the results did indicate that the membrane is suitable for long term use in a PEMFC as it is oxidatively stable at elevated temperatures for prolonged periods of time.

5.5.2 Type B Blend 1 Optimisation: Thermal Testing Results: DSC

DSC experiments were performed to determine whether or not there were any phase changes in the membranes over the operational temperature of a PEMFC. Typically experiments were performed on heating from 10 °C to 150-180 °C and on cooling back to 10 °C over a total of 3 heating and cooling cycles. Membranes with a wide variety of acid content (from 0 to 35%), prehydrolysed and non-prehydrolysed were examined. In all cases the DSC traces were similar, where the membranes were hydrated prior to measurement there was only a broad endothermic and exothermic process on the first heating cycle (as seen in Fig. 5.11), whilst the other heating and all the cooling cycles show a featureless flat line. This indicated that there was no glass transition (T_g) in the temperature range recorded. The DSC traces were recorded under a nitrogen atmosphere.

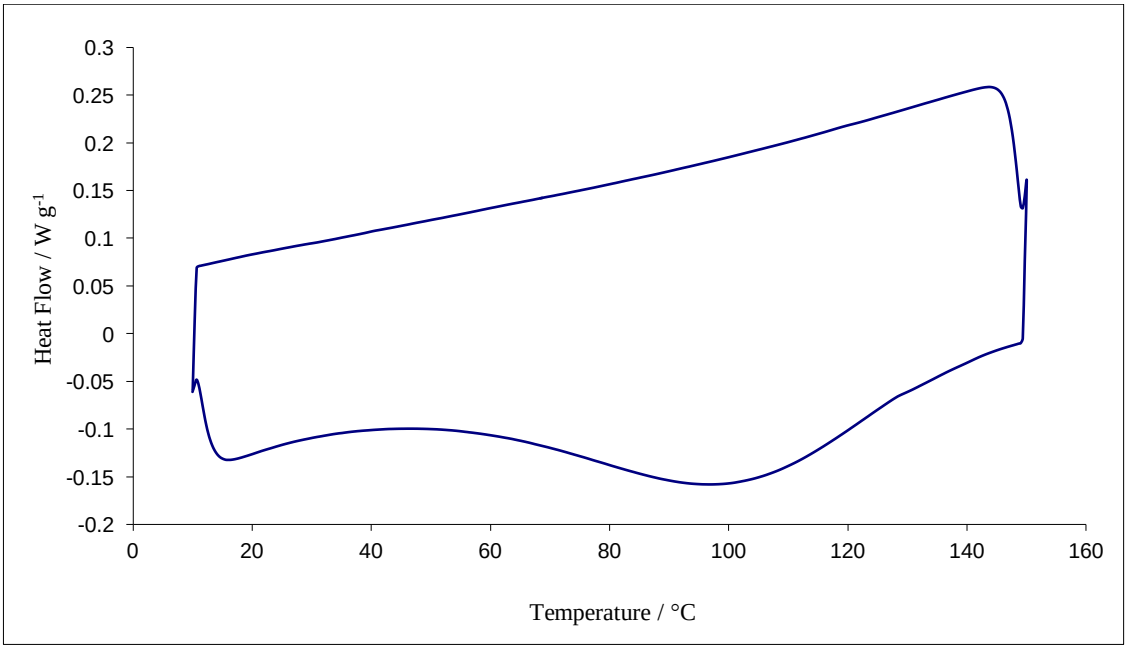

Fig. 5.11. DSC trace of hydrated membrane 064, first heating (bottom trace) and cooling cycle (upper trace)

To determine whether or not the broad peak observed in the first heating cycle hid any features, the DSC traces of a dry membrane were recorded using the same experimental settings, and are shown in Fig. 5.12, with the trace for a hydrated membrane for direct comparison. The second and third heating cycles of the anhydrous membrane showed

similar trends to that of the subsequent cycles for the hydrated membrane. There were unsurprisingly large differences in the recorded DSC traces for the first heating cycle of the hydrated and non-hydrated membranes. In the trace for the non-hydrated membrane there were two small steps visible, one at approximately 50 °C and a second at approximately 75 °C.

Although DSC is not a technique that directly measures mass change (unlike TGA), a DSC experiment can still detect mass change in a sample as it is heated (or cooled), provided the mass change is associated with a change in enthalpy. As a membrane dehydrates, it is reasonable to assume that the membrane will reorganise its internal structure to fill the space that was occupied by water, giving rise to the broad endothermic peak from 70 – 130 °C as seen in Fig. 5.12. The DSC trace for the dry membrane on the first heating cycle (Fig. 5.13) showed a shallow endothermic peak indicating that this membrane retained some water (or possibly NMP solvent) after drying over phosphorus pentoxide for 24 hours, or from absorbed water from the atmosphere immediately prior to the DSC trace being recorded.

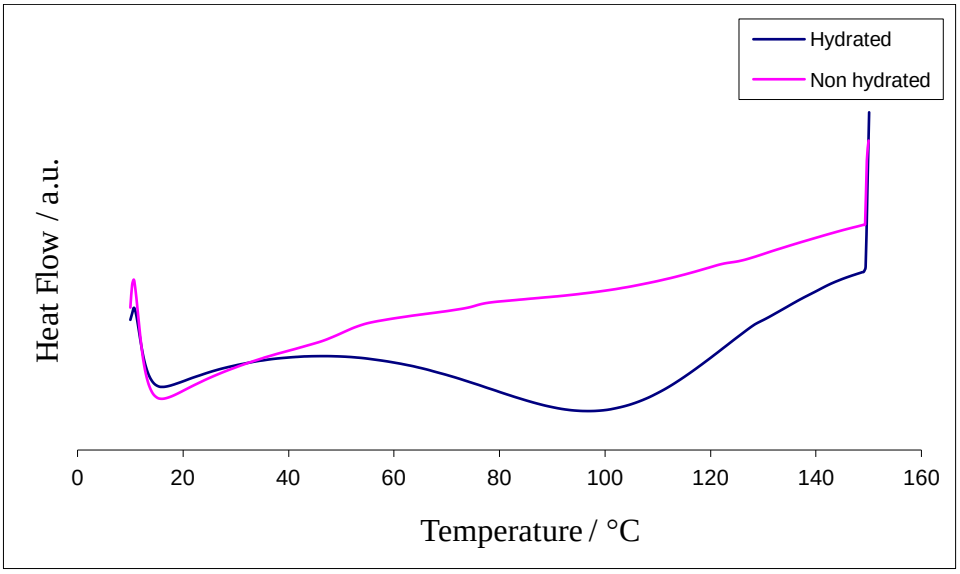

Fig 5.12: DSC traces of membrane 064 1st heating cycle for both hydrated and anhydrous samples

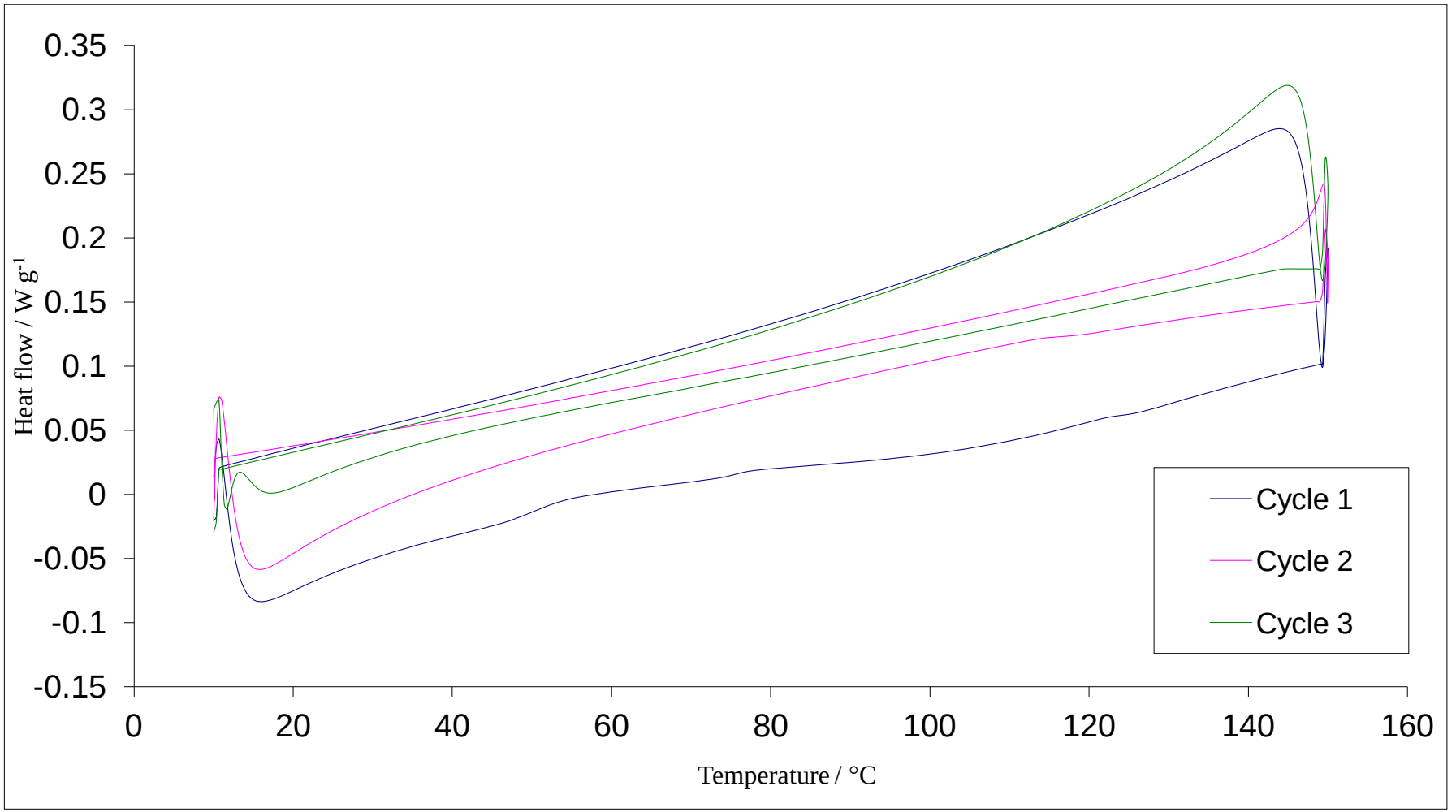

Fig. 5.13. DSC traces of dried membrane 064 over several heating and cooling cycles. The lower traces are the heating cycles and the upper traces are the cooling cycles

After the first heating cycle neither the hydrated nor the non-hydrated membranes showed any further thermal events as can be seen in Fig. 5.12. This implied that after the heating run, the majority of the absorbed water had evaporated and agrees with the results of the TGA experiment.

A second DSC experiment was performed on a sample of hydrated membrane 064, a freezing water experiment. In this experiment a segment of hydrated membrane was cooled to –20 °C for 15 minutes before being gradually heated to above room temperature. There are two possible types of water present below 0 °C, that of frozen water, which could be considered as bulk or free water, and that of liquid water, which could be considered as bound water. Bulk water would freeze at (and below) 0 °C, thus would be the source of frozen water. However if the water interacts with the polymer matrix (via hydrogen bonding) then it is not in the bulk state and thus would exhibit different physical properties, most notably that of melting point.

From this experiment, if there was any frozen water present then an endothermic peak on the DSC trace would be present upon heating the sample (where the ice melts). Integrating the endothermic peak would provide the energy absorbed to melt the ice, so the quantity of frozen water could be evaluated. However, the results are qualitative at best, as the results are highly dependent on experimental conditions (initial temperature, length of time of equilibration, heating ramp etc).

The results indicated that there was no frozen water present as there was no endothermic peak below, at or above 0 °C. These results were not unexpected considering the total volume of water in the hydrated membrane was only *ca.* 13%, the high concentration of PA and hence a low λ value of 2.7, for the membrane. It has been determined that Nafion has a large portion of absorbed water that is in the bulk-state, *i.e.* would be frozen and melted in this experiment.[101] However, Nafion absorbs a higher mass percentage of water (38%) and has a much higher λ value of 21. The PTFE backbone of the Nafion polymer does not form

hydrogen bonds or other strong physical attractions between the water molecules and PTFE chains.[4] There are relatively few sites in the Nafion polymer for water to interact with; these are either the oxygen atoms forming an ether link or the sulfonic acid functional groups. However, in Nafion there are relatively fewer sulfonic acid groups as determined by IEC (0.91 mmol g^{-1}) and EW (1100). The conjugate base of the sulfonic acid ($-SO_3^-$) and the ether oxygens in Nafion do not display the same properties as similar groups in hydrocarbons due to the electron withdrawing properties of fluorine atoms in the polymer matrix. The fluorine atoms make the oxygen atoms less electronegative, which would in turn decrease their interaction with water molecules.

The strong interaction between membrane 064 and water, such that there was no frozen water evident in the DSC experiment, was consistent with the proton conductivity at temperatures above 80 °C. At temperatures above 100 °C in a humidified environment the membrane retained sufficient water to enable efficient proton transport through the membrane via the Grotthuss mechanism, as indicated by the observed low E_a value derived from the conductivity plots. Absorbed liquid water in the bulk state would turn into water vapour above these temperatures, thus resulting in membrane dehydration and a dramatic decrease in proton conductivity which is seen in Nafion membranes.

5.6 Type B Blend 1 Optimisation: IEC

The IECs of the prehydrolysed and non-prehydrolysed membranes were determined by titrimetric analysis. IEC is a useful tool in PEM characterisation as it gives quantitative values for available acid content in the PEM. IEC is typically determined by immersing a portion of the membrane (*ca.* 300 mg) in dilute sodium chloride solution for an extended duration, typically 24-48 hours.[102,103] During this time, the acid from the membrane exchanges with the salt solution forming an equilibrium as described in equation 5.1.

$$NaCl + R\text{-}SO_3H \rightleftharpoons HCl + R\text{-}SO_3Na \qquad (5.1)$$

An aliquot of this solution was then removed and the acid content of the membrane was determined by titration against dilute sodium hydroxide solution. The end point was determined either by phenolphthalein indicator or by pH meter.

In this project since phosphonic acid was used as the proton donor in the PEM, it was decided to use a salt of an acid with a higher pKa value than that of phosphonic acid. For this reason sodium formate was chosen as its acid, formic acid, has a pKa of 3.74,[104] compared to that of phosphorous acid (the nearest free acid equivalent to phosphonic acid), which has pKa values of 1.3 and 6.7.[105] In both phosphorous and phosphonic acid, the first acidic proton is easily dissociated, whereas the second acid proton is much weaker than that of the first and is comparable in strength to that of carbonic acid (pKa 6.4),[104] so in the IEC as determined by this method, only the first acidic proton should exchange with a sodium ion, forming the equilibrium described in equation 5.2.

$$HCO_2Na + R\text{-}P(O)(OH)_2 \rightleftharpoons HCO_2H + R\text{-}P(O)(OH)(ONa) \qquad (5.2)$$

Initially the IEC was determined by producing titration curves using a pH meter. The advantage of using a pH meter instead of using phenolphthalein indicator was that the entire titration curve could be recorded. Formic acid is a mono acid, thus only one neutralisation event should be possible. If two or even three neutralisation events were visible then this must be due to released phosphonic acid which would have leached out of the membrane. This observation would provide quantitative results on the extent of phosphonic acid leaching, such as was determined for membrane 575C of the original formulation. In all cases for Type B PEMs where the IEC was determined using a pH meter, only one neutralisation point was visible, thus showing that PA leaching was negligible.

The IEC of membrane 046 (0% PA loaded P_2MP_2 membrane) was determined in the same fashion as to those PEMs that contained PA. This value was then used to standardise the IEC values of the other membranes in the series to take into consideration the small volume of dilute HCl added to prehydrolyse the membranes. The determined IEC of membrane 046 was 0.04 mmol g^{-1} equiv. The results are summarised in Table 5.5 and Fig. 5.14.

Table 5.5: IEC and EW of prehydrolysed P_2MP_2 membranes

% PA Loading	Standardised IEC / mmol g^{-1} equiv	EW / g mol^{-1}
0	0	N/A
5	0.120	8475
10	0.91	1099
15	1.43	699
20	1.94	515
25	2.38	420
30	2.59	386
33	2.65	377
35	2.66	376

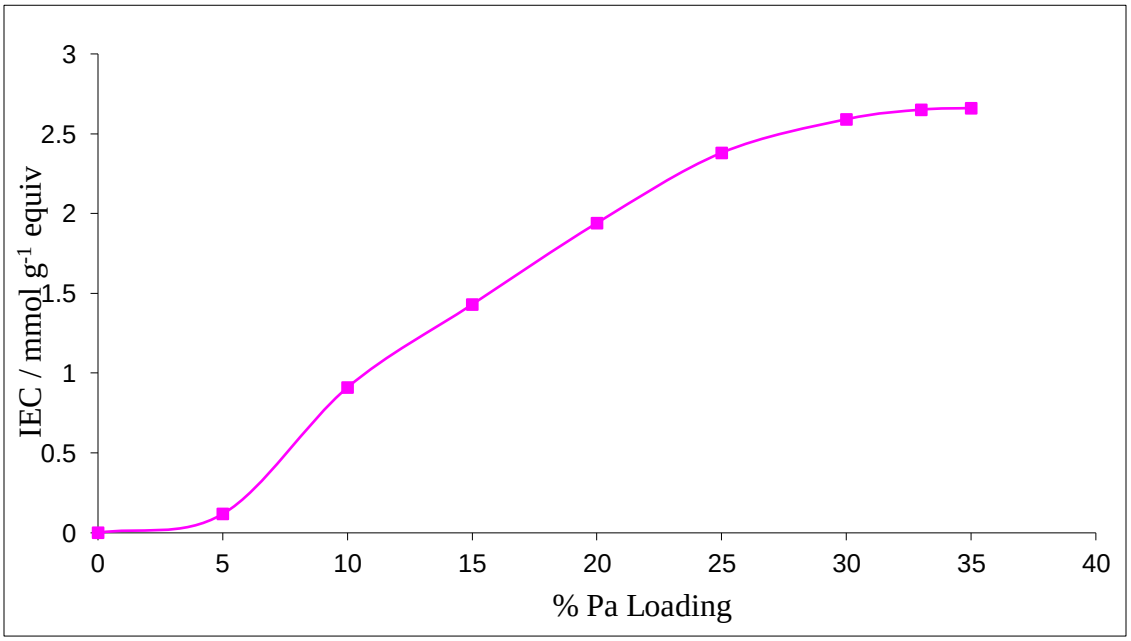

Fig. 5.14. IEC of prehydrolysed P_2MP_2 membranes with increasing PA loadings, as standardised (corrected) data

Initially at 5% PA loading the IEC was 0.12 mmol g^{-1} equiv, which equated to an EW of 8475 g mol^{-1}. Assuming that hydrolysis was 100% complete (evidenced from ^{31}P NMR spectroscopy), and the PA and siloxane end groups on the polymer matrix were fully cross-linked, the IEC was far below the expected PA content of the membrane. The IEC should have been *ca.* 0.5 mmol g^{-1} with the EW 2000 g mol^{-1}. The IECs of the higher PA loaded PEMs also had lower than expected IECs, although the differences between expected and observed IECs were not as great as for the 5% PA membrane.

These lower than expected values for IEC and EW were the result of a lower amount of available acid in the membrane, possibly as a result of acid condensation or silyl and phosphonic acid hydroxyl group condensation, as represented in Fig. 5.15.[61]

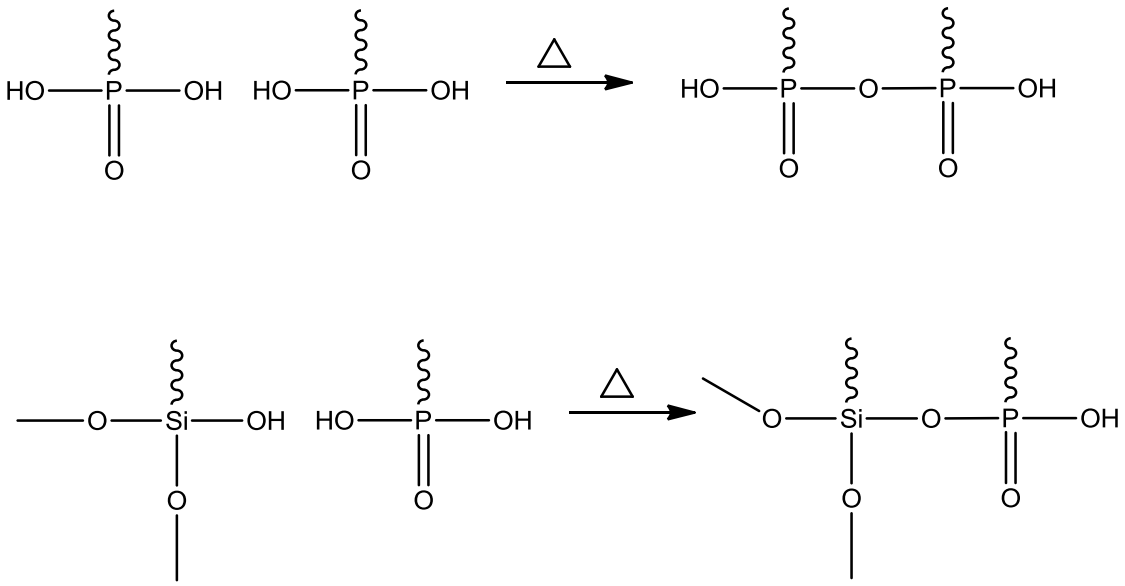

Fig 5.15. Representation of phosphonic acid condition

The phenomenon of a phosphonic acid condensation has been reported in the literature and has been shown to occur at non-humidified elevated temperatures (at and above 90 °C), the poly-condensation of multiple acid groups has also been reported, however this only occurs when the acid is heated for extended periods. This is due to the fact that the condensation reaction itself produces water and is a source of hydration for the membrane, which limits the extent of condensation. For PEMs synthesised in this project, this was most likely to occur during membrane curing. The PA polycondensation was likely to have occurred to some extent in all membranes regardless of PA loading. However in this instance, where the PEM had a 5% PA loading, the effect of the PA condensation was more prominent. This suggests that there was a degree of phase separation of the PA and the rest of the polymer matrix, resulting in larger agglomerates of PA, as in this case, a homogeneous distribution of PA throughout the polymer matrix would have inhibited PA condensation, the other possibility that may have caused the reduction in the IEC was that silyl-PA hydroxyl condensation could have occurred as there would have been a higher concentration of silyl groups in the polymer than other PA hydroxyl groups, or possible could be a mixture of silyl-phosphonic acid and phosphonic acid-phosphonic acid condensation. .

Once the PA loading exceeded 25% the rate of increase of IEC decreased significantly. Between 30 and 35% PA loadings there was only an increase of 0.07 mmol g^{-1}. This was a small increase in IEC and is also consistent with the results of impedance studies, which showed small increases in proton conductivity when increasing the PA loadings from 30, 33 and 35%.

5.7 Type B Blend 1 Optimisation: Water Uptake

The water uptake of a PEM influences many different properties when the PEM is used in a membrane electrode assembly (MEA) and a PEMFC. The more water that a PEM absorbs, the greater the dimensional changes (swelling) that occur, and this can lead to delamination of the gas diffusion electrodes (GDE) in the MEA which can result in higher resistances and more gas (fuel) cross-over. Also, as water has a significant role in proton transport, the volume of water absorbed can directly affect the proton conductivities observed, and as the volume of water absorbed by a PEM increases, it is more difficult to keep the PEMs hydrated at temperatures above 100 °C, as is the case for Nafion membranes. Ideally, the mass of absorbed water should be as low as possible to avoid both swelling and hydration issues at high temperatures.

Water uptake measurements were performed in a similar fashion to that of IEC measurements. The membranes were stored over phosphorus pentoxide for 24 hours to dry. The weight of the membranes was then recorded and used as mass at 0 hours. The membranes were then stored in a sealed container in deionised water. After one hour each membrane was quickly removed from the water and the surface water was removed by wiping with filter paper. The new mass was recorded before the membrane was re-immersed in the deionised water. This procedure was repeated for all membranes (0 – 35% PA loadings) after 1, 2, 3, 4, 24 and 48 hours and the results summarised in Table 5.6 and Fig. 5.17.

Table 5.6: Summary of mass increase (w/w) of dried Type B PEMs (P_2MP_2) stored in deionised water at room temperature over 48 hours

Membrane	0 h	1 h	2 h	3 h	4 h	24 h	48 h
0%	100	120.5	123.5	123.9	128.3	114.2	113.9
5%	100	108.4	113.6	115.0	120.1	114.4	112.0
10%	100	111.4	115.6	115.3	114.5	111.5	109.7
15%	100	108.4	113.3	115.1	114.4	109.7	110.6
20%	100	109.1	113.6	113.9	113.5	108.1	107.5
30%	100	114.8	112.3	112.1	112.4	112.4	112.0
33%	100	113.0	112.4	109.7	109.5	112.1	112.6
35%	100	114.6	112.9	110.5	111.0	113.8	114.1

Surprisingly the membrane that initially absorbed the most water was the one that that contained no phosphonic acid. 20.5% mass of water was absorbed after one hour and 28.3% mass water by 4 hours, however after this time the membrane starts to lose absorbed water, eventually reaching an equilibrium over 24-48 hours to have approximately 14% absorbed water by mass. The membrane which contained 5% PA showed a similar trend to that of the membrane not containing PA, with a steep step in water absorption between 3 and 4 hours. After 24 hours the absorbed water in both membranes reached a similar level, this is clearly seen in Fig. 5.16. This indicated that the PA in this formulation initially inhibited water uptake.

When the PA loading was further increased to 10% the initial water absorption was considerably less than that of the 0% and 5% PA loaded membranes. The mass of absorbed water at equilibrium (after 48 hours) was also comparatively smaller for the 10% PA loaded membrane, 2% less than that of the 5% PA membrane and 4% less than that of the membrane containing no PA. When the PA content was increased to 20% w/w the water uptake of the membrane at equilibrium decreased yet further. This trend indicates that the incorporation of a limited amount of PA into the polymer matrix decreases the hydrophilicity of the membrane.

When the PA content was increased to 30%, the profile of water absorption changed dramatically, with the uptake curves of the 30, 33 and 35% membranes displaying similar trends to each other as shown in Fig. 5.16. The water uptake of these membranes was greater than those of the 15 and 20% PA membranes; however they still absorbed significantly less water than the 0, 5 and 10% PA membranes (as can be seen in Fig. 5.16 and Table 5.6). The final mass of absorbed water increases with increasing PA content. The 35% PA membrane showed slight deterioration in mechanical properties when placed in boiling water, and higher PA content membranes (40% and above) with this polymer matrix formulation showed poor mechanical properties when conditioned for impedance measurements, they were easily torn and were destroyed when perpendicular pressure was applied, thus no further tests or measurements were performed on these membrane.

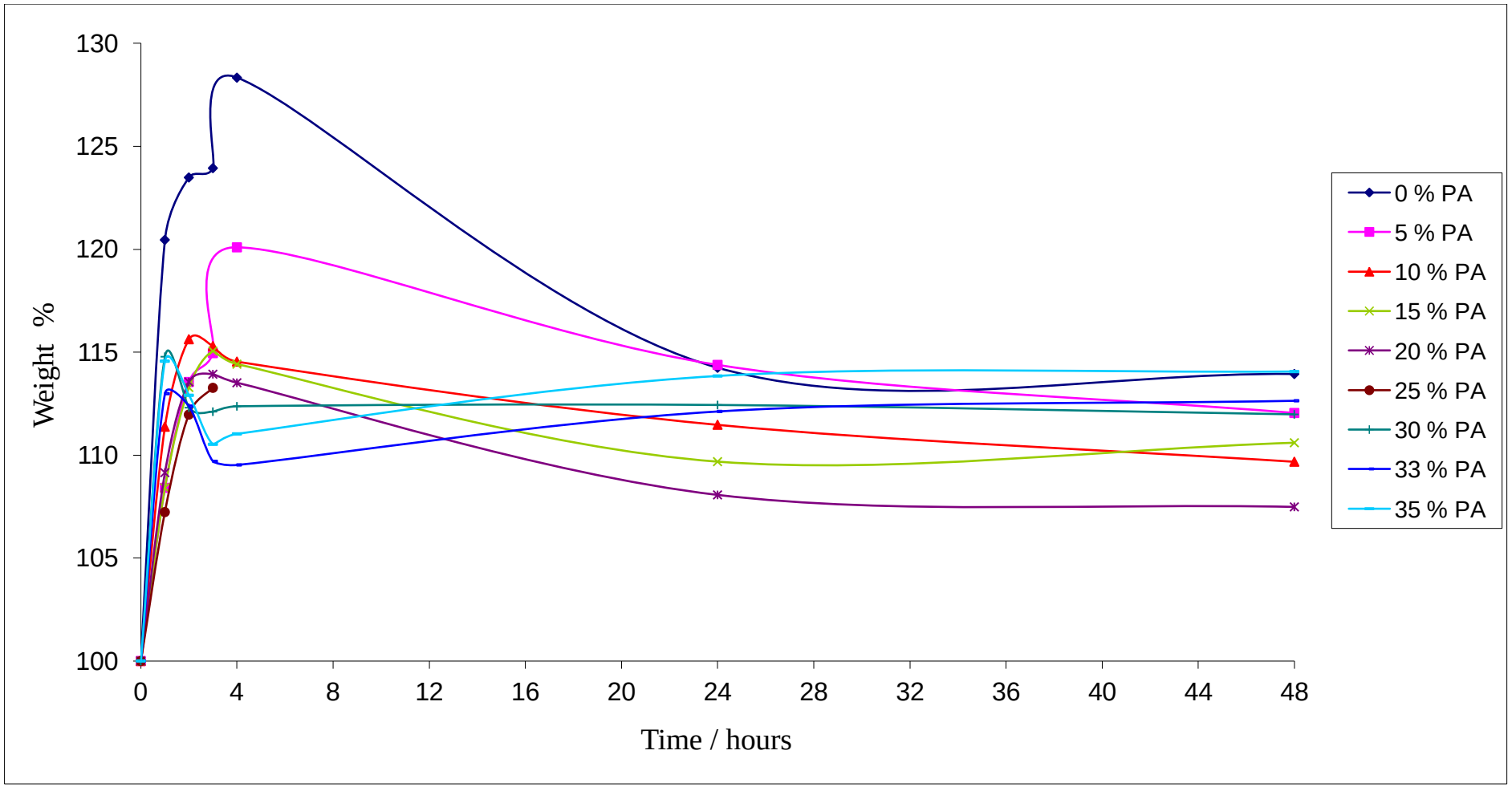

Fig. 5.16. Water uptake of dried Type B PEMs (P_2MP_2 0-35% PA loadings) stored in deionised water at room temperature over 48 hours

The water uptake for membrane 064 (33% PA) was in agreement with the result from the isothermal TGA measurement, the water uptake measurements show that this membrane absorbed 12.7% mass of water when a dry sample is placed in deionised water at room temperature, whereas the TGA experiment showed that the hydrated membrane lost 12% mass when heated at 120 °C over 12 hours. Alberti *et al*. argued to get a true water absorption profile; measurements (for Nafion) should be recorded for at least 150-225 hours, though preferably over the course of a month.[106] However in automotive applications, the PEMFCs would not be routinely allowed to equilibrate at one temperature for this period of time.

5.8 Type B Blend 1 Optimisation: Surface Morphology

To determine the surface morphology of membrane 064, scanning electron microscopy was performed on two samples of this membrane which was first coated with carbon to form a conductive layer. Ideally the surface of a PEM for PEMFC applications should be smooth and featureless, this would aid good adhesion between the PEM and GDE when making MEAs. Pinhole formation in a PEM when in a MEA/PEMFC can lead to hotspots at elevated temperatures which cause further deterioration in the PEM, and can cause higher resistances and gas-crossover decreasing the efficiency of the PEMFC.[107]

The SEM images obtained for the two samples of membrane 064 were markedly different; the first showed a relatively smooth and flat surface that was non-porous (Fig. 5.17). However, in the second sample, small pinholes were observed which are shown in Fig. 5.18, and also in Fig. 5.19 at greater magnification. This indicated that the surface morphology was not homogenous across the membrane, which could be the result of the membrane synthesis procedure.

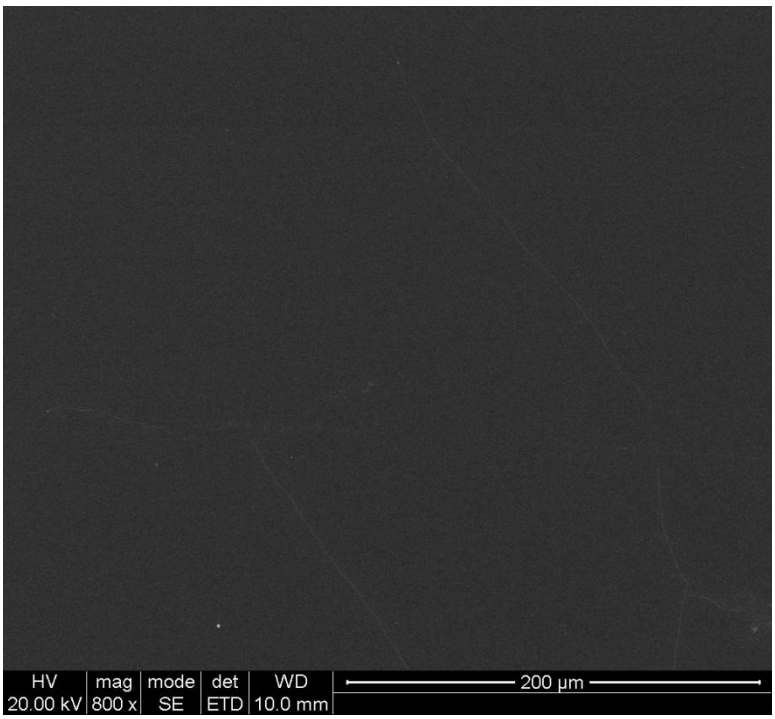

Fig 5.17: SEM image of Membrane 064

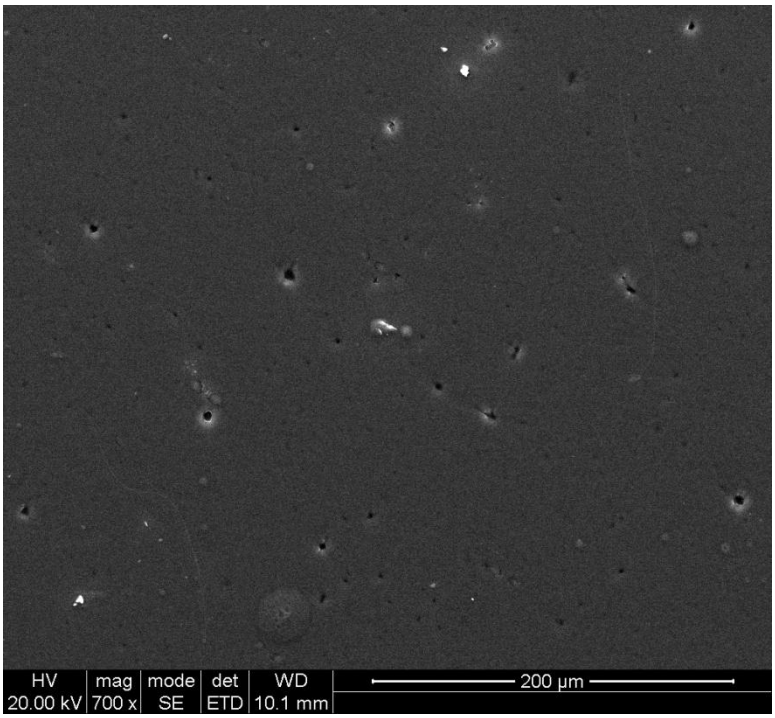

Fig 5.18: SEM image of Membrane 064 showing pinholes

The differences between the micrographs in Figs. 5.17 and 5.18 are clearly visible. One explanation for these differences could be that these images were recorded from different sides of the membrane. The image in Fig. 5.17 being that of the top of the

membrane (when casting) while the micrographs Fig. 5.18 and 5.19 from the bottom of the membrane (when casting), *i.e*. the surface at the coated glass/membrane interface. Any impurities/imperfections on the modified glass substrate surface would transfer to the membrane surface upon casting and this could account for the roughness and pinhole formation on just one side of the membrane surface. Indeed, when the membrane was cast onto a PTFE surface, on one side of the membrane, the side that was in contact with the PTFE surface had a visibly roughened surface whilst the other side of the membrane was completely smooth.

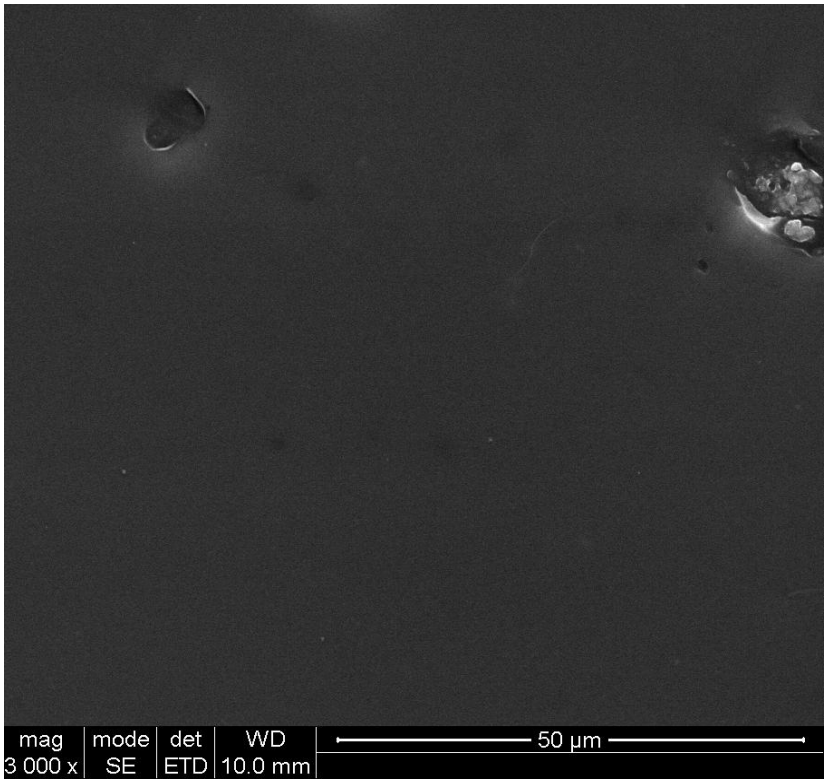

Fig. 5.19. SEM image of membrane 064 showing pinhole (magnified)

EDAX mapping was performed on various samples of membrane 064. EDAX mapping allows the distribution of elements to be determined on a selected portion of the membrane surface. As the membrane was coated in carbon, the carbon from the membrane could not be distinguished from that of the coating. The element which was of most interest was phosphorus. Silicon was present both in the polymer matrix and PA, whereas phosphorus is only present in the PA. Thus EDAX mapping of phosphorus atoms on the membrane surface allowed for the determination of the PA distribution in

the membrane. In this sample, the phosphorus was distributed homogenously throughout the membrane with no large areas devoid of phosphorus signals as shown in Fig. 5.20. This can be rationalised by considering that there was a high concentration of PA present in the membrane and also that the size of the PA particles is in the nanometre range (1-3 nm as determined by DLS). EDAX is a surface selective technique, meaning that only the phosphorus in the first few atomic layers could be detected, this showed that the phosphorus and hence the PA is present on the membrane surface as well as the bulk unlike in Nafion where the sulfonic acid groups are found in the centre of the PEM. This observation can be used to explain the ACIS in the tangential cell where the membrane-electrode response dominates at high frequencies.

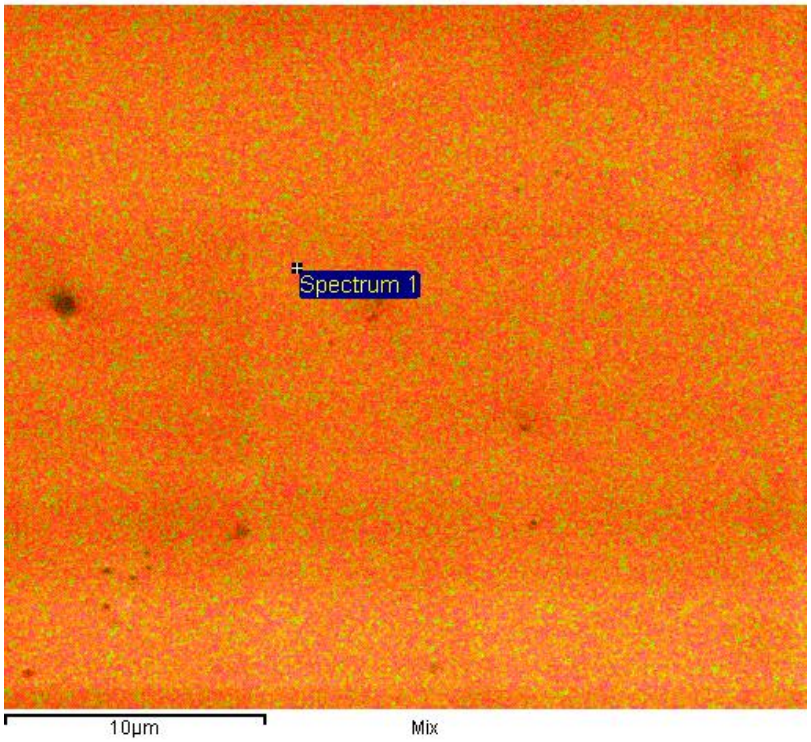

Fig. 5.20. EDAX MAP of surface element composition of membrane 064, orange colour represents silicon distribution and green represents phosphorus distribution

5.9 Type B Blend 1 Optimisation: FT-IR Studies

The structure of the Type B P_2MP_2 PEMs were characterised by ATR FT-IR spectroscopy. This enabled the functional groups present in the polymer to be identified

and assigned. To avoid saturation of the signals in certain regions, the membranes were dried prior to measurement by storing over phosphorus pentoxide.

The peaks expected to be present and their expected frequencies are given in Table 5.7 along with the frequencies the bands were actually observed at. As more PA was added, it was expected that the Si-C and Si-O peaks would become more intense and that the peaks for the P=O and phosphonic acid would become visible on the FT-IR spectra. The FT-IR spectra are shown in Fig. 5.21.

Table 5.7. FT-IR analysis of P_2MP_2 PH PEMs

Expected Band	Approximate frequency expected	Frequency observed / cm^{-1}
Mono substituted amide (urethane bond)	3300-3500 cm^{-1} (m) 1670 cm^{-1} (s)	1629
Ester group (-CO-O-C)	1700 cm^{-1} (s) 1260 cm^{-1} (s)	1706
Ether	1150-1250 cm^{-1} (s)	1230
Aromatic Ring (C-C, C=C, C-H)	750-1250 cm^{-1} (multiple peaks)	-
Alkane Groups (CH_3-C)	1450-1500 cm^{-1} (S)	1446-1454
Alkyl C-H	2850-2950 cm^{-1} (S)	2903-2974
Si-C	600 and 800 cm^{-1} (S)	Not observable
Si-O	450-600 cm^{-1} (S), 1000-1200 cm^{-1}	970-1180
Phosphonic acid (-P(O)-OH)	2550-2700 cm^{-1} (m)	2393
P=O	1230-1260 cm^{-1} (S)	1200

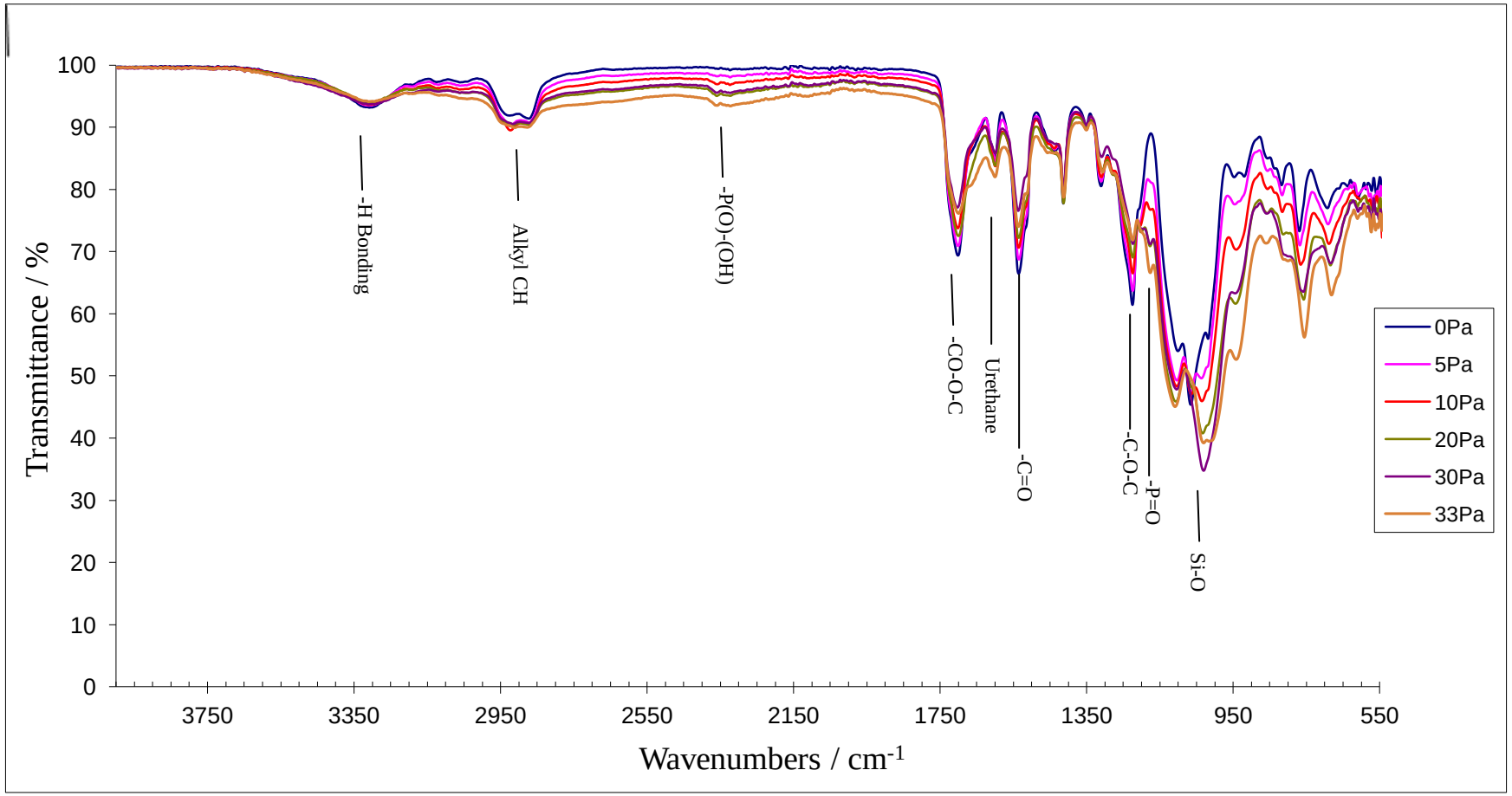

Fig. 5.20. FT-IR spectra of dehydrated P_2MP_2 PH PEMs with assignments of key functional groups

As can be seen from the spectra in Fig. 5.22, with increasing PA content, the most noticeable changes were in the peaks between 970 and 1180 cm^{-1}, which became broader and more intense. This can be explained by considering that the PA introduced more silyl and siloxane groups to the PEM. A small peak was also observed at 1200 cm^{-1}, which was not present in the 0% PA spectrum, and which became more intense as the PA content was increased. This peak was assigned to P=O bond stretching, and is the reason it is not visible in the 0% PA spectrum. A very broad and weak peak became visible, centred at 2393 cm^{-1}. This peak has been attributed in the literature to the PA P-OH functional group, with the broadness of the peak being associated with the hydrogen bonding between the hydroxyl group and electron acceptors in the polymer matrix.[60]

As the PA content of the membrane was increased, the peaks at 1706, 1629 and 1150 cm^{-1}, decreased. These peaks are attributed to the urethane bonds and the ether bonds in the PEG. As the PA content was increased, the concentration of pre-polymer (P_2MP_2) decreased in the membrane. The peak from the Si-C bond, which was expected to be at 600 and 800 cm^{-1} was not observable in any spectra. The FTIR spectrometer used, employed ZnSe lenses which cut out just above 550 cm^{-1}, thus making the 600 cm^{-1} region very noisy in the spectra. Upon adding the PA in higher concentrations, the observed peak at 802 cm^{-1} became broader and more intense. However, the argument that this was caused by a new Si-C peak merging with an existing peak from the aromatic ring (from MDI) cannot be made with certainty.

Other techniques that could be used to probe the structure and morphology of the membrane include Raman spectroscopy which would give complementary information to IR spectroscopy; in IR spectroscopy the selection rules mean that a change in dipole moments need to be observed whereas in Raman spectroscopy the selection rules mean that a change in polarisability needs to be observed. Another useful technique to accurately determine the distribution of PA throughout the membrane would be the use of X-ray topography in association with ion exchange with a heavy metal ion. In this experiment, caesium formate could be employed in much the same way as sodium formate was to determine the IEC of the PEM, the caesium would exchange with a proton and form a caesium phosphate salt which would be detectable in X-ray topography, however the resolution would be similar to that achieved using EDAX

mapping, would take longer to perform with more in depth anaylsis and as the caesium ions are 80% larger than sodium ions, the diffusion of the caesium ions into the PEM bulk would be limited thus making X-ray topography a surface selective technique thus offering no advantages over the simpler and quicker EDAX mapping. Atomic Force Microscopy (AFM) can be used to determine surface morphology and can give atomic level resolution although routinely the resolution is around 0.1-0.4 nm. The advantage of AFM over SEM is that AFM does not require a vacuum to operate, and can even work in a humidified or aqueous environment which resembles the actual environment in which the PEM would be employed, however care needs to be taken to ensure water condensation did not occur in the experiment on the PEM surface. The disadvantage of AFM over SEM is the long scan times needed to build up a micrograph of small sample area which may not be representative of the surface whereas in SEM, the resolution can be lowered to allow a large area of the membrane to be scanned before increasing the resolution to examine any features in more detail.

5.10 Membrane 064 Thickness Studies

Of all the membranes synthesised in this project, membrane 064 (P_2MP_2, 33% PA PH) displayed the most desirable overall properties for use in automotive PEMFCs, even though some Type A PEMs displayed higher proton conductivities. Although this PEM has not met the US DoE target of 0.1 S cm^{-1} at 120 °C at 100% RH,[6] the conductivity was still 17 mS cm^{-1} with immersion conditioning and 64 mS cm^{-1} with steaming conditioning, which was still an order of magnitude greater than that of Nafion under the same conditions. However PEMs for PEMFC applications are not just dependent on the proton conductivity, but also membrane thickness.

The thicker a membrane is, the larger the area specific resistance (ASR) is (if the conductivity is independent of membrane thickness). In 2009 the US DoE HTWMG set the membrane ASR targets,[7] at 30 °C, 0.2 Ω cm^2 and at 120 °C, 0.02 Ω cm^2. Membrane 064 was 270 microns thick and had conductivities of 4.2 and 17 mS cm^{-1} at 30 and 120 °C respectively (with immersion conditioning). This equates to ASR values of 6.5 and 1.6 Ω cm^2 respectively and with steaming condition the ASR reduced to 0.42 Ω cm^2 at 120 °C. Therefore to achieve values close to the targets, the membrane thickness needed

to be reduced in thickness to less than 10 microns. At 10 microns the ASR would be 0.24 Ω cm^2 at 30 °C and 0.056 Ω cm^2 at 120 °C for an immersed membrane if conductivity is independent of thickness. DuPont have successfully decreased the thickness of Nafion films from 258 μm (NE-1110) to 25.4 μm (NRE-211), with the largest decrease in thickness resulting from a change in casting method from extrusion to dispersion cast.[108]

To decrease the thickness of membrane 064 several different methods were attempted. Firstly, less polymer solution was cast into the frame. Whereas previously, the entire polymer solution batch was cast, only half of the solution was cast onto the tray instead, in theory reducing the membrane thickness by half. However, this was not successful, as the polymer solution did not stay spread out over the casting substrate (PTFE or OTS coated glass) during curing, thus a relatively thick membrane (*ca*. 700 μm), which was curled and brittle was formed. This process was repeated with a modification in processing conditions; firstly the polymer solution was cast and then aged for 2 hours prior to heating. However, this did not improve the resultant membrane. A second modification was then tried, where after aging; the membrane was then heated to 60 °C for four hours prior to further curing at 100 °C for 12 hours. Again this did not improve the resultant membrane.

The next step was to try to cast a dilution of polymer solution. Initially, this was tried by halving the quantities of reagents used, but keeping the same volume of solvent. However, this reduced the reactant concentrations by half, thus the kinetics of the reaction were not the same. After the usual reaction times, the polymer solution was cast and cured using the same procedure as the original membrane. When the cast membrane was removed from the oven, the membrane appeared to be visually inhomogeneous. Thus the membrane was unsuitable for further testing.

The next attempt at making a more dilute polymer solution was attempted by reducing all the reactants by half, including the solvent. Then just before the addition of hydrochloric acid, a further 10 mL of solvent was added. The polymer solution was then

stirred for 15 minutes before hydrolysis. The membrane was cast onto an OTS coated glass slide and cured under the original conditions. Upon removal from the oven, the membrane was visibly homogeneous; however the membrane would not peel of the OTS coated glass slide in one piece.

This process was repeated, with the membrane cast onto polished PTFE sheet in place of OTS modified glass. The membrane was easily removed from this surface and then the thickness was measured to be 100 μm. Although this membrane was still relatively thick compared to the desired thickness of 10 μm, it was substantially thinner than the previous membrane, which was 270 μm.

The physical properties of this membrane were superior to that of the thicker membrane. The membrane was more flexible and when cut did not fracture, the tear resistance of the membrane also improved. This membrane was also boiling water stable, and thus the decreased thickness did not seem to have any detrimental effects on the membrane.

The membrane conductivity was measured in the same way as that of membrane 064. The membrane was firstly conditioned by immersing in deionised water at room temperature, before the conductivity was measured in the normal cell. When hydrated, the membrane had increased in thickness by ten microns to 110 μm. The membrane absorbed 12.5 % mass water with an IEC of 2.61 mmol g^{-1} equiv.

As can be seen in Fig. 5.22, the proton conductivity of the thinner membrane was somewhat different to the thicker version of the same membrane formulation. At lower temperatures (below 60 °C), the proton conductivity of the thinner membrane was an order of magnitude less than that of the thicker membrane, although at high temperatures (60 °C and above) the proton conductivities were similar. The resultant ASR values are shown in Table 5.8.

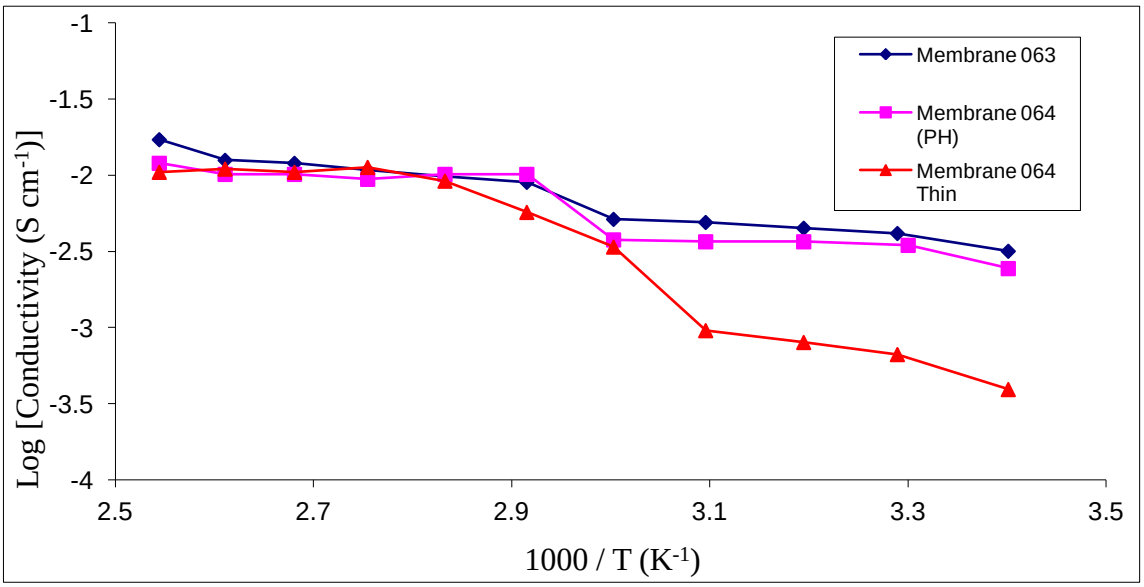

Fig. 5.22. Total proton conductivity of Type B membranes 063, 064 (270 μm) and thin 064 (110 μm) heated to 120 °C over one heating cycle at 100% RH, all membranes were immersed preconditioned

Table 5.8 Calculated ASR for membrane 064 (270 μm) and thin 064 (110 μm) at each temperature measured for the first heating cycle

Temperature / °C	ASR 064 / Ω cm^2	ASR 064 Thin / Ω cm^2
21	8.5	28
30	6.5	16.5
40	6.0	13.75
50	5.5	11.5
60	5.25	3.25
70	3	1.925
80	2.75	1.2
90	2.5	0.975
100	2.25	1.05
110	2.15	1
120	1.575	1.05

The ASR for the thin membrane at 80 °C was under half that of the thicker membrane (1.2 compared to 2.75 Ω cm^2), whilst the difference drops to two-thirds at 120 °C. If the

proton conductivity of the PEM was independent of thickness then the ASR at 30 °C should have been 2.7 Ω cm^2 and at 120 °C it should have been 0.65 Ω cm^2 (based on the results of the 270 μm thick membrane which underwent the same conditioning) whereas at low temperatures the observed ASR were far greater than expected for the thin membrane.

When the third heating cycle of measurements was performed on the thin membrane the profile of proton conductivity drastically changed, as shown in Fig. 5.23. The low temperature values were greater than in the 1st heating cycle, whilst the values at higher temperatures had reduced, although overall, across the entire temperature range, the E_a of proton transport was comparatively smaller.

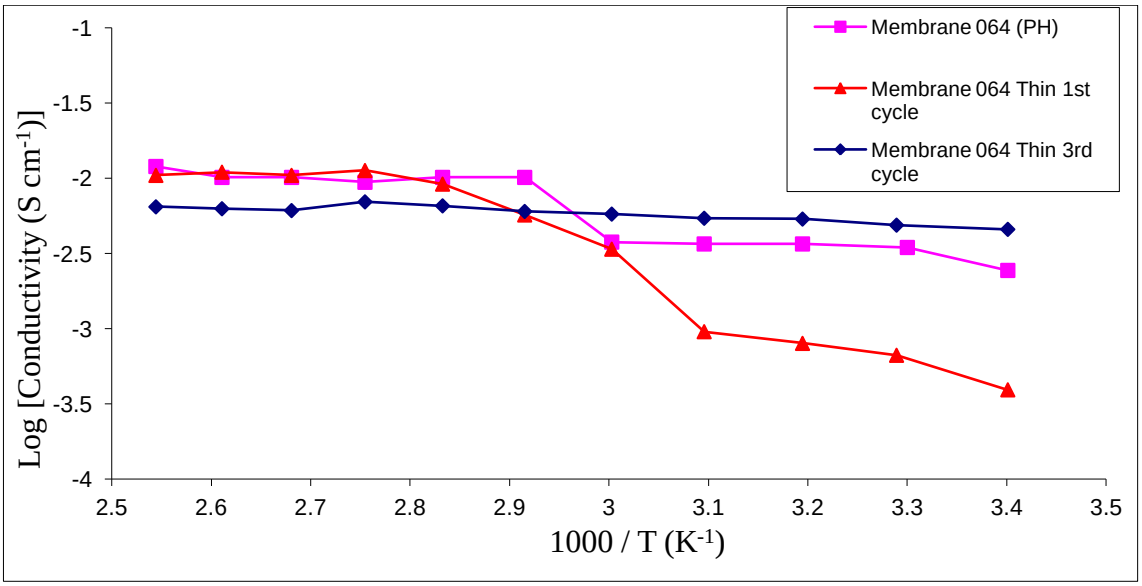

Fig. 5.23. Total proton conductivity of thin 064 (110 μm) heated to 120 °C over three heating cycle at 100% RH

At 120 °C the proton conductivity of the thin membrane fell from 10 to 6.5 mS cm^{-1} on the third heating cycle. This increased the ASR from 1.05 to 1.7 Ω cm^2 which was the same value as the thicker membrane on the first, second and third heating cycles. At 30 °C the ASR dropped to 2.5 Ω cm^2, which was half that observed for the thicker membrane on any heating cycle and was close to the expected ASR value at this temperature (2.7 Ω cm^2).

The thinner membrane swelling and water uptake was comparable to that of the thicker membrane (10% swelling and 12.5% water uptake), so the water uptake could not be directly causing the differences in conductivity and the ASR values. The conductivity of the membrane changed during the course of 3 heating cycles. The conductivity values at 120 °C dropped from 10 to 6.5 mS cm^{-1}, however the fact that the proton conductivity of the PEM increased significantly at lower temperatures (from 0.3 to 6.3 mS cm^{-1}) rules out both PA acid leaching out of the membrane (which was corroborated by titrametric analysis of water a large piece of membrane was conditioned in) as well as physical deterioration of the membrane during the period over which the conductivity was measured. Indeed after the third heating cycle, the cell was removed and the membrane inspected and no visible deformation or creep had occurred. The drop of only 3.5 mS cm^{-1} could even be attributed to experimental error due to the qualitative nature of ACIS as described previously.

Indeed the errors of accurately determining resistances and conductivities of membranes in the normal cell dramatically increase when thinner membranes are measured. If the conductivity is independent of thickness, or is not affected by thickness to a high degree then for a thinner membrane to have a similar conductivity the resistance must be much smaller. For the thicker membrane (270 μm) the resistance measured for a conductivity of say 12 mS cm^{-1} would be 9 Ω whereas for the thin membrane (100 μm) the resistance would be just 3 Ω and for a membrane which was just 30 μm thick the resistance would be 0.8 Ω. The smaller the measured resistance the greater the error, as at these low resistance values the internal resistances of the cell (leads and connections) as well as the interfacial (membrane-electrode) resistances become comparable to that of the resistances measured. If for instance the internal resistance at a given temperature was ≈ 0.25 Ω and the interfacial resistance ≈ 1 Ω then this value would be around half that of the 3 Ω resistance of the 100 μm membrane whereas it would be one seventh of the 9 Ω resistance of the 270 μm membrane, and for the 30 μm membrane the internal and interfacial resistances would be greater than that of the membrane itself. This effectively makes accurate determination of resistances (and conductivities) of thin highly conductive samples impossible when using a normal cell and hence emphasises the importance of a well designed tangential cell that can be used in routine impedance

measurements, where resistances measured are in kilo Ohms for even highly conductive samples. To increase the resistances measured in the normal cell the area of the membrane measured could be decreased, (in the present work in the normal cell it was kept constant at 0.25 cm^2).

5.11 Comparison of Membrane 064 with other PA/hybrid PU Membranes

There have been several reports in the literature of PEMs containing a phosphonic acid as the proton source. In this section, membrane 064 is compared to other membranes containing a phosphonic acid group as well as the original hybrid polyurethane membranes synthesised by Honma *et al*. The membranes that contained polysilsesquioxane phosphonic acid groups where synthesised by Li *et al*., were either fluorinated or non-fluorinated.

The proton conductivities of membrane 064 can be directly compared to that of the membranes synthesised by Li *et al.*, which have comparable acid loadings,for example,2M-2Oc-6CP and 2M-2Be-6CP (CP=PA and both have approximate PA loadings of 30%, structures of precursors M, Oc and Be are given in Fig. 5.24).[60] The proton conductivities of these membranes are shown in Fig 5.25. At low temperatures, all three membranes have similar conductivities, however at higher temperatures, the membranes synthesised by Li *et al.* have higher conductivities. The 2M-2Oc-6CP membrane has a conductivity of 65 mS cm^{-1} at 100 °C, which is approximately 5 times greater than that of membrane 064 (immersion conditioning), but similar to that of membranes 037 and 038 (Type A Peg 1000 30 and 40% PA respectively). The main difference between the polymer matrix in membrane 064 and those of 2M-2Oc-6CP and 2M-2Be-6CP is that the polymer matrix of membrane 064 should be more hydrophilic as it contains more heteroatoms (from the urethane bonds and ether links) than those of membranes 2M-2Oc-6CP and 2M-2Be-6CP. However, these two membranes absorbed considerably more water than that of membrane 064 (Table 5.9) which could in some way explain the observed higher proton conductivities.

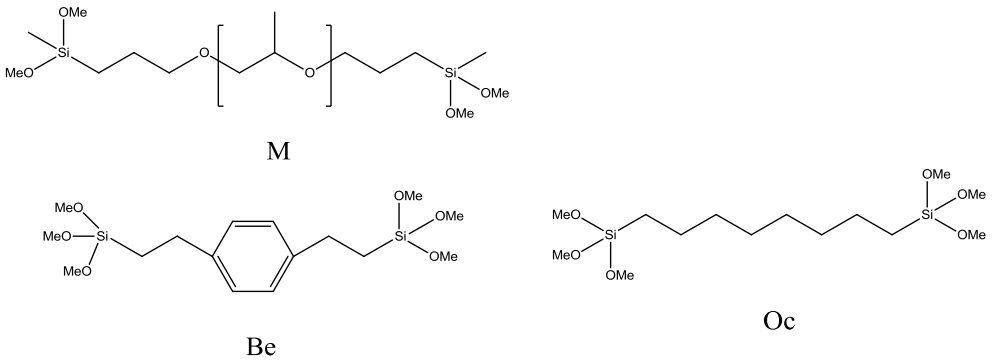

Fig. 5.24. Structures of precursors M, Be and Oc

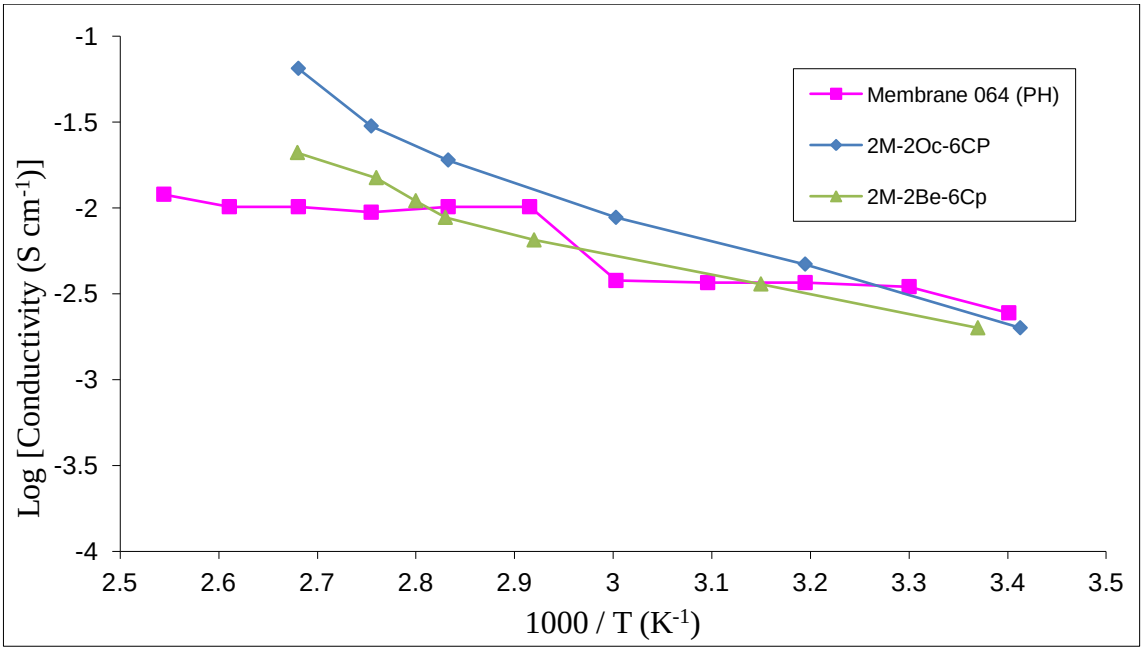

Fig. 5.25. Comparison of total conductivities of membranes containing PA, membrane 064 and those reported by Li *et al.*

Table 5.9. Water uptake and λ values of membranes containing PA, membrane 064 and those reported by Li *et al*

Membrane	Water Uptake / %	λ
Membrane 064	12.6	2.1
2M-2Oc-6CP	23.6	4.4
2M-2Be-6CP	26.5	5.1

The membranes synthesised by Li *et al.* absorbed more water, as shown in Table 5.9, despite being theoretically less hydrophilic. This could have resulted from two factors, firstly the shorter polymer chains means that the siloxane linkages were closer together, whereas in membrane 064 there was one polymer chain significantly longer than both Oc and Be. Thus the second shorter network former present could alter the membrane structure or morphology. Secondly the PA hydrolysis used a different method than employed in this project. This could have resulted in different particle sizes of PA present in the membranes produced by Li *et al.* compared to those in the present work. No PA particle size measurements were reported by Li *et al*.

The differences in proton conductivity may also be explained by differences in the synthesis of the PA rather than of just the water uptake or PA particle size. Membrane 064 was remade with PA hydrolysed by method 3 which had not been washed with either methanol or water, before being dispersed in deionised water, as Li *et al.* did not wash the condensed PA before dispersing in solvent. To make this membrane the PA (10 mL) was refluxed in 6M HCl (10 mL) for 24 hours instead of 3.28 g PA refluxed in 50 mL 12 M HCl as reported by Li *et al*. The proton conductivity of this modified membrane, as well as those synthesised by Li *et al* are shown in Fig 5.26.

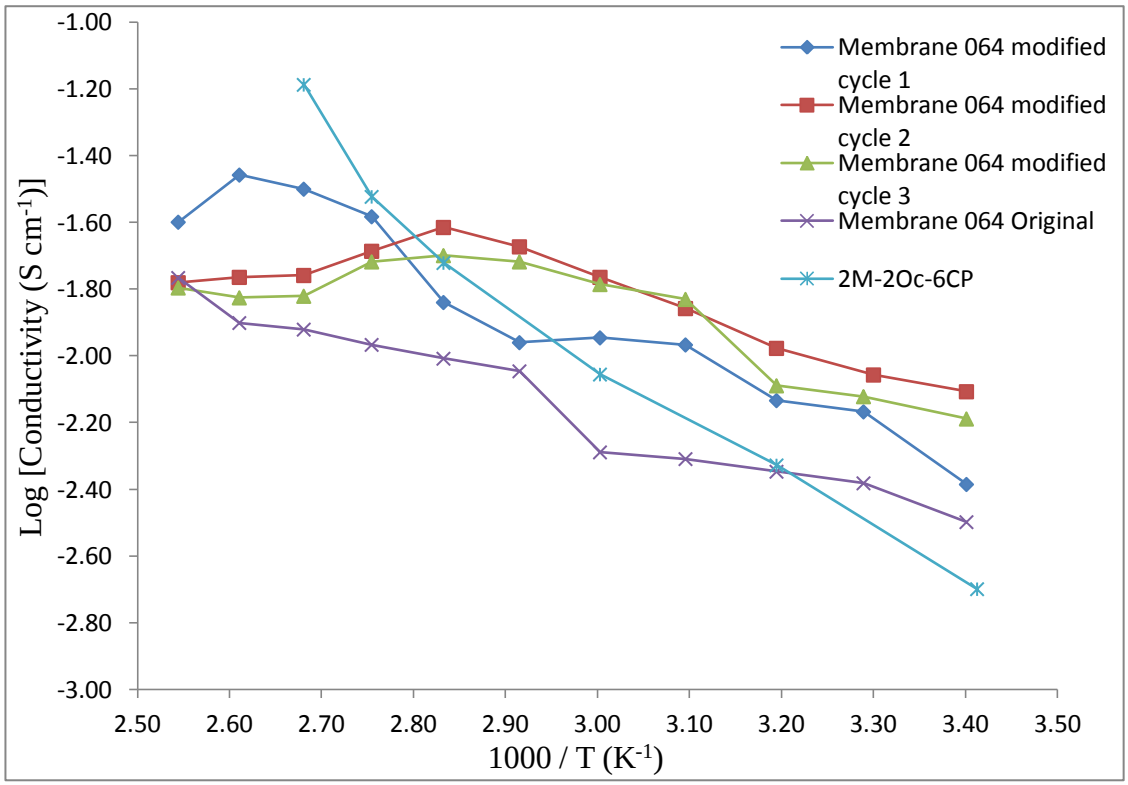

Fig. 5.26. Total Proton Conductivity of modified PA membrane heated to 120 °C over three heating cycle at 100% RH, membrane 064 (original) and 2M-2Oc-6CP shown for comparison

As can be seen from the graph in Fig. 5.26 the proton conductivity for the modified membrane 064 was significantly higher than that of original membrane 064 over all temperatures in the first heating cycle. However, in the subsequent heating cycles the proton conductivities of the modified membrane were the same as the original membrane 064 at 120 °C. In the second and third heating cycles the proton conductivity reached a maximum at 80 °C, before dropping to the same proton conductivity as the original membrane 064. The third heating cycle of the modified membrane showed the lowest conductivities over the entire temperature range of the three heating cycles over which proton conductivity was measured (except room temperature measurement of the first heating cycle). This change in proton conductivity was a result of the residual HCl from PA hydrolysis slowly leaching out of the membrane, thus the gradual decrease in proton conductivity. However Li *et al.* did not report the long term proton conductivity of any membrane synthesised or whether membrane proton conductivities were measured or consistent over more than one heating cycle.

The hybrid membranes synthesised by Honma *et al.*[49,50] (similar to Type A PEMs) which contained an acid dopant (MDP) all saw a dramatic decrease in proton conductivities above 100 °C. This indicated the these membranes dried out above 100 °C. Membranes with a dopant level of 30 and 40% w/w MDP showed similar conductivity to membrane 064 at room temperature (1 to 4 mS cm^{-1}) reaching a maximum at 60 °C. The conductivity of the membranes was approximately 1 to 2 mS cm^{-1} at 100 °C dropping to around 0.5 mS cm^{-1} at 120 °C. So not only is the acid dopant able to leach out from the membrane over time thus further decreasing the proton conductivity of these membranes, but also the conductivity values obtained were two orders of magnitude lower than that of membrane 064 when steam conditioned. When the MDP was exchanged with PWA, the conductivity of the hybrid membranes synthesised by Honma *et al.* remained in the 1 to 5 mS cm^{-1} range up to 120 °C, with a decrease to 0.5 mS cm^{-1} at 140 °C. However, when the PEG was changed for PTHF (similar to type F polymers) or a PTHF/PEG blend, then the conductivity (in the 1 to 4 mS cm^{-1} range) was reportedly stable to 140 °C. The values reported are still comparatively low and would not make suitable PEMs for PEMFC applications. As in this project the proton conductivities were only measured to 120 °C, due to experimental limitations (PTFE cell design), this observation of retaining water at 140 °C could not be confirmed for Type F blended membranes.

Lin *et al.* replaced MDP with DBSA as the proton source in PEG hybrid membranes.[51] The proton conductivities were only recorded at room temperature and for a 20% loading the proton conductivities ranged from 1 to 8 mS cm^{-1}, decreasing with increasing inorganic filler. These results are comparable to those obtained from membrane 064, however the problem still remains that these membranes have non-covalently bound surfactant acid groups which could leach out over time, thus reducing the proton conductivity to even lower values. The high temperature conductivities of these membranes were not reported, however they should be similar to those of MDP containing membranes. These membranes displayed significantly lower IEC values than for membrane 064 (0.4 compared to 2.65 mmol g^{-1}) and significantly higher water uptakes ranging from 56 to 154% which would make these membranes also unsuitable for PEMFC applications.

Umeda *et al*. reported the use of Ethyl 2-[3-(dihydroxyphosphonyl)-2-oxopropyl] acrylate (EPA), shown in Fig. 5.27, as a phosphonic acid proton source which was bound into an inorganic polymer framework by free-radical polymerisation across vinyl bonds in the EPA and synthesised inorganic precursors ((dimethylmethoxysilylmethyl)styrene or (methyldimethoxysilylmethyl)styrene).[109] Conductivities were reported of up to 50 mS cm^{-1} at 120 °C and 1.8 mS cm^{-1} at 40 °C, both at 100 % RH when a molar ratio of 1:6 inorganic:EPA was employed. When the ratio was reduced to 1:2 the proton conductivities reported were similar to that of membrane 064. These membranes would theoretically have higher IEC and EW than membrane 064. The high proton conductivities reported for the higher acid loading membranes are adequate for use in PEMFCs. However, the membrane water uptake, chemical stability, mechanical properties or long term conductivities were not reported, so their overall suitably for use in PEMFC cannot be determined.

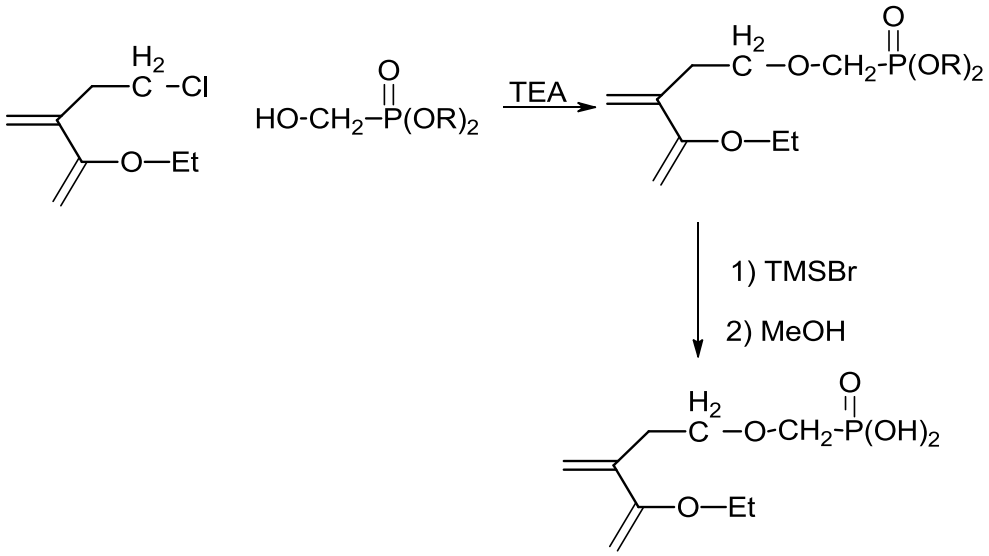

Fig 5.27: Synthesis and structure of EPA

According to Kreur *et al*. the proton conductivities of phosphonic acid can be sensitive to aggregation of acid moieties which would reduce the observed conductivities over time. It is also reasoned that the incorporation of phosphonic acid functional groups to some backbone via long, flexible spacers is also anticipated to reduce the proton conductivity, as the overall concentration of phosphonic acid in the membrane would be reduced, compared to a neat phosphonic acid (whether EPA, PA or other).[61] However,

when large concentrations of phosphonic acid moieties are close together, condensation across acid groups can result in a loss of a substantial amount of available acid, thus a compromise of concentration of phosphonic acid functional groups is needed to maintain long-term and stable conductivities.

5.12 Conclusions

The effect that increasing PA content has on the Type B P_2MP_2 PEM formulation has been explored. It was found that increasing PA both increased the observed proton conductivities and the IEC of the PEMs. Surprisingly however, there was a different trend in water uptake of the PEMs, with the water uptake decreasing with increasing PA content from 0 to 20%, whereupon further addition of PA did start to increase the water uptake. Of the membranes evaluated, membrane 064 displayed the highest proton conductivities, both at room temperature and 120 °C, with conductivities of 48.2 mS cm^{-1} and 33.5 mS cm^{-1} respectively when steamed conditioned and reduced to 4 and 17 mS cm^{-1} when the membrane was conditioned in a milder fashion, immersion in deionised water at room temperature. When the PA synthesis procedure was changed to a similar method employed by Li *et al*. the proton conductivity for the immersed conditioned membrane increased to 35 mS cm^{-1} at 110 °C. When the bis component content of the PA was increased, the proton conductivity of the PEMs decreased, thus showing the PA synthesis conditions, as well as membrane conditioning all dramatically affect the proton conductivities of the membranes at all temperatures.

Chapter 6

Concluding Remarks and the direction of future work

This project has been successful in that the aims have been met, namely that the synthesis and characterisation of the properties of a new type of PEM with covalently bound phosphonic acid, which exhibited high proton conductivities up to 120 °C, and which can be made from cheap and readily available precursors using simple bench-top chemistry, has been achieved.

The membrane that showed the most promise for use in PEMFC automotive applications was that of the Type B membrane 064 (P_2MP_2 33% PA PH). Although this membrane did not exhibit the highest conductivities in the present work, it fulfilled more of the requirements (Fig. 6.1) to be a good PEM, than any other synthesised PEM and as such shows that compromise is often needed to take PEM development further ahead.

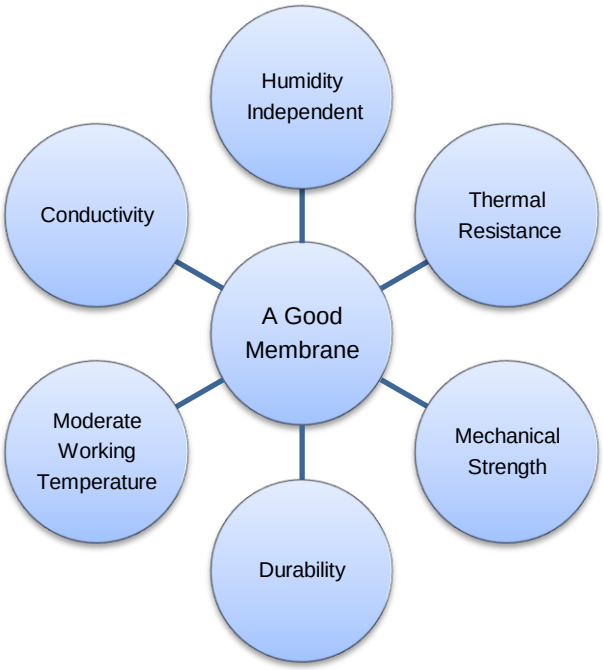

Fig 6.1: Requirements for a good PEM

Membrane 064 displayed conductivities of 17 mS cm^{-1} at 120 °C and 4 mS cm^{-1} at 20 °C, both at 100% RH when conditioned by immersion in deionised water at room temperature, which was reproducible over several heating cycles, extended periods (100

hours) and for different samples. The membrane also exhibited limited swelling and water uptake of just 10% and 12.7% respectively, and was stable in boiling water and also boiling Fenton's Reagent (3% H_2O_2, 5 ppm Fe^{2+}). The proton conductivities were found to be sensitive to conditioning regimes, for instance when the membrane was steamed, the conductivities at 20 and 120 °C showed a dramatic increase to 48 and 33.5 mS cm^{-1} respectively (Nafion 117 had a conductivity of 58 mS cm^{-1} at 80 °C when measured under identical experimental conditions). The proton conductivity was also shown to be adversely affected by addition of extra bis component in the PA (Blend 2). When the bis content was further increased, the resultant membranes were visually inhomogeneous. This membrane was also shown to be thermally stable in an oxidative environment, with no glass transition visible in the operating temperatures in which the PEM would be employed in a PEMFC.

However the PEMs in the present work were too thick to be able to be made into MEAs. This means that the thickness of the PEMs needs to be decreased, whilst maintaining proton conductivity, but reducing ASR. There was an initial investigation exploring the methods to achieve this which had limited success, the thickness was decreased, but the proton conductivity also decreased. Further work needs to be carried out achieve these goals. This might include varying reaction conditions and times, use of a catalyst for urethane formation (such as 1,4-diazabicyclo[2.2.2]octane (DABCO)), or by changing casting and curing conditions and times employed in PEM synthesis. For example, the biggest change that has been made to Nafion, was by changing the production of the PEM from extrusion casting to dispersion casting. This allowed a reduction in thickness from 170 μm to just 25 μm whilst maintaining the same proton conductivity.

The proton conductivity of this membrane also needs to determined at different levels of relative humidity (or water vapour pressure, which is the preferred target used by the HTMWG of the US DoE) at operational temperatures, *i.e.* 120 °C, which is equal to 40 to 80 kPa or 20 to 40% RH. At this temperature in a fuel cell, this would be achieved by humidifying the hydrogen gas stream with steam before passing it through the MEA. In the PEM testing in the present work, this would be harder to achieve. The testing of the membrane at different RH values would also give valuable insight into the role which water plays in proton transport through the membrane. Preliminary results at 0% RH

and 100% RH show that the difference in proton conductivities are extremely large, ranging from 10^{-6} to 10^{-2} S cm^{-1}. Due to the relatively low λ values observed for this membrane, and the strong interaction between the water and the polymer matrix (as shown by the frozen water DSC experiment and TGA results), a significant decrease in RH may not dramatically reduce the proton conductivity as observed in other PEMs, for example Nafion (which has a λ value of 21) shows a dramatic drop in proton conductivity at even 75% RH at 80 °C.

The next step for testing the suitability of membrane 064 for use in PEMFCs would be to use this membrane formulation to make a MEA, and to test a single cell under fuel cell conditions. Again for this membrane to be made into an efficient MEA, the thickness needs to be reduced, to enable the effective output voltage of the cell to be increased to draw usable power. However this membrane would not suffer from delaminating of the membrane and gas-diffusion electrode of the MEA to the same extent as Nafion, due to the lower swelling and strong adhesion to most surfaces.

As membrane 064 does not meet all the criteria for a PEM for PEMFC application at a 120 °C operating temperature, most notably that of the high ASR, further development of the PEMs made in this project should be investigated.

The proton conductivity could be improved by the addition of a secondary dopant acid, such as phosphoric acid, PWA, dodecylsulfonic acid or monodecylphosphonic acid. However, the increase in proton conductivity these dopants may provide would have to outweigh the negative impact of the dopant acid leaching out of the membrane.

Another method for improving the PEM properties that needs investigating thoroughly is the addition of other inorganic network formers, (see Table 4.1 for a non-comprehensive list of examples). In this project, this has been briefly explored by incorporating a small amount of inorganic components from either TEOS or Glysil into the polymer matrix by addition prior to hydrolysis. In the case of TEOS this has been shown to have a dramatic effect on proton conductivity, albeit negative. It is conceivable that certain additional network formers may boost the proton conductivity or improve other properties of the membrane such as mechanical or chemical stability.

Alternatively, blends of type B with different PEG MW could be explored, when blends of Type A were explored there was no significant improvement in either proton conductivity or water stability, so alternative blends containing both of type B and C polymer matrixes could be synthesised and evaluated for use in high temperature PEMs.

As Type A PEMs exhibited the highest conductivities for any PEM investigated in this study (including that of neat PA), these could similarly be made containing Type E and/or F polymers as well. Honma *et al*.[49,50] reported the blend of polymers containing both PEG and PTHF chains. These polymers exhibited improved water stability over those membranes just containing PEG, with conductivities at higher temperatures which were comparable to that of the non-blended polymer which displayed the highest conductivity. This trend may also be observed with PEMs with covalently bound phosphonic acid moieties.

Another blend that could be evaluated is that of type A and B polymers. The combination of Type A Peg 1000 and Type B P_2MP_2 polymers for example, may show the higher conductivities observed with the type A PEM, whilst showing the water stability of the type B PEM.

Future work should also not be limited by using just the precursors in this project for polymer formulation, there is a host of other diols and diisocyanates such as 1,6-hexanediol, TDI and 2',4-MDI. Alternatively, to form more cross linked polymers, which would also improve water stability, but probably diminish the resultant PEM flexibility, triols (or higher polyols) could be used, such as glycerol, trimethylolpropane and pentaerythritol based polyethers.

Thus using the knowledge gained during the course of this project, more efficient PEMs can be designed and tested which could come closer to meeting all the requirements/targets for use in high temperature PEMFCs for automotive applications.

References

[1] A. Bıyıkoğlu, *International Journal of Hydrogen Energy*, 2005, **30,** 1181.

[2] J-H. Wee, K-Y. Lee and S. H. Kim, *Journal of Power Sources*, 2007, **165**, 667.

[3] Y.H. Cho, S. J Yoo, Y. H Cho, H-Y. Park, I-S. Park, J. K. Lee and Y-E Sung, *Electrochemica Acta*, 2008, **53**, 6111

[4] K. A. Mauritz and R. B. Moore, *Chem.Rev*, 2004, **104**, 4535.

[5]US DoE HTMWG research and development plan http://www1.eere.energy.gov/hydrogenandfuelcells/pdfs/htwg_rd_plan.pdf (accessed 10/09/10)

[6]US DoE HTMWG PEM targets http://www1.eere.energy.gov/hydrogenandfuelcells/pdfs/technical_targets_membr_auto.pdf (accessed 10/09/10)

[7] US DoE, Membrane and MEA Accelerated Stress Test Protocols, HTMWG Meeting May 14, 2007 http://www1.eere.energy.gov/hydrogenandfuelcells/pdfs/htmwg_may09_membrane_projects.pdf (accessed 30/08/2011)

[8] D. Marx, Chem. Phys. Chem., 2006, **7**, 1848.

[9] C. I. T. de Grotthiuss (C. J. T. De Grotthuss), *Philos. Mag. (Lond)*, 1806, **25**, 330.

[10] K. D. Kreuer, S. J. Paddison, E. Sphor, M. Schuster, *Chem. Rev*., 2004, **104**, 4637.

[11] Web of Science search topic Nafion performed 21/12/2010 (Search keyword: Nafion)

[12] W. G. F. Grot, V. Mehra, G. E. Munn and J. C. Solenberger. *J. Electrochem. Soc*. 1975, **122**, C104.

[13] T. E. Springer, T. A. Zawodzinski and S. Gottesfeld. *J. Electrochem. Soc*. 1991, **138**, 2334.

[14] T. Malinski and Z. Taha. *Nature*. 1992. **358**. 676.

[15] M. A. Harmer, W. E. Farneth, and Q. Sun. *J. Am. Chem. Soc*, 1996, **118**. 7708.

[16] M. A. Hickner and B. S. Pivovar, *Fuel Cells*, 2005, **5,** 213

[17] T. A. Zawodzinski, M. Neeman, L. O. Sillerud and S. Gottesfeld. *J. Phys. Chem.*, 1991, **95**, 6040.

[18] DuPont Nafion PFSA extrusion cast membranes technical datasheet, http://www2.dupont.com/FuelCells/en_US/assets/downloads/dfc101.pdf (accessed 15/12/2010)

[19]T. A. Zawodzinski, C. Derouin, S. Radzinski, R. J. Sherman, V. T. Smith, T. E Springer and S. J. Gottesfeld. *J. Electrochem. Soc*. 1993, **140**, 1041.

[20]W. Y. Hsu and T. D. Gierke, *J. Mem. Sci*. 1983, **13**, 307.

[21] H. G. Haubold, T. Vad, H. Jungbluth and P. Hiller. *Electrochim.Acta* 2001, **46**, 1559.

[22] DuPont Nafion PFSA dispersion cast membranes technical datasheet, http://www2.dupont.com/FuelCells/en_US/assets/downloads/dfc201.pdf (accessed 15/12/2010)

[23]DuPont Fuel Cells, *Fuel Cells Bulletin*, 2007, **1**, 7

[24] Z. G. Shao, P. Joghee and I. M. Hsing. *J. Mem. Sci.*, 2004, **229**, 43.

[25] P. L. Antonucci, A. S. Arico, P. Creti, E. Ramunni and V. Antonucci, *Solid State Ionics*, 1999, **125**, 431.

[26]P. L. Shao, K. A. Mauritz and R. B. Moore. *Chem. Mater.*, 1995, **7**, 192.

[27] V. Ramani, H. R. Kunz and J. M. Fenton, *J. Mem. Sci.*, 2005, **226**, 110.

[28] M. B. Gieselman and J. R. Reynolds. *Marcromolecules*. 1992, **25**, 4832.

[29] J. S. Wainright, J. T. Wang, D. Weng, R. F. Savinell and M. Litt, *J. Electrochem. Soc.*, 1995, **142**, L121.

[30] X. Glipa, M. E. Haddad, D. J. Jones and J. Rozière, *Solid State Ionics*, 1997, **97**, 323.

[31] R. Bouchet and E. Siebert, *Solid State Ionics*, 1999, **118**, 287.

[32] J. T. Wang, S. Wasmus and R.F. Savinell. *J. Electrochem. Soc.* 1996, **143,** 1233.

[33] Q. Li, R. He, J. O. Jensen, and N. J. Bjerrum. *Chem. Mat.* 2003, **16**, 4896.

[34] G. Liu, H. M. Zhang, J. W. Hu, Y. F. Zhai, D. Y. Xu and Z. G. Shao, *J. Power Sources*, 2006, **162**, 547.

[35] F. Seland, T. Berning, B. Børresen and R. Tunold, *J. Power Sources*, 2006, **160**, 27.

[36] P. T. McGrail, *Polymer International*, 1996, **41**, 103.

[37] T. Kobayashi, M. Rikukawa, K. Sanui and N. Ogata, *Solid State Ionics*, 1998, **106**, 219.

[38] S.M.J. Zaidi, S.D. Mikhailenko, G.P. Robertson, M.D. Guiver and S. Kaliaguine, *J. Mem. Sci.*, 2000, **173**, 17.

[39] F. Wang, T. Chen and J. Xu, *Macromol. Chem. Phys.*, 1998, **199**, 1421.

[40] M. T. Bishop, F. E. Karasz, P. S. Russo and K. H. Langley, *Macromol*., 1985, **18**, 86.

[41] M. Gil, X. Ji, X. Li, H. Nab, J. E. Hampsey and Y. Lu, *J. Mem. Sci.*, 2004, **234**, 75.

[42] M. L. Di Vona, D. Marani, A. D'Epifanio, E. Traversa, M. Trombetta and S. Licoccia, *Polymer*, 2005, **46**, 1754.

[43] M. L. Di Vona, Z. Ahmed, S. Bellitto, A. Lenci, E. Traversa and S. Licoccia, *J. Mem. Sci.*, 2007, **296**, 156

[44] B. Bonnet, D. J. Jones, J. Roziere, L. Tchicaya, G. Alberti, M. Casciola, L. Massinelli, B. Bauer, A. Peraio and E. Ramunni, *J. New Mater Electrochem. Systems*, 2000, **3**, 87

[45] S. M. Haile, D. A. Boysen, C. R. I. Chisholm and R. B. Merie, *Nature*, 2001, **410**, 910.

[46] D. A. Boysen, T. Uda, C. R. I. Chisholm and S. M. Haile, *Science*, 2004, **303**, 68.

[47] T. Uda and S. M. Haile, *Electrochemical and Solid-State Lett.*, 2005, **8**, A245.

[48] C. Damian, E. Espuche, M. Escoubes, S. Cuney and J.P. Pascault, L. *Appl. Poly. Sci.*, 1998, **65**, 2579.

[49] I. Honma, S. Hirakawa, k. Yamada and J. M. Bae, *Solid State Ionics*, 1999, **118**, 29.

[50] I. Honma, Y. Takeda and J. M. Bae, *Solid State Ionics*, 1999, **120**, 255.

[51] C. W. Lin and R. Thangamutha, *Solid State Ionics*, 2005, **176**, 531.

[52] Z. Ma, J. Gao, Y. Huai, J. Guo, Z. Deng and J. Suo, *J. Sol-Gel. Sci. Technol.*, 2008, **48**, 267.

[53] Adapted from J. R. MacDonald and E. Barsoukov, *Impedance Spectroscopy. Theory, Experiment, and Applications*, 2nd Edition, Wiley Interscience, New Jersey,2005

[55] S.D. Mikhailenko, M.D. Guiver and S. Kaliaguine, *Solid State Ionics*, 2008, **179**, 619.

[56] D.T. Sawyer, A. Sobkowiak, J.L. Roberts, Jr., *Electrochemistry for Chemists*, 2nd edition, John Wiley and Sons, Inc., New York, 1995.

[57] D. R. Lide, *CRC Handbook of Chemistry and Physics*, 87th Ed. CRC Press, Boca Raton, 8-42

[58] C. Kantipuly, S. Katragadda, A. Chow and H. D. Gesser, *Talanta*, 1990, **37**, 491.

[59] M. Jurado-Gonzalez, D. L. Ou, B. Ormsby, A. C. Sullivan and J. R. H. Wilson, *Chem. Comm.* 2001, 67.

[60] S. Li, Z. Zhou, H. Abernaty, M. Liu, W. Li, J. Ukai, K. Hase and M. Nakanishi, *J. Mater. Chem.*, 2006, **16**, 858.

[61] H. Steininger, M. Schuster, K. D. Kreuer, A. Kaltbeitzel, B. Bingöl, W. H. Meyer, S. Schauff, G. Brunklaus, J. Maier and H. W. Spiess. *Phys. Chem. Chem. Phys.*, 2007, **9**, 1764.

[62] D. Mecerreyes, H. Grande, O. Miguel, E. Ochoteco, R. Marcilla and I. Cantero, *Chem. Mater.*, 2004, **16**, 604.

[63] G. Liu, H. M. Zhang, J. W. Hu, Y. F. Zhai, D. Y. Xu and Z. G. Shao, *J. Power Sources*, 2006, **162**, 547.

[64] F. Bauer, H. J. Gläsel, U. Decker, H. Ernst, A. Freyer, E. Hartmann, V. Sauerland and R. Mehnert, *Progr. Org. Coatings*, 2003, **47**, 147.

[65] P. Lesot, S. Chapius, J. P. Bayle, J. Rault, E. Lafontaine, A. Campero and P. Judeinstein, *J. Mater. Chem.*, 1998, **8**, 147.

[66] H. Y. Chang, R. Thangamuthu and C. W. Lin, *J. Membr. Sci.*, 2004, **228**, 217.

[67] M. Khiterer, D. A. Loy, C. J. Cornelius, C. Y. Fujimoto, J. H. Small, T. M. McIntire and K. J. Shea, *Chem. Mater.*, 2006, **18**, 3665.

[68] F. Croce, G. B. Appetecchi, L. Persi and B. Scrosati, *Nature*, 1998, **394**, 456.

[69] J. Y. Song, Y. Y. Wang and C. C. Wan, *J. Power Sources*, 1999, **77**, 183.

[70] F. Croce, R. Curini, A. Martinelli, L. Persi, F. Ronci, B. Scrosati and R. Caminiti, *J. Phys. Chem. B*, 1999, **103**, 10632.

[71] W. T. Grubb, *J. Am. Chem. Soc.*, 1954, , **76**, 3408.

[72] S. X. Zhou, L. M. Wu, J. Sun and W. D. Shen, *J. Appl. Polym. Sci.*, 2003, **88**, 189.

[73] D. K. Chattopadhyay and K. V. S. N. Raju, *Progr. Polym. Sci.*, 2000, **32**, 352.

[74] W. J. Liang, C. P. Wu, C.-Y. Hsu and P. L. Kuo. *J. Polym. Sci.: A: Polym. Chem.*, 2006, **44**, 3444.

[75] I. Honma, S. Nomura, H. Nakajima, *J. Membr. Sci.*, 2001, **185**, 83.

[76] E. Yılgör, İ. Yılgör and E. Yurtsever, *Polym.*, 2002, **43**, 6551.

[77] L. Di Landro, M. Pegoraro and L. Bordogma, *J. Membr. Sci.*, 1991, **64**, 229.

[78] L. F. Wang, Q. Ji, T. E. Glass, T. C. Ward, J. E. McGrath, M. Muggli, G. Burns and U. Sorathi, *Polym.*, 2000, **41**, 5083.

[79] D. Randall and S. Lee, *The Polyurethanes Book*, , John Wiley & Sons, New York, 2002.

[80] C. M. Brunette, S. L. Hsu and W. J. MacKnight, *Macromolecules*, 1982, **15**, 71.

[81] R. W. Seymour, G. M. Estes and S. L. Cooper. *Macromolecules*, 1970**, 3**, 579**.**

[82] I. Clemitson, *Castable Polyurethane Elastomers*, CRC PRESS, Boca Raton, 2008

[83] G. Woods, *The ICI Polyurethanes book*, , John Wiley & Sons & ICI Polyurethanes, New York, 1990.

[84] L. Wang, Y. Shen, X. Lai and Z. Li., *J. Appl. Polym. Sci*., 2010, **119**, 3521.

[85] H. Goda and C. W. Frank, *Chem. Mater.*, 2001, **13**, 2783.

[86] K. K. Jena and K. V. Sn. N. Raju, *Ind. Eng. Chem. Res.*, 2008, **47,** 9214.

[87] Y. K. Seo, S. B. Park and D. H. Park, *J. Solid State Chem.*, 2006, **179**, 1285.

[88] S. I. Lee, Y. B. Hahn, K. S. Nahm and Y. S. Lee, *Polym. Adv. Technol.*, 2005, **16**, 328.

[89] Q. Fan, J. Fang, Q. Chen and X. Yu, *J. Appl. Polym. Sci*, 1999, **74**, 2552.

[90] X. Dai, J. Xu, X. Guo, Y. Lu, D. Shen, N. Zhao, X. Luo, and X. Zhang, *Macromolecules*, 2004, **37**, 3615.

[91] A. Razatos, Y. L. Ong, F. Boulay, D. L. Elbert, J. A. Hubbell, M. M. Sharma and G. Georgiou, *Langmuir*, 2000, **16**, 9155.

[92] P. Costamagna, C. Yang, A. B. Bocarsly and S. Srinivasan, *Electrochim. Acta*, 2002, **47**, 1023.

[93] Alfa Asear, www.alfa.com date accessed 05/05/11

[94] Tetrathane Technical Information Datasheet, Invista Corp, http://terathane.invista.com/doc/files/813/TERATHANE_PTMEG_PUSH%20Bulletin_April11.pdf, (accessed 8/7/11)

[95] J. Zhang, G-P. Yin, Z-B. Wang, Q-Z. Lai and K-D. Cai, *J. Power. Sources*., 2007, **165**, 73

[96] S. Song, G. Wang, W. Shou, X. Zhao, G. Sun, Q. Xin, S. Kontou and P. Tsiakaras., *J. Power. Sources.*, 2005, **140**, 103

[97] Z. Xie, C. Song, B. Andreaus, T. Navessin, Z. Shi, J. Zhang and S. Holdcroft, *J. Electrochem. Soc.*, 2006, **153**, E173.

[98] Y. Sone, P. Ekdunge and D. Simmonsson, *J. Electrochem. Soc*, 1996, **143**, 1254.

[99] Ed P. G. Bruce, *Solid State Electrochemistry*, 1997, Cambridge University Press, Cambridge, pg 228

[100] E. Barsoukov and J. R. Macdonald, *Impedance Spectroscopy , Theory, Experiment, and Applications,* 2nd Ed., Wiley Interscience, New Jersey, 2005, pg 79

[101] E. L. Thompson, T. W. Capehart, T. J. Filler and J. *J. Electrochem. Soc*, 2006, **153**, A2351.

[102] B. Smitha, S. Sridhar and A. A. Khan, *J. Membr. Sci*, 2003, **225**, 63.

[103] C. Zhao, X. Li, Z. Wang, Z. Dou, S. Zhong and H. Na, *J. Membr. Sci*, 2006, **280**, 643.

[104] D. R. Lide, *Handbook of Chemistry and Physics*, 84th Ed, CRC Press, Boca Raton, 2003, 8-48

[105] D. R. Lide, *Handbook of Chemistry and Physics*, 84th Ed, CRC Press, Boca Raton, 2003, 8-47

[106] G. Alberti, R. Narducci and M. Sganappa, *J. Power. Sources*., 2008, **178**, 575

[107] W. Lü, Z. Liu, C. Wang, Z. Mao and M. Zhang, *Int. J. Energy Res.*, 2011, **35**, 24.

[108] J. Peron, A. Mani, X. Zhao, D. Edwards, M.Adachi, T. Soboleva, Z. Shi, Z. Xie, T. Navessin and S. Holdcroft, *J. Membr. Sci.*, 2010, **356**, 44

[109] J. Umeda, M. Moriya, W. Sakamoto and T Yogo, *Electrochim. Acta*, 2009, **55,** 298.